A Designer's Guide to:

Innovative Linear Circuits

As featured in EDN Magazine

By Jim Williams

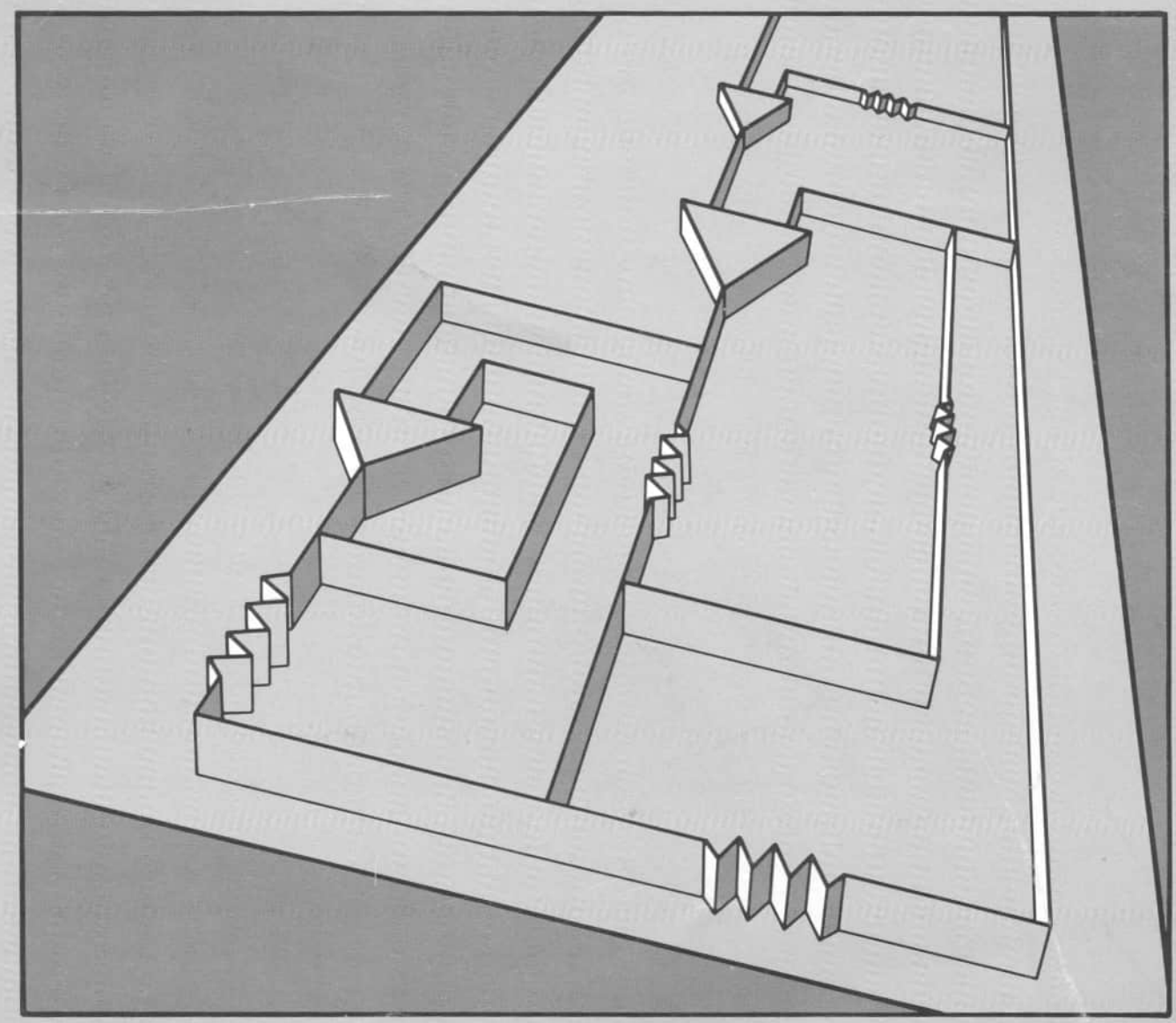

INTRODUCTION

Writing about applications, like all engineering tasks, involves compromises and limitations. An author must, for example, consider the editorial standards of the publication he writes for, his readers' interests, his employer's commercial aspirations, and the time available. And then, the author must simply desire to do the work. Without this drive, there's no point in even starting.

Balancing these sometimes conflicting considerations can be difficult, but not unduly so. You can, for example, balance a publication's needs, its readers' interests, and your employer's needs. After all, a successful publication must reflect its readers' interests. An astute employer will understand that serving the readers' interests can benefit the company as well. Such an employer realizes that the true value of publishing an applications article can't be measured in the immediate sales the article generates.

Instead, a stream of useful articles sponsored by a certain company lets readers know that the company can provide solutions to engineering problems. Such articles are a subtle and effective form of advertising. Instead of generating immediate sales, applications articles establish credibility. They become powerful long-term sales tools because they win customers' confidence by portraying the company as a problem-solving ally.

Of course, producing an applications article takes a lot of time. Typically, I need more than 100 hours to complete each article, and some articles take 200 to 300 hours. The actual writing takes up less than 10% of all the time I spend developing an article. The bulk of my article-development time is consumed by the lab work that I write the article around.

Because engineers are basically skeptical, a good author must address them in the language of working circuits and systems: The author must use laboratory-based material that's worked out and documented. Too, it's important to know when to stop. The author should work out his material well, but he doesn't have to refine it to the highest possible degree. An article's primary function is to be a catalyst—to start the reader thinking.

Finally, an author must simply desire to do the work. Applications work allows more freedom and flexibility than almost any other engineering job. And conceiving ideas and developing them into circuits is an enjoyable way to spend one's time.

Doing applications work has allowed my hobby and my vocation to become an indivisible entity, hopefully to the benefit of EDN and its readers. This state of affairs is made possible by you, EDN's readers, and I appreciate your support.

James M Williams
Linear Technology Corp
Milpitas, CA

PREFACE

Analog design is not dead. Neither is interest in it. Although digital design techniques have become the primary focus of most electronics trade journals and design magazines, the need for linear applications material remains strong. Designers continue to make significant advances in linear ICs, and using these new devices is anything but a trivial task.

EDN has regularly published design features that help readers get the most from the latest, most sophisticated linear ICs. And EDN's readers have written time and time again to thank us for continuing to print linear-design articles as well as for introducing the latest digital techniques.

Among all the contributors of linear-design features to EDN, one author stands out, both because of the large volume of material he's written for EDN and because of the originality and usefulness of his ideas. This man is Jim Williams. Since he first wrote for EDN in the mid 1970s, Jim has become a regular contributor and a favorite with readers. In fact, many readers have requested that we publish a compilation of his work. This book is a direct result of such requests.

In this preface, EDN would like to thank Jim for the time and effort he's invested in the many articles he's written for us. We hope that you find this material useful; we know that by reading it, you'll gain a similar appreciation for this man's talents.

EDN Staff

This book is dedicated
to the memory of
EDN Associate Editor George Huffman

EDN, a Cahners Publication, Cahners Building, 275 Washington St, Newton, MA 02158

TABLE OF CONTENTS

Test your analog-design IQ

Skilled analog-circuit designers are rapidly becoming a rare breed; for you diehards, here's a good test of your circuit-design acumen.

Jim Williams

Circuit design is very much the art of making imperfect components function "perfectly" together. Prepared with this consideration in mind, the questions in this test require a knowledge of components and circuit configurations, as well as an ability to identify and focus on the important issues affecting a circuit. The answers given are accurate, although in a few cases they have been left incomplete in a deliberate attempt to stimulate the kind of discussion that should occur in a circuit-design lab.

These problems are practical ones—solving them requires both experience and thought. The solutions are open to debate—alternative, perhaps better, ones are possible. But leave your Karnaugh maps at home and forget everything you know about bits and bytes; wonderful things are going on in the forgotten land between ONE and ZERO. This is Real Electronics.

Pencils ready? Begin!

1. Synthesizing the variable-resistance function (2-terminal) with decade switches is easy; clever designs minimize the number of resistors per decade by using series-parallel resistor combinations. Synthesizing the potentiometer (3-terminal) or ratio function, however, is not so obvious. Design a 4-decade switched potentiometer that has a constant impedance from end to end, regardless of the wiper arm's setting. You may use a standard pot for the final decade.

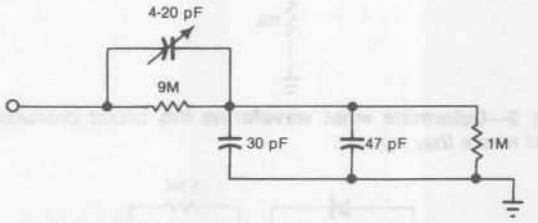

Fig 2—What function *might this network serve? Determine its response characteristics.*

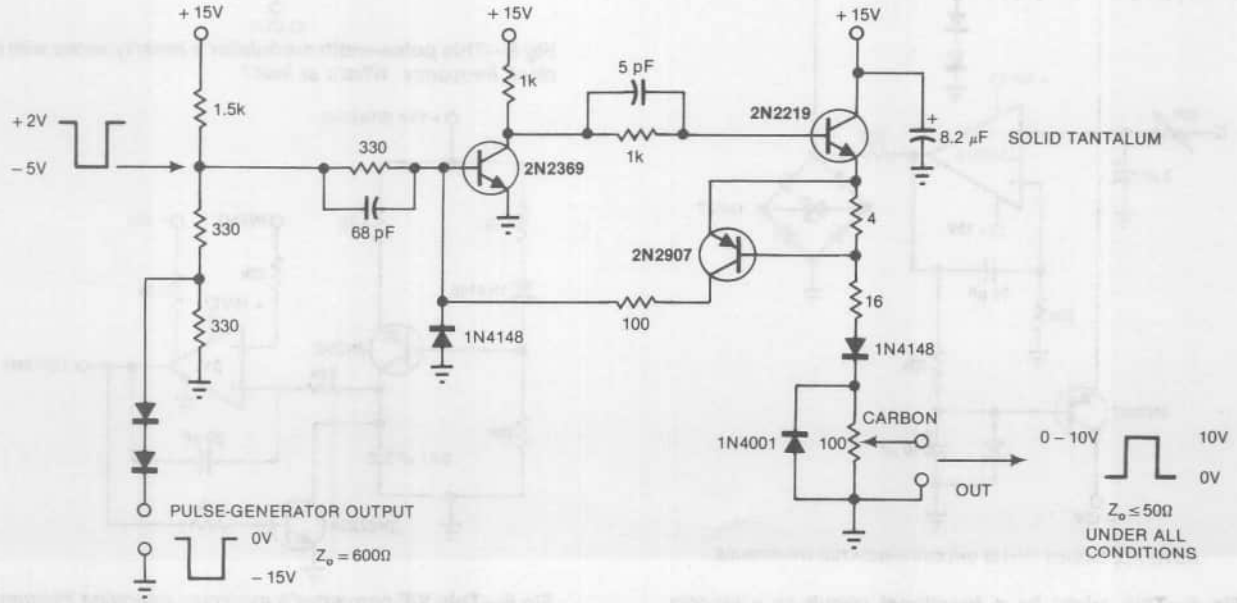

Fig 1—Reconfigure *this converter to correct its shortcomings: 30-nsec rise time and duty-cycle inversion.*

Why does a pulse-width modulator's linearity vary with clock frequency?

2. The circuit shown in **Fig 1** converts the negative-going output of pulse generators used in vacuum-tube work into a positive-going output compatible with solid-state circuits. Its low-impedance output is fully variable and capable of withstanding shorts to ground or either power-supply rail. This circuit works well, with two exceptions: First, the output appears as the inverse of the input, and second, the output pulse's rise time is about 30 nsec—a respectable time span that's nonetheless relatively short for a pulse-generator output. Reconfigure the circuit to correct these deficiencies, using a minimum number of component additions.

3. Determine the response characteristics of the network shown in **Fig 2.** What useful function might such a network serve? Why?

4. The circuit shown in **Fig 3** produces three waveforms. What are they and at what points do they appear?

5. What is the function of the circuit depicted in **Fig 4?** Does this circuit really do anything or is it just a random collection of parts?

6. Assuming the circuit shown in **Fig 4** does provide some useful function, what role does the 2N2907 play?

7. The circuit shown in **Fig 5** is a pulse-width modulator. At a given clock frequency, its linearity (E_X vs pulse width out) is good (typically 0.01%), but when the clock frequency changes, the linearity varies slightly. What is at fault and why?

8. The circuit displayed in **Fig 6** is a voltage-to-frequency converter. What is this circuit's chief limitation on maximum operating frequency? If you snip out the 20-pF capacitor, what would happen? Why? Are there any other significant considerations involved in setting up and using this circuit?

9. The configuration shown in **Fig 7** is a pulse-width-to-voltage converter—it provides a voltage proportion-

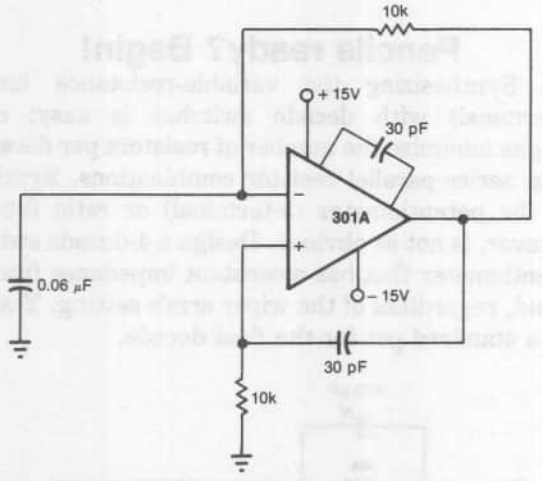

Fig 3—Determine what waveforms *this circuit produces and where they appear.*

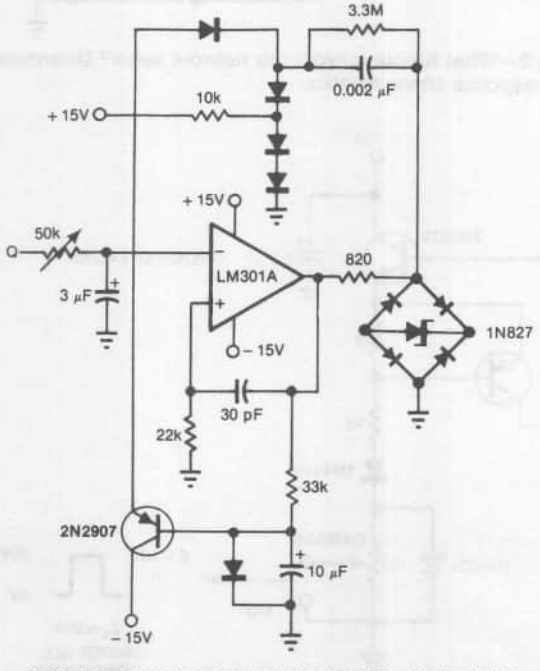

NOTE: ALL DIODES 1N4148 UNLESS INDICATED OTHERWISE

Fig 4—This might be a functional circuit *or a random collection of components—can you tell which?*

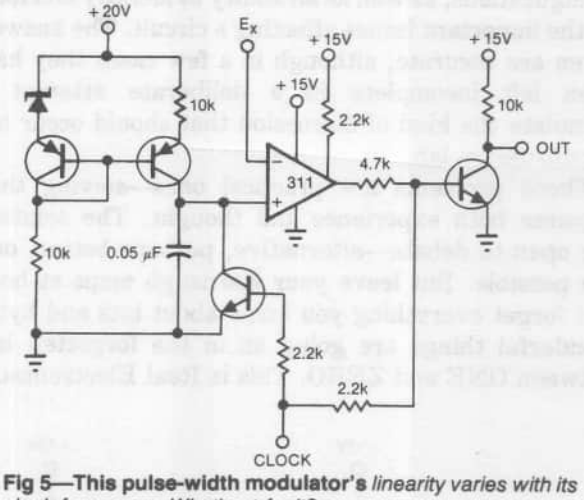

Fig 5—This pulse-width modulator's *linearity varies with its clock frequency. What's at fault?*

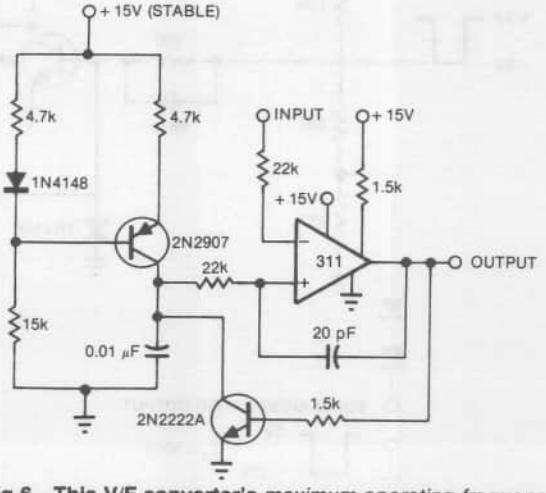

Fig 6—This V/F converter's *maximum operating frequency is limited by which component?*

al to the width of the most recent pulse applied to its input. Typically, this voltage must be "held" by the integrating capacitor for a few milliseconds. Aside from the small error caused by the reset one-shot's "holding down" the integrating capacitor for a few microseconds, performance is adequate. Unfortunately, the circuit suffers serious errors above about 8 or 9V output. Why? Add whatever components are necessary to fix this problem.

10. Given four 7.5V batteries and a Type 741 operational amplifier, construct a unity-gain, noninverting follower. The 741's positive input cannot be the signal input. Assume that the signal to be followed will range between +2 and −3.4V.

11. A 3-terminal black box is connected to the base, emitter and collector terminals of a transistor curve tracer. With the curve tracer set up to display the characteristics of an npn transistor, the familiar family

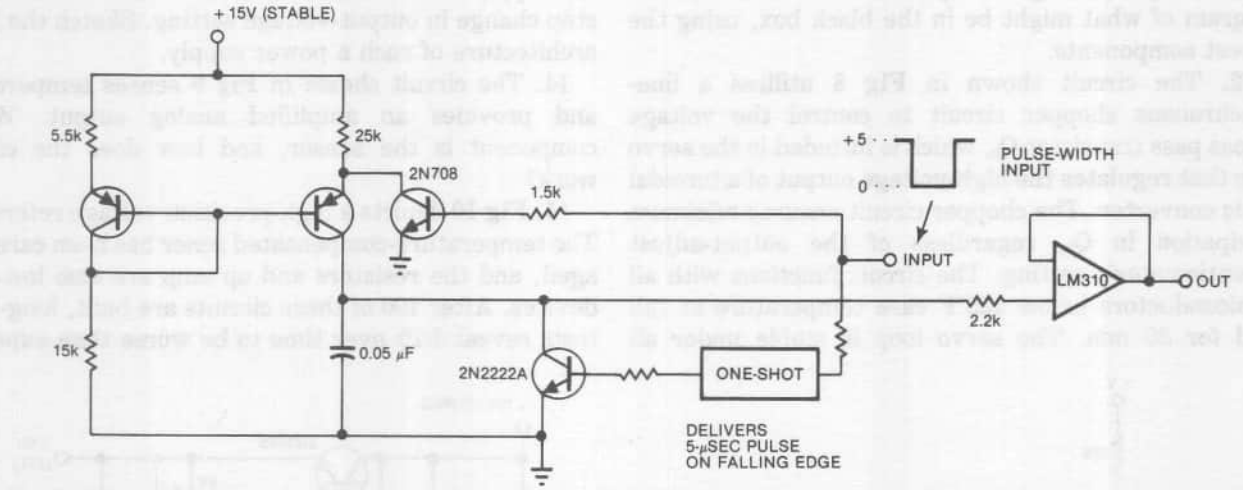

Fig 7—Conversion of pulse widths to voltages *suffers serious errors above 8 or 9V when this circuit is configured as shown. What's the problem?*

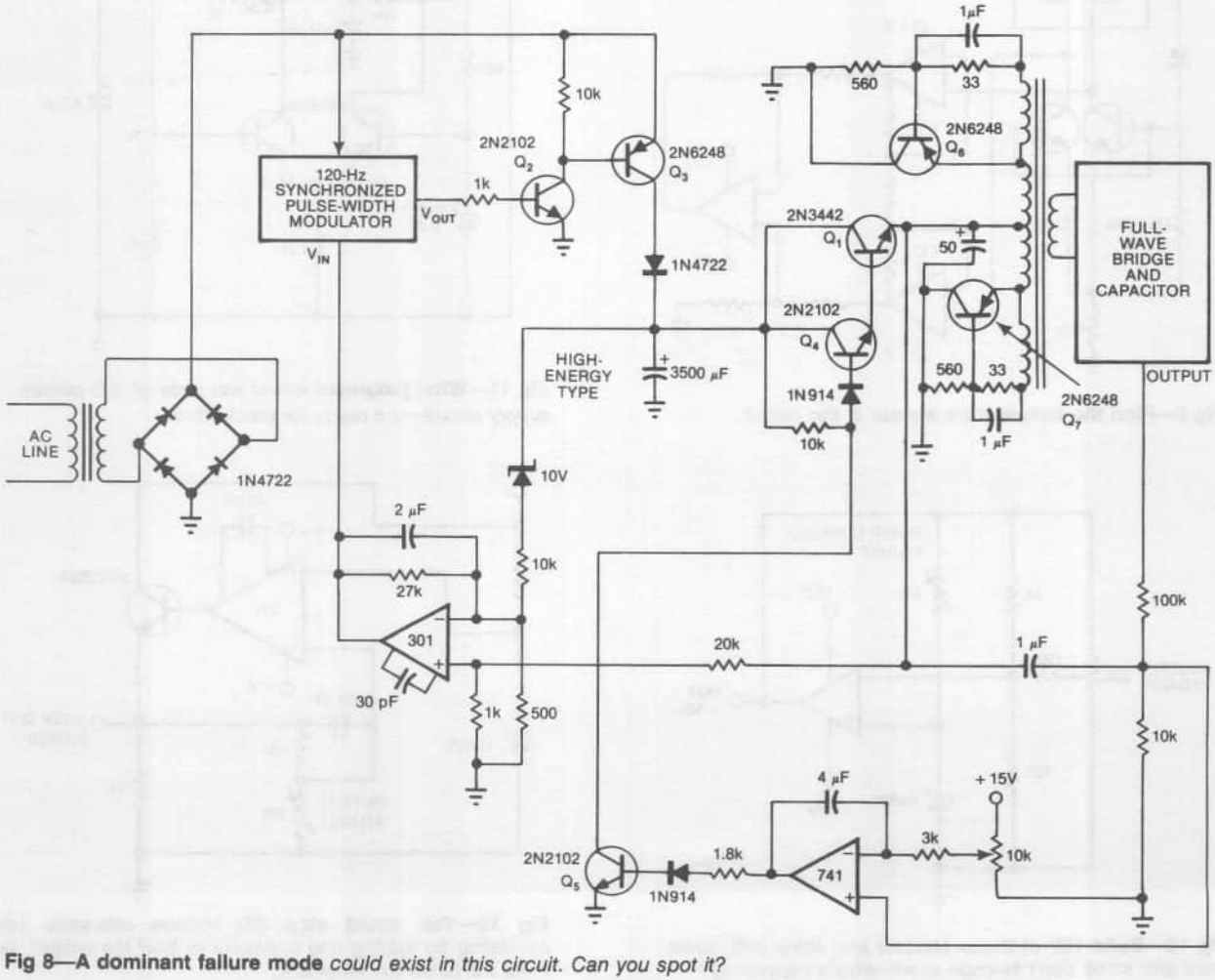

Fig 8—A dominant failure mode *could exist in this circuit. Can you spot it?*

Discover the source of erratic unit-to-unit performance

of curves appears on the screen. The gain appears quite low. Without touching the lead connections from the black box, you can reconfigure the curve tracer to display the curves of a pnp transistor...and they appear! Again, the gain is quite low. Draw the circuit diagram of what might be in the black box, using the fewest components.

12. The circuit shown in **Fig 8** utilizes a line-synchronous chopper circuit to control the voltage across pass transistor Q_3, which is included in the servo loop that regulates the high-voltage output of a toroidal dc/dc converter. The chopper circuit ensures minimum dissipation in Q_3, regardless of the output-adjust potentiometer's setting. The circuit functions with all semiconductors below 125°F case temperature at full load for 30 min. The servo loop is stable under all conditions, and performance appears good. But before you ship 100 of these systems, think twice. A dominant failure mode could exist. What might it be?

13. A requirement for a power supply with a 2000V output capable of providing 30 mA at 0.01% regulation (dc to 100 kHz) sends you to the design board. The load is active and inductive and also presents a 10Ω equivalent impedance for 100 msec every 2.5 min; during these periods, regulation may suffer. Finally, the supply should be able to settle within 100 μsec for a step change in output-voltage setting. Sketch the basic architecture of such a power supply.

14. The circuit shown in **Fig 9** senses temperature and provides an amplified analog output. Which component is the sensor, and how does the circuit work?

15. Fig 10 depicts a high-precision voltage reference. The temperature-compensated zener has been carefully aged, and the resistors and op amp are also low-drift devices. After 100 of these circuits are built, long-term tests reveal drift over time to be worse than expected

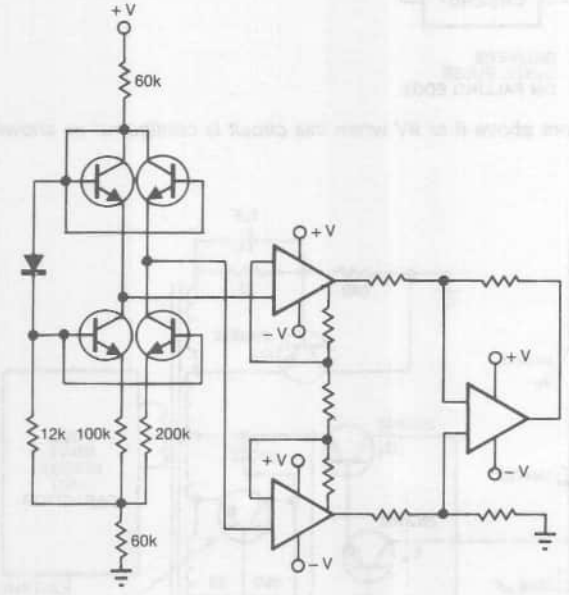

Fig 9—Find the temperature sensor *in this circuit.*

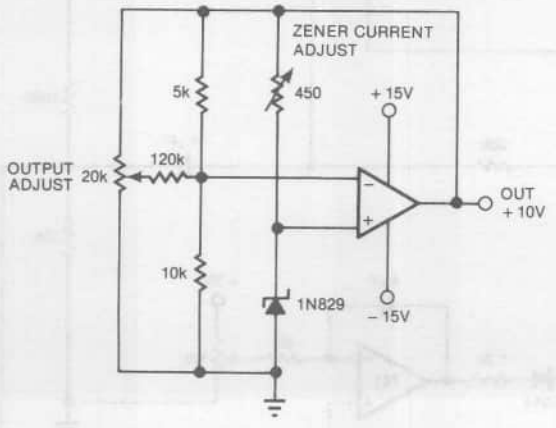

Fig 10—Build 100 of these circuits *and some drift, some work and some don't function at all—what's happening?*

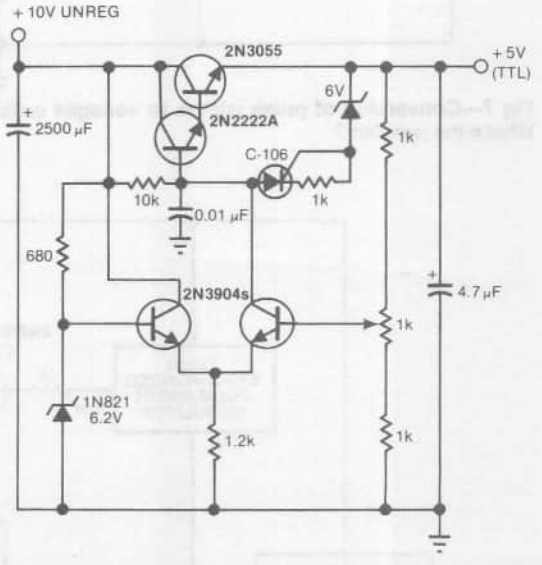

Fig 11—What judgment *would you pass on this power-supply circuit—is it ready for production?*

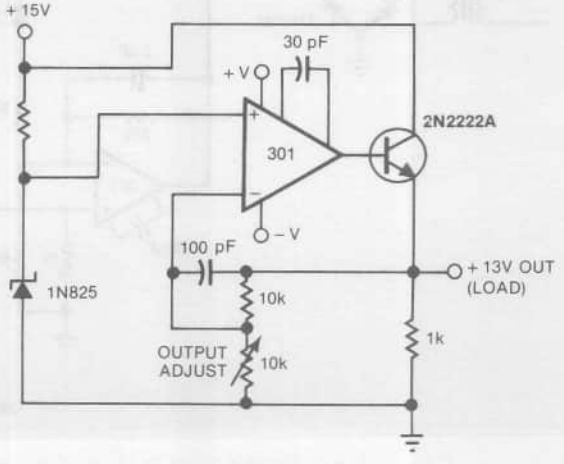

Fig 12—You could stop *this voltage reference from oscillating by adding one capacitor to load the emitter, but there's a better fix. What is it?*

in many units. Others work, while the remainder do not function properly at all. What's going on, what's the fix and why?

16. The data-acquisition power-supply circuit shown in **Fig 11** is on your desk for final approval before going to production. Any comments?

17. Fig 12 shows another voltage-reference circuit. Its output, instead of being dc, oscillates at 10 MHz. Using a 10-μF capacitor to load the emitter stops the oscillation, but this is a crude solution to the problem. What's the real fix?

18. Fig 13 shows a high-efficiency, precision temperature-control circuit designed to maintain a small oven at 198°C. Any comments?

19. In response to an input positive step function, what will be the output of the circuit shown in **Fig 14?** When the input steps back to zero, what will the output do?

20. The voltage-to-frequency-converter circuit shown in **Fig 15,** intended for electronic-music applications, features an output frequency exponentially related to its input voltage. For the values shown, the circuit produces a precise doubling of frequency output for each volt of input applied, from 20 Hz to 14 kHz. From 15 to 45°C, the circuit achieves negligible drift and exponential conformity within 0.2% over its entire operating range. The op amps run off ±15V supplies, the transistors are contained within a monolithic-array IC and the metal-film resistors specified are RN55 types. The current into the LM301A input is exponentially related to the circuit's input voltage because of the well-known logarithmic relationship between current and V_{be} in a transistor. The 301A and its associated components convert the emitter current into the output-frequency sawtooth. The 1N825 provides a reference for stability against supply changes. The 3-kΩ resistor establishes a 20-Hz frequency for 0V input, while the 10.5-kΩ resistor trims the gain to 1V in for each doubling of frequency out. The 1-MΩ/1.2-kΩ divider constitutes a first-order pass at canceling nonideal parasitic vagaries of Q_1. Most of the error in this circuit at low frequencies comes from the bias current of the LM301A and may be eliminated by substituting an FET device, such as an LF356. Discuss the function of the 741 op amp and its associated components. What are they doing and why?

21. Absolute zero is the temperature at which

(a) Type 3762 Josephson-effect ICs operate

(b) All molecular motion ceases

(c) Power transistors run most effectively

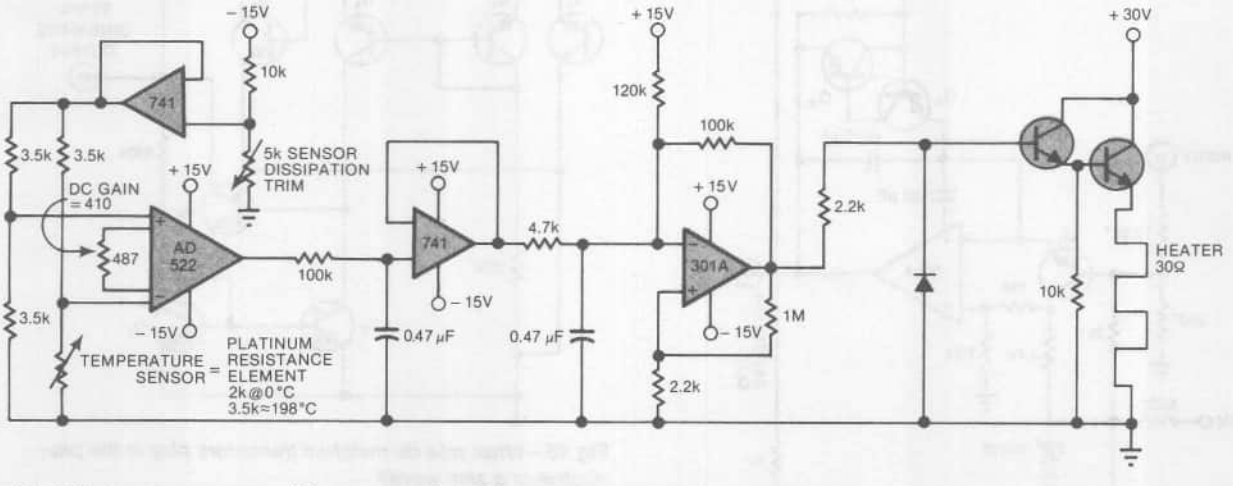

Fig 13—What performance *could you expect from this temperature-control circuit?*

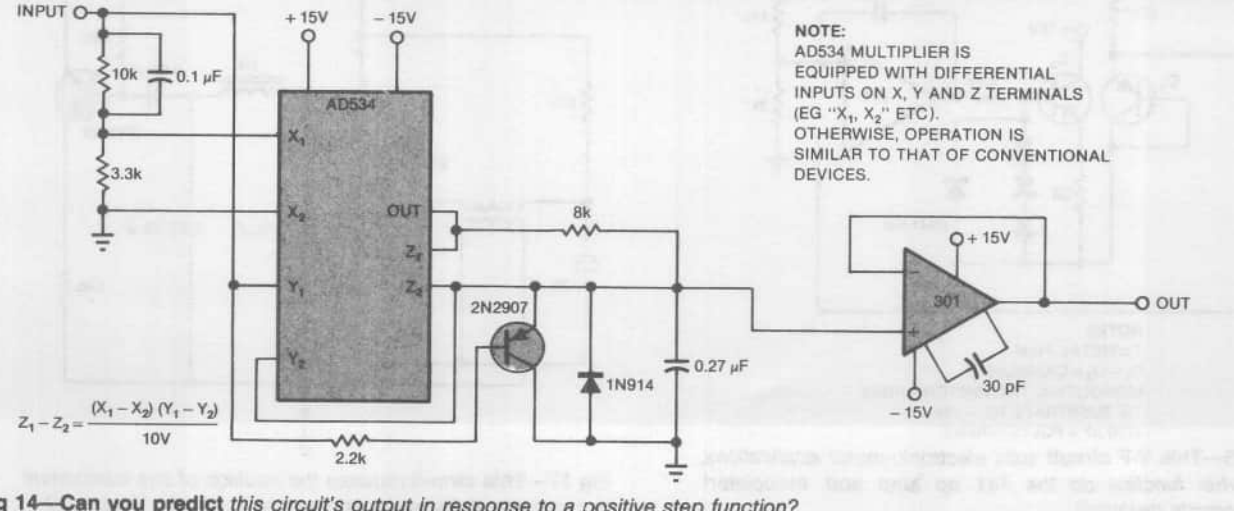

Fig 14—Can you predict *this circuit's output in response to a positive step function?*

Analyze the performance of an electronic-music circuit

(d) Lord Kelvin's body is refrigerated in the British Museum.

22. You want to invert (at unity gain) a 0 to +20V signal with a 741-type op amp. The 741 must run on ±15V supplies, although a −25V supply is available. Using no transistors, sketch the basic circuit.

23. Temperature is the most common physical phenomenon an EE is asked to consider. Which of these devices provides the most accurate and repeatable performance as a temperature sensor?

(a) Thermocouple
(b) Thermistor
(c) Type 8007 op amp
(d) Platinum wire
(e) 15-ft McPhearson thermometer.

24. The circuit shown in **Fig 16** generates a 75-kHz sine wave with about 2% distortion. Total supply-current drain is about 2.5 μA. Q_1 functions as a temperature-compensated reference diode to stabilize the circuit against supply and temperature shifts. The Q_1/Q_5 combination bootstraps off the reference-diode potential to provide a 1.2V potential to Q_6 via the LC circuit. Q_2, Q_3, Q_6, Q_7 and Q_8 actually produce the sine wave. Explain how. Hint: Assume all the transistors are matched.

25. One component is required to make the circuit depicted in **Fig 17** oscillate with good stability and output-wave purity. Put it in.

Pencils down

After you're sure of your answers, compare them with the ones presented on pg 145. You'll even find a chart there that lets you score your performance. **EDN**

Article Interest Quotient (Circle One)
High **476** ***Medium*** **477** ***Low*** **478**

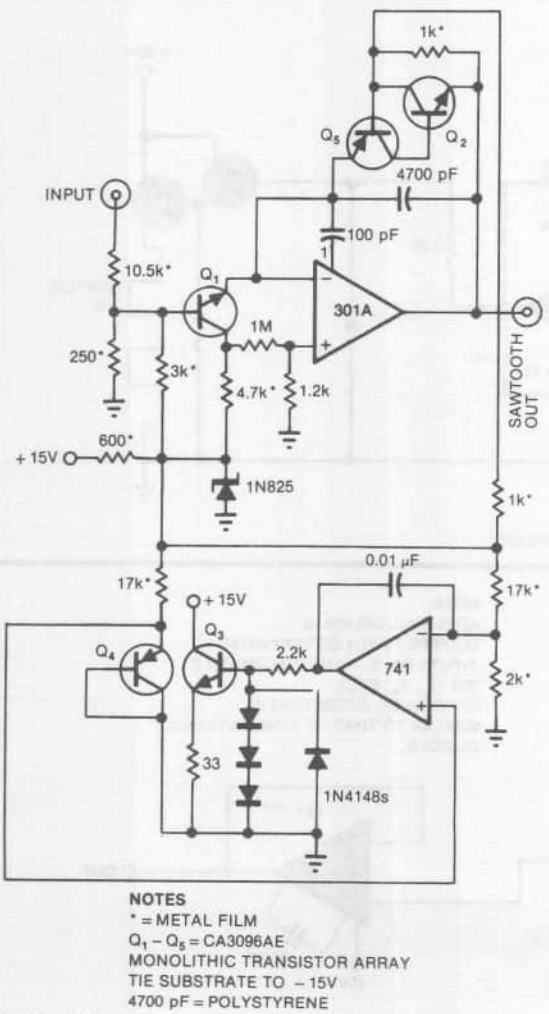

Fig 15—This V/F circuit *suits electronic-music applications, but what function do the 741 op amp and associated components perform?*

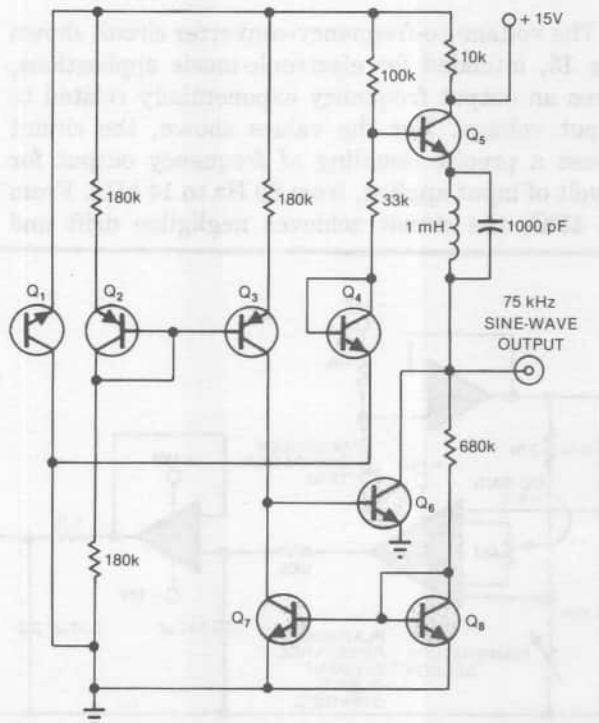

Fig 16—What role *do matched transistors play in the production of a sine wave?*

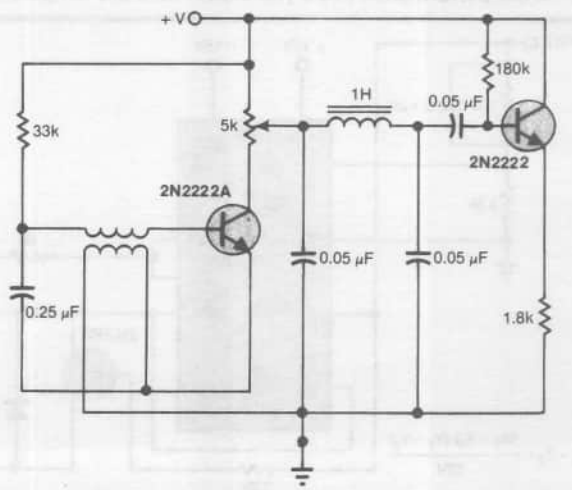

Fig 17—This circuit *requires the addition of one component to provide stability and output-waveform purity. What is it?*

Presenting the answers to EDN's analog-design quiz

Realizing that the answers might be debatable, get ready to score your paper. Each correct answer gets one point.

1. Several forms work; the most widely known solution is the Kelvin-Varley divider (named after Lord Kelvin) shown in **Fig 1.** All you must do is label the values of the resistors.

2. Less is better! In the original circuit, level shifting and voltage gain come from the popular high-speed 2N2639 transistor. The common-emitter configuration proves relatively slow (due to storage charge) and inverts the signal. The improved version (**Fig 2**) uses the common-base configuration because of its high speed and noninverting characteristics. This arrangement provides 10-nsec rise and fall times plus lower component count.

3. You should recognize the network as a common 10× scope probe connected to a scope. The variable capacitor allows you to precisely cancel the effects of cable and scope capacitance; the circuit provides high input impedance and very low input capacitance.

4. To understand this circuit (**Fig 3**), consider the effects of lightly compensating the 301. What if you put a very high-slew-rate amplifier in its place?

5. This circuit is a high-performance "charge-dispensing" voltage-to-frequency converter. "Packets" of charge, dumped into the summing junction by the amplifier output's switching action, servo-control the voltage there. The zener bridge and the 0.002-μF capacitor determine the amount of charge in each packet; the voltage applied to the input determines the number of packets dumped per unit time. The transistor and associated circuitry protect against lock-up, while the additional diodes provide the bridge's temperature compensation. For waveforms and details of operation, see EDN, August 5, 1978, pg 101.

6. The 2N2907 provides latch-up reset—latch-up can occur if the circuit's input is driven above the normal operation range (0 to 12V). In normal operation, the transistor is biased off.

7. The villain of this piece is dielectric soakage in the capacitor.

8. Maximum frequency is limited by the saturation voltage of the 2N222A. If you snip out the 20-pF capacitor, the 311's output never stays high long

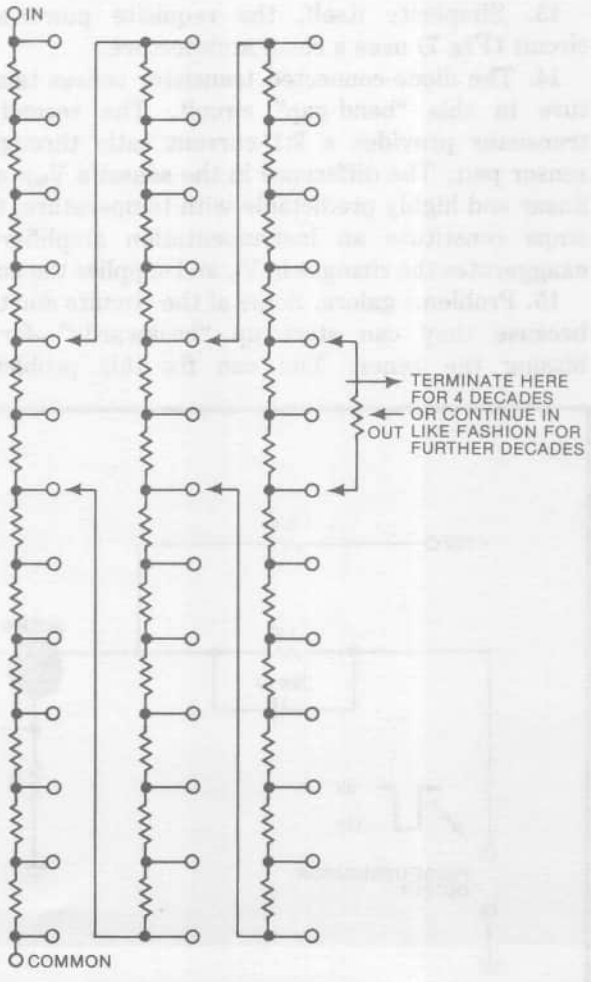

Fig 1—The Kelvin-Varley divider *allows you to add decades easily.*

SCORE YOURSELF

NUMBER OF QUESTIONS ANSWERED CORRECTLY	RATING
20-25	CIRCUIT DESIGNER
15-20	ELECTRICAL ENGINEER
10-15	TTL JOCKEY
5-10	MICROPROCESSOR SCHOLAR
0-5	COMPUTER PROGRAMMER

A current-source transistor bleeds charge from a capacitor

enough for the 0.01-μF integrator to completely discharge—the circuit's transfer characteristics go awry. Incidentally, the transfer characteristic creates an *inverse* relationship between input voltage and output frequency, as shown in **Fig 4.**

9. The circuit works well—up to where the current-source transistor suffers reverse breakdown (typically 8 to 9V in a small transistor). When the 2N708 comes on, if the 0.05-μF capacitor's voltage is above 8 to 9V, the current-source transistor breaks down and bleeds charge from the capacitor. One fix adds a diode in each emitter; two diodes are required to maintain temperature stability in the current source.

10. The circuit shown in **Fig 5** produces an output equal to its input, satisfying the stated requirements.

11. The black box need contain only a C-106B SCR, as shown in **Fig 6.**

12. A number of weak spots exist—Q_3 drives an enormous load, for example—but the ac power transformer presents the most important problem. Unless carefully designed, it will burn up (literally). Can you figure out why?

13. Simplicity itself, the requisite power-supply circuit (**Fig 7**) uses a clean architecture.

14. The diode-connected transistor senses temperature in this "band-gap" circuit. The second dual transistor provides a 2:1 current ratio through the sensor pair. The difference in the sensor's V_{be}s will be linear and highly predictable with temperature; the op amps constitute an instrumentation amplifier that exaggerates the changes in V_{be} and supplies the output.

15. Problems galore. Some of the circuits don't work because they can start up "backwards"—forward-biasing the zener. You can fix this problem by grounding the op amp's −15V terminal or inserting a diode in the output line. If you add the diode, run a 33-kΩ resistor from the top of the bridge to +15V to ensure starting. The units with long-term drift suffer from transient forward biasing of the zener. Precision zeners respond to any applied forward bias, however brief, by drifting slowly over time.

16. Place the SCR crowbar across the supply's output. (If the pass or driver transistor failed, the SCR shunt path to ground wouldn't be worth much.) Add a slow-blow fuse in the collector line. The turn-on provided for the SCR works, but sloppily and slowly—perhaps too slowly to save the TTL. Also, the SCR requires a capacitive bypass to avoid "rate effect" nuisance tripping. Anything else? You bet.

17. Add 100Ω to the base of the transistor and the oscillation ceases. Can you explain why?

18. Precision is fine but efficiency only results when the heater is placed in the collector line. The 301A pulse-width modulator only swings to +12V—most of the 30V supply ends up across the poor emitter-follower "switch."

19. Initially, the multiplier's output responds to the derivative of the input step (signal); after the capacitor at the input settles from the step input, the output is filtered at a frequency determined by the input's dc potential. **Fig 8** shows the effective time-constant

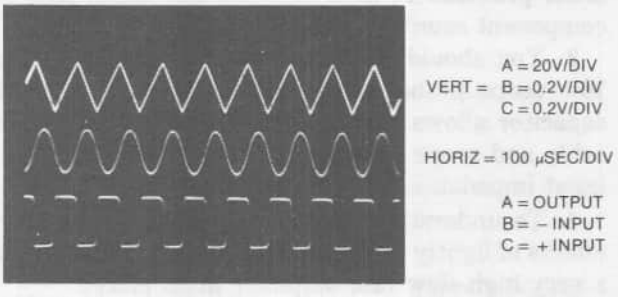

Fig 3—Three waveforms, *one at the negative input, one at the positive input and one at the output, characterize this circuit.*

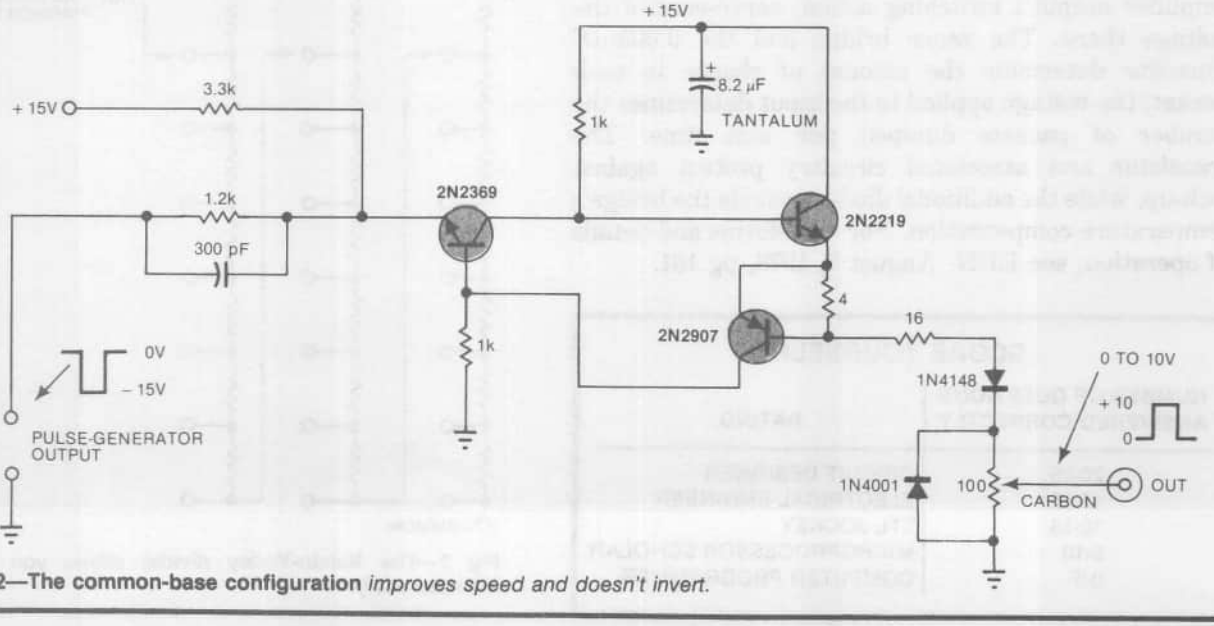

Fig 2—The common-base configuration *improves speed and doesn't invert.*

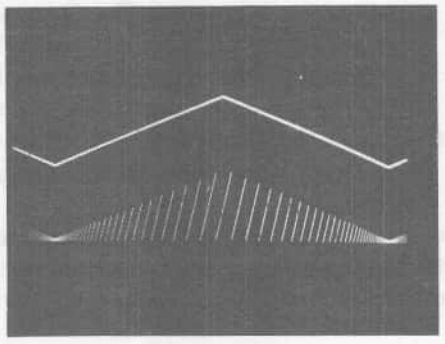

Fig 4—The V/F converter *provides an inverse relationship between input voltage and output frequency.*

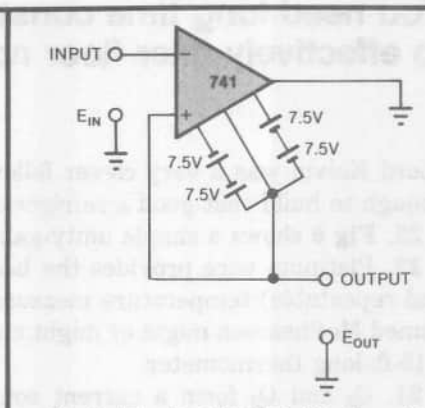

Fig 5—E_{IN} is mirrored by E_{OUT} *in this unity-gain, noninverting follower.*

change of the circuit caused by derivative response. The diode and transistor prevent derivative-controlled response on the trailing edge by clamping the 0.27-μF capacitor to ground. This circuit has proved itself in electronic weighing applications, where rapid signal acquisition is required yet "floor noise" calls for long time constants to provide effective filtering. Additional information on this circuit appears in the "Multiplier Application Guide," available free from Analog Devices Inc, Norwood, MA.

20. Q_1, unless compensated for shifts in ambient temperature, drifts wildly, rendering the circuit virtually useless. This problem is characteristic of the logging configurations, and several methods can correct it. Q_3, Q_4 and the 741 form a temperature-control loop that thermally stabilizes the entire monolithic transistor array at about 50°C. The loop prevents shifts in ambient temperature from affecting Q_1, stabilizing its operating point. Q_4's V_{be} junction senses the temperature, while Q_3 acts as the chip heater. The 741 adjusts Q_3's conductivity, dissipating enough power on chip to keep the voltage across the 2-kΩ resistor equal to Q_4's V_{be} potential. The 33Ω resistor, along with the diode string, determines the maximum power Q_3 can dissipate and prevents servo lock-up during circuit start-up. Note that Q_2 and Q_5 (responsible for resetting the integrator) constitute part of the monolithic array and thus are immune to ambient-temperature shifts. The 4700-pF integrating capacitor, which should be polystyrene, creates all thermal drift of any consequence in this circuit.

21. (b). All molecular motion stops at absolute zero.

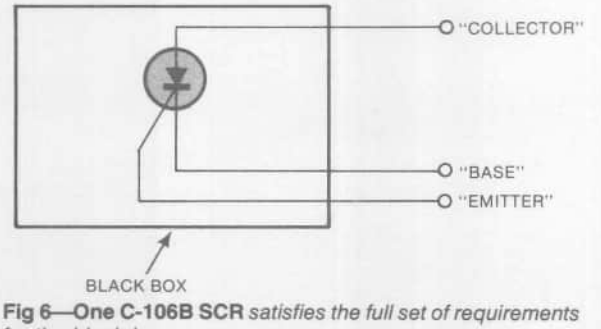

Fig 6—One C-106B SCR *satisfies the full set of requirements for the black box.*

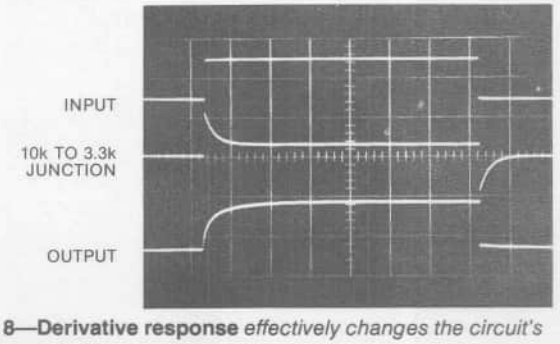

Fig 8—Derivative response *effectively changes the circuit's time constant.*

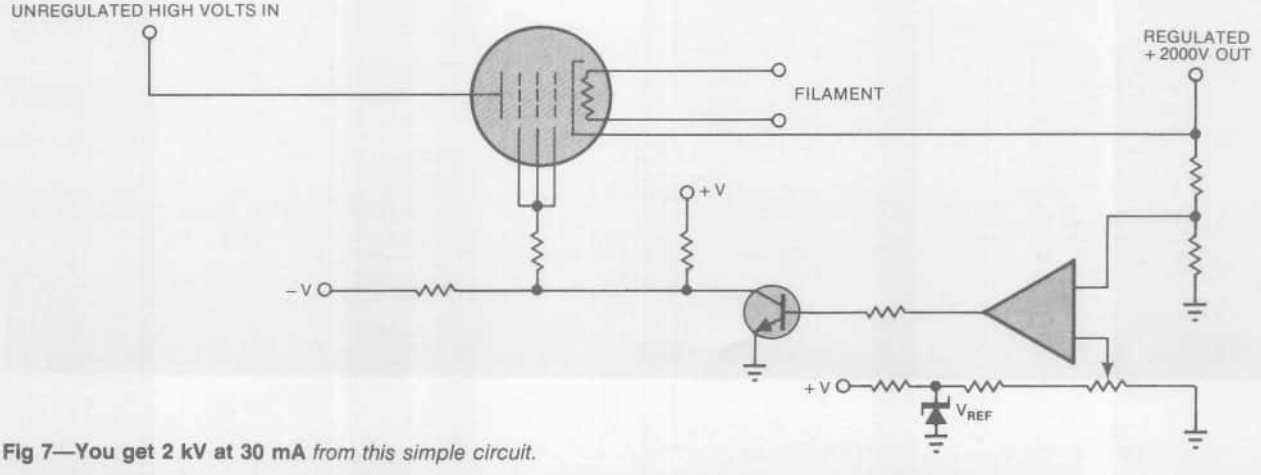

Fig 7—You get 2 kV at 30 mA *from this simple circuit.*

You need long time constants to effectively filter floor noise

(Lord Kelvin was a very clever fellow, but not clever enough to build that good a refrigerator.)

22. Fig 9 shows a simple unity-gain inverter.

23. Platinum wire provides the best (most accurate and repeatable) temperature measurements. Someone named McPhearson might or might not have ever made a 15-ft-long thermometer.

24. Q_2 and Q_3 form a current source that delivers about 15 μA to Q_3's collector. Q_3's collector current determines Q_6's peak collector current. The 680-kΩ resistor plus Q_7 and Q_8 accomplish a voltage-to-current conversion that decreases Q_6's base current whenever its collector potential rises. This provision gives the configuration a negative resistance characteristic that permits oscillation. The LC circuit determines the operating frequency. The Q_1 zener diode and the Q_4/Q_5 regulator provide supply-voltage-variation immunity—the circuit operates from 8.5 to 50V with constant output amplitude. At operating frequencies above 100 kHz, you might stiffen Q_5's output impedance by bypassing the emitter to ground with a 0.1-μF capacitor.

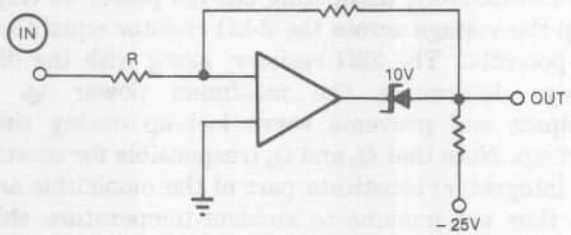

Fig 9—You can invert *a 0 to 20V input easily with one 741.*

25. Insert a 600-Hz tuning fork between the primary and secondary of the feedback transformer. **EDN**

Author's biography

Jim Williams, now unemployed, was a consultant at Arthur D Little Inc, Cambridge, MA, when this article was written. Before that, he was a senior engineer in MIT's Dept of Nutrition and Food Science, where he designed experimental biomedical instrumentation. Jim's interests transcend analog design to include sculpture, art, skiing, tennis and collecting antique scientific instruments.

Use comparator ICs in new and useful ways

You can use the unique differential-input/digital-output characteristics of comparators to implement a wide range of circuit functions.

Jim Williams, National Semiconductor Corp

Perhaps the most underrated and underutilized of monolithic ICs, comparators are among the most flexible and universally applicable components in your design arsenal. With their differential linear inputs and very-fast-switching digital outputs, these devices can help you implement unusual circuit functions at favorable cost and low component count compared with other approaches. Examples ranging from a shaft-angle encoder to a V/F converter show how you can exploit comparators' unique abilities.

Variable capacitor makes shaft-angle encoder

If, for example, you need to convert a shaft angle to a digital bit stream, you can employ **Fig 1**'s comparator-

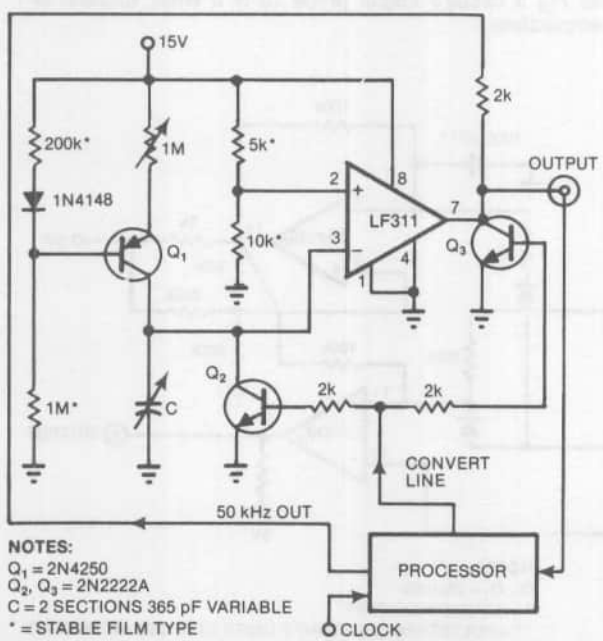

Fig 1—Employing a variable capacitor and a comparator, *a single-supply circuit yields a pulse burst—triggered by a Convert-line HIGH-to-LOW transition—whose duration is a ±0.1% linear function of the capacitor's shaft angle.*

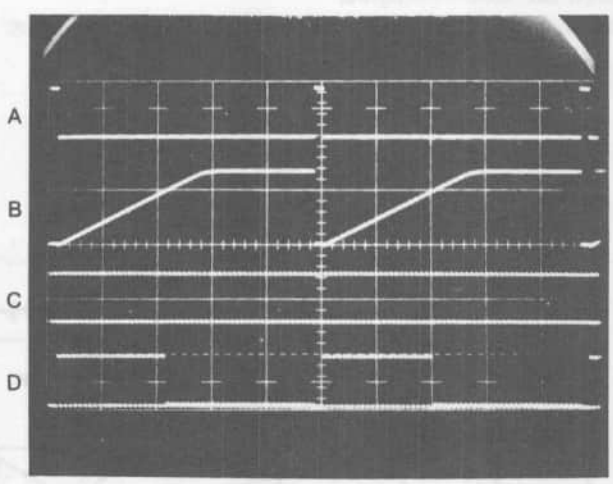

TRACE	VERTICAL	HORIZONTAL
A	5V/DIV	200 μSEC/DIV
B	10V/DIV	200 μSEC/DIV
C	5V/DIV	200 μSEC/DIV
D	5V/DIV	200 μSEC/DIV

Fig 2—When the linear charging ramp *(trace B) of* **Fig 1***'s variable capacitor reaches 10V, it signals a comparator to shut off the trace D output pulse burst.*

Obtain shaft-angle readings with a comparator-based circuit

based circuit. It uses a standard AM-radio dual 365-pF variable air capacitor to generate a controlling-processor-triggered constant-frequency pulse burst. The burst's duration—or the number of pulses it contains—indicates shaft position to within a ±0.1% typ accuracy. Moreover, the capacitor has essentially infinite life—unlike potentiometers, which can wear quickly and require frequent replacement in high-usage applications such as video arcade games.

In operation, transistor Q_1 and associated components form a ground-referred current source that linearly charges the variable capacitor. When the controlling processor needs a shaft-angle conversion, it drives the Convert line HIGH (**Fig 2,** trace A), turning Q_2 on and discharging the capacitor. Concurrently, Q_3 turns on, forcing the circuit output to zero.

To continue the conversion, the processor pulls the Convert line LOW, and the constant-current-source-driven capacitor voltage begins to ramp linearly toward the 15V supply (**Fig 2,** trace B). This Convert-line HIGH-to-LOW transition simultaneously unclamps the LF311's output, thus triggering a pulse burst by causing the processor's clock (**Fig 2,** trace C) to appear as a serial bit stream at the output (**Fig 2,** trace D).

The circuit continues to transmit this bit stream until the capacitor's voltage crosses the level established by the 5-kΩ/10-kΩ resistor divider; at that point the comparator output clamps, inhibiting pulses. Note that each Convert-line HIGH-to-LOW transition initiates an updated bit-stream output.

The circuit is insensitive to supply shifts because the resistor-divider trip point and the current-source reference are ratiometrically related. The FET-input comparator does not appreciably load other circuit components, so linearity is excellent. With a standard variable air capacitor (General Radio Type 722) substi-

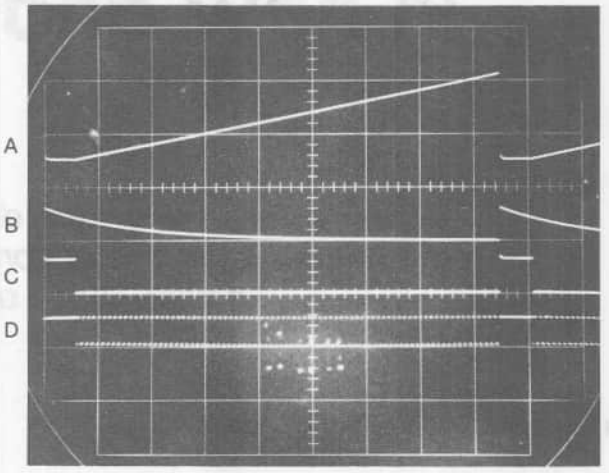

TRACE	VERTICAL	HORIZONTAL
A	0.5V/DIV	1 mSEC/DIV
B	0.1V/DIV	1 mSEC/DIV
C	5V/DIV	1 mSEC/DIV
D	10V/DIV	1 mSEC/DIV

Fig 4—The number of pulses *between bit-stream gaps in the* ***Fig 3*** *circuit's output (trace D) is a linear function of temperature.*

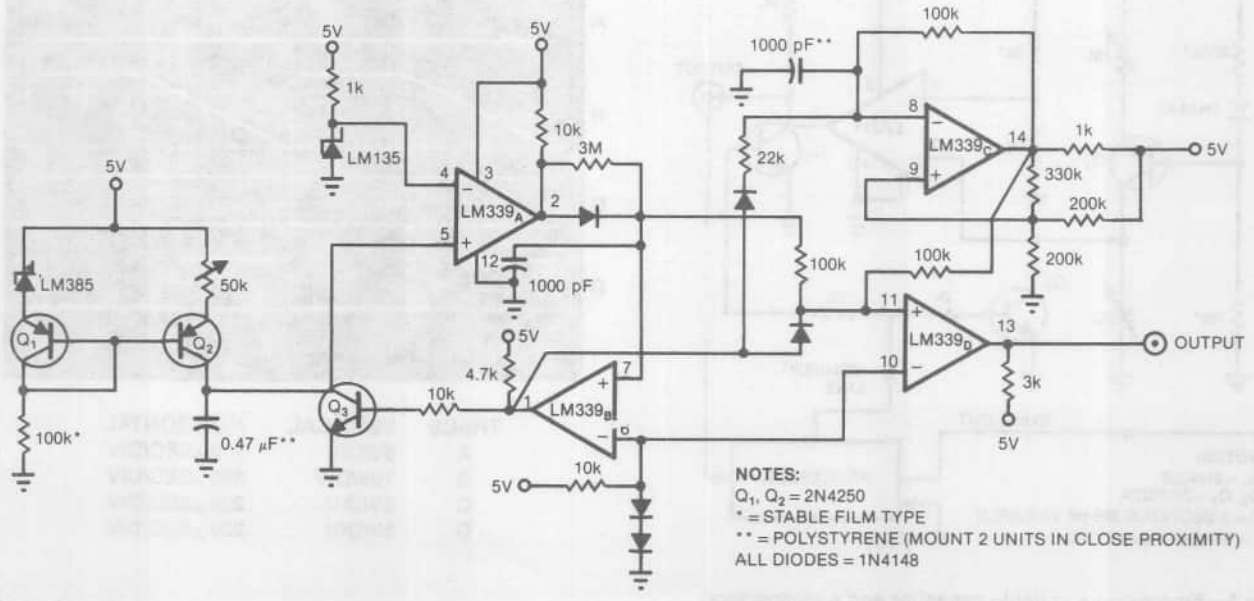

Fig 3—Furnishing an output pulse count proportional to temperature, *this LM135-sensor-based circuit requires no external clock. A gap in the output bit stream indicates the end of conversion.*

tuted for the dual 365-pF unit, linearity is well within ±0.1%. Use the 1-MΩ potentiometer to set the desired scale factor.

Convert temperatures to bit streams

Fig 3 shows another serial-output converter, one that requires only a 5V supply. Generating this circuit's output, which indicates the temperature at the LM135 sensor, doesn't require an external command—instead, the circuit clocks itself continuously and inserts gaps in the output stream to indicate the end of one conversion and the beginning of a new one.

Q_1 and Q_2 form a temperature-compensated current source whose output is referenced to the LM385. Q_2's collector current linearly charges the 0.47-μF capacitor (**Fig 4**, trace A) until the ramp voltage exceeds the LM135's voltage. Then, $LM339_A$'s output goes HIGH, dumping charge into the 1000-pF capacitor and forcing $LM339_B$'s positive input (**Fig 4**, trace B) and output (**Fig 4**, trace C) HIGH. This action turns on Q_3, resetting the ramp capacitor.

The 1000-pF capacitor can discharge only through the 3-MΩ resistor paralleling the diode at $LM339_A$'s pin 2. Therefore, the waveform at $LM339_B$'s positive input decays slowly, and the ramp capacitor stays off for an extended period of time. When the 1000-pF capacitor's

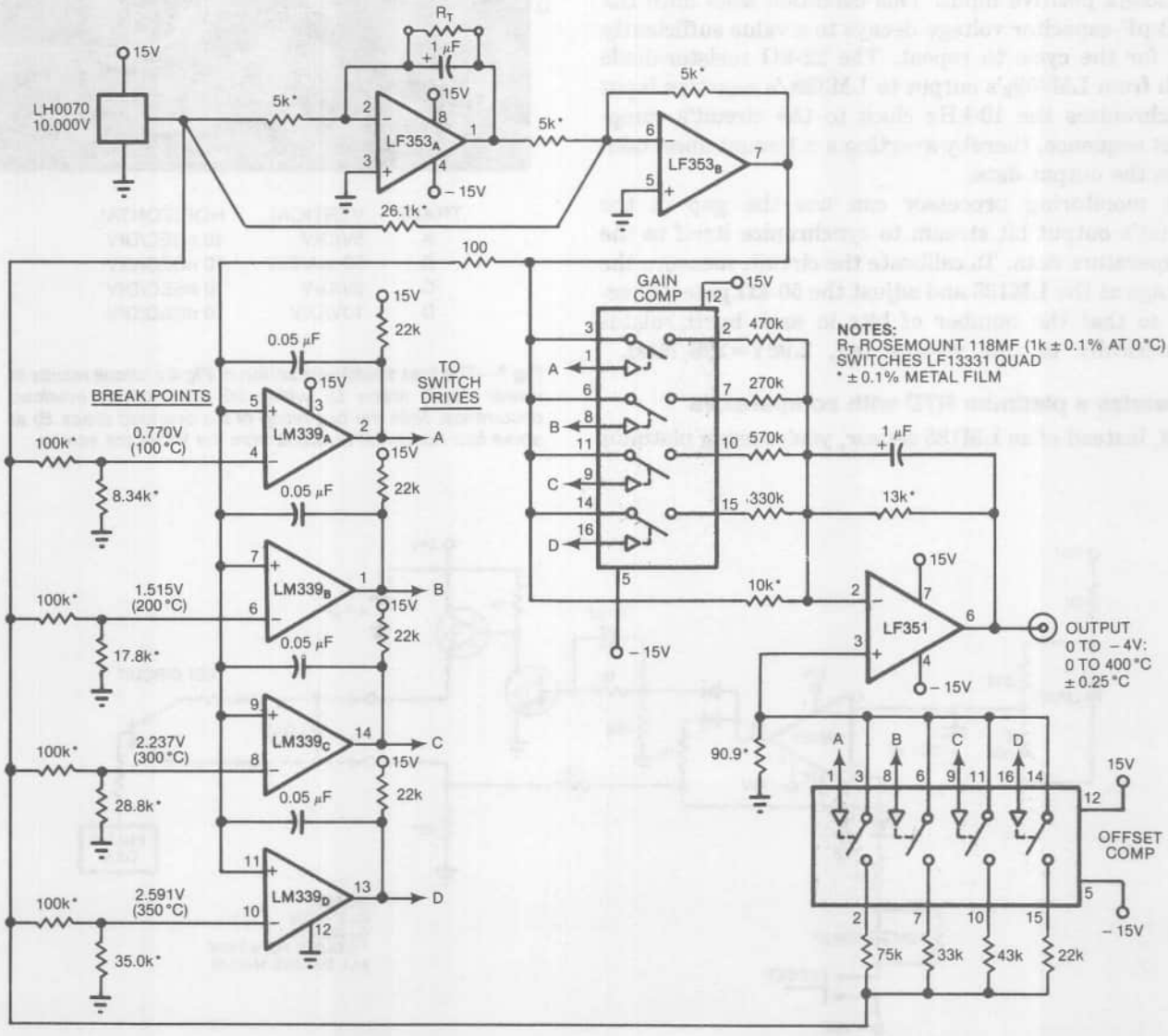

Fig 5—Using breakpoint corrections *at four temperatures and requiring no trimming, this circuit compensates for a platinum RTD sensor's nonlinearity.*

Temperature-sensing scheme uses a 4-comparator IC

voltage finally decays below the 2-diode-drop value at $LM339_B$'s negative input, Q_3 turns off, ramping begins and the cycle repeats.

The oscillation frequency varies inversely with the LM135's output voltage. The ramping time, however, is directly—and linearly—proportional to the LM135's output. While the ramp is running, $LM339_B$'s output is LOW, and $LM339_C$, which functions as a 10-kHz clock, biases $LM339_D$, providing the circuit's output. When $LM339_A$'s output goes HIGH, the 100-kΩ resistor path from $LM339_A$ to $LM339_D$'s positive input in turn forces $LM339_D$'s output HIGH (**Fig 4**, trace D).

Reinforcing feedback results when $LM339_B$'s output goes HIGH and applies bias through the diode path to $LM339_D$'s positive input. This condition lasts until the 1000-pF-capacitor voltage decays to a value sufficiently low for the cycle to repeat. The 22-kΩ resistor/diode path from $LM339_B$'s output to $LM339_C$'s negative input synchronizes the 10-kHz clock to the circuit's ramp-reset sequence, thereby averting a ±1-count uncertainty in the output data.

A monitoring processor can use the gap in the circuit's output bit stream to synchronize itself to the temperature data. To calibrate the circuit, measure the voltage at the LM135 and adjust the 50-kΩ potentiometer so that the number of bits in each burst relates numerically to this voltage (eg, 2.98V=298 bits).

Linearize a platinum RTD with comparators

If, instead of an LM135 sensor, you're using platinum RTDs (resistance temperature detectors) to take advantage of their extremely wide operating-temperature ranges and their long-term stability under adverse environmental conditions, consider the **Fig 5** linearizing

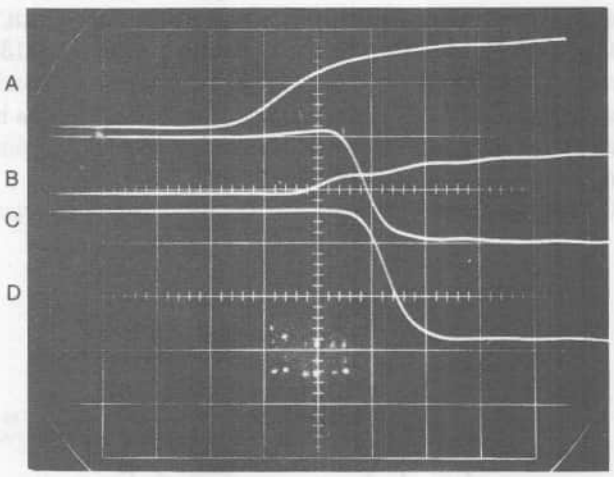

TRACE	VERTICAL	HORIZONTAL
A	5V/DIV	10 nSEC/DIV
B	50 mA/DIV	10 nSEC/DIV
C	5V/DIV	10 nSEC/DIV
D	10V/DIV	10 nSEC/DIV

Fig 7—The fast shutdown action *of* ***Fig 6****'s circuit results in power cutoff (trace D) within 30 nsec of an overload occurrence. Note the beginning of the overload (trace B) at about four horizontal divisions from the left of the screen.*

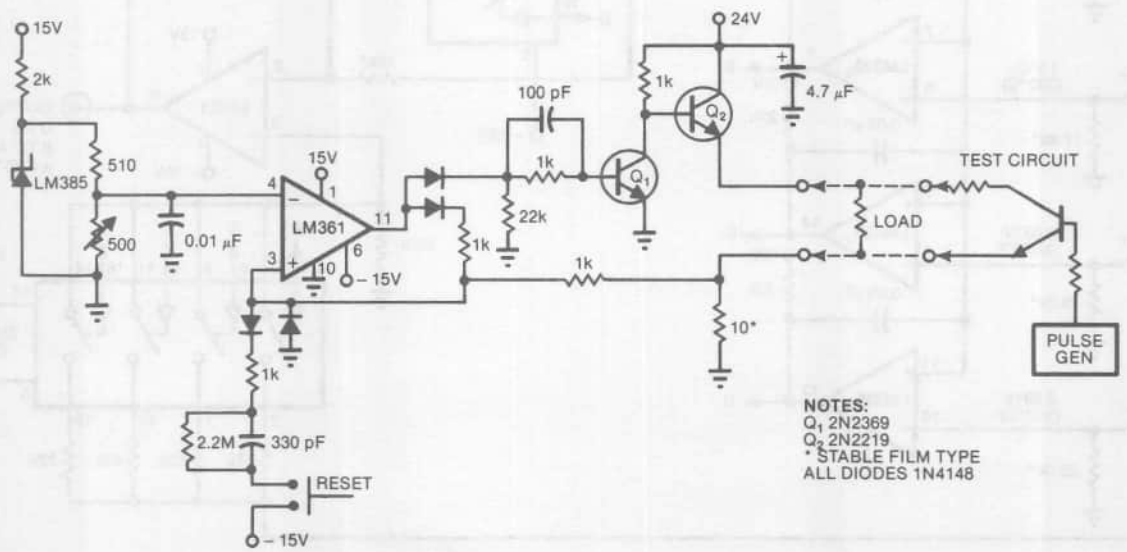

Fig 6—A fast-acting power-shutdown circuit can protect sensitive components. *The one shown here employs a comparator and a 10Ω sense resistor to establish a 100-mA trip point.*

circuit. It overcomes an RTD's inherent nonlinearity (>6° error from 0 to 400°C) by using an LM339 quad comparator to apply a 4-section breakpoint correction. In contrast to other RTD-linearizing circuits, **Fig 5**'s design needs no calibration.

Because of the RTD sensor's positive temperature coefficient, op amp $LF353_A$'s output rises with increasing temperature. Summing the output with a constant current at $LF353_B$'s negative input results in a 0V $LF353_B$ output at 0°C; this output increases as a direct but nonlinear function of the RTD's temperature.

$LF353_B$'s temperature-dependent output drives the positive inputs of the LM339 comparators and provides the input to the output gain stage, $LF351_C$. The threshold voltages at the LM339 negative inputs cause the respective comparators to switch at the $LM353_B$ voltages corresponding to 100, 200, 300 and 350°C.

When a comparator output switches HIGH, it switches in gain- and offset-changing resistors via the LF13331 JFET switches. The four slight gain adjustments compensate for the RTD's nonlinearity, and the introduced offsets ensure a monotonic increase in output as temperature rises. The 0.05-μF capacitors at the LM339 outputs prevent chattering at the trip points; the 1-μF capacitor in the LF351's feedback loop eliminates transient switching signals from the output.

If you use the **Fig 5** circuit values and RTD sensor, you can obtain ±0.15°C accuracy over 0 to 400°C with no trimming of any kind.

Do you have need to protect expensive components in a system—perhaps, for example, during the final phases of trimming and calibration? If so, consider the **Fig 6** circuit—it shuts down power within 30 nsec of an overload occurrence (in this case, for load currents greater than 100 mA).

When the current is less than or equal to 100 mA, the LM361's output is LOW, Q_1 is OFF and emitter follower

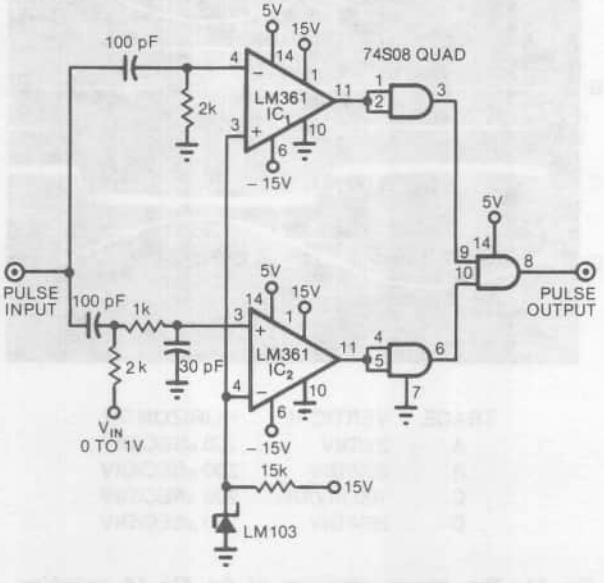

Fig 8—A circuit based on two comparators *and an AND gate can generate 6-nsec-wide pulses with 2-nsec rise and fall times. The V_{IN} level determines pulse width.*

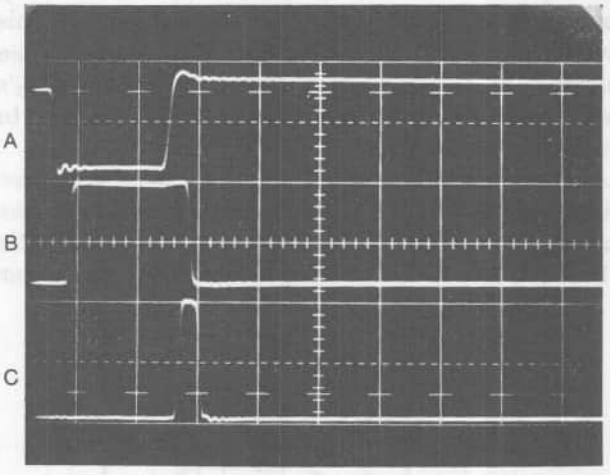

TRACE	VERTICAL	HORIZONTAL
A	2V/DIV	200 nSEC/DIV
B	2V/DIV	200 nSEC/DIV
C	2V/DIV	200 nSEC/DIV

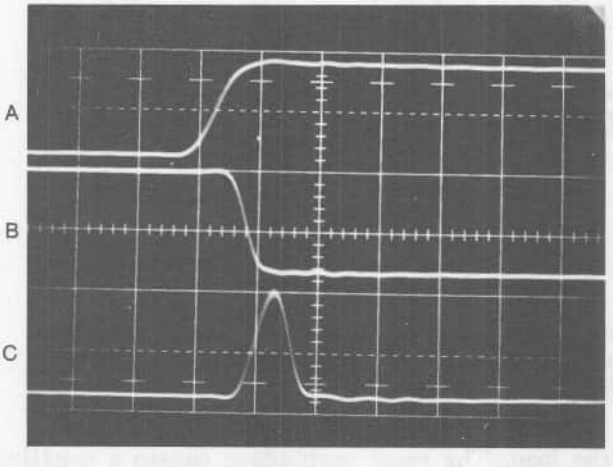

TRACE	VERTICAL	HORIZONTAL
A	5V/DIV	10 nSEC/DIV
B	5V/DIV	10 nSEC/DIV
C	5V/DIV	10 nSEC/DIV

Fig 9—The ANDing action *of **Fig 8**'s 74S08 gate yields a narrow pulse (**(a)**, trace C) because of time displacement between comparator outputs (traces A and B). The traces in **(b)** show the signals at these same circuit nodes for a 100-mV V_{IN}.*

Comparator high-speed switching eases pulse-generation tasks

Q_2 sources power to the load and the 10Ω sense resistor. When an overload occurs (in this case via the test circuit, whose output appears in **Fig 7,** trace A), the current through the 10Ω sense resistor begins to increase. (Note the slight load-current rise in **Fig 7,** trace B.)

This rise in current produces a corresponding voltage increase at the LM361's positive input. The comparator's output then rises (**Fig 7,** trace C) and drives Q_1 through a heavy feedforward network. Although this network degrades the LM361's output rise time somewhat, Q_1 responds very quickly and clamps Q_2's base to ground, causing load voltage (**Fig 7,** trace D) to immediately decay to zero.

As noted, the total elapsed time from overload onset to circuit shutdown is 30 nsec. Once the shutdown has occurred, the resistor-diode network from the LM361's pin 11 to pin 3 provides latching feedback to keep power

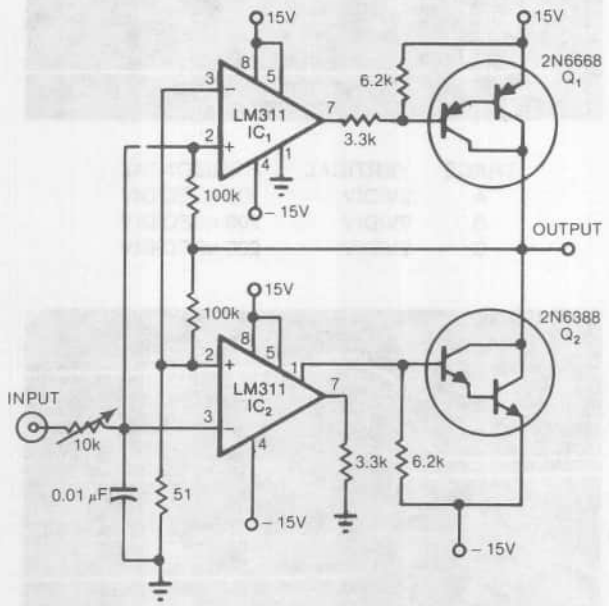

Fig 10—A comparator-based 400-Hz switching amplifier *is inexpensive, requires few components and can provide a 6A output.*

off the load. The reset pushbutton causes a negative spike to appear at the LM361's positive input, breaking the latching feedback and allowing the loop to function normally again. Use the 500Ω potentiometer to set the trip point at the desired value (for the **Fig 6** circuit, 1V=100 mA).

Comparators make 2-nsec pulse generator

Similarly benefiting from the LM361's high-speed performance, the **Fig 8** ultra-high-speed pulse generator furnishes voltage-controllable pulse widths. Its differentiator networks generate a pair of pulses with slightly different durations; the comparators and a Schottky TTL gate extract the difference between two widths and present it as a single fast-rise-time pulse at the circuit output.

When you apply a positive input pulse, the two 100-pF/2-kΩ differentiator networks yield positive outputs. When the positive-going steps exceed the 2V threshold established by the LM103, both LM361s switch output states. For a 0V control input, the differentiator networks and the LM361s respond simultaneously, and both output transitions line up.

As you increase the control voltage, however, the spike produced by IC_2's differentiator arrives at the 2V threshold earlier than does that of IC_1. IC_2 also normally takes longer to decay through the 2V threshold, appearing to lead to a situation in which IC_2's output would remain HIGH longer and switch earlier than would IC_1's.

IC_2's 30-pF/1-kΩ network, however, provides a delay that shifts the IC_2 output so that IC_1's leading and trailing edges occur first (**Fig 9a,** traces A and B). The length of time between the comparator outputs' edges depends on the input control voltage.

For the **Fig 8** circuit, a 0 to 1V control range produces a trailing-edge timing difference of 0 to 100 nsec. The

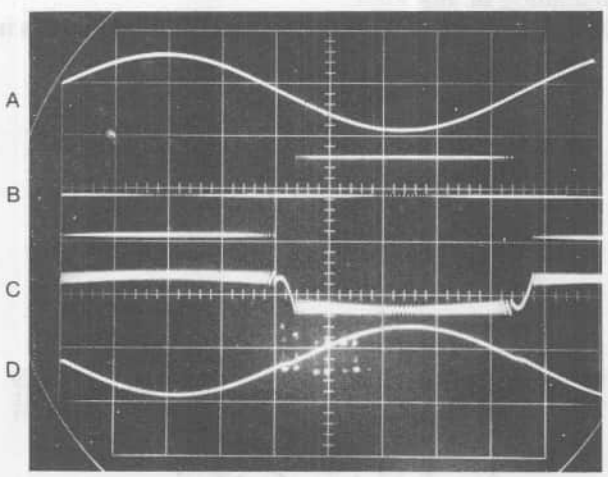

TRACE	VERTICAL	HORIZONTAL
A	2V/DIV	200 μSEC/DIV
B	20V/DIV	200 μSEC/DIV
C	100 mV/DIV	200 μSEC/DIV
D	20V/DIV	200 μSEC/DIV

Fig 11—The power envelope *of the* ***Fig 10*** *switching amplifier's output (trace D) is sinusoidal when the circuit is driven by a sine-wave input (trace A). Note the high-frequency charging and discharging of the circuit's 0.01-μF capacitor (trace C).*

Comparator circuit handles frequency-division chores

DM74S08 ANDs the two comparators' outputs to obtain the single-pulse circuit output (**Fig 9a,** trace C).

The gate and comparator switching speeds limit the minimum pulse width to 6 nsec; rise and fall times are approximately 2 nsec. **Fig 9b** shows an example of the high-speed operation that the **Fig 8** circuit can achieve (control input=100 mV). Traces A and B represent IC_1 and IC_2 outputs, respectively; trace C is the circuit's output pulse.

If you need a simple, inexpensive 400-Hz amplifier, consider the **Fig 10** circuit. It uses ±15V supplies,

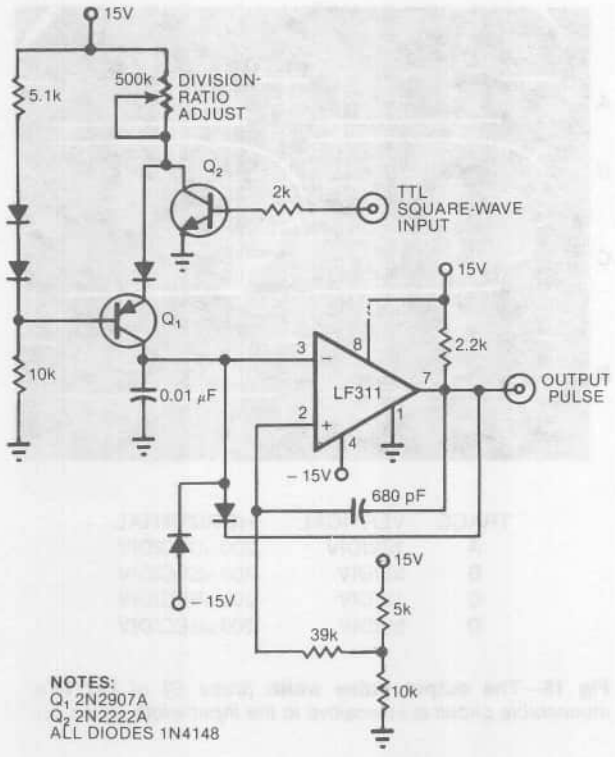

Fig 12—Divide and conquer *your frequency-reduction problems with this synchronous circuit. You can vary the division ratio over a 1:1,000,000 range.*

provides full bipolar swing and has a 1.5-kHz full-power bandwidth with a 6A pk output capability.

If the input voltage is negative, IC_2's output is LOW (note that IC_2 operates in an emitter-follower mode, so its output is in phase with its negative input), cutting Q_2 off. Concurrently, IC_1's output goes LOW, turning Q_1 on and thereby driving the load and the 100-kΩ resistors connected to the comparators' positive inputs. This feedback produces a small voltage at IC_1's negative input.

When the 0.01-μF capacitor charges to a level high enough to offset the negative input, IC_1's output changes state, turning Q_1 off. At this point, the input draws current from the capacitor, forcing IC_1's positive input to a lower state and consequently driving IC_1's output LOW again, turning Q_1 on.

The switching action occurs continuously; repetition rate depends on the input voltage. For positive inputs, IC_2 and Q_2 perform similar action. To avoid cross-current conduction in the output transistors, tie the comparators' offset-adjust terminals to the 15V supply.

Fig 11 trace B shows the circuit output resulting from the trace A input; the trace C waveform represents current flow in and out of the capacitor. (Think of the IC_2 pin 3 point as a digitally driven summing junction.) Trace D is a lightly filtered version of trace B; it clearly shows that the circuit output has a sinusoidal power envelope. You can vary the amplifier gain with the 10-kΩ input potentiometer.

Divide frequencies over a 1:1,000,000 range

Using the **Fig 12** circuit, you can divide a frequency over a $1:10^6$ range, adjustable via a single potentiometer. Moreover, the output frequency you obtain is synchronously related to the input frequency. You can use this circuit to obtain simultaneous oscilloscope observations of low-frequency signals and the fast clock

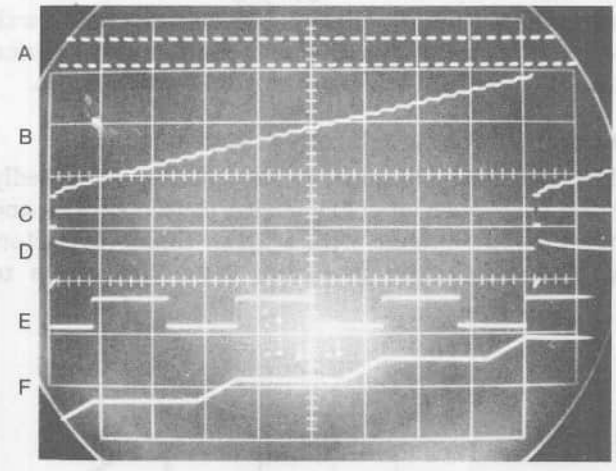

TRACE	VERTICAL	HORIZONTAL
A	10V/DIV	100 μSEC/DIV
B	5V/DIV	100 μSEC/DIV
C	50V/DIV	100 μSEC/DIV
D	20V/DIV	100 μSEC/DIV
E	10V/DIV	10 μSEC/DIV
F	0.2V/DIV	10 μSEC/DIV

Fig 13—Using a step-charging technique *that results in the trace B capacitor voltage,* ***Fig 12****'s circuit yields an output frequency proportional to and synchronized with an input signal's frequency (trace A). In the example shown here, the output (trace C) contains a pulse after 32 input pulses.*

Manipulate pulses with comparator-based circuits

from which they're derived or to synchronously trigger an A/D converter at a variable rate.

The circuit functions by step-charging a capacitor with a switched current source and using a comparator to determine when to reset the capacitor. **Fig 13,** trace B, shows the step-charging waveform; each time the pulse input (**Fig 13,** trace A) goes LOW, a current-source pulse causes a capacitor-voltage positive step. You can control the step height—and therefore the division ratio—with the 50-kΩ potentiometer.

When the staircase waveform reaches the voltage at the LF311's positive input, the comparator output goes LOW (**Fig 13,** trace C) and stays LOW until the positive feedback through the 680-pF capacitor ceases. The delay produced by this feedback ensures a complete reset for the 0.01-μF capacitor, which discharges through the steering diode into the comparator output.

The diode connected from LF311 pin 3 to −15V provides first-order compensation for the steering diode's leakage effects during the charge cycle. **Fig 13,** trace D, shows the waveform at the LF311's positive input. Traces E and F show in an expanded time scale the relationship between the input waveforms and the step-charged ramp.

When using this circuit, remember that although the output frequency is always synchronously related to the input frequency, its absolute value can vary with time and temperature. Typically, the trip point—hence, the output frequency—moves back and forth along the horizontal portion of a step at low division ratios and changes from step to step at high ratios.

Overcome TTL multivibrators' shortcomings

If you've used TTL monostables, you've undoubtedly noticed their poor input triggering characteristics and limited dynamic range with a given timing capacitor. The **Fig 14** circuit surmounts these limitations to provide a true level-triggered input and a single-resistor-programmable 10,000:1 output-pulse range. It delivers a preprogrammed output pulse width regardless of the input pulse duration. (The minimum input trigger-pulse width is, however, 3 μsec.)

When you apply an input pulse (**Fig 15,** trace A) to the circuit, $LM393_A$'s output goes LOW (**Fig 15,** trace B), producing reinforcing feedback for its own positive input (**Fig 15,** trace C). This causes $LM393_B$'s output to go HIGH, providing additional feedback to $LM393_A$'s positive input via the 1-MΩ resistor.

When the 50-pF capacitor ceases to provide feedback

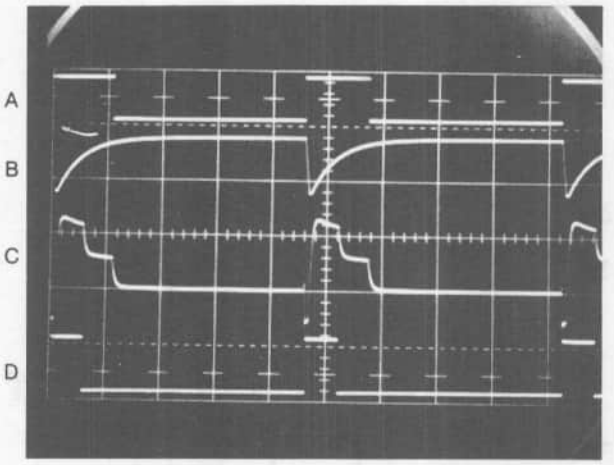

TRACE	VERTICAL	HORIZONTAL
A	10V/DIV	200 μSEC/DIV
B	5V/DIV	200 μSEC/DIV
C	1V/DIV	200 μSEC/DIV
D	5V/DIV	200 μSEC/DIV

Fig 15—The output pulse width *(trace D) of* ***Fig 14****'s monostable circuit is insensitive to the input width (trace A).*

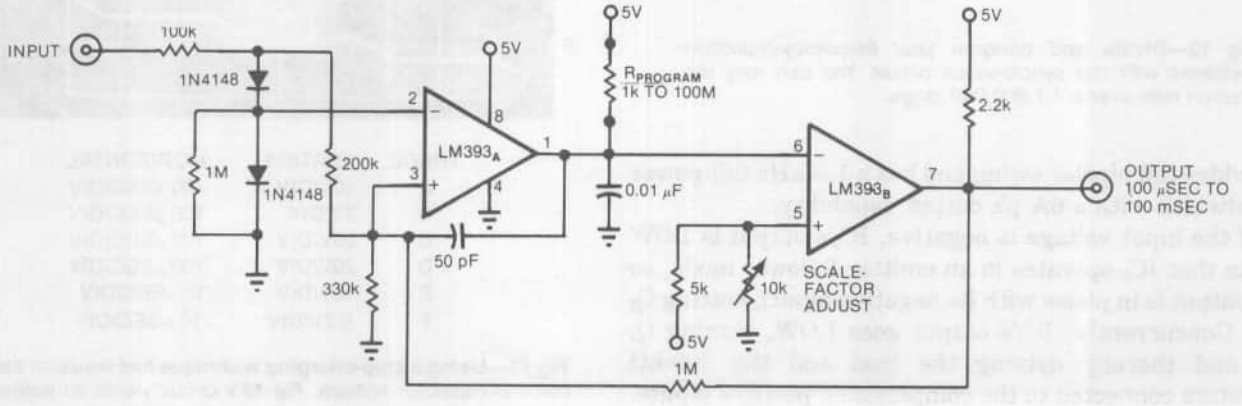

Fig 14—Better than a multivibrator, *this monostable circuit provides a true level-triggered input and a 10,000:1 output pulse range. You program the output pulse width with one resistor.*

Make a better monostable with a 2-comparator IC

to $LM393_A$'s positive input, this comparator's output goes HIGH, allowing the 0.01-μF timing capacitor to charge (**Fig 15,** trace B). When the capacitor voltage exceeds $LM393_B$'s positive input voltage, $LM393_B$'s output (**Fig 15,** trace D) goes LOW, terminating the output pulse.

With the 0.01-μF timing capacitor, you can obtain output pulse widths of 10 μsec to 100 msec, with a scale factor (trimmable with the 10-kΩ potentiometer) of 100Ω/μsec.

Get variable width and delay with one IC

If you need a known-width pulse that's delayed with respect to another pulse, consider the **Fig 16** circuit. It works from one 5V supply and requires only one dual-comparator IC.

When you apply a TTL input (**Fig 17,** trace A), $LM319_A$'s output stays LOW until the 1500-pF capacitor at its positive input charges beyond the negative input's 1.2V level. The resistor-diode clamp from the circuit input to $LM319_A$'s pin 5 provides immunity to input-amplitude variations.

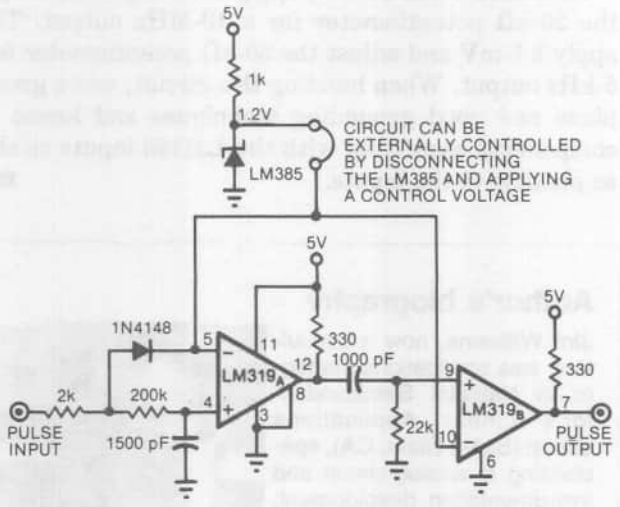

Fig 16—Form a pulse *having the parameters you need from this simple 1-IC circuit. The 1500-pF/200-kΩ network determines delay relative to a triggering pulse; the 1000-pF/22-kΩ differentiator sets the width.*

When $LM319_A$'s output goes HIGH (**Fig 17,** trace B), the transition is coupled via the 1000-pF/22-kΩ differentiator to $LM319_B$'s positive input (**Fig 17,** trace C), causing $LM319_B$'s output to rise and stay HIGH (**Fig 17,** trace D) until the differentiator output drops below the 1.2V level at $LM319_B$'s negative input.

You can tailor both the delay time and the output pulse width to your requirements by altering the values of the RC networks. Alternatively, you can control these parameters externally by applying variable voltages to the comparators' negative inputs.

Make an ultrafast V/F converter

Using two comparator ICs, you can build a V/F converter that yields a 5-kHz to 10-MHz output, with better than ±1% linearity, from a 0 to 5V input. The LM160's 20-nsec propagation delay allows **Fig 18**'s circuit to run much faster than monolithic VFCs.

The LM160's output switches the 50-pF capacitor between a reference voltage (furnished by the LM385) and the comparator's negative input. The comparator's output pulse width is unimportant so long as it permits complete charging and discharging of the capacitor. The LM160 also drives the 5-pF/510Ω network, providing regenerative feedback to reinforce its output transitions.

When this positive feedback decays, any negative-going LM160 output is followed by a positive-going edge after an interval determined by the 5-pF/510Ω time constant (**Fig 19,** traces A and B).

The actual integration capacitor—the 0.01-μF unit—never charges beyond 100 mV because it's constantly reset by charge dispensed from the switched 50-pF capacitor (**Fig 19,** trace C). When the LM160's output goes negative, the 50-pF capacitor takes charge from

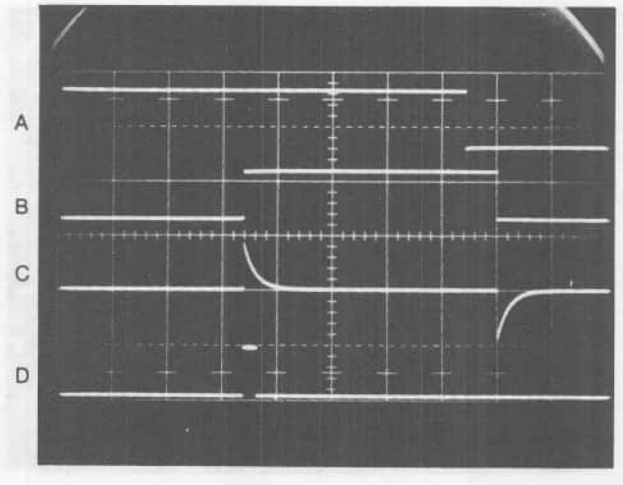

TRACE	VERTICAL	HORIZONTAL
A	5V/DIV	100 μSEC/DIV
B	5V/DIV	100 μSEC/DIV
C	5V/DIV	100 μSEC/DIV
D	5V/DIV	100 μSEC/DIV

Fig 17—A delayed narrow pulse *(trace D) from* **Fig 16**'s *1-IC circuit specs delay and width of 340 and 30 μsec, respectively.*

Two comparator ICs yield a fast, linear VFC

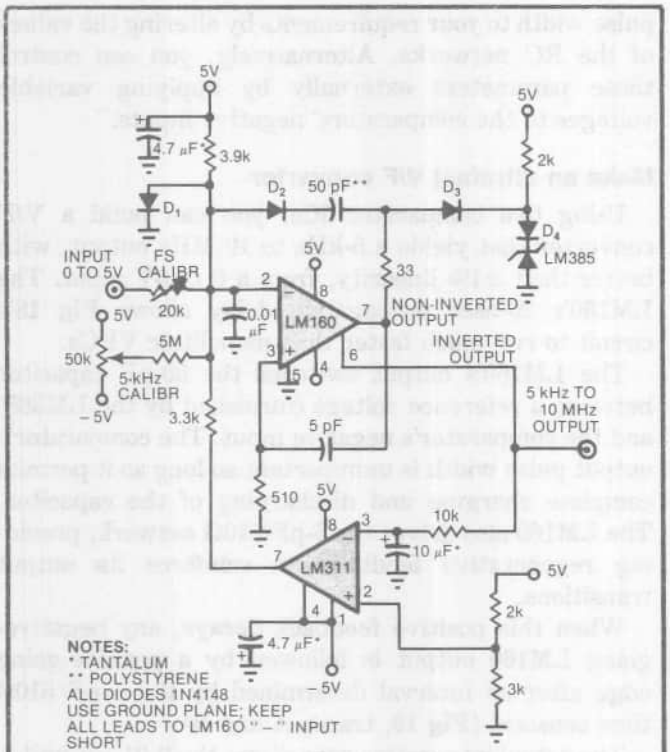

Fig 18—Producing 5-kHz to 10-MHz output, *this V/F-converter circuit uses two comparator ICs and features ±1% linearity. The LM160 is the heart of the converter; the LM311 prevents lockup.*

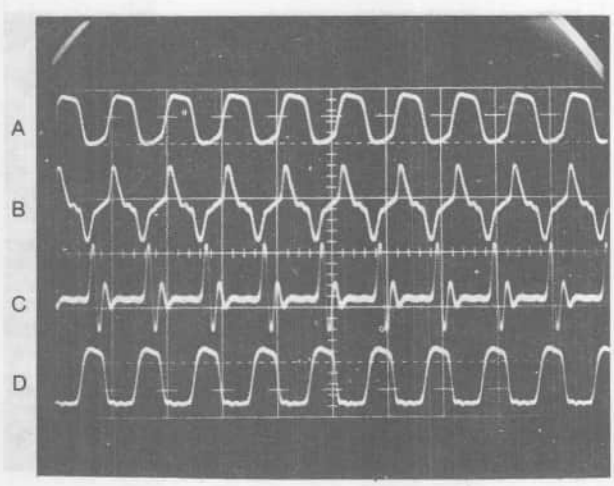

TRACE	VERTICAL	HORIZONTAL
A	5V/DIV	100 μSEC/DIV
B	0.5V/DIV	100 μSEC/DIV
C	10 mA/DIV	100 μSEC/DIV
D	5V/DIV	100 μSEC/DIV

Fig 19—A clean 10-MHz output *(trace D) results from an LM160's action in* **Fig 18***'s V/F converter. Trace C shows the charge-dispensing current from* **Fig 18***'s 50-pF capacitor.*

the 0.01-μF capacitor, resulting in a lower voltage.

The LM160's negative-going output also produces a short negative pulse—via the 5-pF/510Ω feedback—at its positive input. When this negative pulse decays to a point where the positive input is just higher than the negative input, the 50-pF capacitor again receives a charge, and the entire cycle repeats. Diodes D_1 and D_2 compensate for diodes D_3 and D_4, minimizing temperature drift.

The LM160's inverted output (**Fig 19,** trace D) serves as circuit output and also drives the LM311 comparator circuit to prevent LM160 lockup. Without it, any condition (such as startup and input overdrive) that allows the 0.01-μF capacitor to charge beyond its normal operating point could cause the LM160's output to go to the −5V rail and stay there.

The LM311 prevents lockup by pulling the LM160's negative input toward −5V. The 10-μF/10-kΩ network determines when the LM311 switches on. When the VFC runs normally, the 10-μF capacitor charges to a negligibly small voltage, holding the LM311 off. The LM160's inverted output stays HIGH if the VFC stops running (if lockup occurs), forcing the LM311 to turn on and restarting the circuit.

To calibrate the circuit, apply a 5V input and adjust the 20-kΩ potentiometer for a 10-MHz output. Then apply 2.5 mV and adjust the 50-kΩ potentiometer for a 5-kHz output. When building this circuit, use a ground plane and good grounding techniques and locate the components associated with the LM160 inputs as close as possible to the inputs. **EDN**

Author's biography

Jim Williams, now a consultant, was applications manager in National Semiconductor's Linear Applications Group (Santa Clara, CA), specializing in analog-circuit and instrumentation development, when this article was written. Before joining the firm, he served as a consultant at Arthur D Little Inc and directed the Instrumentation Development Lab at the Massachusetts Institute of Technology. A former student of psychology at Wayne State University, Jim enjoys tennis, art and collecting antique scientific instruments in his spare time.

Use off-the-shelf linear ICs for sophisticated audio designs

With a little creativity and a good understanding of common linear circuits, you can produce high-performance audio designs—such as V/F converters, VCAs, preamps and panning circuits—with simple, inexpensive parts.

Jim Williams, National Semiconductor Corp

Op amps can serve in applications other than audio amplifiers; you can apply them and other off-the-shelf linear ICs to create more sophisticated audio and electronic-music circuits. And although these applications present stringent performance demands, don't assume you'll need excessively complicated and expensive designs; the linear circuits described here achieve high performance at low cost.

As an example of the unusual use of conventional components, consider **Fig 1**'s exponential V/F converter. Suitable for use in music synthesizers, this circuit provides an output that changes its frequency one octave in response to a 1V control-input variation. Similar to conventional nonlinear converters, it exploits

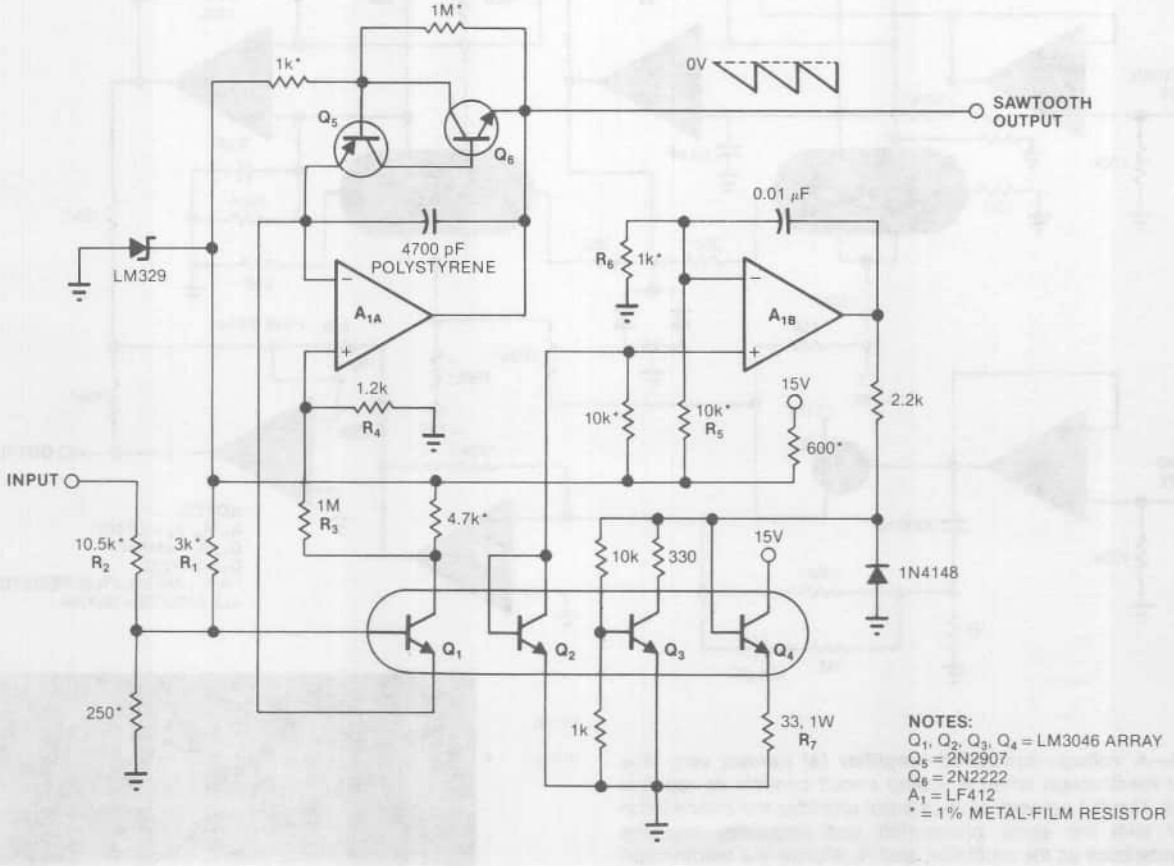

Fig 1—A temperature-compensated transistor array *stabilizes this exponential voltage-to-frequency converter. Q_2 senses the array's temperature and A_{1B} drives chip heater Q_4, maintaining a stable operating environment for logarithmic converter Q_1. The circuit's negative-going sawtooth output results from A_1's integration of Q_1's collector current until it reaches Q_5 and Q_6's threshold.*

A servo loop eliminates temperature-dependent drift

the logarithmic relationship between a transistor's base-emitter voltage and collector current. However, a unique thermal servo loop eliminates temperature-dependent transfer-function errors.

Generating the circuit's negative-going sawtooth output, op amp A_{1A} integrates Q_1's collector current until Q_5 and Q_6 turn on. These feedback transistors then discharge the integrating capacitor, the output rises to 0V and the cycle repeats.

Q_1 is a vital element in this circuit because its V_{BE}/I_C characteristics ensure that A_{1A}'s input current—and thus the output frequency—remain an exponential function of the control voltage. Assisting Q_1, transistors Q_2, Q_3, Q_4 and op amp A_{1B} form a temperature-controlled loop that stabilizes Q_1's operating point by thermally compensating the LM3046 transistor array.

To perform this compensation, Q_2's base-emitter junction senses array temperature, and Q_4 heats the chip. A_{1B} varies this heater transistor's dissipation until Q_2's V_{BE} drop equals the reference level set by R_5 and R_6. Furthermore, Q_3 and R_7 limit Q_4's maximum operating power and ensure proper servo functioning during circuit power-up.

In addition to stabilizing Q_1's collector bias, the LM329 6.9V reference also fixes the Q_5/Q_6 firing point. These two transistors exhibit opposing temperature coefficients, so their switching threshold is compensated to approximately 100 ppm/°C. The polystyrene integrating capacitor's −120-ppm/°C TC cancels remaining firing-level uncertainty.

To establish a 20-Hz quiescent output frequency, R_1 biases the circuit's input. R_2 trims the converter's transfer gain. Op-amp input resistors R_3 and R_4 maintain exponential conformity to within 0.5% from 20 Hz to 15 kHz by providing first-order compensation for Q_1's bulk emitter resistance.

Reduce VCA feedthrough

The next circuit, a voltage-controlled amplifier (VCA), also uses a simple error-correction scheme to improve its performance (**Fig 2**). Commonly employed

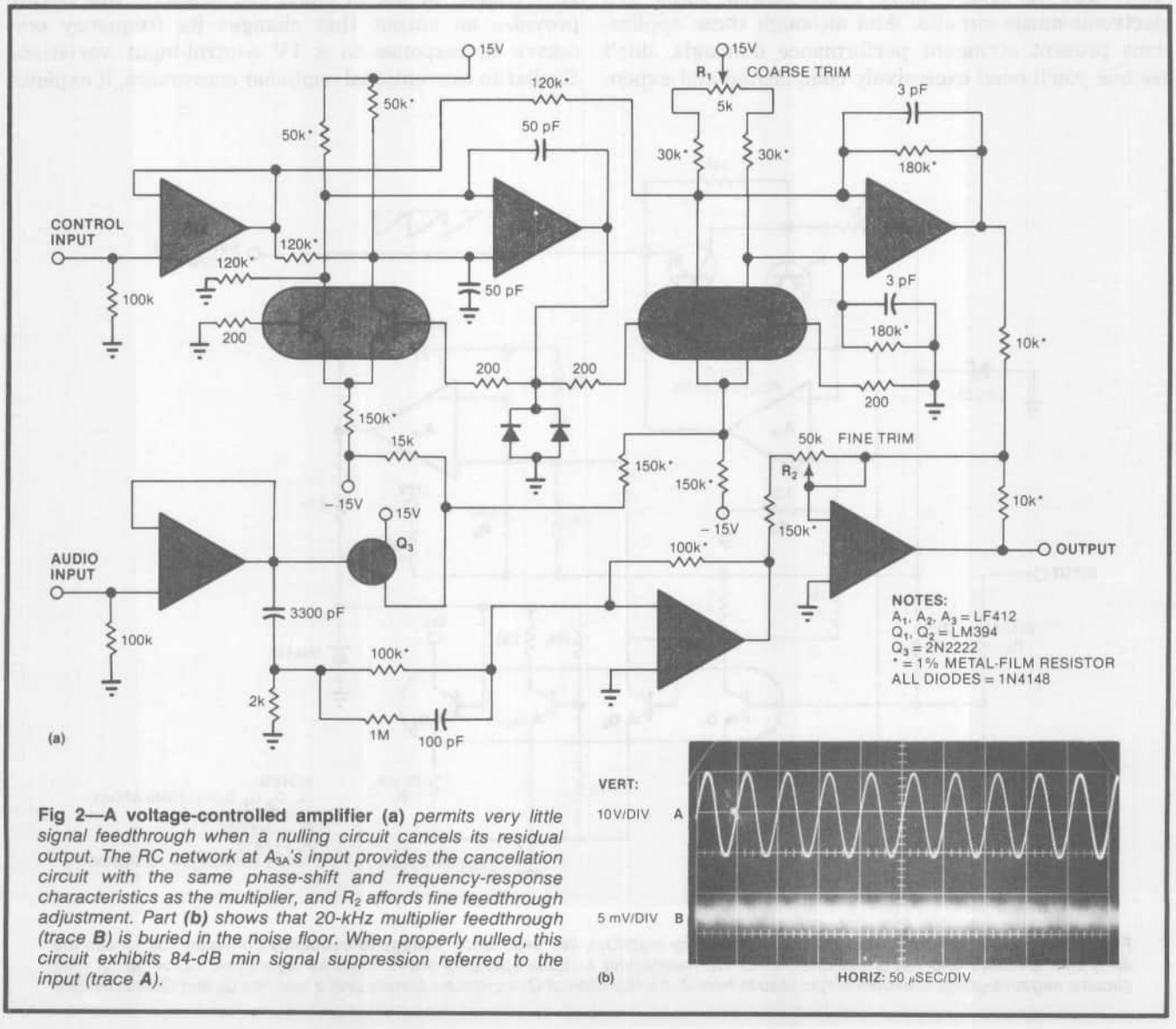

Fig 2—A voltage-controlled amplifier (a) *permits very little signal feedthrough when a nulling circuit cancels its residual output. The RC network at A_{3A}'s input provides the cancellation circuit with the same phase-shift and frequency-response characteristics as the multiplier, and R_2 affords fine feedthrough adjustment. Part* **(b)** *shows that 20-kHz multiplier feedthrough (trace* **B***) is buried in the noise floor. When properly nulled, this circuit exhibits 84-dB min signal suppression referred to the input (trace* **A***).*

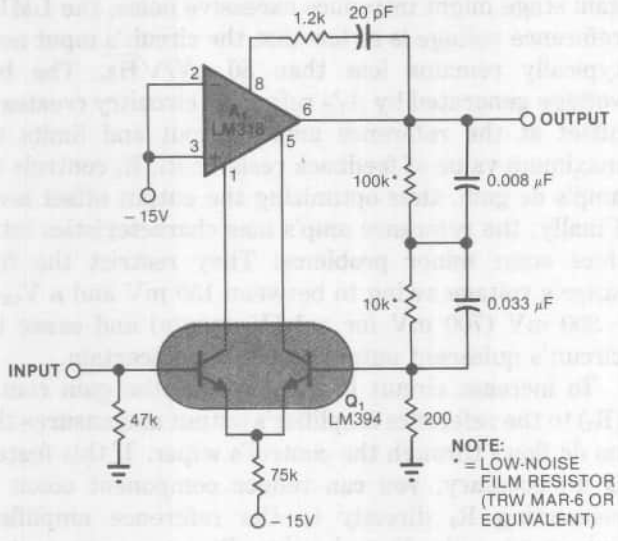

Fig 3—Lower input noise *results when an external transistor pair replaces the first stage of an op amp. This design avoids the loop-instability problems often caused by adding external stages to an op amp because the additional transistors replace rather than complement the LM318's input devices.*

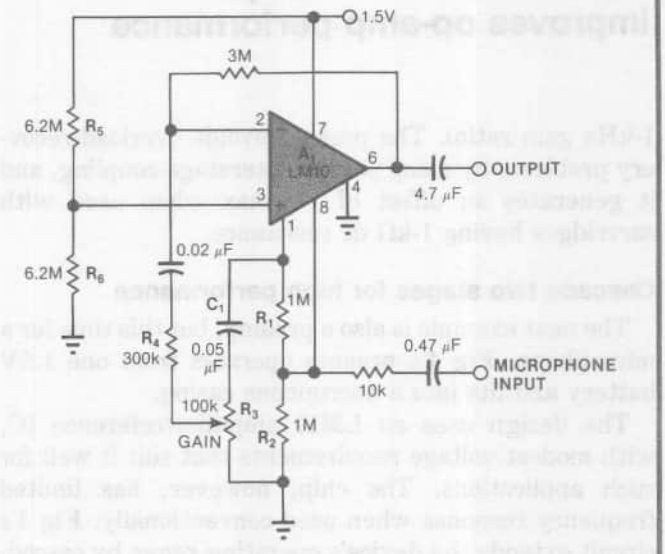

Fig 4—This microphone preamp *operates from supplies as low as 1.5V. Its LM10 reference amplifier provides a voltage gain of 100 with an input noise level of less than 50 nV/√Hz. The chip's op-amp section amplifies the reference output by an additional 20 dB.*

in recording-studio mixing consoles, VCAs must permit minimal signal feedthrough when their control inputs reach 0V. Conventional analog multipliers aren't optimal for this application; although they behave well in high-gain regions, they afford inadequate high-frequency signal suppression with their control channels off.

To reduce the feedthrough levels of its simple VCA, **Fig 2a**'s design uses a nulling technique. Op amps A_{1A} and A_{1B} and emitter-follower Q_3 buffer the circuit's control and audio inputs and then feed these signals to a transconductance multiplier composed of A_{2A}, Q_1 and Q_2. A_{2B} converts Q_2's differential collector currents to a single-ended audio output. R_1 allows coarse feedthrough trimming at 10 kHz to approximately −65 dB (relative to the input signal level).

To further reduce feedthrough, A_{3A} and A_{3B} null the multiplier's OFF-state output with the audio input. The RC network at inverter A_{3A}'s input provides phase shift and frequency response similar to the multiplier's feedthrough characteristics—thus, residual signals cancel out when A_{3B} combines the outputs from A_{3A} and A_{2B}. The nulling circuit's gain control, R_2, allows fine feedthrough trimming to −84 dB at 20 kHz.

To adjust this VCA, apply a 20V p-p, 20-kHz sine wave to the audio input, and with the control input grounded, adjust R_1 for minimum output from A_{2B}. Then trim R_2 for the lowest level at A_6's output. **Fig 2b** illustrates the circuit's typical feedthrough signal (trace **B**) for a 20-kHz input (trace **A**) when properly trimmed. Note that circuit noise almost obscures the waveform.

In addition to its excellent feedthrough suppression, this VCA exhibits only 0.05% total harmonic distortion (THD) throughout its 60-kHz power bandwidth. To obtain best circuit performance, construct it on a rigid circuit board, enclose it in a well-shielded box and employ proper grounding and noise reduction.

Replace an op amp's inputs

Instead of correcting a circuit's inherent errors as in the previous designs, you can use your knowledge of an IC's internal workings to eliminate deficiencies before they occur. For example, **Fig 3** illustrates an RIAA-equalized phono preamp with a noise figure less than 2 dB typ; it uses an LM394 ultralow-noise transistor pair at an LM318's compensation inputs instead of the device's internal input transistors.

This technique achieves lower noise than the unaltered op amp without introducing loop instability. Stability criteria become especially critical in RIAA circuits because the equalization function requires 100% feedback at high frequencies. Connecting the op amp's unused inputs to the negative supply shuts off the device's first differential pair and allows the external devices to operate into the LM318's output stages.

The distortion performance of **Fig 3**'s circuit exceeds the measurement capability of most test equipment: THD within the audio band remains less than 0.002% for outputs to 0.1V rms, and 20-kHz distortion rises only to 0.007% at 5V rms. Referred to a 10-mV input, the preamp's noise level equals −90 dB, with absolute values measuring 0.55 μV and 70 pA rms over a 20-kHz bandwidth—levels below the noise generated by most phono cartridges.

Fig 3's phono preamp also performs well in transient-intermodulation (TIM) tests. When fed with a 200-mV input—consisting of 10- and 11-kHz sine waves equally mixed—the circuit generates a 1-kHz output of only 80 μV. The TIM level, therefore, is 0.004% (or 0.0008% if you include the RIAA function's 14-dB (5:1) 10- to

An external transistor pair improves op-amp performance

1-kHz gain ratio). The preamp avoids overload-recovery problems by using only dc interstage coupling, and it generates an offset of 1V max when used with cartridges having 1-kΩ dc resistance.

Cascade two stages for high performance

The next example is also a preamp, but this time for a microphone. **Fig 4**'s preamp operates from one 1.5V battery and fits into a microphone casing.

The design uses an LM10 amplifier/reference IC, with modest voltage requirements that suit it well for such applications. The chip, however, has limited frequency response when used conventionally. **Fig 4**'s circuit extends the device's operating range by cascading its reference amplifier and op amp to form a high-gain preamp.

Here are the details. The microphone input drives A_1's reference amplifier, which has a unity-gain bandwidth of 500 kHz. Feedback around this stage yields an ac voltage gain of 100. The op amp, which operates more slowly than the reference amp, provides an additional 20 dB of voltage amplification, resulting in overall circuit gain of 60 dB. The preamp's bandwidth extends to 10 kHz unloaded and reaches 5 kHz with a 500Ω load.

Although using a reference amplifier as a low-level gain stage might introduce excessive noise, the LM10's reference voltage is so low that the circuit's input noise typically remains less than 50 $nV/\sqrt{Hz}$. The bias voltage generated by A_1's reference circuitry creates an offset at the reference amp's output and limits the maximum value of feedback resistor R_1. R_2 controls the amp's dc gain, thus optimizing the output offset level. Finally, the reference amp's bias characteristics introduce some minor problems: They restrict the first stage's voltage swing to between 150 mV and a V_{CC} of −800 mV (700 mV for a 1.5V supply) and cause the circuit's quiescent output to become uncertain.

To increase circuit life, C_1 couples the gain control (R_3) to the reference amplifier's output and ensures that no dc flows through the control's wiper. If this feature is unnecessary, you can reduce component count by connecting R_4 directly to the reference amplifier's output (A_1, pin 1) and using R_1 as a gain control. However, the 70-nA bias current that normally flows through the feedback resistor might increase noise.

DAC pans audio signal

Another approach to solving audio-design problems involves multiplying DACs. **Fig 5** shows a digitally programmable panning circuit that splits an input between two output channels. The DAC input code (D) determines the relative levels of the two channels, and op amps A_{1A} and A_{1B} convert the DAC's complementary current outputs into voltages. The relationship of the

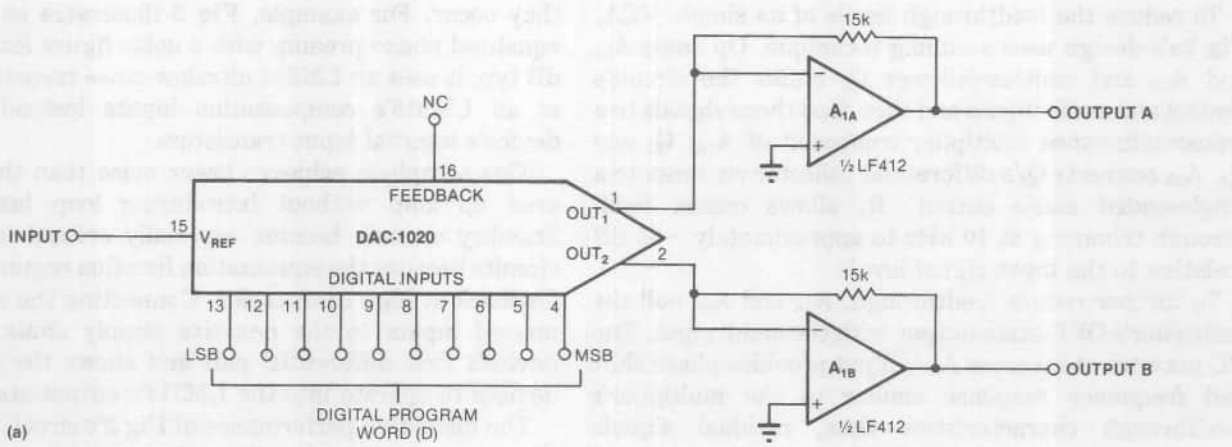

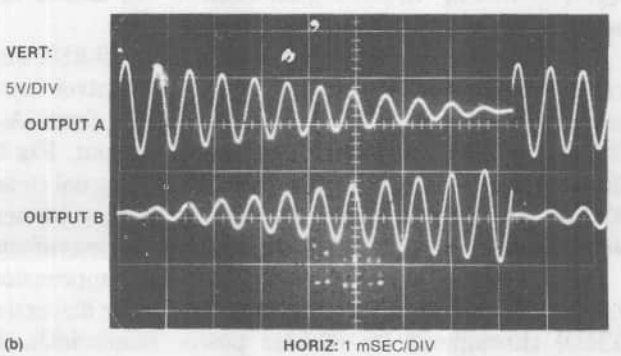

Fig 5—A DAC controls the ratio of two output signals *in the pan-pot circuit shown in* ***(a)****. Op amps A_{1A} and A_{1B} convert the DAC's complementary output currents to voltage signals. The ratio of the pan pot's outputs* ***(b)*** *changes as a digital ramp drives the DAC input. The sum of the two signals remains constant, regardless of the digital control word.*

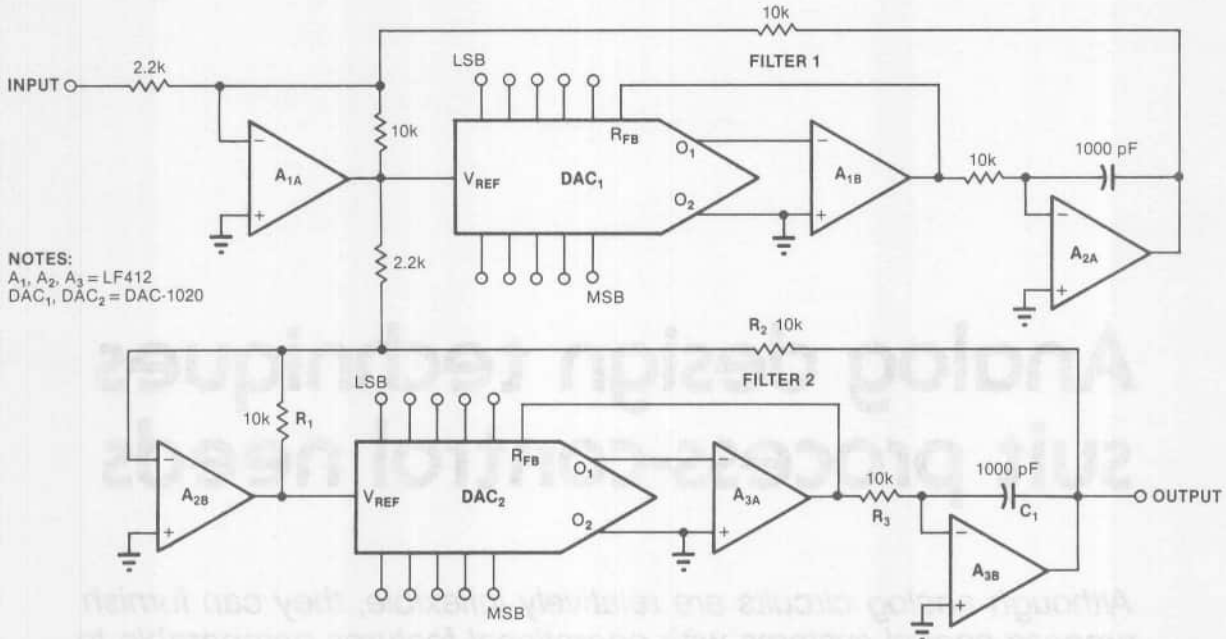

Fig 6—Two DACs control the passband *of this first-order filter. The input codes determine the gains of integrators A_{2A} and A_{3B}.*

two output signals to the digital input in **Fig 5**'s design is given by:

$$\text{OUTPUT A} = -\left[\text{INPUT} \times \left(\frac{3D}{2048}\right)\right],$$

$$\text{OUTPUT B} = -\left[\text{INPUT} \times \frac{3(1024 - D)}{2048}\right]$$

and **Fig 5b** illustrates the circuit's operation when a digital ramp controls the DAC inputs.

This circuit differs from conventional DAC applications because the converter's internal feedback resistor remains unconnected; the circuit's discrete resistors permit better matching of the output channels. Each op amp exhibits 300-ppm/°C gain drift arising from mismatches between the DAC's ladder resistors and op-amp feedback elements. You can eliminate these small errors, though, by using a separate DAC, with complementary digital inputs, for each channel.

You can also employ DACs in programmable-audio-filter designs. **Fig 6**'s circuit, a first-order bandpass network, utilizes two identical state-variable filters. The DACs control the gains of integrators A_{2A} and A_{3B} and thus determine the filters' cutoff frequencies.

You achieve a bandpass characteristic by connecting the first filter's high-pass output (taken from the output of A_{1A}) to the second filter's input. Filter 2's low-pass output then contains only those signals that lie within the passband established by the DACs' input codes.

You can determine filter 2's low-pass cutoff frequency (f_C) as a function of DAC_2's program input (D) with

$$f_C = \frac{R_1}{R_2}\left[\frac{D}{2048\pi R_3 C_1}\right].$$

For **Fig 6**'s components,

$$f_C = \frac{D}{2048\pi(10k)(1 \times 10^{-9})}.$$

Filter 1's high-pass output function equals the derivative of the low-pass expression **(reference)**. **EDN**

Reference

Analog Devices Inc, *Application Guide to CMOS Multiplying D/A Converters*, 1978, pg 32.

Author's biography

Jim Williams, applications manager of National Semiconductor's Linear Applications Group (Santa Clara, CA), specializes in instrument development and analog circuit design. Before joining National, he served as a consultant at Arthur D Little Inc and ran the Instrumentation Development Lab at the Massachusetts Institute of Technology. A former student of psychology at Wayne State University, Jim lists spare-time interests that include tennis, art and collecting antique scientific instruments.

Analog design techniques suit process-control needs

Although analog circuits are relatively inflexible, they can furnish process-control systems with operational features comparable to those attainable using digital methods. A stepper-motor pump-drive application illustrates the techniques involved.

Jim Williams, National Semiconductor Corp

For many process-control applications, analog control circuits prove a better choice than their digital counterparts, especially when you expect low product volumes and when fast design time and high noise immunity are design priorities. In fact, if you're working with well-defined operational specifications and don't anticipate having to make major modifications, analog methods serve as viable alternatives to intelligent but dedicated and expensive hardware/software approaches.

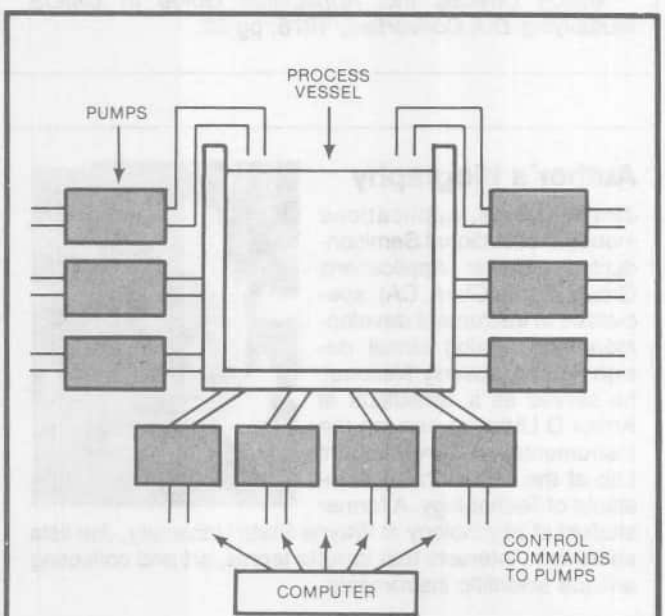

Fig 1—In this conceptual computer-controlled chemical-mixing system, *the computer governs several pumps delivering chemicals to the process mixing vessel by periodically sending updated pulse-width-modulated commands that control the pumps' speeds.*

Controlling a pump's speed

To demonstrate, this article describes the design of an analog pump controller that manipulates computer-generated command pulses to regulate stepper-motor-driven pumps in a critical chemical-mixing process. The controller/pump system furnishes precise fluid delivery at both fast and slow rates, a requirement often arising in chemical and biological process-control systems, which demand high pumping rates for flushing or process startup and slow but accurate flow rates for mixing precise amounts of liquid. Although dc motors can deliver adequate high-speed performance, they often need complex and expensive digital control to perform well at very slow speeds. In contrast, exponentially driven stepper motors can easily handle a pump's conflicting high- and low-speed drive requirements.

Fig 1 diagrams a computer-driven system that governs several pumps feeding an intricate chemical process. The computer controls each pump's speed by periodically sending a pulse-width-modulated control command. Because the computer runs in a time-shared manner, each pump controller must retain the last received pulse width's value.

In this application, each pump gets speed-updated every 30 sec by a 50- to 1000-msec pulse. The pump drive must provide optimum speed-setting resolution for the low-speed ranges to provide increasingly slower

flow rates as the system approaches crucial mixing conditions. And the controller must possess a high degree of noise immunity to prevent spurious noise-induced responses from degrading process quality.

Fig 2 illustrates a μP-based-controller scheme. In this arrangement, the computer delivers an input pulse that gates a clock. The clock in turn serially loads a bank of parallel counters that determine the input pulse width. The counters address a processor section that converts input data to a frequency output, using an exponential transfer function—a nonlinear response that achieves the required high resolution (precise liquid delivery) at slow pump speeds. Finally, the frequency output activates a stepping-motor driver that runs the pump.

On the surface, this digital controller's operation appears relatively simple. However, the application masks some tricky design problems. For example, the lengthy period between speed updates, coupled with the need to avoid erroneous pump responses, mandates careful power-supply design, including provision of such functions as RFI filtering, memory battery backup and self-checking software.

In addition, the need for a high-resolution, smoothly varying frequency-output function demands careful design attention to how the processor synthesizes its

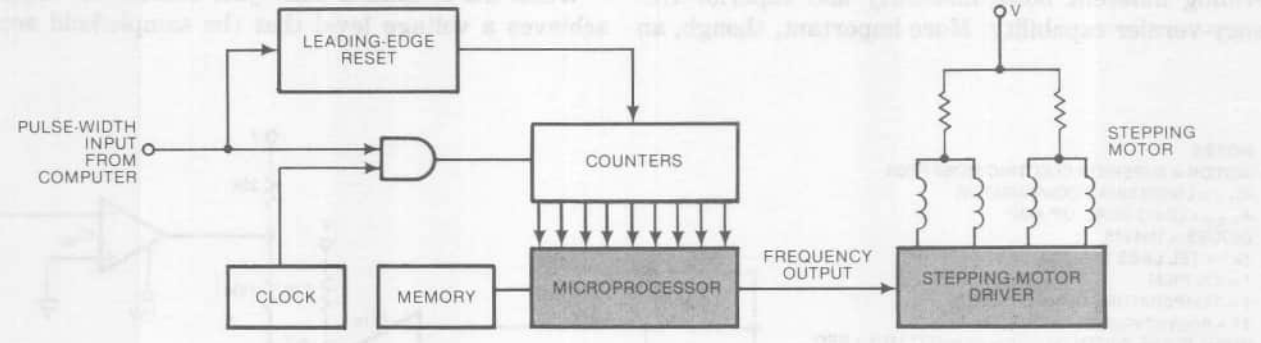

Fig 2—Upon receiving gated pulses, *a μP converts timed computer data into a frequency output, using an exponential transfer function. This nonlinear response results in the necessary high-resolution-at-low-speed characteristics for accurately controlling pump operation with a stepper-motor driver. The problems that can arise with this digital approach to controlling* **Fig 1***'s mixing system include noise sensitivity, memory-retention difficulties and an undesirable quantized frequency-shift characteristic.*

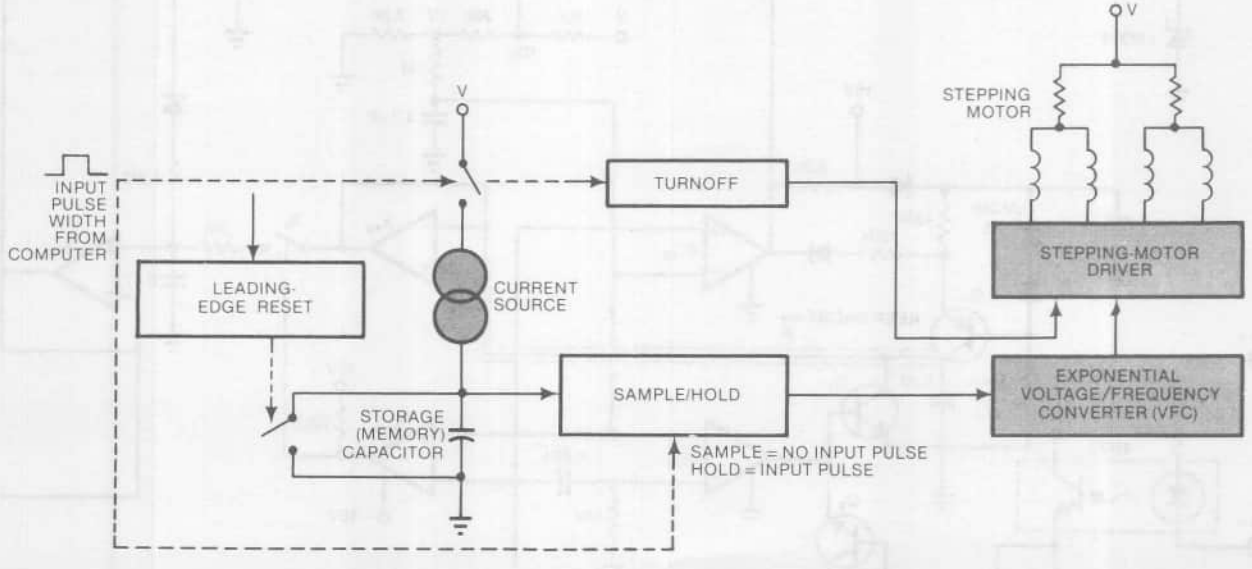

Fig 3—In this analog-pump-controller approach, *a computer's command pulses direct a current source, which in turn charges a storage capacitor that provides noise-immune analog-data retention. When the command pulse ceases, the sample/hold amp receives the capacitor's stored voltage and delivers it to the exponential voltage-to-frequency converter (VFC). The VFC activates the stepper-motor driver in a continuous, smooth manner; the turn-off stage deactivates the motor driver.*

Analog functions prove adequate in simple process-control tasks

output. Although these problems are amenable to solution, they complicate the controller's design and entail lengthy development time and high cost.

Take the analog route

Considering the task's conceptual simplicity, however, reveals a clear edge for an analog-control approach to satisfying this application's critical requirements. A turnkey system, it needs little intelligence or flexibility and can employ a straightforward data-retention structure. And although the digital μP-based approach can also meet these requirements, it involves substantial hardware and software overhead to overcome noise-immunity and frequency-shift-resolution problems.

The analog-based design surmounts these obstacles, providing inherent noise immunity and superior frequency-vernier capability. More important, though, an analog approach eliminates the intensive software effort required by μP-based methods. As a matter of record, the analog pump-controller design was conceived, breadboarded and released for production in just 4 wks—and at a cost competitive with an alternative μP-based method.

Fig 3 depicts the analog system. In this scheme, a capacitor furnishes memory storage. An exponentially responding voltage-to-frequency converter (VFC) fulfills the function of **Fig 2**'s processor. In operation, the computer's command pulse gates a current source that linearly charges the storage capacitor. While the capacitor is charging, the sample/hold stage enters Hold mode, blocking the capacitor's ramping action from the VFC.

When the command pulse just ceases, the capacitor achieves a voltage level that the sample/hold accepts

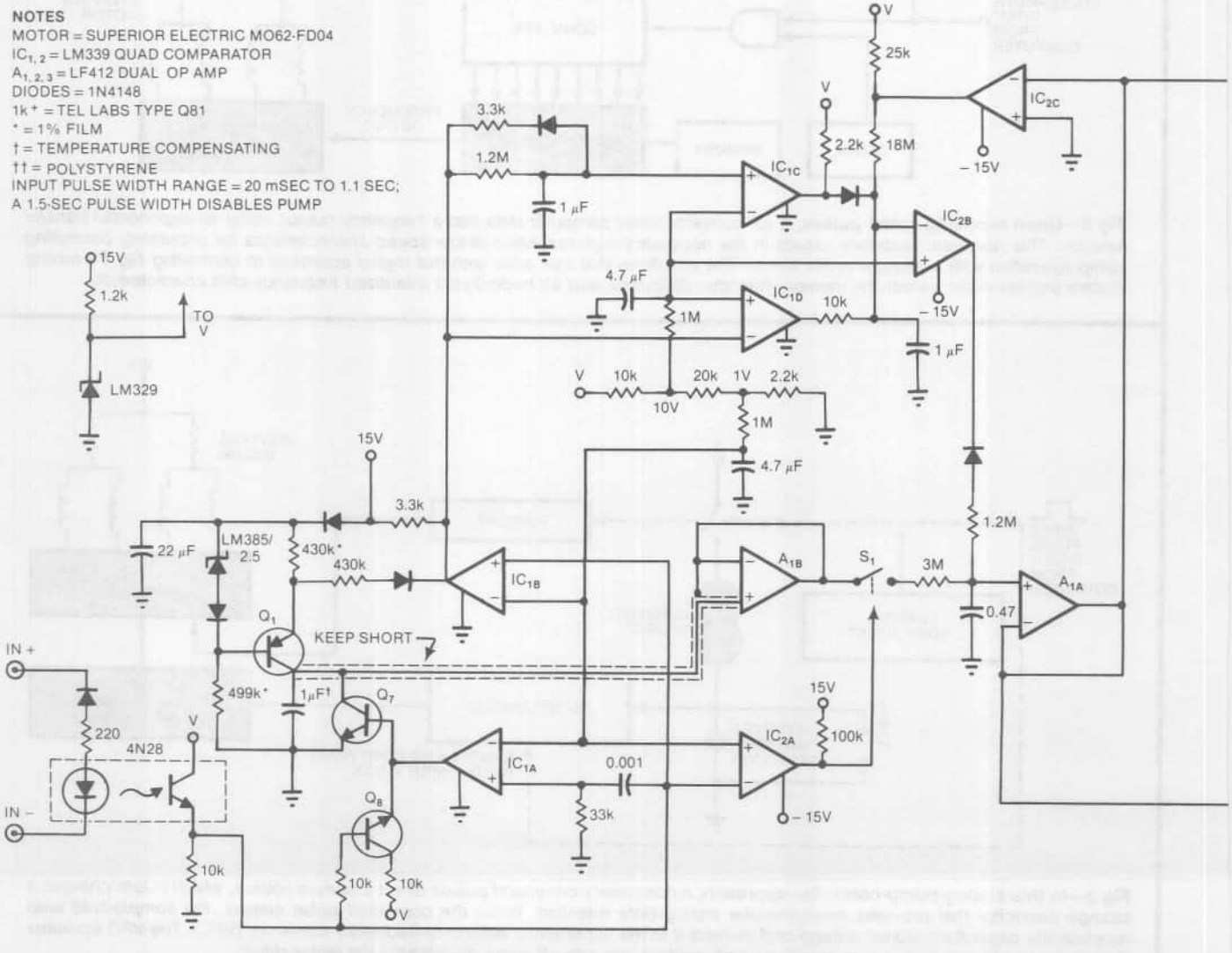

and feeds to the VFC. By issuing an extremely wide pulse, the computer actuates the turn-off stage, which deactivates the stepper-motor drive.

Optoisolation eliminates noise

Fig 4 shows the analog pump controller's schematic diagram. To initiate circuit action, the computer sends an input pulse to the 4N28 optoisolator, which eliminates noise-pickup-induced ground-loop and data-line problems. Appearing at its emitter, the optoisolator's output (**Fig 5,** waveform A) goes to IC_{1A} and IC_{1B}. IC_{1A}'s differentiator setup—a 0.001-μF/33-kΩ combination—generates a short pulse (**Fig 5,** waveform B) that biases Q_7. This transistor in turn resets its associated 1-μF capacitor (**Fig 5,** waveform C).

Note that Q_8's emitter supplies the current to base-bias Q_7 ON because IC_{1A} is an open-collector device. In turn, Q_8 receives its base bias from the optoisolator, which provides a drive output only when a command pulse appears at the controller circuit's input. Consequently, in the highly unlikely event that a severe noise disturbance causes IC_{1A}'s output to rise, Q_7 still doesn't receive a drive pulse, and its 1-μF capacitor does not get reset.

The 1-MΩ/4.7-μF filter, which feeds IC_{1A}'s minus input, provides additional noise immunity by ensuring a stable trip point during noise disturbances. The optoisolator's output also goes to IC_{1B}, which gates the Q_1 current source. When Q_7 turns off, its 1-μF capacitor immediately starts to ramp up (**Fig 5,** waveform C). (Circuit-operation speed in **Fig 5** has been increased to provide optimum waveform photographs.) Then, the A_{1B} follower unloads the capacitor.

Diode/capacitor decoupling of Q_1 assures high noise

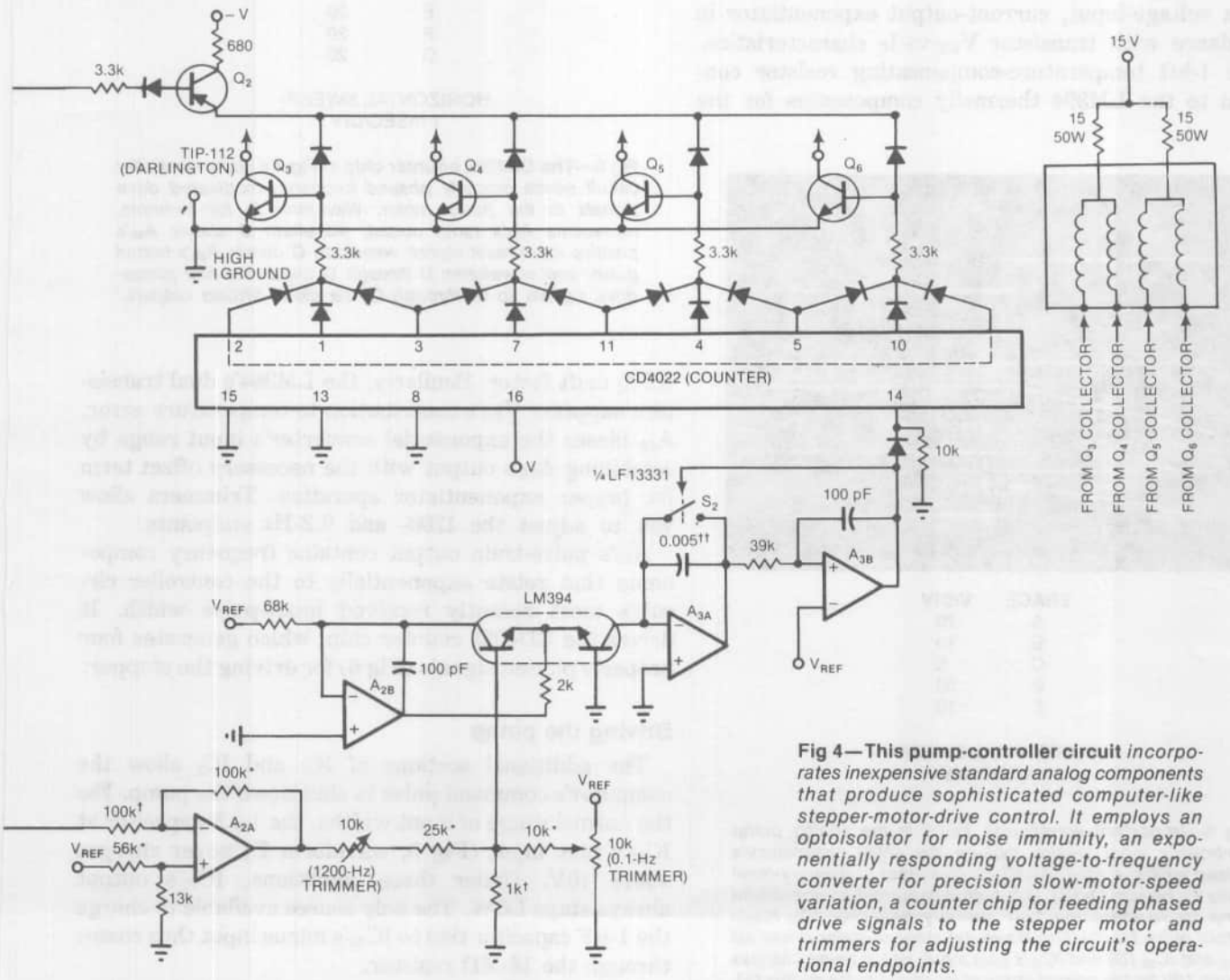

Fig 4—This pump-controller circuit *incorporates inexpensive standard analog components that produce sophisticated computer-like stepper-motor-drive control. It employs an optoisolator for noise immunity, an exponentially responding voltage-to-frequency converter for precision slow-motor-speed variation, a counter chip for feeding phased drive signals to the stepper motor and trimmers for adjusting the circuit's operational endpoints.*

A voltage-to-frequency converter controls stepper-motor drive

rejection, even for supply dropouts, during the capacitor's ramp time. During ramping, IC_{2A}'s output stays LOW and shuts off S_1. This switch maintains A_{1A}'s output at a dc level. When the controller's input pulse ceases, IC_{1B}'s output goes LOW and disables Q_1. The integrating 1-μF capacitor therefore stops charging. Concurrently, IC_{2A}'s output goes HIGH and closes S_1. As a result, A_{1A}'s output changes to the capacitor's newly acquired level. Located in A_{1A}'s input section, the 3-MΩ/0.47-μF filter provides a time constant that limits the stepper motor's acceleration rate, thereby preventing stalling.

Try an exponentiator

Op amp A_{1A}'s output feeds the A_2-A_3 configuration, which forms an exponentially responding VFC that controls the input current to the A_{3A}-A_{3B} integrator-comparator-type oscillator stage. To accomplish this function, A_{2B} and the LM394's dual transistors constitute a voltage-input, current-output exponentiator in accordance with transistor V_{BE}-vs-I_C characteristics.

The 1-kΩ temperature-compensating resistor connected to the LM394 thermally compensates for the KT/Q drift factor. Similarly, the LM394's dual transistors suppress V_{BE}'s contribution to temperature error. A_{2A} biases the exponential converter's input range by combining A_{1A}'s output with the necessary offset term for proper exponentiator operation. Trimmers allow you to adjust the 1200- and 0.2-Hz endpoints.

A_{3B}'s pulse-train output contains frequency components that relate exponentially to the controller circuit's most recently received input-pulse width. It drives the CD4022 counter chip, which generates four properly phased signals (**Fig 6**) for driving the stepper.

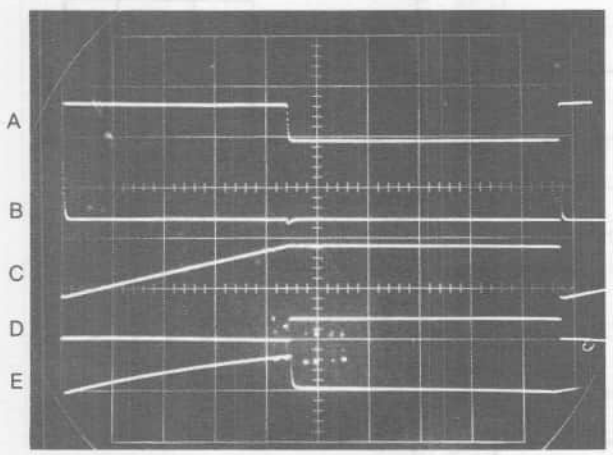

TRACE	V/DIV
A	20
B	10
C	5
D	50
E	10

HORIZONTAL SWEEP-
1 mSEC/DIV

Fig 5—Important waveforms *found in the analog pump controller's input section include the 4N28 optoisolator's pulsed emitter output* ***(A)****, IC_{1A}'s plus input or memory-reset spike for biasing Q_7* ***(B)****, Q_7's output or current-source-driven ramp for resetting the 1-μF memory capacitor* ***(C)****, IC_{1D}'s output pulse for shutting down the stepper-motor driver via IC_{2B} and IC_{2C}* ***(D)*** *and IC_{1C}'s plus input, which never charges above 10V for the normal range of incoming pulse widths* ***(E)****.*

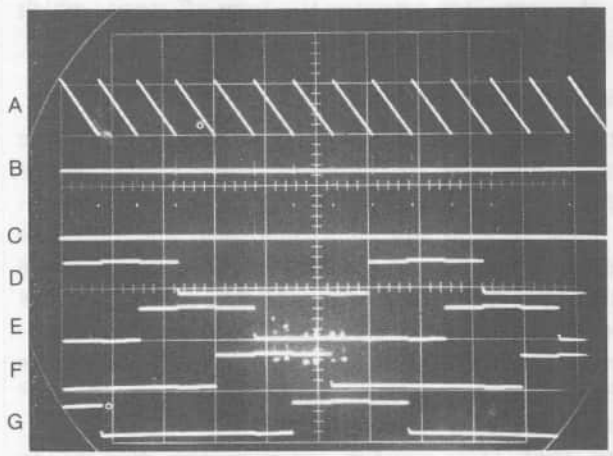

TRACE	V/DIV
A	5
B	50
C	20
D	20
E	20
F	20
G	20

HORIZONTAL SWEEP-
1 mSEC/DIV

Fig 6—The CD4022 counter chip *in* ***Fig 4****'s pump-controller circuit sends properly phased frequency-modulated drive signals to the pump motor. Waveform* ***A****, for example, represents A_{3A}'s ramp output; waveform* ***B*** *shows A_{3B}'s positive input reset signal; waveform* ***C*** *details A_{3B}'s output pulse; and waveforms* ***D*** *through* ***G*** *depict the four phase-drive signals to Q_3 through Q_6 via diode-ANDed outputs.*

Driving the pump

The additional sections of IC_1 and IC_2 allow the computer's command pulse to shut down the pump. For the normal range of input widths, the 1-μF capacitor at IC_{1C}'s plus input (**Fig 5**, waveform E) never charges above 10V. Under these conditions, IC_{1C}'s output always stays LOW. The only source available to charge the 1-μF capacitor tied to IC_{2B}'s minus input thus comes through the 18-MΩ resistor.

However, during normal operation, A_{1A}'s output remains positive, ensuring that IC_{2B}'s negative input

Use an optoisolator to eliminate noise effects

stays that way. This condition forces IC_{2B}'s open-collector output to float. If the controller circuit receives an input pulse substantially wider than the normal maximum, therefore, IC_{1C}'s input charges above 10V. This action quickly dumps a large charge into IC_{2B}'s 1-μF capacitor, forcing its voltage level to rise to the negative rail. This value pulls A_{1A}'s input negative, turns on Q_2 and cuts off all drive signals to the output transistors (Q_3 to Q_6).

A_{1A}'s negative output also feeds back to IC_{2C}, driving that device's output positive. This output supplies a continuous topping-off current to IC_{2B}'s input capacitor. The connection completes a positive feedback latch, which prevents the pump from operating until the counter receives a pulse width within the controller circuit's normal range. IC_{1D} functions to clear out the IC_{2B} capacitor's charging action (**Fig 5,** waveform D) as each new command pulse arrives.

The time constant associated with A_{1A}'s input section lets the controller circuit examine each received pulse and never disables this clamping performance unless the pulse width resides within established limits. Although the latch's positive feedback doesn't require the computer to send successive shutdown instructions to the pump, the controller circuit ensures that the pump's motor can't be energized, even briefly, if successive turn-off-length pulses appear. **EDN**

Author's biography

Jim Williams, now a consultant, was applications manager with National Semiconductor's Linear Applications Group (Santa Clara, CA) when he wrote this article. Before working at National, he was employed by Arthur D Little Inc and the Instrumentation Development Lab at the Massachusetts Institute of Technology. A former student of psychology at Wayne State University, Jim enjoys tennis, art and collecting antique scientific instruments in his spare time.

Apply sample-and-hold techniques for elegant design solutions

More than just a data-acquisition device, a S/H amplifier can also simplify—indeed, make possible—other circuit designs. The applications presented here provide a sampling of ideas ranging from data-link eavesdropping to oven control.

Jim Williams, National Semiconductor Corp

Most designers regard sample/hold amplifiers merely as system components utilized in high-speed data-acquisition work. But they should also consider S/H devices' possibilities as circuit-oriented building blocks.

Sampling techniques can implement circuit functions that are sophisticated in performance, low in cost and not easily realized with other approaches. The designs presented here illustrate a few of the many application possibilities for S/H amplifiers as circuit elements.

Stop fiber-optic eavesdropping

Fig 1 depicts a design that detects attempts to tap a fiber-optic data link. Because the circuit works with pulse-encoded data formats, it detects only short-term changes in the fiber-optic cable's loss characteristics. Thus, long-term changes arising from temperature variations or component aging won't trigger the alarm, but any unauthorized data extraction—a short-term phenomenon—will.

Under normal operating conditions, because the input light pulse's amplitude is constant, so is the level detected by photodiode D_1 and amplified by A_6. A_6's constant-amplitude output pulses are sampled by the S/H amplifier, A_3, which is driven by a delayed S/H pulse generated by A_1 and A_2. (Delaying the sampling ensures that A_6's output settles completely.) Unless

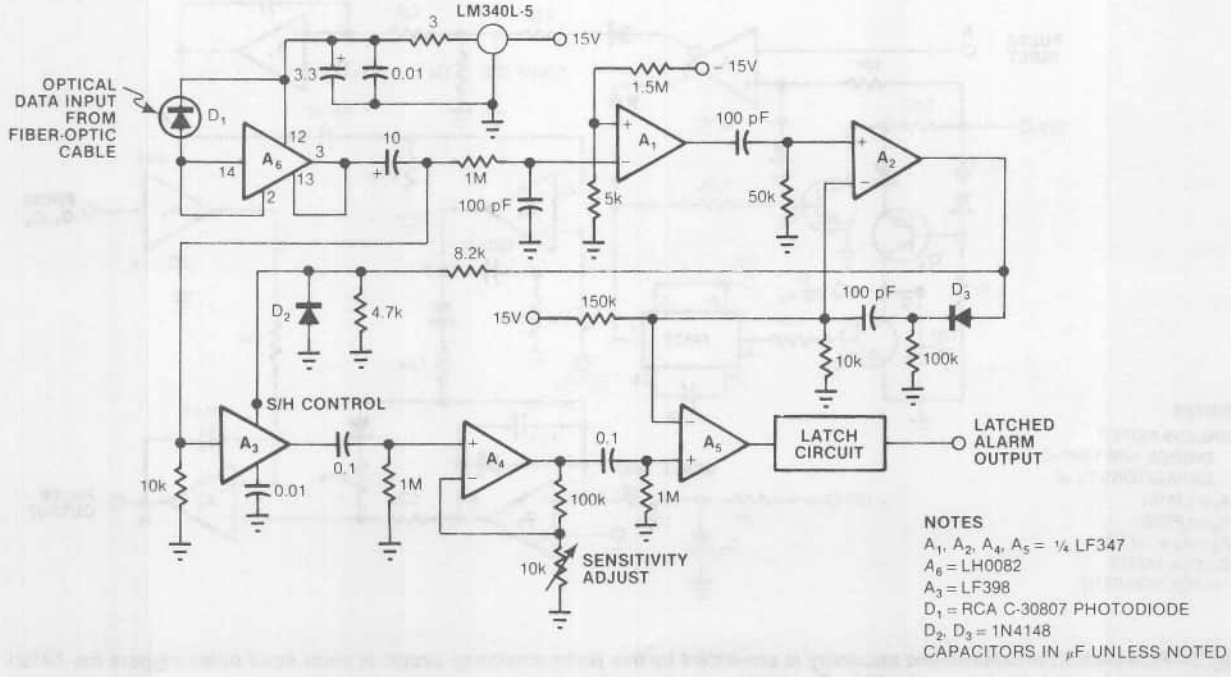

Fig 1—Fiber-optic-link eavesdropping attempts *are immediately detected by this design. Working on a pulse-by-pulse comparison basis, A_3 samples each input pulse and holds its amplitude value as a dc level. Anything that disturbs the next input's amplitude causes a jump in this level; because A_4 is an ac-coupled amplifier, the comparator and latch then activate.*

Sample/hold techniques benefit fiber-optics usage

something changes the input light pulse's amplitude, A_3's output is a dc voltage; because A_4 is ac coupled, its output is 0V.

A link-intrusion attempt disturbs the input pulse's amplitude, causing A_6's output to shift. A_4 ac-amplifies this shift, trips comparator A_5 and activates the alarm latch.

This sequence is represented in **Fig 2**, where trace A is A_6's output, B tracks A_3's S/H control pin and C is the alarm's output. An input disturbance occurs slightly past trace A's midpoint, indicated by A_6's reduced output. The alarm's output latches HIGH just after the Sample command rises—a result of the S/H amplifier's level jumping to A_6's changed output. **Fig 2** shows a large disturbance (10%) for demonstration purposes, but in practice, the design can detect an energy loss of as little as 0.1%.

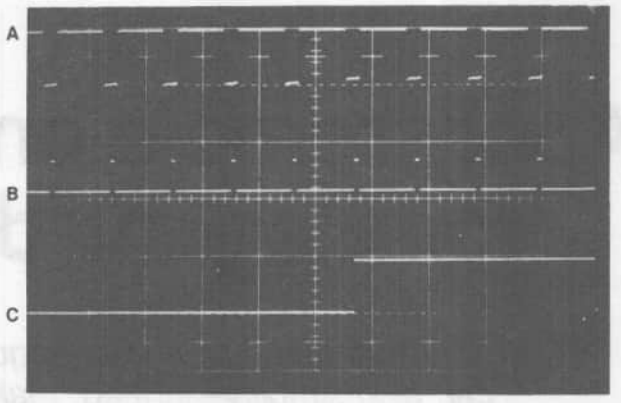

TRACE	VERTICAL	HORIZONTAL
A	0.1V/DIV	500 μSEC/DIV
B	10V/DIV	500 μSEC/DIV
C	5V/DIV	500 μSEC/DIV

Fig 2—An intrusion attempt *occurring just past the midpoint of trace A is immediately detected by* **Fig1***'s circuit. The photodetector's amplifier output (A) shows a slight amplitude drop. The next time the S/H amplifier samples this signal (B), the alarm latch sets (C).*

Stretching pulses proportionally

You can measure short-duration pulses with another S/H circuit, shown in **Fig 3.** The design works for either single-shot or repetitive events.

Assume that you must measure a 1-μsec-wide pulse to an accuracy of 1%. With digital techniques, this task would require use of a 100-MHz clock (1% of 1 μsec). **Fig 3**'s design avoids this requirement by linearly amplifying the pulse's width by a factor of 1000 or more. Thus, a 1-μsec input pulse becomes a 1-msec output pulse—a somewhat easier time duration to measure to 1% accuracy.

Fig 4 shows how this design responds to an even shorter (350 nsec) input pulse (trace A). Comparator A_1's output goes LOW (B), and the 74121-one-shot/Q_1 combination discharges the associated 100-pF capacitor via a 50-nsec pulse (D). Concurrently, Q_2 turns off, allowing current source Q_3 to start linearly recharging

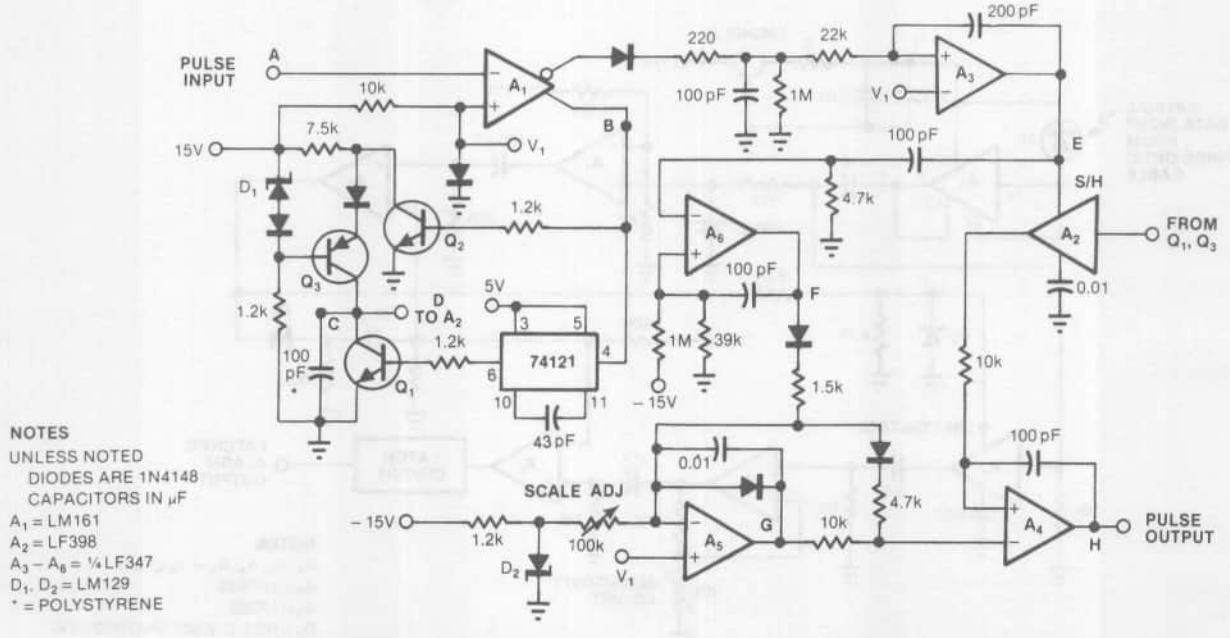

Fig 3—Pulse-width-measurement accuracy *is enhanced by this pulse-stretching circuit. A short input pulse triggers the 74121 one-shot and (via Q_1) discharges the 100-pF capacitor while concurrently turning on the recharging current source, Q_3. So long as the input pulse is present, the capacitor charges; when the pulse ends, the capacitor's voltage is proportional to the pulse's width. S/H amplifier A_2 samples this voltage, and the resultant dc level controls the ON duration of the A_4/A_5 pulse-width modulator. (Letters at key points in the circuit refer to waveforms shown in* **Fig 4.**)

the 100-pF capacitor (C). Charging continues until the input pulse terminates, which causes A_1's output to again go HIGH and cut off the current source. The voltage across the capacitor is then directly proportional to the input pulse width; S/H amplifier A_2 samples this voltage when A_3 generates the command shown by trace E. (Note the horizontal scale's change.) A_3's input derives via a delay network from A_1's inverting output, completing the sampling cycle.

A_2's dc output voltage represents the most recently applied input pulse's width. This voltage feeds to A_4, which works with A_5 as a voltage-controlled pulse-width modulator. A_5's output ramps positive (G) until reset by a pulse from A_6. (A_6 goes HIGH briefly (F) each time A_3's output (E) goes LOW.) To generate the circuit's final output, A_4 compares A_6's output with A_2's and produces a HIGH level (H) for a time linearly dependent upon A_2's output.

With the component values shown in **Fig 3**, the input-to-output time-amplification factor equals approximately 2000. Thus, a 1-μsec input yields a 1.4-msec output. Absolute accuracy is 1% (10 nsec) referred to the input, and the measurement's resolution extends down to 2 nsec. The 74121 one-shot's 50-nsec pulse limits the minimum measurable pulse width.

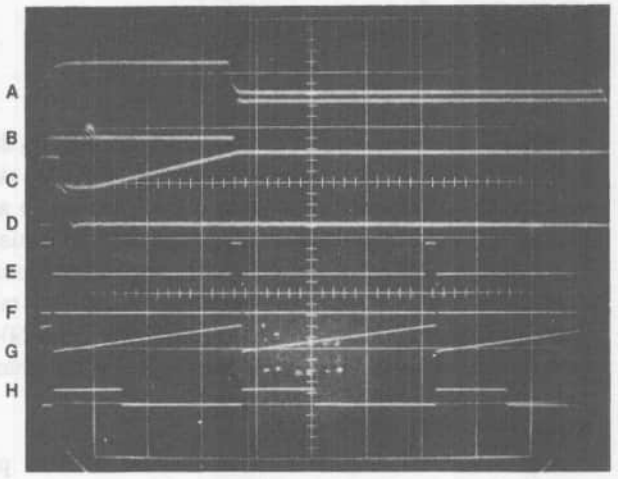

TRACE	VERTICAL	HORIZONTAL
A	10V/DIV	100 nSEC/DIV
B	5V/DIV	100 nSEC/DIV
C	5V/DIV	100 nSEC/DIV
D	5V/DIV	100 μSEC/DIV
E	50V/DIV	500 μSEC/DIV
F	50V/DIV	500 μSEC/DIV
G	20V/DIV	500 μSEC/DIV
H	100V/DIV	500 μSEC/DIV

Fig 4—A sequence of events *in Fig 3's circuit stretches a 350-nsec input pulse (A) by a factor of 2000. When triggered, comparator A_1 goes LOW (B). This action starts the recharging of a capacitor (C) after its previously stored charge has been dumped (D). When the input pulse ends, the capacitor's voltage is sampled under control of a delayed pulse (E) derived from the input amplifier's inverting output (F). The sampled and held voltage then turns off a voltage-controlled pulse-width modulator (G), and a stretched output pulse results (H).*

Control a pulse's amplitude

S/H amplifiers also make possible the amplitude-stabilized pulse generator shown in **Fig 5**; this circuit drives 20Ω loads at levels as high as 10V pk. The pulse's adjustable amplitude remains stable over time, temperature and load changes.

The circuit functions by sampling the output pulse's amplitude and holding this value as a dc voltage. This voltage then connects to a feedback loop that controls the output switching devices' supply voltage.

Specifically, an input TTL-level pulse turns on output drivers Q_2 and Q_3 and simultaneously places S/H amplifier A_1 in Sample mode. When the input pulse ends, A_1 outputs a dc voltage that represents the output pulse's amplitude. A_2 compares this level with the one

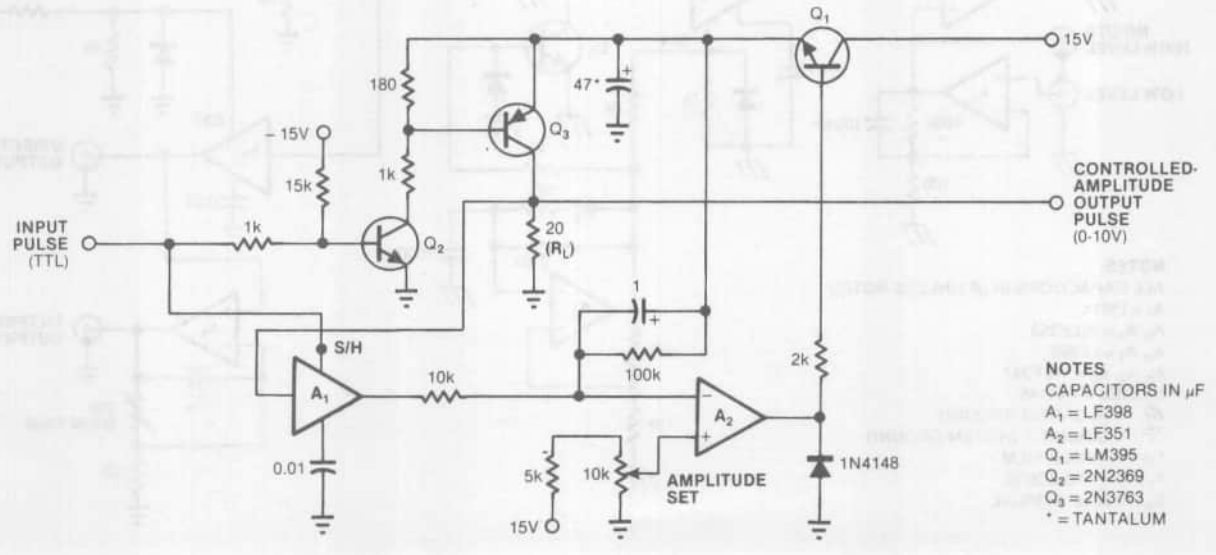

Fig 5—Pulse-amplitude control *results when this circuit samples an output pulse's amplitude and compares it with a preset reference level. When the output exceeds this reference, A_2 readjusts switching transistor Q_3's supply voltage to the correct level.*

Pulse-amplitude control results from S/H designs

established by the Amplitude Set adjustment; A_2 drives emitter follower Q_1, which provides the dc supply voltage to output switches Q_2 and Q_3. This servo action forces the output pulses' peak amplitude to equal the "set" value, regardless of Q_3's losses or output loading.

Fig 6's trace A shows the pulser's overall output wave shape, and traces B and C detail the clean 50-nsec rise and fall times. (Note the horizontal scale change.)

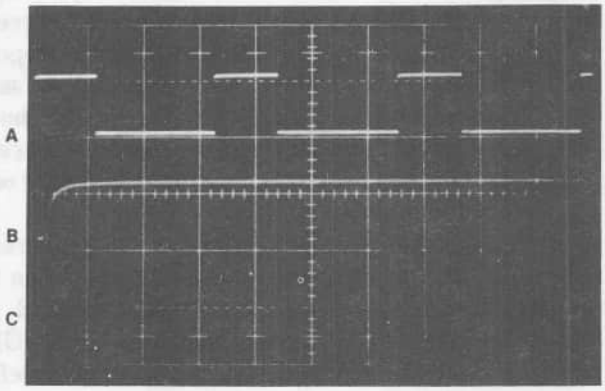

TRACE	VERTICAL	HORIZONTAL
A	10V/DIV	1 mSEC/DIV
B	10V/DIV	100 nSEC/DIV
C	10V/DIV	100 nSEC/DIV

Fig 6—A 10V, 0.5A pulse (A) *is amplitude-stabilized by the S/H technique depicted in* **Fig 5.** *Note the clean 50-nsec rise (B) and fall (C) times.*

Input isolation made easy

Fig 7 shows a powerful extension of the pulse-amplitude-control scheme that permits you to measure low-level signals (eg, thermocouple outputs) in the presence of common-mode noise or voltages as high as 500V. Despite the input terminals' complete galvanic isolation from the output, you can expect a 0.1% transfer accuracy. And by using the optional low-level preamp (A_1), you can measure inputs as low as 10 mV FS.

The circuit works by generating a pulse train whose amplitude is linearly related to the input signal's amplitude. This pulse train drives the input-to-output isolating transformer, T_1. T_1's output, demodulated to a dc level, provides the circuit's system-ground-referenced output. The pulse train's amplitude is controlled by a loop similar to the one employed in the pulse-amplitude-servo design. Here, however, the Amplitude Set doesn't appear, and the servo amplifier's + input becomes the signal input.

Set up as an oscillator, A_2 generates both the sample pulse for S/H amplifier A_3 and the drive for switches Q_2 and Q_3 (**Fig 8**, trace A). The feedback to the pulse-amplitude stabilizing loop comes from T_1's isolated secondary—a trick that ensures highly accurate amplitude-information transfer despite T_1's or Q_2's losses.

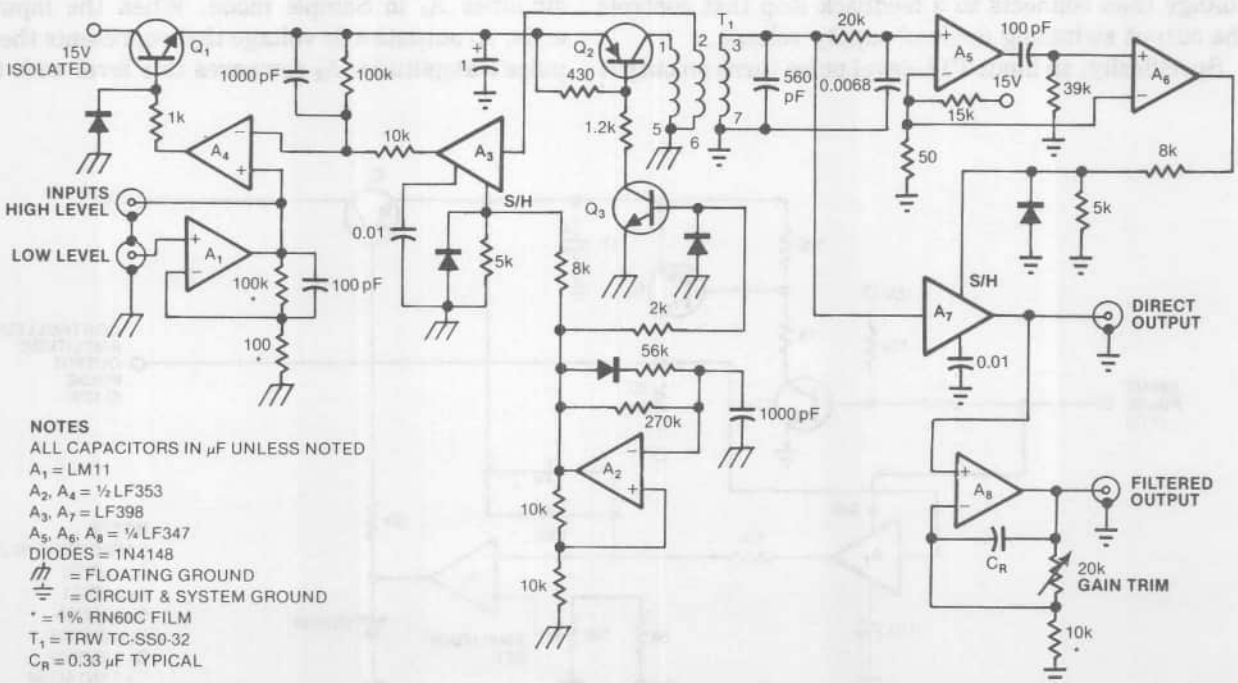

Fig 7—Obtain input-signal isolation *using this circuit's dual-S/H scheme. Analog input signals amplitude-modulate a pulse train using a technique similar to that employed in* **Fig 5**'s *design. This modulated data is transformer coupled—and thereby isolated—to a dc filter stage, where it's resampled and reconstructed.*

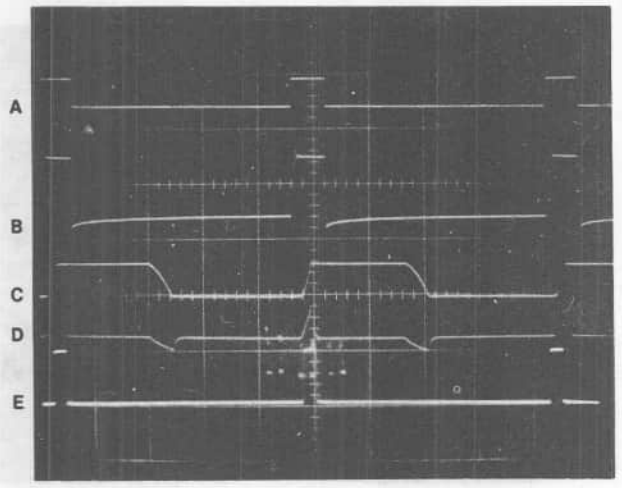

TRACE	VERTICAL	HORIZONTAL
A	50V/DIV	100 μSEC/DIV
B	1V/DIV	100 μSEC/DIV
C	50V/DIV	100 μSEC/DIV
D	10V/DIV	100 μSEC/DIV
E	5V/DIV	100 μSEC/DIV

Fig 8—Fig 7's in-circuit oscillator (A_2) *generates both the sampling pulse (A) and the switching transistors' drive. Modulated by the analog input signal, Q_2's (and therefore T_1's) output (B) is demodulated by S/H amplifier A_7. A_5's output (C) and A_6's input (D) and output (E) provide a delayed Sample command.*

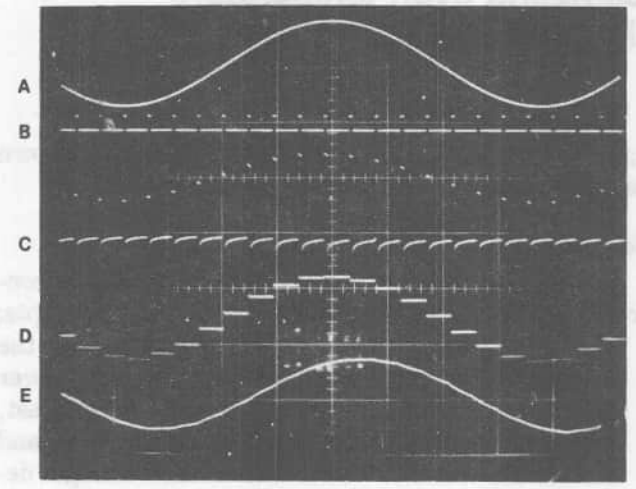

TRACE	VERTICAL	HORIZONTAL
A	5V/DIV	100 mSEC/DIV
B	100V/DIV	
C	5V/DIV	
D	5V/DIV	
E	5V/DIV	

Fig 9—Completely input-to-output isolated, *Fig 7's circuit's analog input signal (A) is sampled by a clock pulse (B) and converted to a pulse-amplitude-modulated format (C). After filtering and resampling, the reconstructed signal (D) is available smoothed (E).*

S/H amplifier A_7 demodulates the amplitude-encoded signal at T_1's output (B) back to a dc level. A_5's output (C) and A_6's + input (D) and output (E) provide A_7's delayed Sample command. A_8 furnishes an optional gain-trimmed and filtered output.

Fig 9 illustrates the design at work. Here, the input signal (trace A) is a dc-biased sine wave. Trace B shows A_2's output clock pulse, and A_7's Sample command

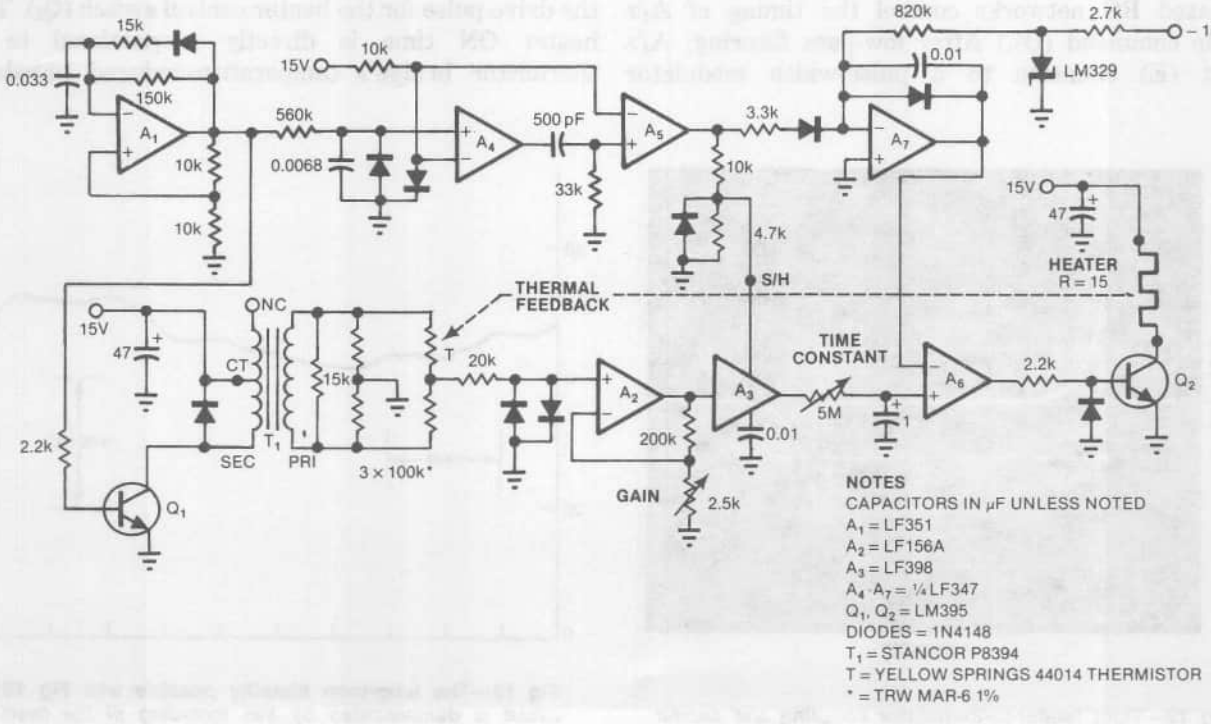

Fig 10—Tight temperature control *results when high-voltage pulses synchronously drive a thermistor bridge—a trick that increases signal level—and are then sampled and used to control a pulse-width-modulated heater driver.*

Sampling oven temperature tightens stability

appears as trace C. A_7's reconstructed output is shown as trace D and A_8's filtered output as trace E.

Sampling holds the temperature

The S/H-based high-stability oven-temperature controller shown in **Fig 10** embodies two unusual concepts:

- High-voltage, low-duty-cycle pulses drive the circuit's bridge and thus provide low power dissipation and high output levels. (In contrast, the power-dissipation limits of the resistors and thermistors in standard thermistor-bridge designs define the maximum dc bias level and therefore the maximum recoverable signal.)
- A S/H amplifier performs as a synchronous detector in the circuit's servo feedback loop. And because the sampling pulse establishes the design's reference level as well as the sampling interval, even the usual drift problems don't arise.

The circuit generates pulses via the oscillator-A_1/amplifier-Q_1 combination, driving a standard 24V transformer (T_1) "backwards." The transformer applies a floating 100V pulse across the thermistor bridge. Because one side of the bridge's output is grounded, this signal becomes the pair of complementary 50V pulses shown in **Fig 11** (traces A and B).

Amplified by A_2 (**Fig 11**, trace C), the bridge's output feeds to S/H amplifier A_3, whose dc output level equals A_2's peak output. (The A_4 and A_5 stages and their associated RC networks control the timing of A_3's Sample command (D).) After low-pass filtering, A_3's output (E) connects to a pulse-width modulator consisting of A_6 and A_7. A_5's output periodically resets A_7's output ramp (F). A_6's output pulse (G) results from the comparison of A_5's and A_3's outputs and serves as the drive pulse for the heater control switch (Q_2). Thus, heater ON time is directly proportional to the thermistor bridge's temperature-induced unbalance.

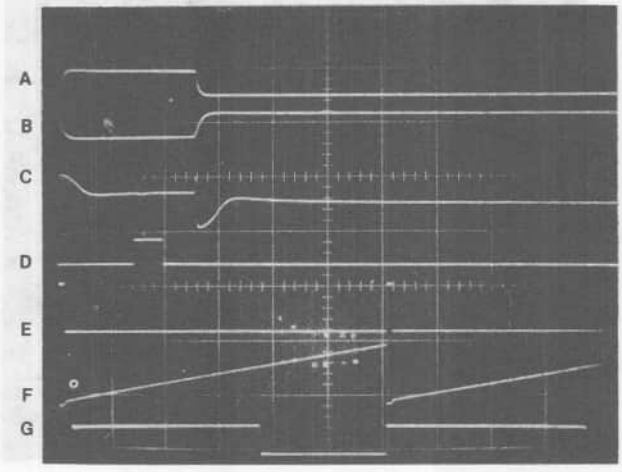

TRACE	VERTICAL	HORIZONTAL
A	100V/DIV	200 μSEC/DIV
B	100V/DIV	200 μSEC/DIV
C	5V/DIV	200 μSEC/DIV
D	10V/DIV	200 μSEC/DIV
E	5V/DIV	1 mSEC/DIV
F	10V/DIV	1 mSEC/DIV
G	50V/DIV	1 mSEC/DIV

Fig 11—Driving a thermistor bridge *with complementary high-voltage pulses (A and B) permits high-gain amplification without drift problems (C). Driven by a delayed Sample command (D), a S/H amplifier converts the bridge's error signal to a dc level (E) that controls a pulse-width-modulated heater driver (F and G).*

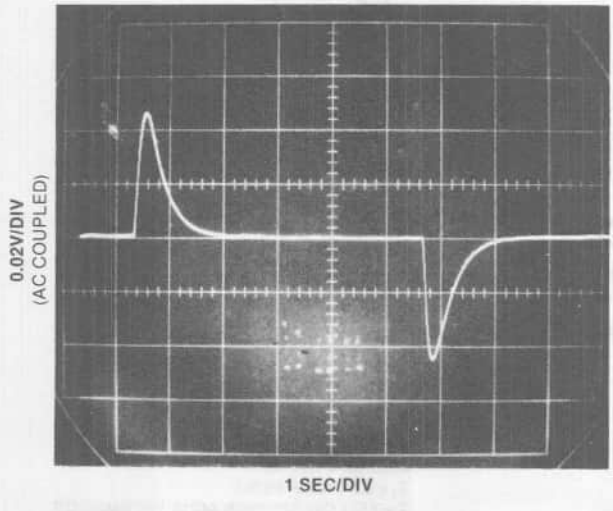

Fig 12—Tight heater-to-thermistor coupling *and careful calibration can provide rapid temperature restabilization. Here the controlled oven recovers within 2 sec after ±0.002°C steps.*

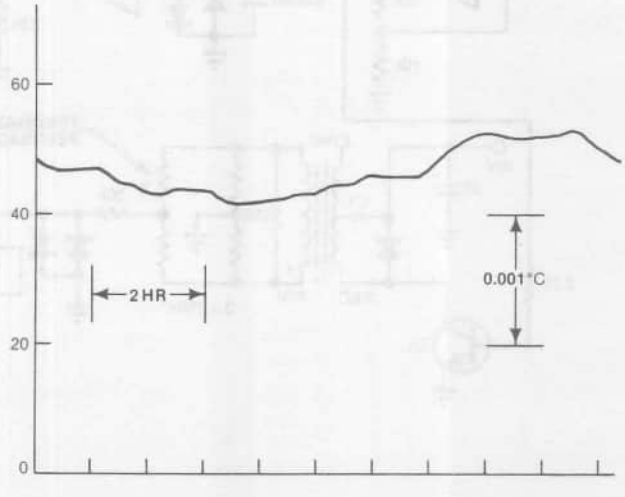

Fig 13—The long-term stability *possible with* **Fig 10**'s *circuit is demonstrated by this recording of the oven's temperature. Set at 50°C, the internal temperature stays within 0.001°C even though the exterior temperature varies by 6°C.*

Oven temperature stabilizes within 2 sec

Heater-to-thermistor thermal feedback completes the servo loop.

To adjust the loop's performance characteristics, apply small step changes in the temperature setpoint by switching a 100Ω resistor in series with one of the bridge's resistors. (For the thermistor shown in **Fig 10**, this modification produces a 0.02°C change.) While monitoring the loop's response at A_3's output, adjust the Gain and Time Constant potentiometers for minimum settling time.

Fig 12 shows how the system stabilizes within 2 sec for both positive and negative steps. And **Fig 13** demonstrates the design's very tight temperature-control capability. Set at 50°C, the oven's interior temperature varies by less than 0.001°C even when the ambient temperature changes by 6°C. Although **Fig 13** shows only a a few hours of operation, the circuit continued this performance over a 48-hr test period. **EDN**

Author's biography

Jim Williams, design engineer with National Semiconductor Corp's Linear Applications Group, Santa Clara, CA, has made a specialty of analog-circuit design and instrumentation development. Before joining National, he was a consultant with Arthur D Little Inc in analog systems and circuits. From 1968 to 1977, Jim directed the Instrumentation Development Lab at the Massachusetts Institute of Technology, where in addition to designing experimental biomedical instruments, he was active in course development and teaching. A former student of psychology at Wayne State University, he lists tennis, art and collecting antique scientific instruments as his leisure interests.

Current-source alternatives increase design flexibility

An op amp's feedback loop is an excellent constant-current circuit. But if your requirements call for a ground-referenced load, high speed or high efficiency, consider several other approaches.

Jim Williams, National Semiconductor Corp

If traditional feedback-loop-based methods of current control aren't adequate for your needs, investigate some alternative approaches to designing constant-current sources. The circuits described here can prove useful in a variety of applications requiring current rather than voltage control—resistance-temperature-detector (RTD) and thermistor excitation, ramp generation and deflection-yoke modulation, for example.

Traditional method exhibits shortcomings

The most commonly used current source—the one most frequently encountered in op-amp cookbooks—is the feedback loop of an operational amplifier (**Fig 1**). Although the amplifier's voltage gain varies with R_{FB}, the current in the feedback loop remains fixed, assuming a fixed E_{IN} and R_{REF}. Thus, the op amp, viewed from the feedback resistor, is a constant-current source. The amplifier inputs accommodate offset and scaling.

In general, this simple op-amp-based circuit provides good results. You can increase current or voltage compliance by adding an output stage, and precision greater than 0.01% is easy to achieve. However, the approach also has limitations. The most serious is that the current-driven load isn't referred to ground. Although the amplifier junction is at 0V, it's forced there by feedback and remains sensitive to noise and lead capacitance. Thus, because remote transducers and test fixtures are often driven with respect to ground, feedback-loop designs often exhibit problems.

Providing a grounded load

The clever circuit shown in **Fig 2,** devised in 1959 by B Howland at MIT, solves this ground-reference

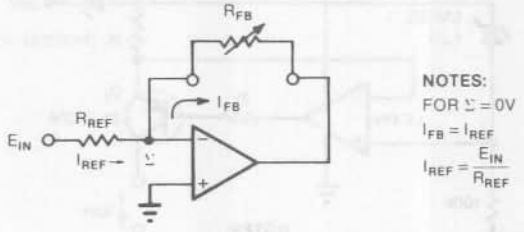

Fig 1—A feedback-loop-based current source *produces excellent results but isn't useful in applications requiring a ground-referenced load.*

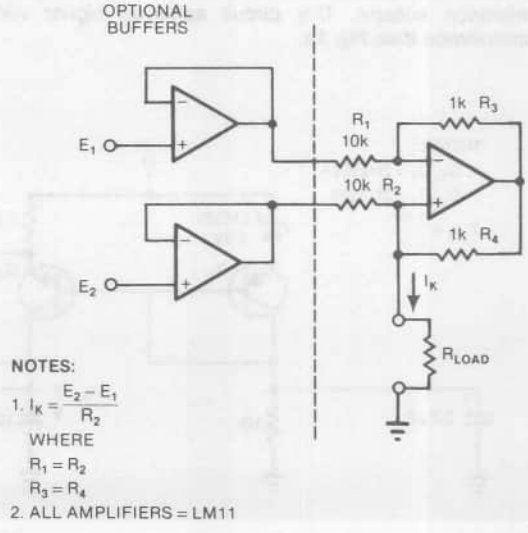

Fig 2—A Howland current-source circuit *supplies a grounded load and has differential inputs.*

problem. This single-amplifier circuit is a true instrumentation-grade current source: It supplies a grounded load and has fully differential inputs. You can delete the input followers if you don't need high input impedance.

Because positive feedback makes the circuit's output impedance appear infinite, understanding circuit operation isn't easy. To start, assume E_1 is 0V, E_2 is some positive value and the load is a short circuit. The configuration is then the well-known inverting amplifier. Because the input E_1 is at 0V, the output is also 0V, and input current E_2/R_2 is the only current flowing into the now-shorted load.

As the current-driven load's resistance increases, the voltage across the load also increases. This increasing voltage at the op amp's noninverting input forces the voltage at the inverting input to rise. As a result, the negative-feedback network causes the op-amp output to rise above the inverting-terminal potential; the op amp supplies the additional current to the load that's no longer supplied from E_2. In other words, as the load value increases, less and less current gets taken from E_2, with the op amp taking up the slack.

For precision results, this circuit demands an op amp with good common-mode rejection; in dc operation, an LM11 provides 0.01% precision without too much difficulty. *(Ed Note: A future article will examine the Howland circuit in greater detail.)*

Increasing voltage compliance

Another way to achieve grounded-load operation involves the circuit shown in **Fig 3**. Here, the op amp forces the voltage across R_1 to equal the LM385 voltage

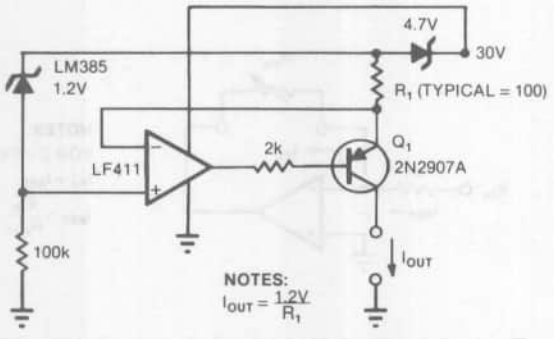

Fig 3—Another way to achieve grounded-load isolation *is to force the potential across R_1 to equal the LM385's 1.2V reference voltage. This circuit achieves higher voltage compliance than* **Fig 2***'s.*

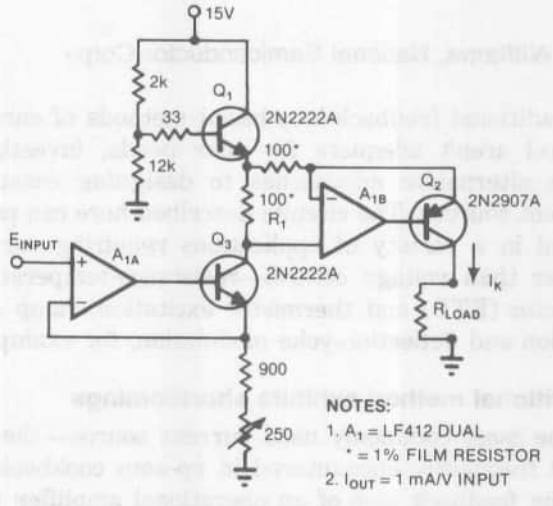

Fig 4—Achieve voltage control *by forcing the voltage drop across R_2 to equal the drop across R_1.*

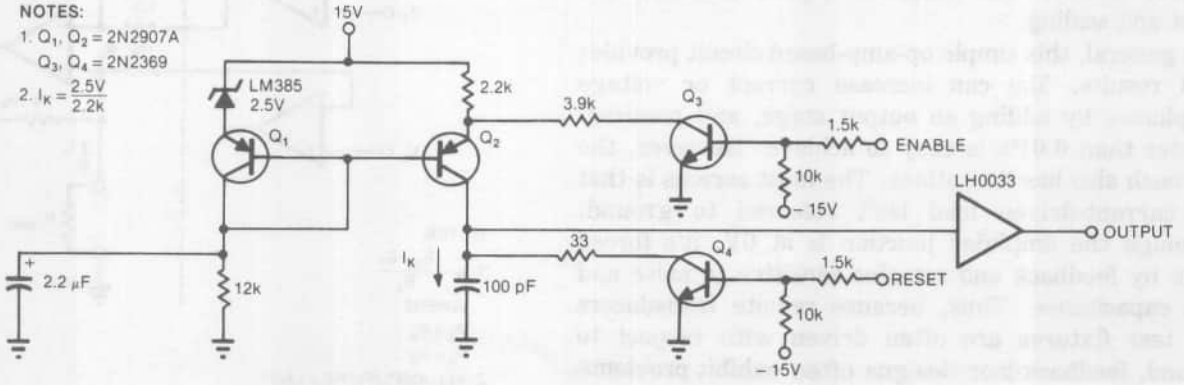

Fig 5—High-speed operation *results when you abandon feedback techniques. Obtain ramp-and-pedestal operation by gating the charging current to the loop's capacitor.*

reference's 1.2V potential, regardless of transistor Q_1's load. The 4.7V zener diode ensures that the op amp's inputs are within its common-mode range. The circuit's output current measures

$$I=1.2V/R_1.$$

This circuit's advantage compared with the Howland design is its greater voltage compliance. That is, it exhibits a greater ability to maintain current in high-resistance loads. (In an ideal current source, the voltage goes to infinity when you increase the load because the source tries to maintain constant current. In **Fig 3**'s circuit, the voltage output rises with increasing load resistance to a maximum value of 24V; beyond this voltage-compliance value, the output source can no longer increase the resistor's voltage, and it clips.)

Voltage-controlled source sports high impedance

If you need a voltage-controlled ground-referenced current source, consider **Fig 4**'s design. This circuit features high input impedance and noninverting operation. A_{1A} and Q_3 act as a voltage follower, producing an input-voltage-controlled drop across R_1. A_{1B} and Q_2 then force this drop to appear across R_2; Q_2's collector supplies the output current. Q_1 acts as a voltage regulator, reducing the supply voltage to 12V so that A_{1A} and A_{1B} operate within their common-mode range.

The 250Ω potentiometer provides trimming, resulting in an input/output relationship of 1 mA/V. To set the scale factor, apply 10V to the input and adjust the potentiometer for 10-mA output. You can alter the scale factor by changing R_2.

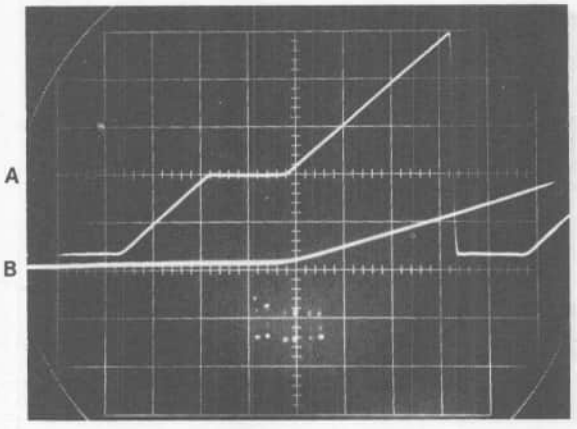

TRACE	VERTICAL	HORIZONTAL
A	2V/DIV	500 nSEC/DIV
B	0.2V/DIV	50 nSEC/DIV

Fig 6—The ramp-and-pedestal operation *of* ***Fig 5****'s circuit shows sharp transitions, with no ripple.*

Abandon feedback for high speed

In addition to lacking the ability to operate with a grounded load, feedback-loop-based circuits can't achieve accurate high-speed operation without using

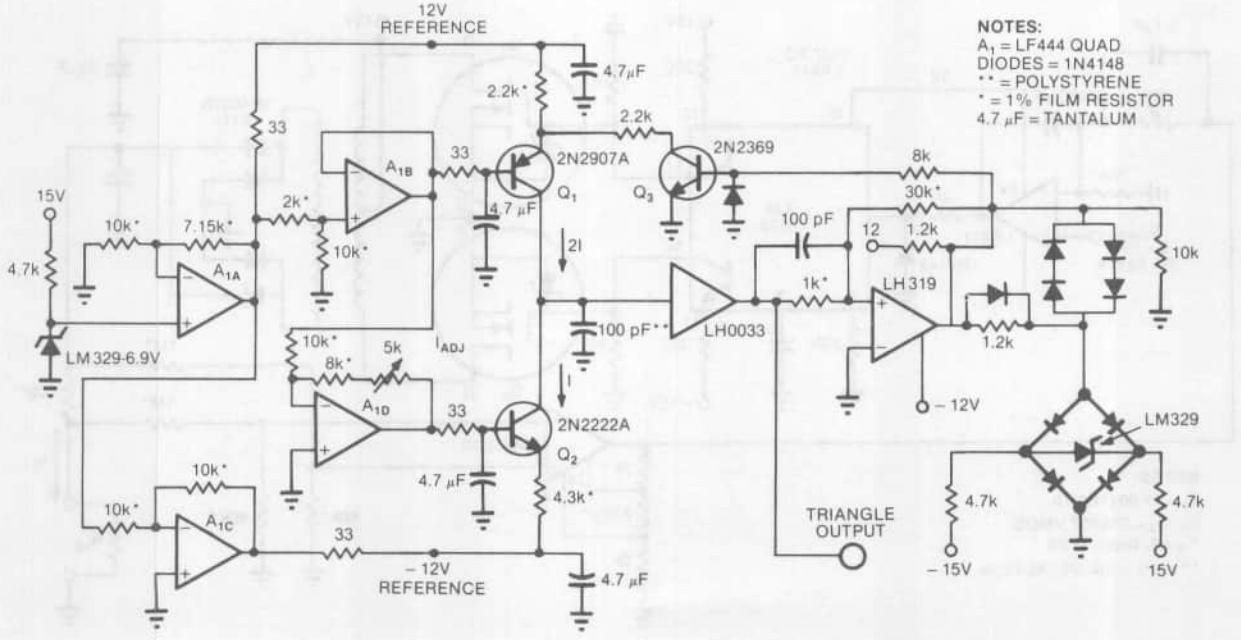

Fig 7—A bipolar current source *generates a highly linear triangular wave. It functions by alternatively charging and discharging a capacitor with positive and negative currents.*

Abandon feedback for high-speed operation

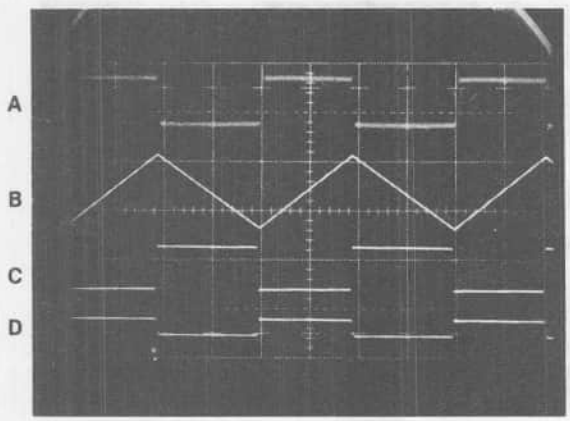

TRACE	VERTICAL	HORIZONTAL
A	2 mA/DIV	200 nSEC/DIV
B	2V/DIV	200 nSEC/DIV
C	20V/DIV	200 nSEC/DIV
D	10V/DIV	200 nSEC/DIV

Fig 8—Performance to several megahertz *characterizes Fig 7's circuit.*

elaborate and expensive op amps. That is, the ac dynamics of maintaining accurate feedback place limitations on loop-based current sources. Fortunately, several high-speed alternatives are available.

In **Fig 5**, for example, the Q_1/Q_2 transistor current source supplies a gateable current to the 100-pF capacitor to produce a very-high-speed voltage ramp. (Q_2 is the actual current source, with Q_1 furnishing V_{BE} compensation.) The LH0033 buffer provides a low-impedance output; the LM385 reference fixes the current, which you can vary by changing the value of Q_2's emitter resistor.

Q_3 gates the current source by reverse-biasing Q_2. This procedure allows you to obtain the high-speed ramp-and-pedestal operation shown in **Fig 6**'s trace A—a common requirement in nuclear- and particle-research instrumentation. Because the design has no feedback loop, operation is quick and clean, even at high speed. **Fig 6**'s trace B shows an expanded version of the center section of trace A. Here, the pedestal begins to ramp as the source is gated ON. The transition is sharp, with no discontinuities.

Another high-speed current source appears in **Fig 7.** Here, alternately charging a capacitor with positive and negative current sources generates a high-linearity 1.5-MHz triangle wave—a capability that op-amp based circuits can't achieve. The positive current source Q_1 supplies a current of value 2I to the 100-pF capacitor, while Q_2 sinks I. The resulting charging current is I, and the capacitor charges linearly. **Fig 8**'s trace A shows the charging current, while trace B depicts the voltage across the capacitor.

When the capacitor voltage ramps sufficiently high, the LM319 comparator changes state (trace C), turning transistor Q_3 ON. This action back-biases Q_1 (trace D),

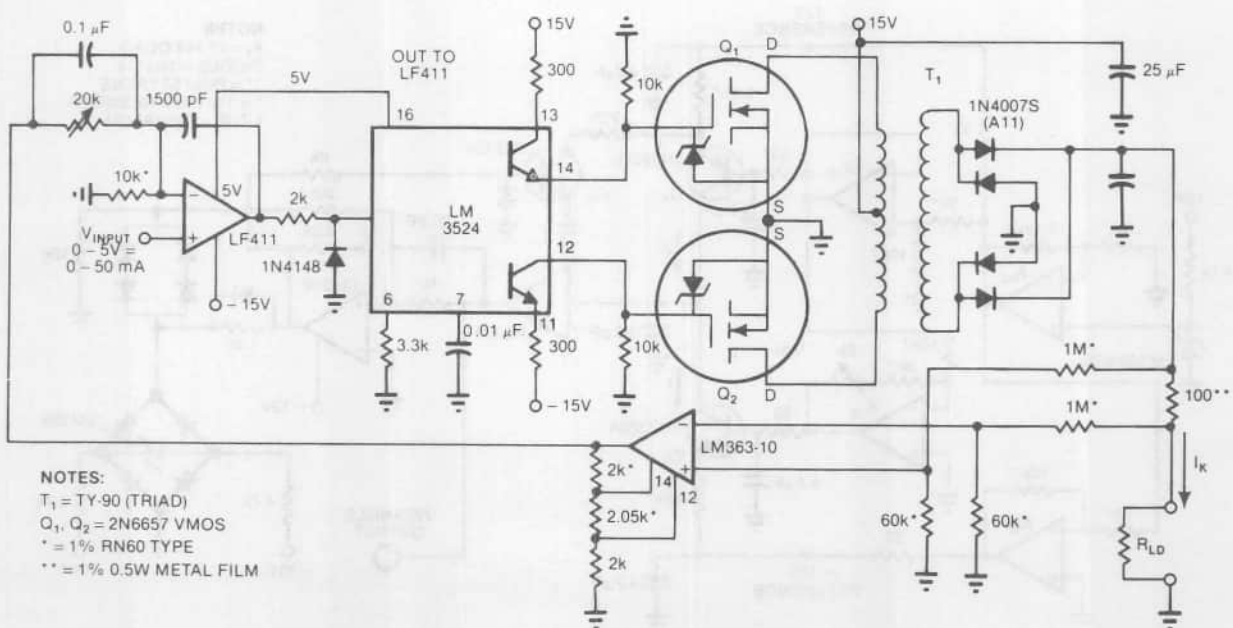

Fig 9—A switching converter *provides 0 to 50 mA into a load, with a compliance of 200V.*

shutting off the 2I current flow. From this point on, the capacitor discharges at a rate proportional to I until the LM319 changes state again, reinitiating the cycle.

The zener bridge and associated diodes ensure a stable, bipolar comparator trip point, while the 100-pF comparator input capacitor compensates for propagation delay. The LH0033 unloads this capacitor, and the quad op amp sets the bias points for the current sources, using the LM329 as the master reference. A_{1A} and A_{1C} generate ±12V for the Q_1 and Q_2 emitters, while A_{1B} and A_{1D} bias the transistors' bases. The 33Ω/4.7-μF combinations furnish decoupling, and the ±12V emitter voltage also biases the comparator's output stage.

You can vary the triangle-wave frequency by driving A_{1B} directly, changing the current sources' base bias. With a good ground plane and a low-capacitance wiring technique, the current sources can generate good triangle waveforms out to several megahertz. To adjust the circuit, trim the I_{ADJ} potentiometer until the triangle waveform is symmetrical. This action essentially adjusts the I/2I ratio and also corrects for propagation-delay-induced errors.

Use a switched-mode source for efficiency

Some current-source applications require high current or high compliance voltage, and in these cases, efficiency suffers. The source shown in **Fig 9,** however, operates in switched mode to achieve low losses.

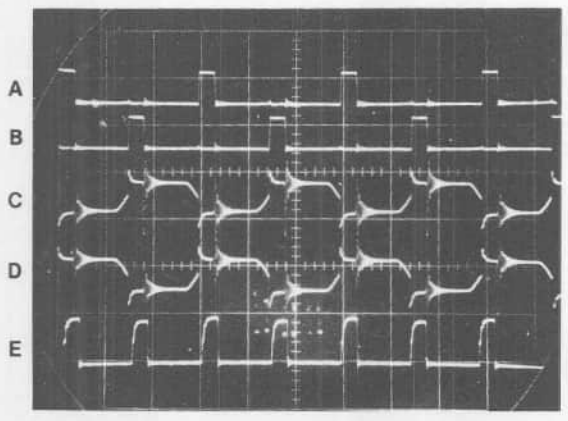

TRACE	VERTICAL	HORIZONTAL
A	20V/DIV	20 μSEC/DIV
B	20V/DIV	20 μSEC/DIV
C	20V/DIV	20 μSEC/DIV
D	20V/DIV	20 μSEC/DIV
E	2A/DIV	20 μSEC/DIV

Fig 10—Because the pulse drive of Fig 9's switching converter *is not a square wave, the waveforms appear distorted. But the current in the transformer primary is clean and distortion free.*

This current source provides 0 to 50 mA into a load with a compliance limit of 200V. The LF411 receives the control-voltage input and biases the LM3524 pulse-width modulator. The complementary LM3524 outputs (**Fig 10,** traces A and B) drive the VMOS transistors at 30 kHz. The toroidal transformer provides a voltage step-up when excited by these VMOS transistors (drain waveforms appear in traces C and D). Because the pulse drive is not a square wave, the drain-voltage waveforms appear distorted. But the current in the transformer primary is clean and orderly (trace E). The transformer output gets rectified and filtered to produce the current output.

The LM363 divides down the voltage across the 100Ω shunt resistor to a usable level; it also transforms the voltage to single-ended form. The LM363 is trimmed to

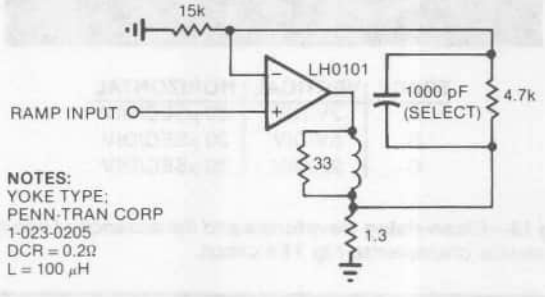

Fig 11—A deflection-yoke driver *achieves precision current drive, avoiding display distortion.*

a gain of 30; its output returns to the LF411, completing a loop that forces the pulse-width modulator to run at whatever duty cycle is required to keep the current through the 100Ω shunt constant, regardless of loading conditions. Although the pulsed transformer can develop a 200V output, it's loop-limited to produce only the voltage required to satisfy the circuit's current output. The result? High efficiency.

The VMOS devices permit high-speed operation while requiring little drive. The LF411 gets driven from the LM3524's internal 5V regulator, ensuring that the LM3524 input can't be overdriven during startup or transients. The capacitors at the op amp ensure loop stability, and the 20-kΩ potentiometer trims the circuit's 100-mA/V scale factor.

Deflection yokes require current drive

As a final example of a constant-current source, consider the circuit shown in **Fig 11.** It provides a carefully controlled current drive—useful in a precision display's deflection yoke, whose magnetic field is proportional to the current through it.

The LH0101 power op amp provides a current-controlled drive to the yoke at a scale factor of 1V/A.

Obtain high efficiency with a switching converter

The 33Ω resistor furnishes yoke damping; without it, a high inductive flyback voltage would be produced at a step discontinuity. The 1000-pF capacitor trims the circuit. For a ramp input (**Fig 12**, trace A), the yoke input current (trace C) rises cleanly with no ripple or discontinuities. When the ramp resets, the inductor current falls to zero, and the op-amp output (trace B) must swing sharply negative to compensate for the inductive flyback. Because damping is optimized, the yoke-current sweep reset is clean and doesn't cause display distortion. **EDN**

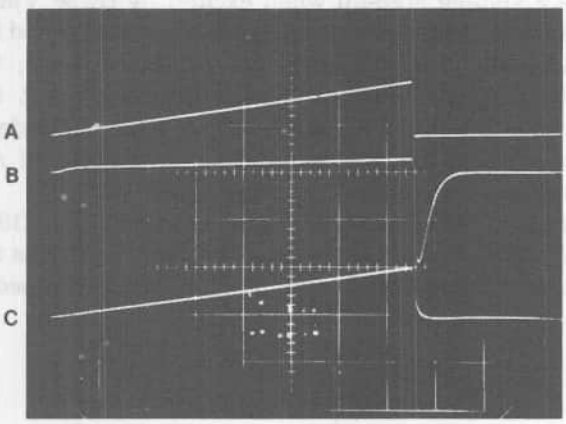

TRACE	VERTICAL	HORIZONTAL
A	2V/DIV	20 μSEC/DIV
B	5V/DIV	20 μSEC/DIV
C	2A/DIV	20 μSEC/DIV

Fig 12—Clean-rising waveforms *and the absence of unruly dynamics characterize* ***Fig 11****'s circuit.*

Author's biography

Jim Williams was applications manager in National Semiconductor's Linear Applications Group (Santa Clara, CA), specializing in analog-circuit and instrumentation development, when this article was written. Before joining the firm, he served as a consultant at Arthur D Little Inc and directed the Instrumentation Development Lab at the Massachusetts Institute of Technology. A former student of psychology at Wayne State University, Jim enjoys tennis, art and collecting antique scientific instruments in his spare time.

Designer's Guide to: Temperature control

Nine working circuits and a list of hints emphasize the practical aspects of thermal control systems.

Jim Williams, Dept. of Nutrition and Food Science, Massachusetts Institute of Technology

Once you have selected a temperature sensor (Part 1 of this series, EDN 5/5/77) and developed a measurement scheme (Part 2, EDN 5/20/77), it's theoretically a simple task to create a control loop by well known servo-feedback techniques. Unfortunately, the long time constants inherent in thermal systems present circuit designers with significant challenges. Nowhere is the close relationship between servo systems and oscillators more apparent than in thermal control systems.

A thermal control loop can be simply modeled as a network of resistors and capacitors, where the resistors are equivalent to thermal resistances and the capacitors to thermal capacity. In **Fig. 1,**

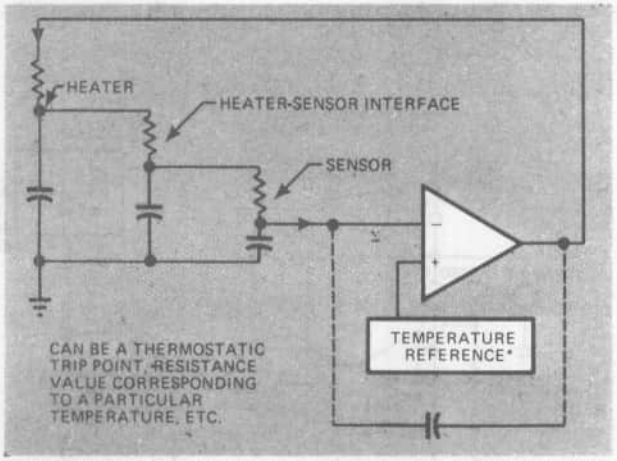

Fig. 1—Electrical model of a thermal-control system shows the RC factors that contribute to the delay in its response to driver inputs.

observe that the heater, heater-sensor interface and sensor all have RC factors that contribute to a lumped delay in a thermal system's ability to respond to its driving device. The designer must minimize these delays, and in so doing he must make a number of tradeoffs. The heater element's physical size and electrical resistivity determine its time constant. And the heater-sensor interface time constant can be minimized by placing the sensor in intimate contact with the heater.

Keep the thermal time constant small

We cannot overstate the importance of a minimized heater-sensor thermal time constant, because this interface is the most commonly mis-designed part of thermal-control systems. When working with a still-air oven, you should make every attempt to mate the sensor very tightly to the heater. With baths the same provision applies, but some relaxation can be tolerated if you use adequate and truly isothermal mechanical stirring of the liquid. You can operate forced air ovens with the sensor somewhat removed from the heater, but only if the air moves fast enough from the heater to the sensor to inhibit significant phase shift.

Generally speaking, in a well designed thermal-control system *the heater and sensor are always at the same temperature.*

You can minimize the sensor RC product by selecting a sensor of small size relative to the capacity of its thermal environment. Clearly, if the wall of your oven is 6-in. thick aluminum, your sensor need not be the smallest available size. Conversely, if you are controlling the temperature of a 1/16-in. thick glass microscope slide, you need a very tiny sensor (i.e., a fast one).

After minimizing the thermal time constants relating to the heater and sensor, you should choose some form of insulation for the system. The type of thermal load will dictate the optimum type and amount of insulation. Remember that the function of insulation is to keep the loss rate down so the temperature-control device can keep up with the losses. For any given system, *the higher the ratio between the insulation time constants and the heater-sensor time constants, the better the performance of the control loop.*

You can compensate thermal loops by adjusting the gain of the control element, limiting its bandwidth to less than the thermal delays, or both. Such practice is consistent with well-known feedback theory. A single bandwidth-limiting element and a single gain-setting adjustment should suffice to stabilize any system. Systems that employ numerous gain and bandwidth ad-

justments, while impressive, are poorly designed.

Thermoswitches can control to 0.01°C

Thermostatic switches can provide adequate temperature control in many applications. You can obtain reasonably high performance by careful consideration of the power supply and the power to be dissipated in the oven. Avoid a supply voltage that's too high; it will cause the system to overshoot when the switch closes. Other refinements include a second "warming" heater which always runs, keeping the oven just below the control point. The warming heater keeps overshoot low because when the thermoswitch closes, the main heater provides only a small amount of additional heat. Another possibility, less costly but also less efficient, is to solder a bleed resistor across the thermoswitch terminals **(Fig. 2).** Properly optimized systems using mercury thermometer-type switches can control

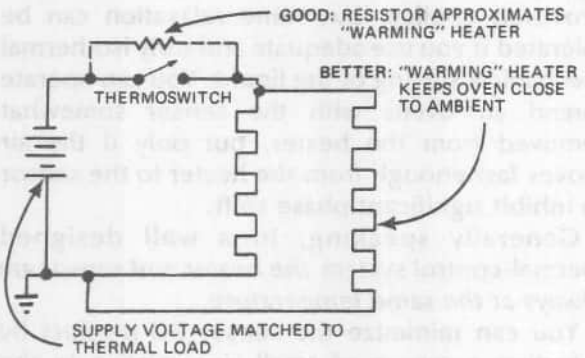

Fig. 2—A bleed resistor and/or warming heater can serve to minimize overshoot in a system with a thermostatic controller.

to better than 0.01°C.

Operational amplifiers can serve to construct "on-off" electronic equivalents of thermoswitch controllers with good performance, high reliability and adjustable set points. In **Fig. 3,** the 301 op amp functions as a comparator. The platinum sensor is in a bridge configuration, and the amplifier looks across the bridge differentially. Initially the sensor resistance is less than 500Ω, so the amplifier saturates positive, turning on the transistor and the heater. As the oven warms, the sensor resistance increases, the bridge balance shifts and the heater cuts off.

If you build **Fig. 3's** circuit and severe overshoot occurs, adjust the heater supply, change the heater resistance and/or place a resistor across the transistor in a manner similar to **Fig. 2.** Also check thermal contact between the heater and sensor to ensure minimum phase delay.

Timer output must vary with ambient

The circuit of **Fig. 4** operationally resembles **Fig.**

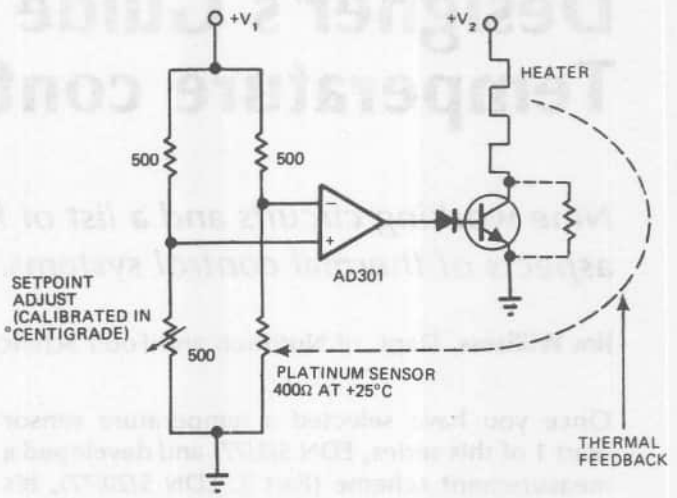

Fig. 3—With good thermal contact between the heater and sensor to minimize phase delay, circuits of the type shown here can control to better than 0.01°C over wide set-point ranges.

3 except that it includes a scheme that precisely compensates for overshoot. This approach proves extremely effective in applications where the heat source is not electrically adjustable or that demand fine tuning of an electrically heated system. For instance, many industrial situations utilize gas-fired heaters of enormous thermal capacity. These heating units cannot be "tuned"

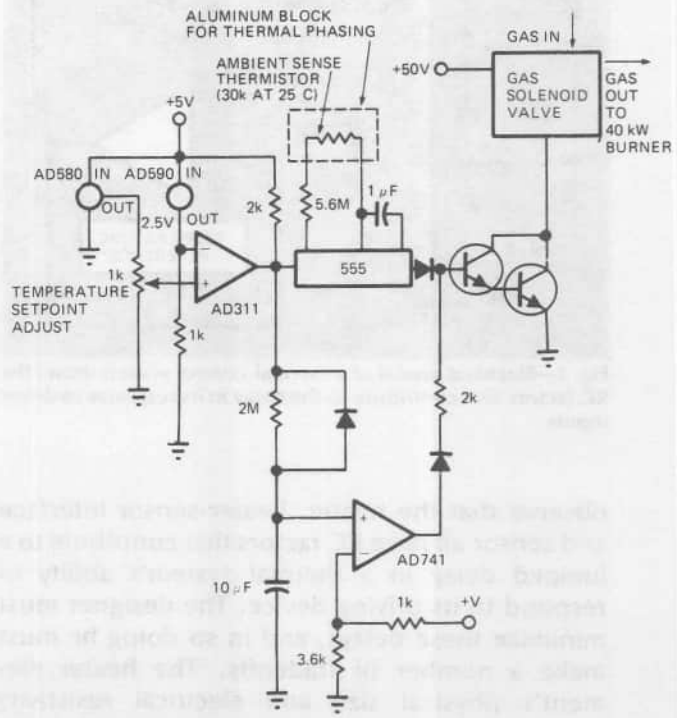

Fig. 4—Precise overshoot compensation is provided by this 555 timer-based circuit. The 741 op amp and its input and output circuitry effectively bypass the 555 one-shot during start-up conditions and if the one-shot fails to fire.

as easily as an electrical heater to achieve minimum overshoot.

The circuit illustrates the latter situation. It functions by comparing the output of the AD590 IC temperature transducer with a stable voltage reference. When the 311 comparator trips at the set-point temperature, the 555 one-shot causes the transistors to turn on the gas solenoid and light the 40 kW burner. When the 555 times out, the burner is extinguished—regardless of the 311's output state. The time constant of the 555 compensates for lags in the system by turning off the heater before the phase-lagged sensor actually hits cutoff value.

As the ambient temperature around the thermal load changes, the amount of time the 555 is on must also change to maintain optimum control. Why? Because the 555 effectively breaks the control loop. As the ambient temperature changes, the dissipation constant of the system varies and the 555's output pulse width must vary correspondingly. The thermistor across the timing resistor serves this function, sensing ambient temperature and providing proper time-constant trimming. It is mounted in an aluminum block whose time constant ensures proper phasing.

Fig. 4's basic approach has been used to control a 5000 gal. vat at 100°C to 0.1°C. It has also provided 0.001°C control for a quartz delay-line oven in a retrofit application where heater and power-supply parameters could not be altered.

Phase-fired systems are efficient

Any thermostatic control loop, even one as sophisticated as **Fig. 4,** still suffers from its unrealistic correction characteristic. Thermostatic systems tend to control about, rather than at, a desired set point. Since energy is leaving the controlled environment at all times, it follows that even the most carefully optimized thermostatic circuit cannot provide the best possible performance for a given application. Phase-fired control circuits, however, can more closely approximate a linear system.

In phase-fired circuits an ac waveform across the heater is chopped at a servo-controlled phase angle to provide nearly linear response. Since thermal control-loop response crosses over long before 60 Hz, the assumption is that the thermal components of the loop will nearly perfectly integrate the chopped heater drive into a thermal dc level. Typically, phase-fired systems use SCR's as choppers and are capable of good efficiency at high power.

In **Fig. 5,** the AD580 band-gap voltage reference furnishes power to a bridge circuit, while the platinum sensor provides the sensing function. The AD504 amplifies the bridge output; its 110k feedback resistor allows maximum loop gain without oscillation. The op amp's output biases a 2N2907 whose collector potential controls a 60 Hz syncronized unijunction transistor (UJT) oscillator. The UJT's output drives the SCR gate via an

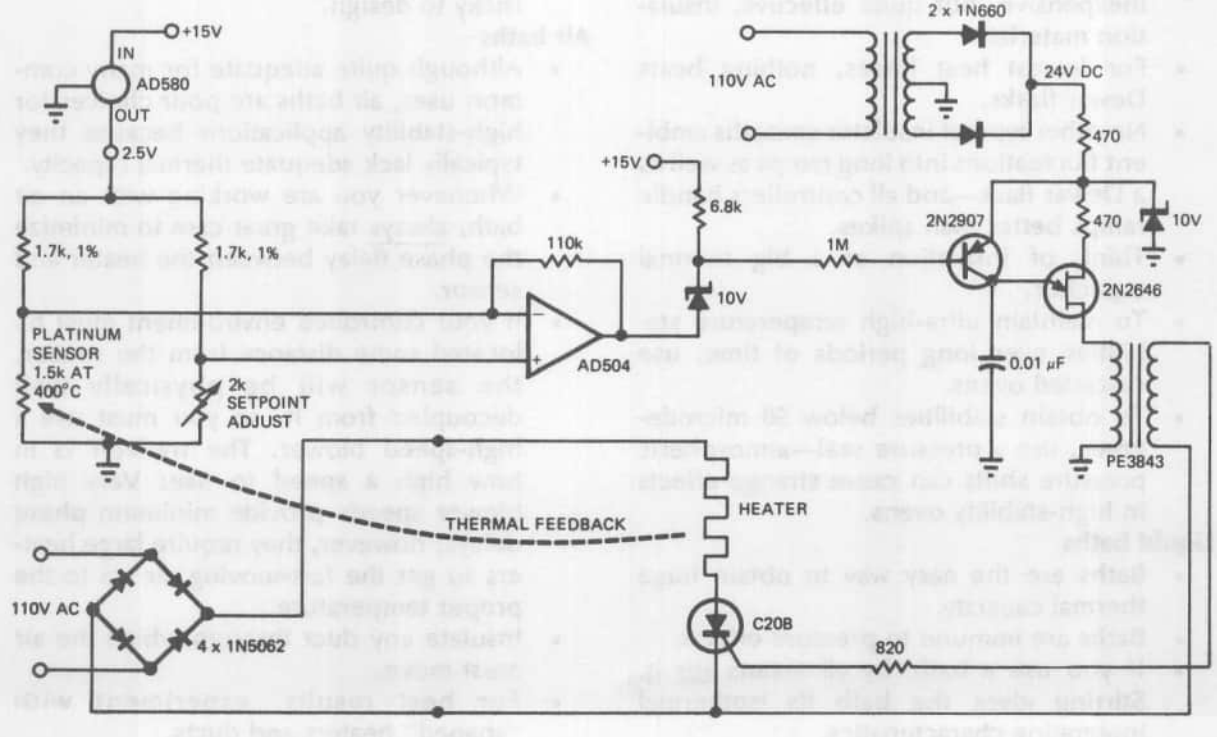

Fig. 5—Servo-controlled phase-angle firing of an SCR can provide linear thermal control to 0.001° stabilities with a properly designed thermal load. Beware of the RFI generated, however.

isolation transformer.

This system provides analog temperature control as the AD504 biases the 2N2907-2N2646 combination to fire at different points on the ac waveform. The 2N2646 always runs at 60 Hz, but the op amp's servo action controls the phase angle at which it fires. The integral of the ac waveform across the heater equals the dc level of the energy leaving the oven.

Phase-fired circuits of this type should be arranged so that the SCR chops at the peak of the waveform, thereby ensuring the highest gain. And the higher the gain, the more closely this circuit can approximate "energy in equals energy out" operation. The gain, in turn, is limited by that eternal problem of thermal control loops—phase delay.

Typically, a circuit of this type can exceed 0.001° stabilities if the thermal load is properly designed.

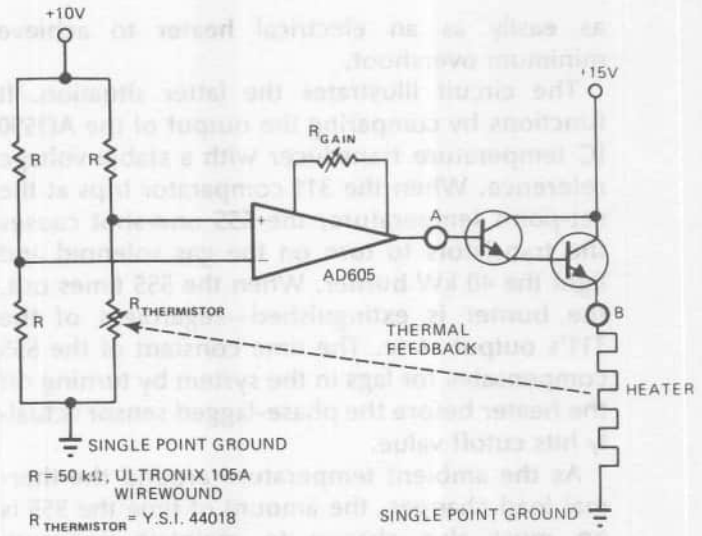

Fig. 6—Instrumentation-amplifier gain resistor sets the loop gain in this linear thermal controller. Circuit can control an oven or bath to stabilities of 75 microdegrees.

Thermal-control system design hints

Ovens

- Always pay careful attention to oven geometry.
- Thick walls help reduce heat losses.
- Spheres, though cumbersome, are the best choice for a super stable oven.
- Cylindrical ovens provide good performance, but the heater wires must be wound more densely on the ends to compensate for losses there.
- Styrofoam and fiberglass are relatively inexpensive, but quite effective, insulation materials.
- For lowest heat losses, nothing beats Dewar flasks.
- No other type of insulator smooths ambient fluctuations into long ramps as well as a Dewar flask—and all controllers handle ramps better than spikes.
- Think of insulation as a big thermal capacitor.
- To maintain ultra-high temperature stabilities over long periods of time, use cascaded ovens.
- To obtain stabilities below 50 microdegrees, use a pressure seal—atmospheric pressure shifts can cause strange effects in high-stability ovens.

Liquid baths

- Baths are the easy way to obtain huge thermal capacity.
- Baths are immune to pressure effects.
- If you use a bath, by all means stir it. Stirring gives the bath its isothermal integrating characteristics.
- Use caution in the design of a stirred bath. Carefully evaluate propellor type and placement, as well as the type, size, shape and placement of all baffles. In particular, watch out for layering effects.
- Heater placement deserves extra thought and experimentation. Consider evenly distributed heater schemes such as the concentric spiral.
- Multisensor schemes can take advantage of a bath's fast integration property. However, such configurations can be tricky to design.

Air baths

- Although quite adequate for many common uses, air baths are poor choices for high-stability applications because they typically lack adequate thermal capacity.
- Whenever you are working with an air bath, always take great care to minimize the phase delay between the heater and sensor.
- If your controlled environment must be located some distance from the sensor, the sensor will be physically well decoupled from it, so you must use a high-speed blower. The tradeoff is in how high a speed to use: Very high blower speeds provide minimum phase delays; however, they require large heaters to get the fast-moving air up to the proper temperature.
- Insulate any duct through which the air must move.
- For best results, experiment with "shaped" heaters and ducts.

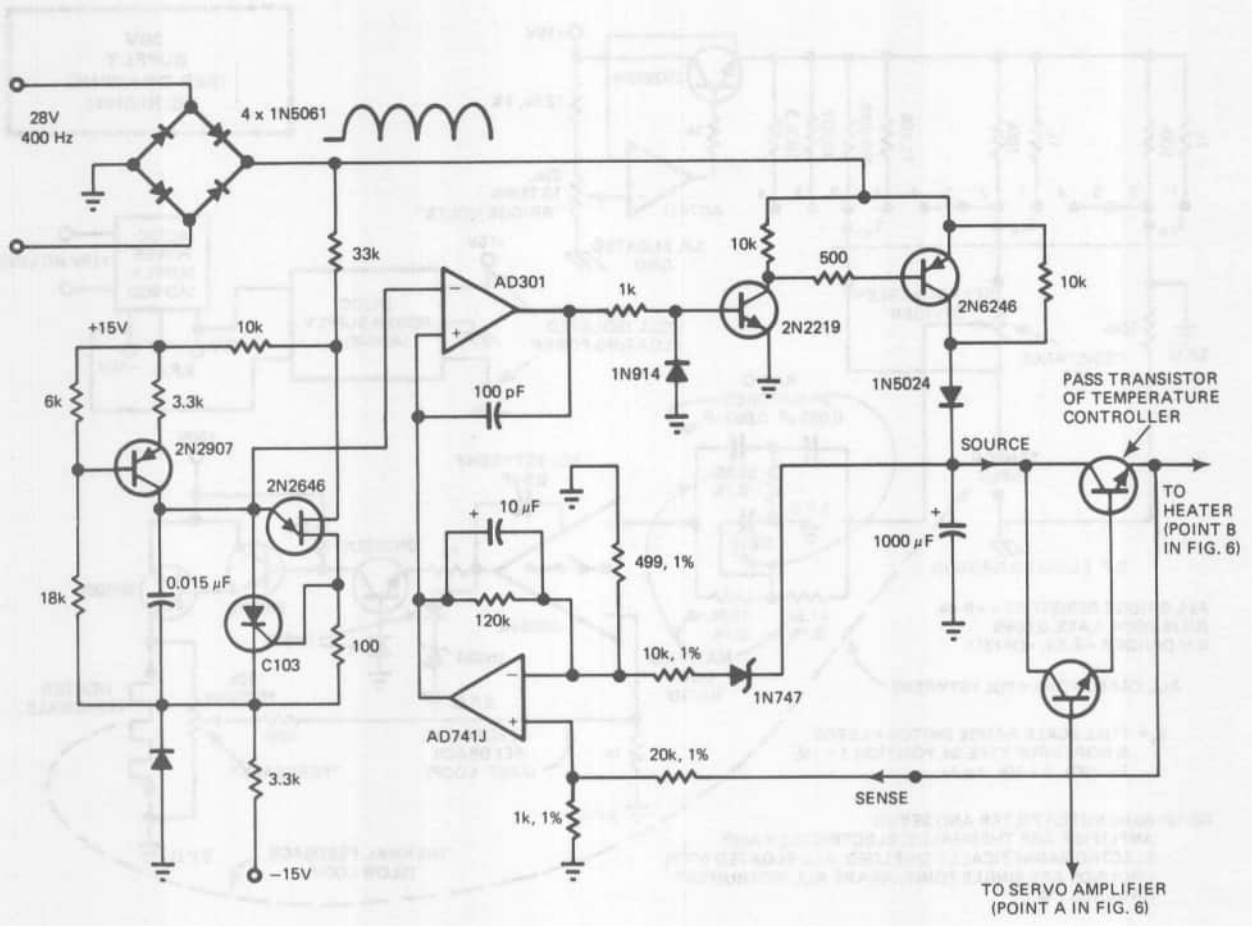

Fig. 7—To reduce the power dissipated in Fig. 6's pass transistor, this circuit maintains a constant 3V across it.

However, note that it generates significant RF noise because the SCR chops in the middle of the waveform. This noise can be especially troublesome if the circuit serves to control an oven containing RFI-sensitive low-level electronics.

For applications demanding the very best

Certain situations require ultra-stable temperature control that can only result from a true linear system. Zener reference and quartz crystal time-drift studies, laser micro-interferometry, crystal growing and (especially) biochemical microcalorimetry have benefitted from the development of ultra-stable thermal control. Temperature controllers with a stability of 3 microdegrees at 50°C have been constructed. That's just 0.06-ppm drift!

To achieve such spectacular performance, you must use components with the ultimate in specifications and pay strict and careful attention to every detail of the thermal system. **Fig. 6** shows a circuit that will control an oven or bath to stabilities of about 75 microdegrees at 37.5°C.

In operation, the bridge offset is sensed by an instrumentation amplifier that features high common-mode rejection, low drift and balanced inputs. The amplifier drives a Darlington pair that provides current gain to the heater. Loop gain, controlled by the gain-setting resistor at the instrumentation amplifier, is adjusted so that the loop is stable and a dc voltage appears across the heater.

One of the penalties of this circuit is that the pass transistor must dissipate any power not delivered to the heater. Since an ample collector supply must be available for turn-on and low-temperature ambient conditions, the device may have to handle a sizeable amount of power within many operating environments.

Fig. 7 shows an accessory circuit that you can add to **Fig. 6's** controller to eliminate this problem. Developed for an aerospace application that requires high efficiency, the circuit is essentially a servo that maintains a constant 3V across the pass transistor regardless of the controller's demand for power.

The 741 looks differentially across the transistor, with its negative input biased through a 3.3V zener. The op amp's output is compared to a 400 Hz line-synchronized ramp by a 301A amplifier that functions as a pulse-width modulator and drives a 2N2219-2N6246 switch. In turn, the switch delivers phase-controlled power to the 1000 µF integrating capacitor and the temperature-controller pass transistor. The 1N5624 diode

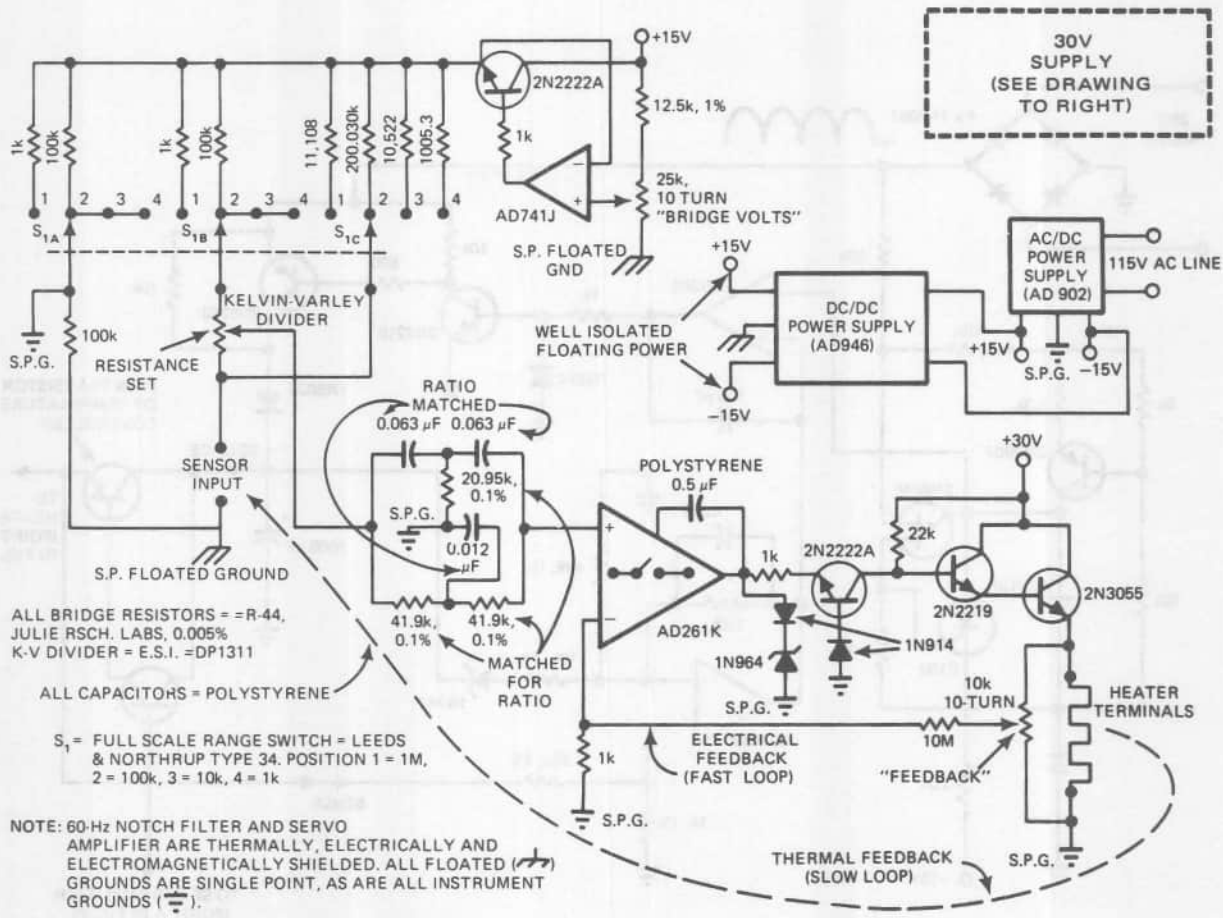

Fig. 8—Kelvin-Varley divider dials out the resistance control point directly in this circuit that accommodates sensor resistances from 10Ω to 1 MΩ. The feedback potentiometer provides adjustable global feedback.

ensures that the 2N6246 will not be reverse biased when the 400 Hz signal falls below the dc value of the 1000 μF capacitor.

This circuit avoids the unpleasant surprises that may arise when a servo loop is run within a servo loop by giving the dissipation-limiting servo a much slower time constant than the thermal-control servo. The 10 μF capacitor across the 301A serves this function.

Settling in 2.5 sec for a 500 μ° step

Chopper-stabilization techniques and other refinements embodied in the circuit of **Fig. 8** provide the ultimate in temperature control. The circuit features a multiranging bridge that accommodates sensors from 10Ω to 1 MΩ—a Kelvin-

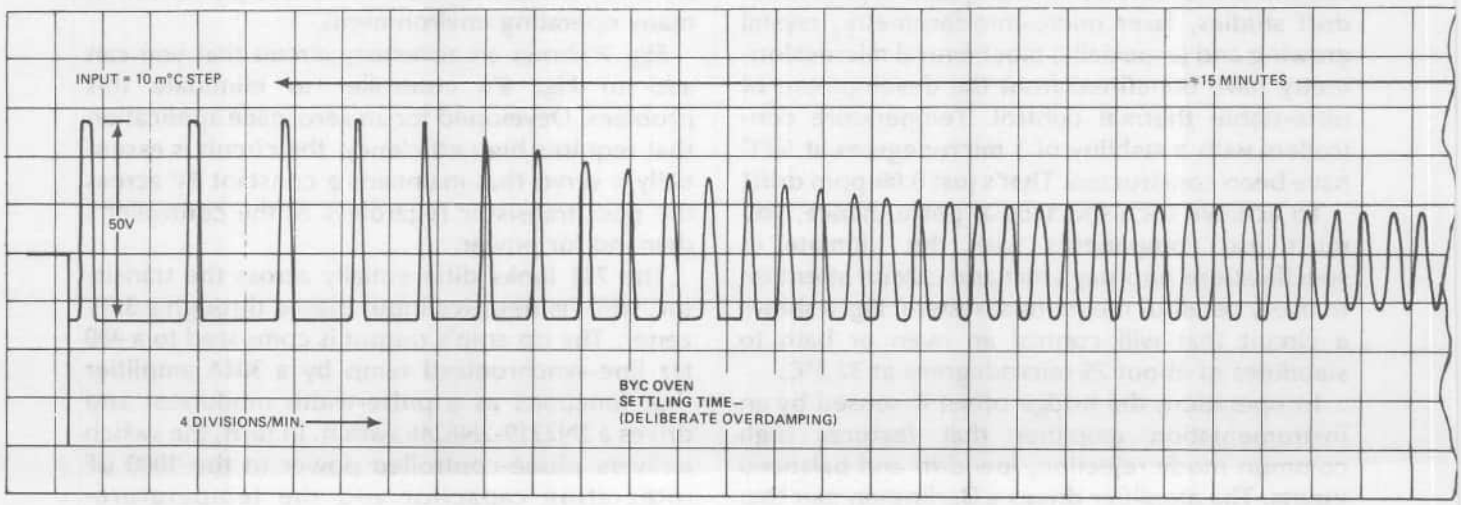

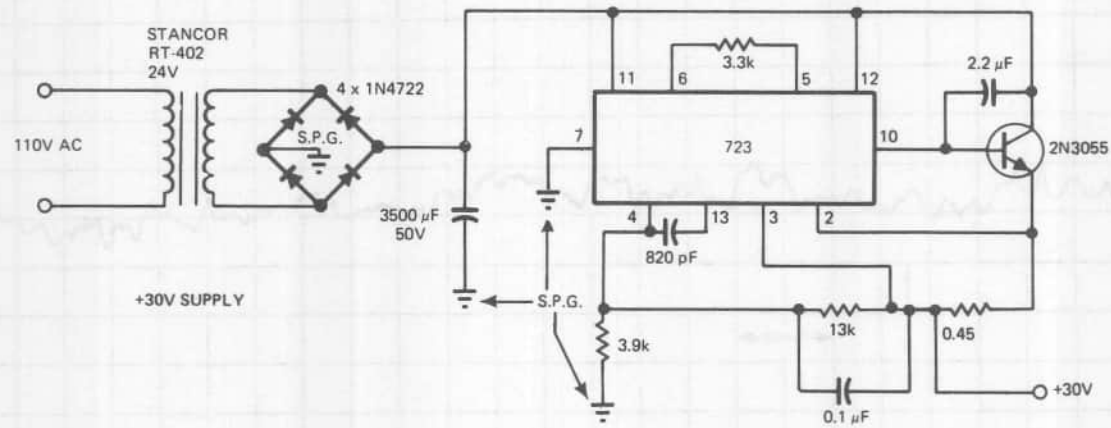

Varley divider dials the sensor-resistance control point directly to five digits.

A floated power supply drives the bridge. This approach allows the single-ended noninverting chopper-stabilized amplifier to take a differential measurement, and also completely eliminates the common-mode voltage error an instrumentation amplifier would contribute. A passive 60 Hz notch filter eliminates the pick-up noise of the floated bridge. The common base-amplifier transistor at the 261K's output provides sufficient amplification to permit the Darlington pair to drive up to 30V across the heater. Note that the feedback potentiometer is across the total of all gain elements in the circuit and supplies adjustable global feedback.

The thermal loop operates separately from the electrical loop, with the latter functioning to set the circuit gain at maximum; i.e., the feedback setting at which the system exhibits a nearly perfect response. **Fig. 9** shows an optimum response waveform obtained by step changing the temperature set point by 500 microdegrees.

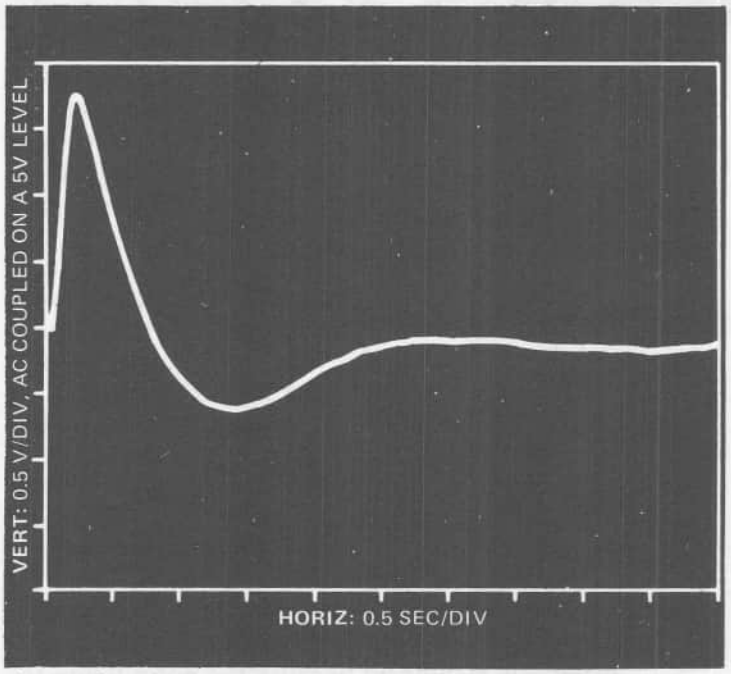

Fig. 9—Changing the temperature set point by 500 microdegrees causes **Fig. 8's** entire loop to settle within 2.5 sec, indicating that the gain is set for optimum response.

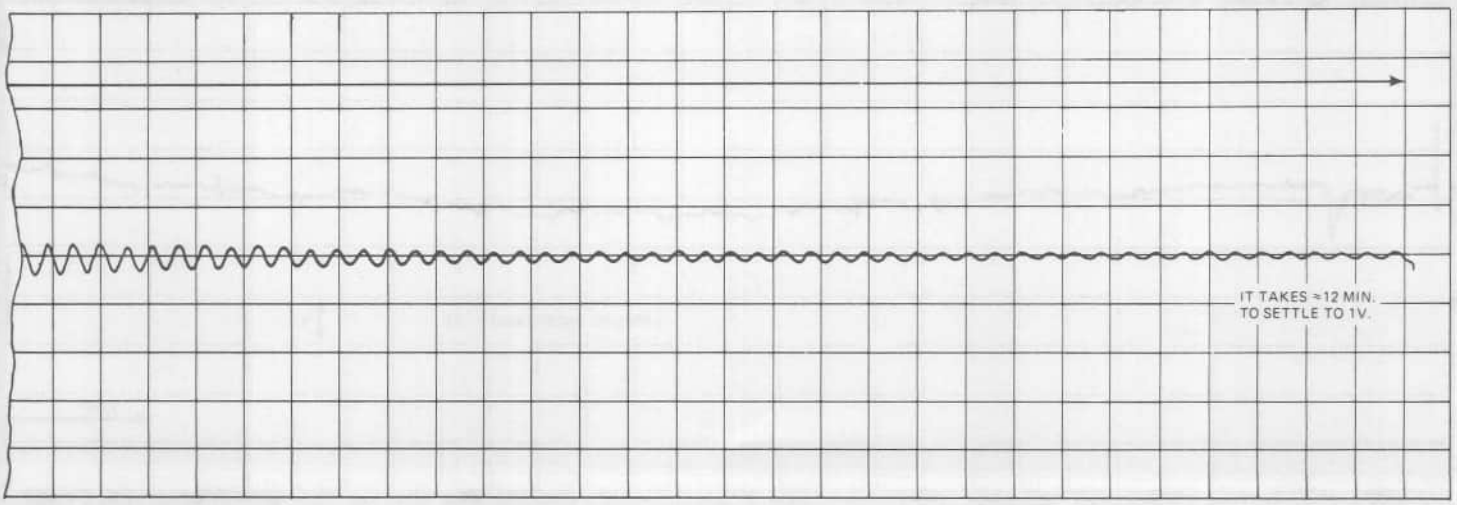

Fig. 10—High loop gain puts the circuit of **Fig. 8** on the verge of oscillation. Ringing resulting from a 10 millidegree step set-point change lasts almost 15 min.!

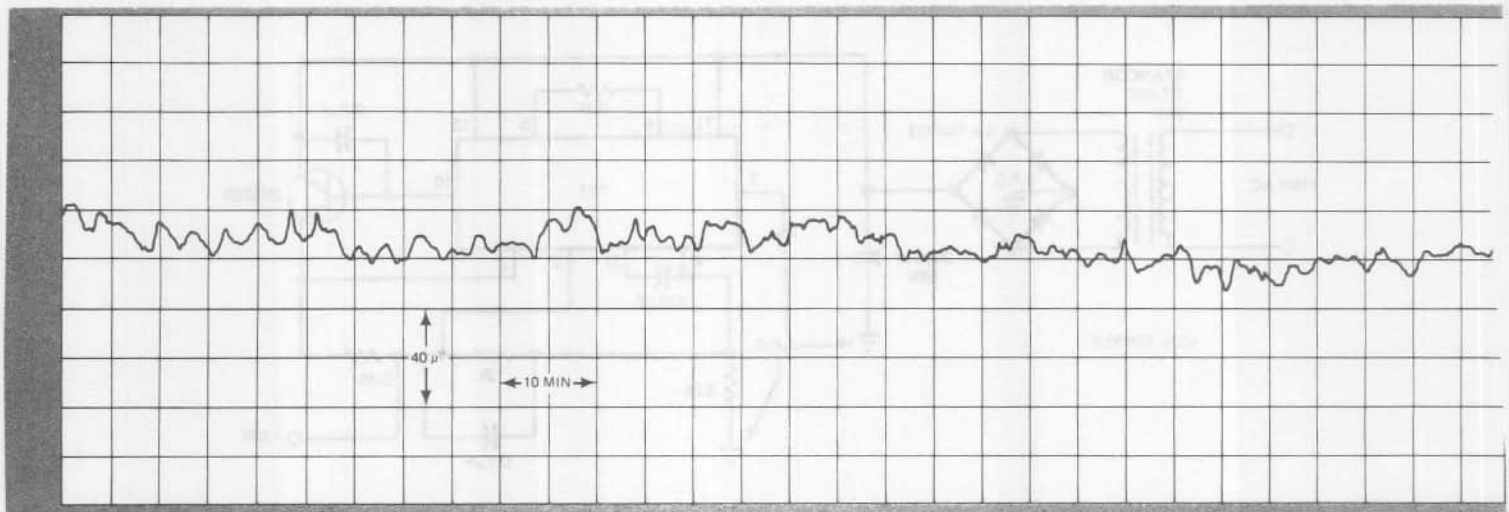

Fig. 11—Stability of spherically shaped, Dewar enclosed, pressure-sealed oven is measured at 3.3 microdegrees over a 3-hr period, despite the sensor's 3 microdegree (calculated) noise figure. (Only part of the trace is shown.)

The same loop can also generate some extraordinary waveforms. When the loop gain was set so high that the circuit was on the verge of sustaining oscillation, a 10 millidegree step setpoint change produced a damped, ringing response of almost 15 minutes duration **(Fig. 10)!**

Would you believe 3.3 μ° control?

High-quality control loops equipped with thermally optimized ovens and operating under tightly controlled laboratory conditions can provide amazing results. The strip chart of **Fig. 11** shows the stability of a spherically shaped, Dewar enclosed, pressure-sealed oven (since PV=nRT, ultra-high stability control requires pressure sealing to avoid atmospheric pressure shifts from causing temperature deltas inside a fixed-volume oven). Observe that the servo holds the monitoring sensor in the oven to within just 3.3 millionths of a degree for over three hours. This proves especially significant because the noise figure for the particular sensor used was calculated at about 3 microdegrees.

Fig. 12 shows what happens to the stability baseline when a 20 nW pulse—generated by putting 20 mV across a 1 MΩ resistor for 15 sec—is released into the oven 1 inch from the monitoring sensor. Temperature rise at the sensor is 7 μ° peak; setting time, about 11 min. to within 2 μ° of the initial baseline. Note that this performance is achieved despite the fact that most of the energy released is not picked up by the monitoring sensor. (As a point of reference, a single human cell operates at about the nanowatt level.)

Other controllers provide special functions

Some temperature-control applications require other than simple stability. **Fig. 13's** circuit furnishes a linear temperature shift from 45°C to 45.2°C over a 10,000-hr period. It drives a controller similar to the one in **Fig. 8** and consists of a voltage referenced half-bridge, a 16-bit digital-to-analog converter and an integrator.

Initially, the DAC's output is zero and the oven

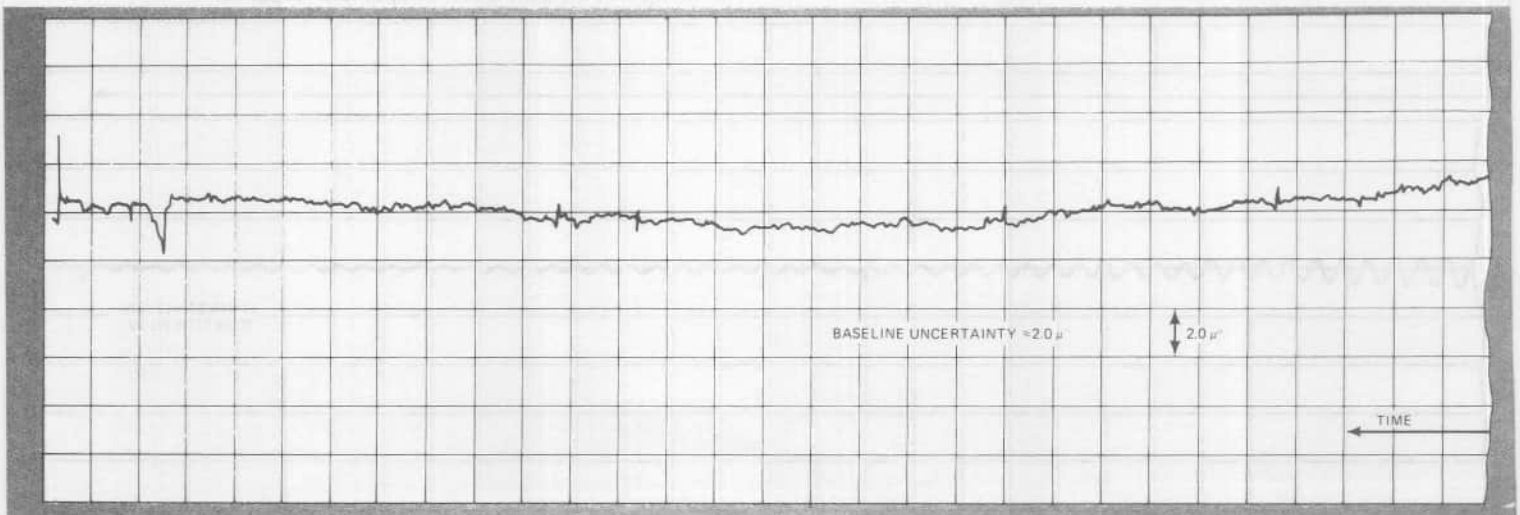

Fig. 12—A 20 nW pulse released 1 in. from the monitoring sensor into the oven described in **Fig 11** produced this extraordinary trace. Peak temperature rise is 7 microdegrees.

is running at 45°C and stabilized. Then, every 10 min. the DAC is clocked one step, each time producing a set-point change of 3 microdegrees via the summing amplifier. The amplifier's output is integrated with a time constant slightly greater than 10 min., producing the obsolutely smooth ramp that feeds the temperature controller's reference input. Over 10,000 hours time the temperature of the controlled environment slews from 45°C to 45.2°C in a highly linear fashion. Nonlinear functions can also be obtained by clocking the DAC aperiodically.

Other special-type controllers include feed-forward systems and heater-sensed controllers. In a feed-forward system the temperature of the ambient surrounding the controlled environment is sensed, differentiated with the appropriate time constant and summed with the servo sensor's signal. The advantage of this type of system is that it gives the controller the "look ahead" capability it needs to offset large ambient shifts. Feed-forward systems particularly suit situations such as large buildings where the controlled environment lacks good insulation characteristics. In general, they are cost effective when designed properly, which proves no easy task. Results range from excellent to catastrophic.

Because heater-sensed controllers use the heater itself as a sensor, they offer very fast response and are perhaps more reliable and cost effective than separate sensor types. However, they are usually somewhat lacking in precision because most heater materials exhibit only small changes in resistivity with temperature. Most controllers of this type time-share the heater/sensor function. □

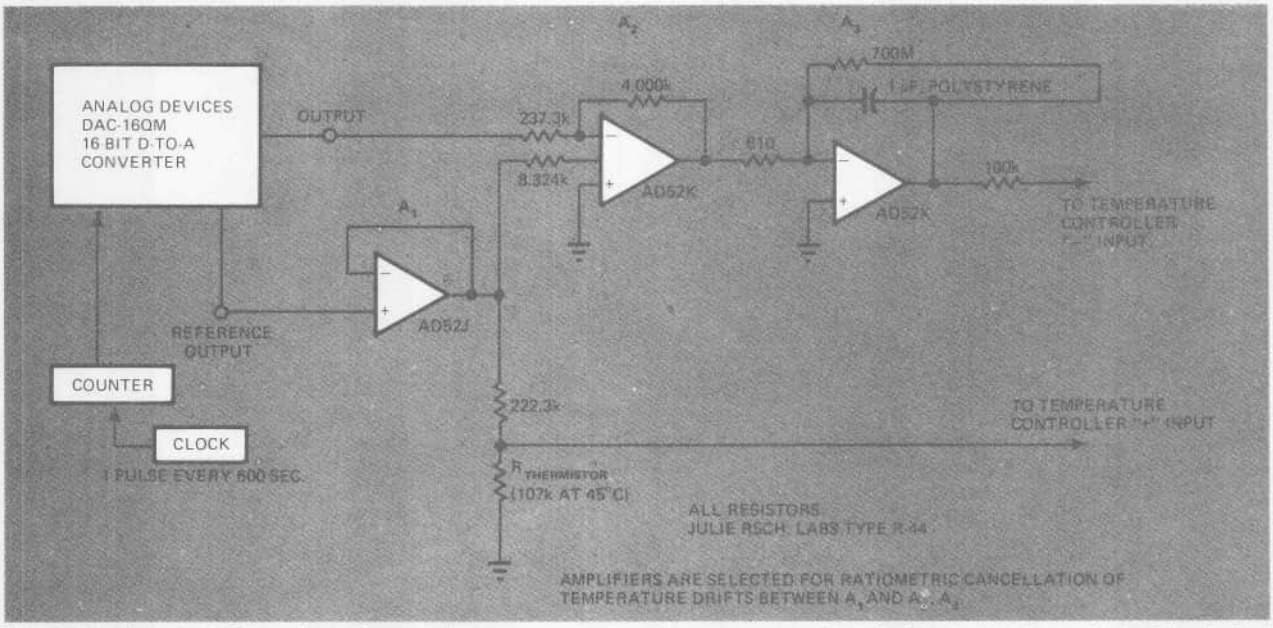

Fig. 13—It takes 10,000 hrs. to linearly ramp the oven temperature from 45.0 to 45.2°C with this circuit. The 16-bit DAC is clocked one step every 10 min. to produce a 3 μ° set-point change.

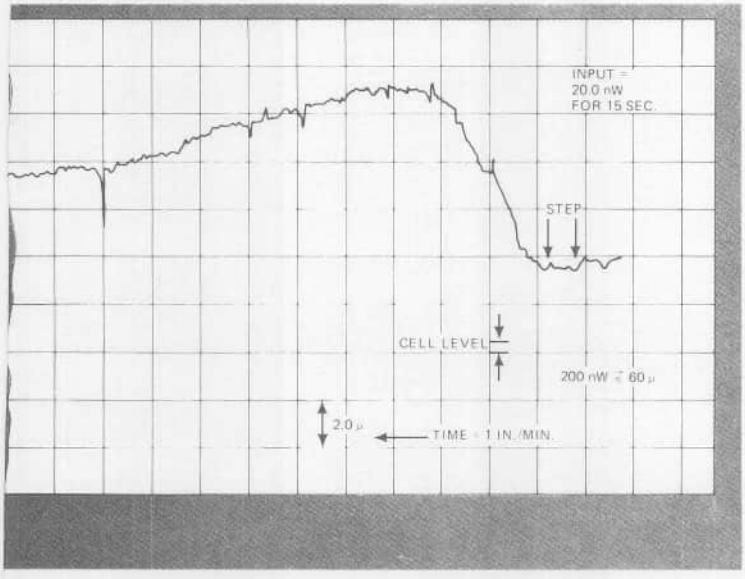

Bibliography

1. *Fulton, S.P., "The Thermal Enzyme Probe," S.B. Thesis, M.I.T., Cambridge, MA, 1975.*
2. *Harvey, M.E., "Precision Temperature Controlled Water Bath," Review of Scientific Instruments, 39-1, 1968.*
3. *Krasner, M., "Precision Control of Temperature," Dept. of Electrical Engineering, M.I.T., Cambridge, MA, 1974.*
4. *Olson, J.V., "A High Stability Temperature Controlled Oven," S.B. Thesis, M.I.T., Cambridge, MA, 1974.*
5. *Williams, J.M., "Temperature Control of Microdegrees," Educational Research Center, M.I.T., Cambridge, MA, 1971.*
6. *Williams, J.M., "Portable Wide Range Chopper Stabilized Temperature Controller," Dept. of Nutrition and Food Science, M.I.T., Cambridge, MA, 1974.*
7. *Williams, J.M., "Split a Temperature Degree to 10 Microdegrees," Electronic Design, May, 1974.*

Employ pulse-width modulators in a wide range of controllers

Generally considered a power-supply controller, the pulse-width modulator suits many other applications such as lamp-intensity control and motor-speed regulation.

Jim Williams, National Semiconductor Corp

By applying the pulse-width-modulator (PWM) capabilities that serve so well in high-efficiency power supplies, you can control many diverse functions. PWM ICs such as the LM3524 contain several operational blocks (see **box,** "A pulser plus"), giving them the versatility to simplify control tasks.

Level a lamp's luminosity

As a first example, consider what happens when evaluating optoelectronic sensors or trying to accurately duplicate a 35-mm color slide. The light source used must maintain constant intensity. **Fig 1** demonstrates how you can combine a PWM with a photodiode/amplifier stage to servo-level a lamp's output intensity and thereby meet this need.

In this design, the LF356 op amp functions as a current-to-voltage converter. Thus, as the lamp's output increases, the resulting higher radiant energy causes the photodiode to draw more current out of the op amp's summing junction. The amp responds by generating a positive-going output voltage that feeds back into the input and re-establishes the summing junction's requisite zero balance.

The op amp's output voltage—a function of the photodiode's light-induced current flow—also feeds the PWM's on-chip error amplifier. This amplifier compares the unknown voltage at pin 1 with the intensity-control value set by the 2.5-kΩ potentiometer. (Note that the reference voltage for the intensity setting comes from the PWM's on-chip 5V supply.) This error voltage, amplified by approximately 70 dB as determined by the 1-MΩ resistor loading pin 9, controls the PWM's ON time.

In addition to the 1-MΩ resistor, a 0.001-μF capacitor loads pin 9. This RC combination provides the feedback loop with the proper frequency compensation

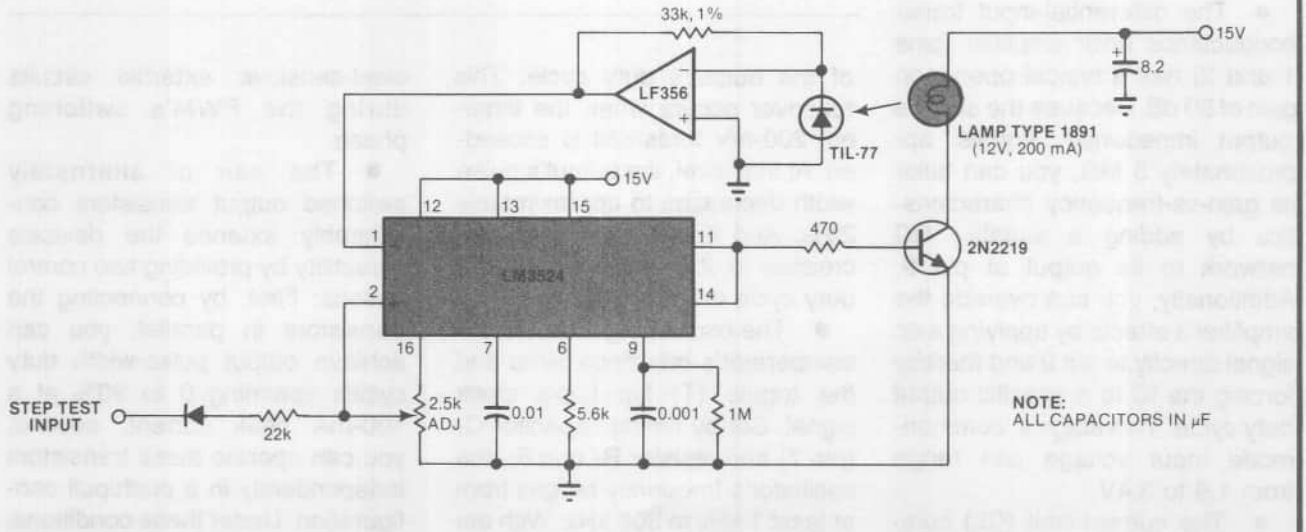

Fig 1—A lamp's intensity remains constant *when you drive the lamp with a pulse-width modulator (PWM) in an optical closed-loop feedback scheme. Here the PWM's ON time is controlled by comparing a photodiode's output with a preset intensity reference level.*

Pulse-width-modulate a lamp to keep its brightness constant

by rolling off with a 1-msec time constant. Similarly, the 5.6-kΩ/0.01-μF combination connected to pins 6 and 7 sets the PWM's oscillator frequency to about 30 kHz.

The lamp is driven by a combination of the IC's on-chip transistors and a discrete 2N2219. **Fig 2a** shows the design's servo action; note that when the 2N2219's collector pulses ON (upper trace), the LM356's output ramps up rapidly (lower trace). But when the drive ramps up rapidly (lower trace). But when the drive-transistor turns off, the resultant negative-going signal ramps much slower because the lamp accepts energy more readily than it gives energy up.

Figs 2b and **c** better illustrate the lamp's action. Here the servo loop is artificially upset by introducing an external pulse via **Fig 1**'s circuit's Step Test port. As shown in **Fig 2b,** when the input pulse (upper trace) goes HIGH, the diode blocks any bias injection, and the op amp's output (lower trace)—and therefore the lamp's brightness—remains constant. However, when the input pulse goes LOW, current flows out of the intensity-control potentiometer's wiper via the 22-kΩ

A pulser plus

Pulse-width-modulator (PWM) ICs —such as the LM3524—include several on-chip function blocks that aid application to circuit designs other than regulated power supplies. By gaining an understanding of these circuits' operation, you'll discover how to employ a PWM in many applications.

The **figure** depicts the PWM's major functions:

- An on-chip voltage regulator supplies a stable 5V, 50-mA output for external usage in addition to handling all on-chip supply requirements. Capable of operating over an input voltage range of 8 to 40V (pin 15), this stage's output (pin 16) varies no more than 30 mV with a varying input. Thus, it provides an excellent reference level for closed-loop feedback schemes.
- The differential-input transconductance error amplifier (pins 1 and 2) has a typical open-loop gain of 80 dB. Because the stage's output impedance equals approximately 5 MΩ, you can tailor its gain-vs-frequency characteristics by adding a suitable RC network to its output at pin 9. Additionally, you can override the amplifier's effects by applying a dc signal directly to pin 9 and thereby forcing the IC to a specific output duty cycle. This stage's common-mode input voltage can range from 1.8 to 3.4V.
- The current-limit (CL) comparator (pins 4 and 5) can override the error amplifier and take control of the output's duty cycle. This takeover occurs when the inherent 200-mV threshold is exceeded. At that level, the output's pulse width decreases to approximately 25%. And if the input signal increases to 210 mV, the output's duty cycle drops to 0%.
- The oscillator generates the comparator's reference ramp and the toggle (T) flip flop's clock signal. Set by timing capacitor C_T (pin 7) and resistor R_T (pin 6), the oscillator's frequency ranges from at least 1 kHz to 300 kHz. With the oscillator's output pulse (pin 3), you can disable ("blank") transient-sensitive external circuits during the PWM's switching phase.
- The pair of alternately switched output transistors considerably extends the device's versatility by providing two control options: First, by connecting the transistors in parallel, you can achieve output pulse-width duty cycles spanning 0 to 90% at a 100-mA peak current; second, you can operate these transistors independently in a push/pull configuration. Under these conditions, you can vary the duty cycle for each device from 0 to 45%.

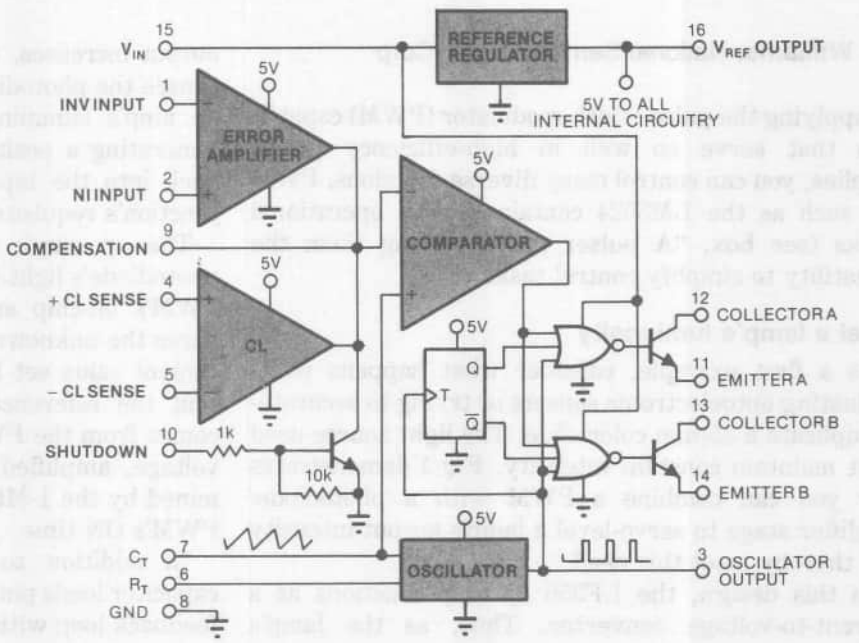

Pulse-width-modulator ICs *contain several sense-and-control function blocks that extend the device's capabilities to other application areas. Error-voltage-amplifying, current-sensing and logic-level-shutdown stages are part of the chip's resources.*

resistor. This action causes the servo loop to lower the drive level to the lamp proportionately.

Note again how the lamp's ON and OFF times differ. But at high intensity levels, the lamp's on/off characteristics reverse themselves (**Fig 2c**) because the lamp then acts as a more efficient radiant-energy source.

μPs read pulse width vs temperature

In a second application, a μP-based data-acquisition system can directly monitor a wide temperature range, using **Fig 3**'s design. The temperature transducer, an LM135 IC, provides a highly linear 10-mV/°K output voltage over its calibrated range of −55 to +150°C. (You can operate the IC to 200°C on an intermittent basis.) The voltage-to-pulse-width conversion circuits—the op amp, PWM and associated networks—can convert any slowly changing 0.1 to 5.0V input signal to a 0 to 500-μsec-wide output pulse with 0.1% linearity. Thus, this scheme satisfies many data-acquisition requirements without modification; just connect an unknown signal to the 100-kΩ input resistor.

In **Fig 3**'s configuration, the input resistor string divides down the temperature transducer's output and applies it to the op amp's noninverting (+) input. This positive input voltage, once amplified, directly drives the PWM's on-chip comparator. (The on-chip error amplifier isn't used because its limited common-mode input range of 1.8 to 3.4V can't encompass the overall design's full capability. The off-chip LM358, on the other hand, handles inputs down to 0V.)

The PWM responds to a variable input voltage by generating a variable-width output pulse: 0.1V yields a zero-width output pulse and 5V produces a 500-μsec-wide output. The resulting TTL-compatible output pulse is clipped to 1.235V by the LM185 and integrated by the 1-MΩ/0.1-μF network. This dc feedback voltage gets summed at the op amp's inverting (−) input and linearizes the voltage-to-pulse-width conversion. (The 1000-pF feedback capacitor provides loop stability.) Adjusting the converter to data-acquisition requirements proves simple: Trim the 5-kΩ potentiometer for the proper pulse width at a known input temperature.

Pulse-width-control an oven

Fig 4 shows how you can regulate an oven's temperature using just the pulse-width-modulator chip. Here, a platinum resistance temperature detector (RTD) functions as the variable element in a resistive-bridge circuit. When you first apply power, the RTD—with its positive temperature coefficient—has a lower resistance than the corresponding 2-kΩ resistor in the bridge, and as a result, the LM3524's + input is at a more positive voltage than its inverting input. This imbalance forces the PWM's output pulse to its maximum value of 90%; it also turns on the 2N3507 power transistor and thus the oven's heater. When the oven reaches its operating temperature, the servo shuts down to the value needed to maintain temperature equilibrium.

The 330-kΩ/4.7-μF combination sets the servo's gain

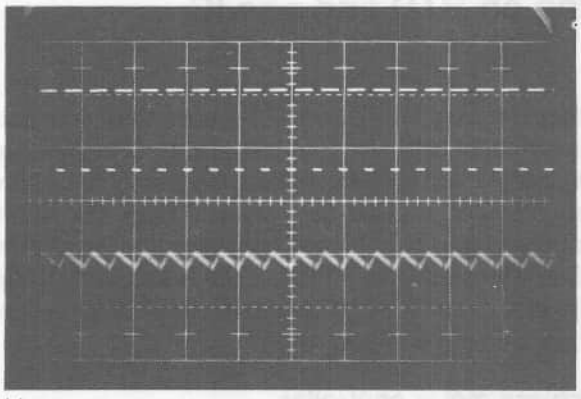

(a)

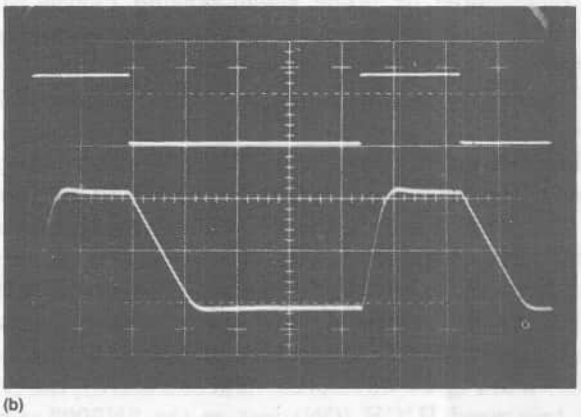

(b)

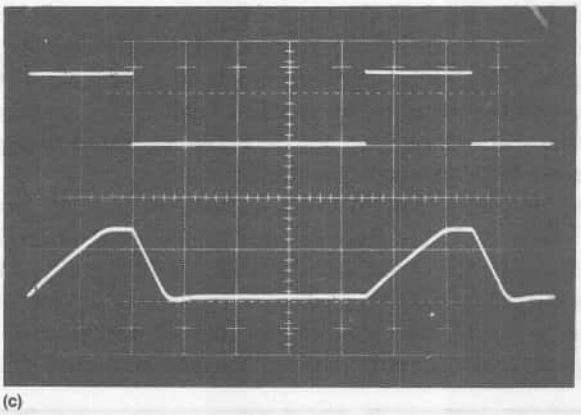

(c)

PHOTO	TRACE	VERTICAL	HORIZONTAL
(a)	UPPER	10V/DIV	100 μSEC/DIV
	LOWER	0.005V/DIV (ON 1V DC LEVEL)	
(b)	UPPER	5V/DIV	1 mSEC/DIV
	LOWER	0.05V/DIV (ON 1V DC LEVEL)	
(c)	UPPER	5V/DIV	1 mSEC/DIV
	LOWER	0.05V/DIV (ON 1V DC LEVEL)	

Fig 2—A closed-loop-servo design *closely tracks and corrects for a lamp's changing intensity. As shown in* ***(a)****, when* ***Fig 1****'s lamp-driver transistor pulses ON (upper trace), the loop amplifier's output starts ramping up to re-establish the loop's stability. Note how the lamp's turn-on time is shorter than its turn-off time when operating at low intensity levels* ***(b)****. This situation reverses* ***(c)****, however, at high output levels.*

Hold an oven to within 0.1°C using an RTD and one IC

to approximately 55 dB at 1 Hz—more than adequate for most applications. Similarly, the 2.7-kΩ/0.2-μF timing components set the pulse's frequency to approximately 15 kHz, a point far removed from the servo's 1-Hz pole frequency. If you maintain a close thermal proximity between the RTD and the heater, this design easily maintains a 0.1°C control point over widely varying ambient temperatures.

A tachless motor controller

A tachometer or other speed-sensing device isn't necessary when you employ **Fig 5**'s motor controller. Instead of a tach, this scheme uses the motor's back EMF to bias the feedback loop that governs the motor's speed.

When you apply power, the PWM's + input lies at a higher potential than its − input. The PWM outputs a 90% ON pulse that (via the 2N5023) starts the motor turning (**Fig 6**) and feeds the 1000-pF/500-kΩ differentiator network. The LM393 compares this level with the PWM's 5V reference, and the resulting delayed pulse triggers the LF198 sample-and-hold (S/H) device. As shown in **Fig 6**'s waveforms (traces b and d), the S/H IC is triggered HIGH (ON) just as the 2N5023 stops supplying current to the motor (traces a and c). At this instant, the motor coils generate a flyback pulse that's damped by the shunt-opposed diode. But even after the flyback pulse decays, the motor's back EMF remains, and this voltage, held by the S/H chip when the trigger pulse ceases, then controls motor speed.

The 10-kΩ/4-kΩ divider attenuates the motor's back EMF to ensure that the S/H output doesn't exceed the PWM's common-mode input range. Additionally, the S/H's output is filtered to keep things quiet during the sampling period and clamped to prevent any negative-going signals from damaging the PWM input. (The S/H's 10-MΩ bleeder resistor prevents the servo from never achieving stability in the unlikely event that the 0.01-μF sampling capacitor charges to a level greater than the motor's back EMF.) The 39-kΩ/100-μF time constant sets the loop's frequency response, and the 60-kΩ/0.1-μF combination determines the pulse-modulation frequency (300 Hz). You avoid overshoot problems and aid the loop's transient response by employing the 2-kΩ resistor divider and diode network; this configuration limits the maximum output duty cycle to 80%.

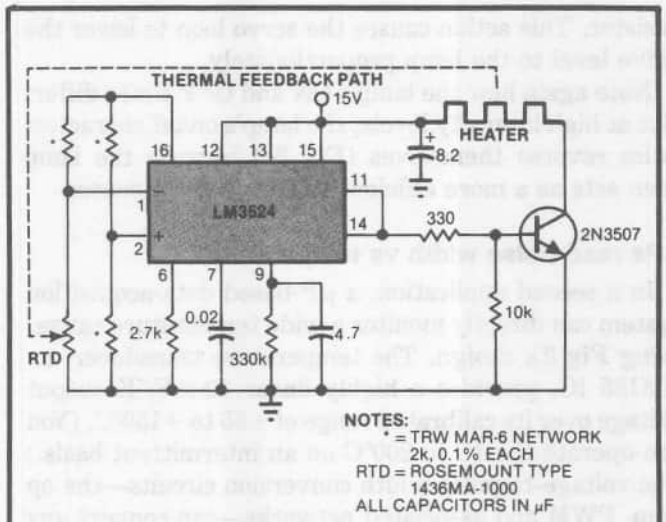

Fig 4—An oven's temperature remains constant *to within 0.1°C when a pulse-width modulator (PWM) controls the heater's power. Switching at 15 kHz, the PWM obtains the error signal from a platinum resistance temperature detector.*

Supply analog circuits at ±15V

Analog designers interested in the previous circuit seldom have much use for the 5V-only dc power supplies that digital designs thrive on. They will, however, find plenty of use for **Fig 7**'s design; it converts a 5V source into a ±15V, 100-mA supply suitable for analog designs.

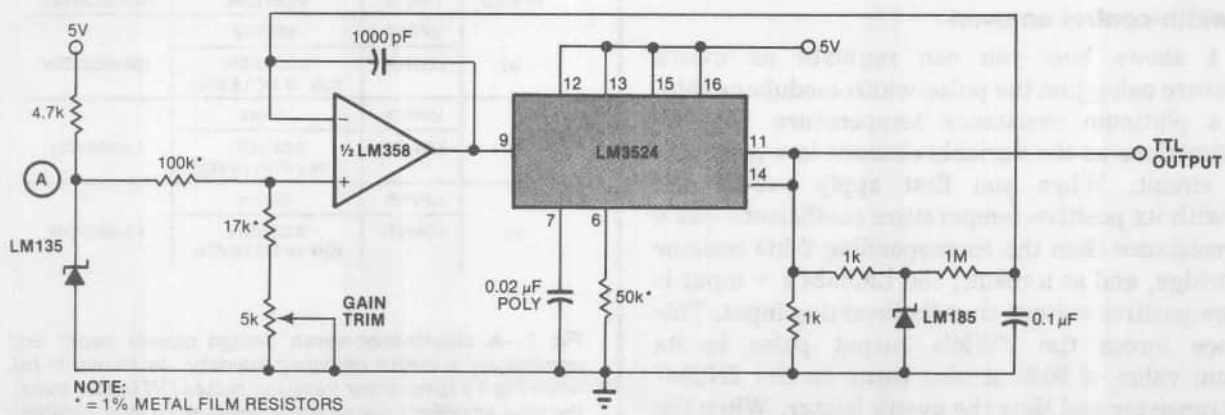

Fig 3—Temperature-to-pulse-width conversion *results when an LM135 transducer provides a temperature-dependent error signal directly to the pulse-width modulator's comparator input. The TTL output's pulse width varies from 0 to 500 μsec for a 0.1 to 5V input swing at point A.*

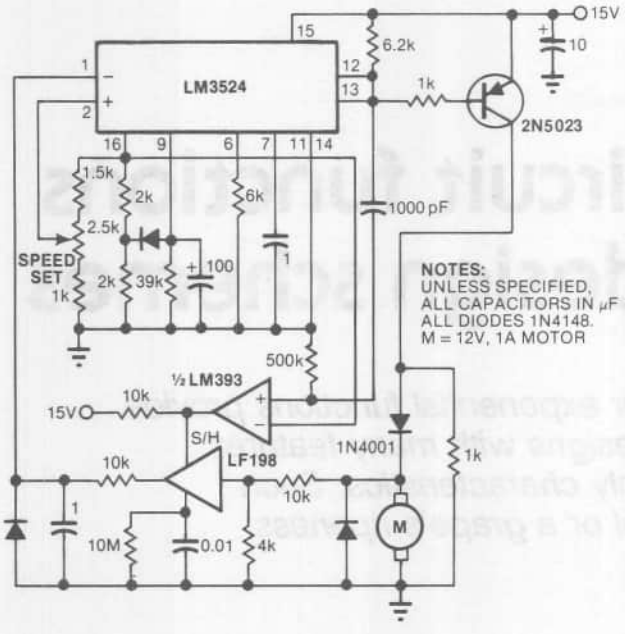

Fig 5—A motor's back EMF *provides the error signal in this motor-speed-control servo loop. After passing through a sample/hold stage* ***(Fig 6),*** *the smoothed error signal feeds the pulse-width modulator's control input.*

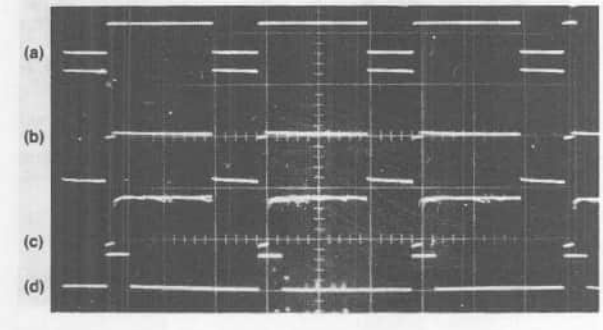

Fig 6—The motor's back EMF is sampled *(traces b and d) at the time* ***Fig 5****'s motor-drive transistor stops conducting (traces a and c). Although the motor generates a flyback pulse when the drive current stops, the remaining back voltage is what's held.*

Unlike the previous examples, the LM3524's on-chip output transistors here operate out of phase to provide a pulse-width-modulated push/pull signal to the transformer's driver transistors. Switching at 30 kHz, the transformer's output is rectified and filtered to obtain complementary but unregulated dc output voltages. The 15V output feeds back via an adjustable resistor divider and is compared with a reference voltage by the PWM's error amplifier. (The reference must stay at 2.4V to ensure that the error amplifier operates within its common-mode range.) This feedback loop regulates the +15V output, and an LM137 supplies the −15V.

Overcurrent protection results when the PWM's on-chip current-limit comparator senses a 200-mV level across the 2N2219s' 0.33Ω emitter resistor. When the current exceeds this threshold level, the comparator shuts down the chip's internal drivers and thus the entire converter. You can disable the converter during, for example, power-up sequencing by applying a TTL HIGH at pin 10. **EDN**

Author's biography

Jim Williams, applications manager with National Semiconductor's Linear Applications Group (Santa Clara, CA), specializes in analog-circuit and instrumentation development. Before joining the firm, he served as a consultant at Arthur D Little Inc and directed the Instrumentation Development Lab at the Massachusetts Institute of Technology. A former student of psychology at Wayne State University, Jim enjoys tennis, art and collecting antique scientific instruments in his spare time.

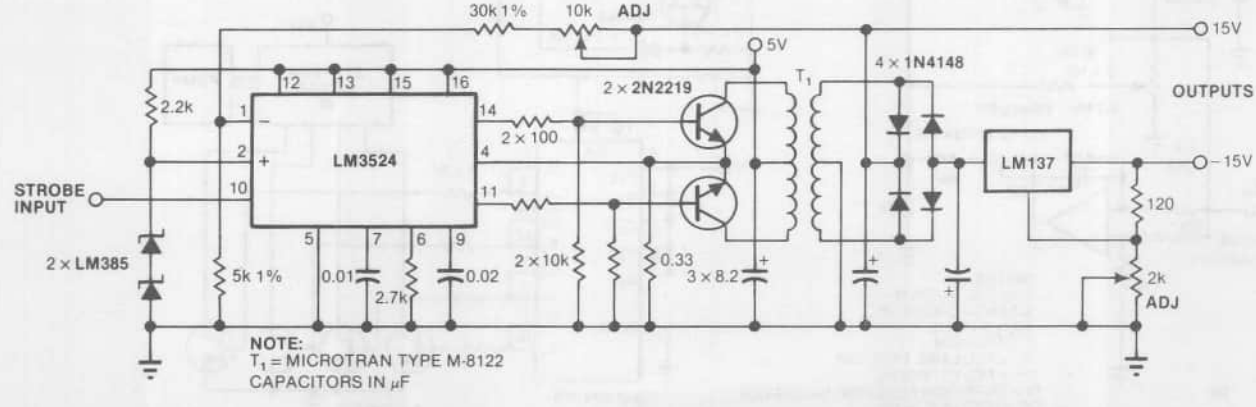

Fig 7—Convert a 5V digital-IC power supply *into a ±15V analog supply by using a pulse-width modulator to control the driver transistor's ON time. The PWM compares the 15V output against a reference and adjusts its output pulse widths accordingly. Overcurrent protection comes from sensing the driver transistors' emitter current, and a TTL-level input permits power-up sequencing.*

Expand linear circuit functions with nonlinear design schemes

Circuits implementing logarithmic or exponential functions provide instrumentation and control designs with many features unobtainable using linear-only characteristics. Such circuits can gauge fuel level or a grape's ripeness.

Jim Williams, National Semiconductor Corp

Just because a control or instrumentation design requires a logarithmic or exponential transfer function, don't assume that it must be complex, troublesome and expensive. It needn't be if you employ the correct basic circuit (see **box,** "Straightforward nonlinear circuits"). Indeed, the same concepts apply whether you must measure a tank's contents or control a motor's speed.

Govern a pump's rate

Although peristaltic pumps are generally driven by a continuously rotating motor, this technique isn't suitable when your application requires precise delivery at low rates as well as a high-throughput capability. (This situation often occurs in chemical or biological process-

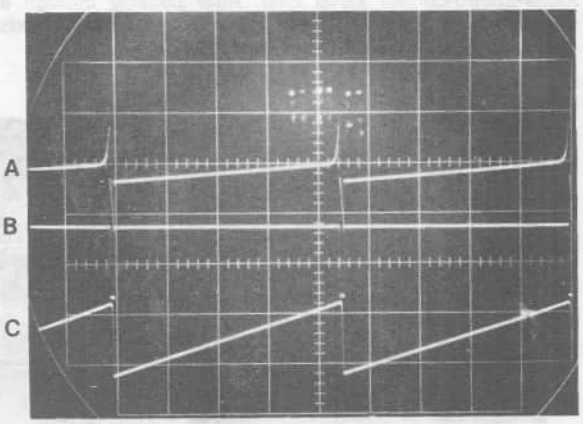

TRACE	V/DIV
A	5
B	20
C	20

HORIZONTAL
(b) SWEEP = 200 μSEC/DIV

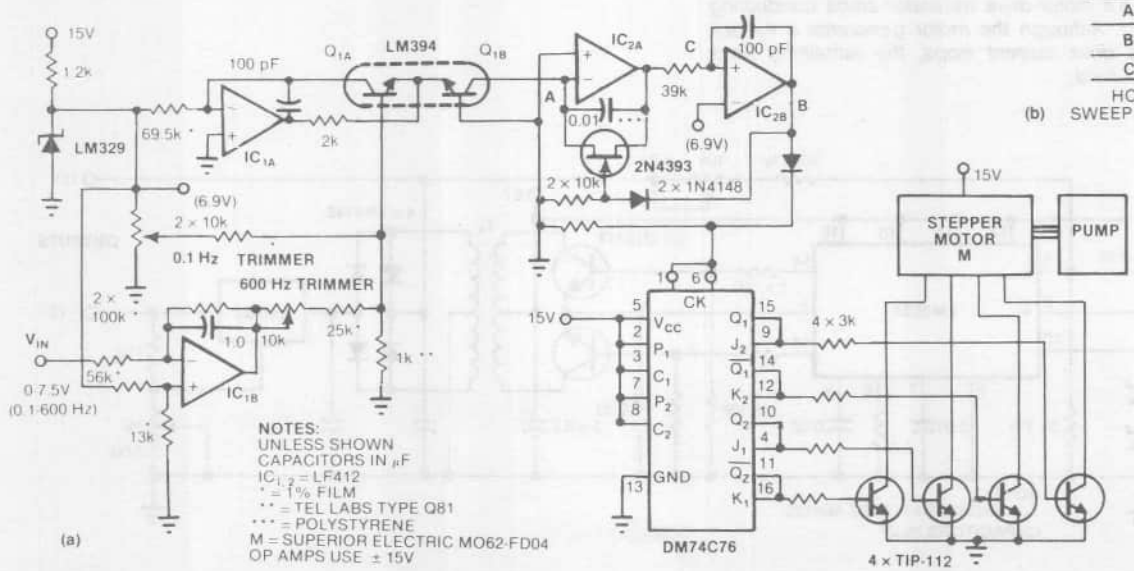

Fig 1—A stepper motor's speed varies exponentially *when driven by this voltage-to-4-phase converter. Using this approach, you can precisely govern a peristaltic pump's output flow for tight process control at low rates, yet speed it up for high throughputs. The waveforms correspond to points indicated on the schematic.*

Exponential expansion provides an 8-octave audio sweep signal

Straightforward nonlinear circuits

The theory and construction of logarithmic and exponential circuits isn't difficult, just different from what linear circuits require. By applying a few basic concepts, you can adapt the **figure**'s logarithmic **(a)** and exponential **(b)** schemes to a wide range of applications.

Capable of transforming a linear input voltage or current to a logarithmically equivalent output voltage, the design in **(a)** exhibits a 1% current-to-voltage conformity over a range of nearly six decades. This design, like most log circuits, is based on the inherently logarithmic relationship between a bipolar transistor's collector current (I_C) and base-emitter voltage (V_{BE}).

In the design, Q_{1A} functions as the "logging" device and is included within op amp A's feedback loop along with the 15.7-kΩ/1-kΩ divider. An input to A forces the amp's output to achieve the level required to maintain its summing-junction input at zero potential. But because Q_A's response is dictated by its I_C/V_{BE} ratio, A's output voltage is the log of its input.

Op amp B and Q_B provide compensation for Q_A's temperature-dependent V_{BE}. B servos Q_B's I_C to equal the 10-μA current established by the 6.9V LM329 voltage reference and its associated 700-kΩ resistor. This action fixes Q_B's collector current and therefore its V_{BE}. And under these conditions, Q_A's V_{BE} varies only as a function of the input, yielding

$$E_{OUT} = \left(\frac{15{\cdot}7k+1k}{1k}\right) \times (Q_B V_{BE} - Q_A V_{BE}).$$

With Q_A and Q_B operating at different I_Cs, the differential V_{BE}s are

$$\Delta V_{BE} = \left(\frac{KT}{q}\right) LOG_e\left(\frac{Q_A I_C}{Q_B I_C}\right),$$

where K=Boltzmann's constant, T=temperature in degrees Kelvin and q=electron charge.

To find the circuit's output, combine these equations to yield

$$E_{OUT} = \left(\frac{-KT}{q}\right)\left(\frac{15{\cdot}7k+1k}{1k}\right) \times LOG_e\left(\frac{E_{IN}\ 700k}{6{\cdot}9V\ 100k}\right).$$

Here, 6.9V equals the LM329's output, 100k is the input resistor and $E_{IN}>0V$.

Although this relationship confirms the circuit's linear-to-log transfer function, it's not the whole solution; without some form of compensation, the circuit's scale factor varies with temperature. The simplest solution is to have the 1-kΩ resistor also vary with temperature; using the indicated resistor, the design is compensated to within 1% over −25 to +100°C.

If your application needs an exponential expansion instead of a logarithmic compression, just turn the circuit in **(a)** around. In the resulting exponentiator scheme **(b)**, Q_A gets driven via the 15.7-kΩ/1-kΩ divider. Here Q_B's I_C varies exponentially with its V_{BE}, and op amp B converts this current into an output voltage.

Although these circuits are easy to construct and use, you must take one precaution: Because of the devices' V_{BE} temperature dependency, you must keep the transistors and the 1-kΩ resistor at the same temperature. The transistors are a dual unit and thus track each other. The 1-kΩ resistor must be mounted as closely as possible to this unit, and the entire network must be isolated from air drafts and changing thermal currents on the pc board. The KT/q factor for which the resistor compensates varies by approximately 0.3%/°C; a few degrees difference between the components therefore introduces a significant error.

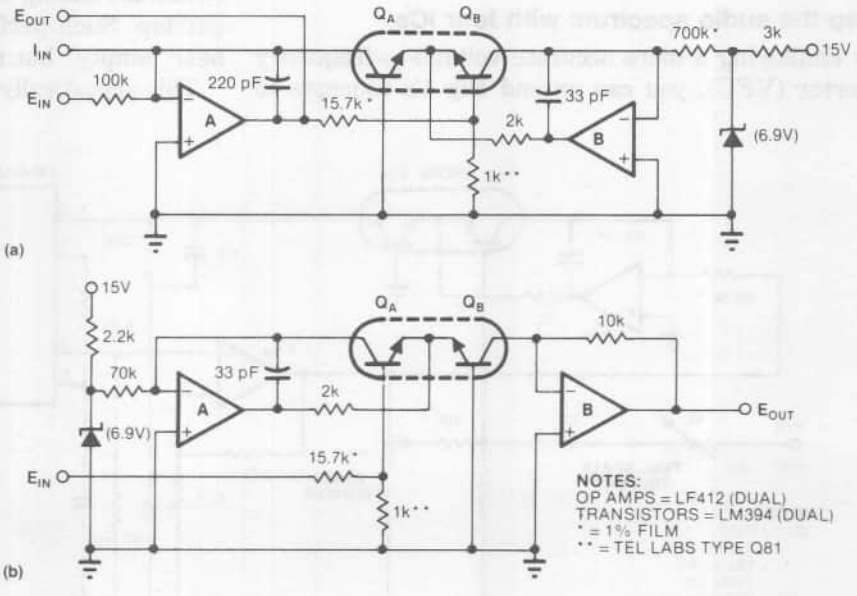

Logarithmic and exponentiating circuits *employ the inherent logarithmic relationship of a bipolar transistor's collector current to its base-emitter voltage. The logging circuit* ***(a)*** *displays an input-current-to-output-voltage transfer conformity within 1% over an input-current range of nearly six decades. Similar performance results when you reverse the circuit to form* ***(b)****'s exponentiator. A temperature-compensating resistor provides −25 to +100°C stability.*

control environments. Such applications require a high pumping rate for system flushing or process startup but a much lower, very accurate flow for maintaining the process.) Trying to meet these requirements with, say, a dc motor is difficult at best: If the motor can deliver high-speed performance, accurate control at, say, 0.1% of its maximum speed proves difficult.

Fig 1's design, however, satisfies a pump's conflicting high/low-speed drive requirements by employing an exponentially controlled stepper motor as the prime mover. In this scheme, the exponentiator—comprising IC_{1A} and Q_{1A}—gets driven by IC_{1B}. But here, unlike the version discussed in the **box**, Q_{1B}'s collector *draws* current from integrator IC_{2A}. This stage ramps up (trace **A**) until reset by level-triggered IC_{2B} (trace **B**). (Trace **C** shows how the 100-pF capacitor provides positive ac feedback to this stage's + input.) In this fashion, the oscillator's frequency follows the amount of current that Q_{1B} draws from IC_{2B}'s input. (Note that because IC_{2A}'s summing junction is always at virtual ground, this circuit is similar to the one in the **box**.)

IC_{2B}'s output clocks a dual JK flip flop that's wired to provide the 4-phase signal needed to drive the stepper motor. Using an exponentiator in this way, you achieve a very fine and predictable low-speed control (for example, 0.1 to 10 rpm), yet retain the motor's high-speed capabilities. To calibrate this circuit, ground the V_{IN} pin and adjust the 0.1-Hz trimmer until oscillation just ceases. Next, apply 7.5V to V_{IN} and adjust the 600-Hz trimmer for a 600-Hz frequency.

Sweep the audio spectrum with four ICs

By employing a more accurate voltage-to-frequency converter (VFC), you can extend **Fig 1**'s concepts to cover the complete audio spectrum **(Fig 2)**. Intended for laboratory and audio-studio applications, this design provides an output frequency that varies exponentially with a linear input-voltage sweep. Because the scheme uses a VFC IC, its transfer specs remain within 0.15% from 10 Hz to 30 kHz. Thus, it's suitable for use in music synthesizers or for making swept distortion measurements. In the latter application, its output drives a sine-encoded ROM/DAC or analog shaper.

In the **Fig 2** circuit, IC_{1B} derives the voltage that drives IC_{1A}'s input and the zero trimmer from the VFC's internal reference. The exponentiator functions exactly like the design described in the **box** to convert a linear input voltage into a nonlinear collector current for driving the VFC. The VFC's direct 10-Hz to 30-kHz output also clocks a D flip flop and thus provides a 5-Hz to 15-kHz square wave. To align the circuit, ground the V_{IN} port and adjust the zero trimmer until a 2- to 3-Hz oscillation just starts. Then apply −8V and adjust the full-scale trimmer for a 30-kHz signal. For the component values shown, this process yields an exponentiator K factor of 1V/octave.

Try an electronic dipstick

Fig 3 demonstrates how an exponential measuring circuit satisfies the requirement for a noninvasive, high-reliability gasoline gauge. This scheme nonlinearly measures a fuel tank's contents to suit applications—such as remote irrigation-pump installations—that benefit from depleting the tanks as much as possible (without running out of fuel) to eliminate condensation buildup. Such performance requires a scale expansion near "empty" but not near "full."

This acoustically based design operates by bouncing

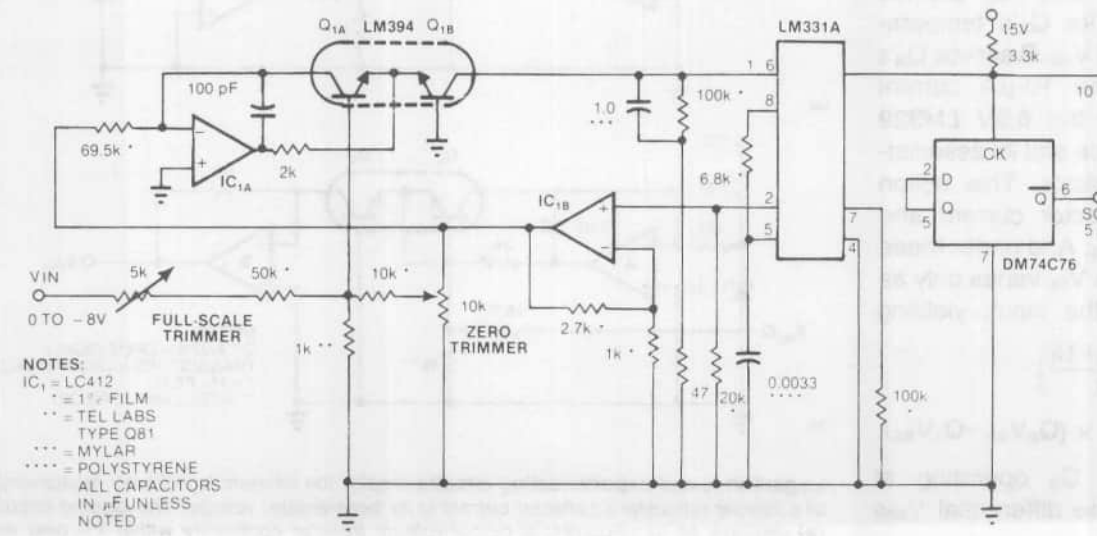

Fig 2—An exponentially swept audio spectrum *results when an input ramp voltage drives a voltage-to-frequency converter. Because the linear input is exponentiated, the circuit's output frequency varies 1V/octave.*

Ultrasonics and time expansion measure a fuel tank's contents

an ultrasonic signal off the fuel's surface and measuring the pulse's round-trip time—the longer the time, the lower the fuel level. Round-trip time gets converted to a voltage that in turn gets exponentiated to yield a high-resolution readout when the tank is nearly empty.

The 60-Hz-based clock pulse (trace **A**) drives a transistor pair and the sonic transducer ST with a 100V pulse. This same clock signal concurrently disables the receiver (to preclude false responses arising from noise) via a one-shot (traces **B** and **D**) and sets a flip flop (trace **C**). The one-shot then again goes HIGH (D), and the receiver (using the same sonic transducer) "hears" the echo and resets the flip flop (**C**). (This elapsed time (**C**) represents the tank's remaining fuel.) The flip flop's output gets clamped by the LM329, integrated by IC_{1D}

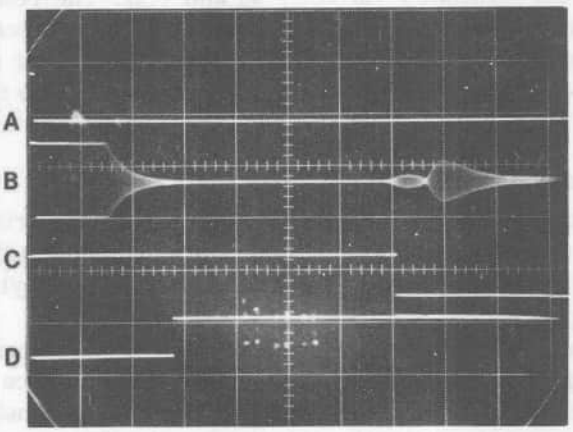

TRACE	V/DIV
A	10
B	20
C	20
D	20

HORIZONTAL SWEEP = 1 mSEC/DIV

(b)

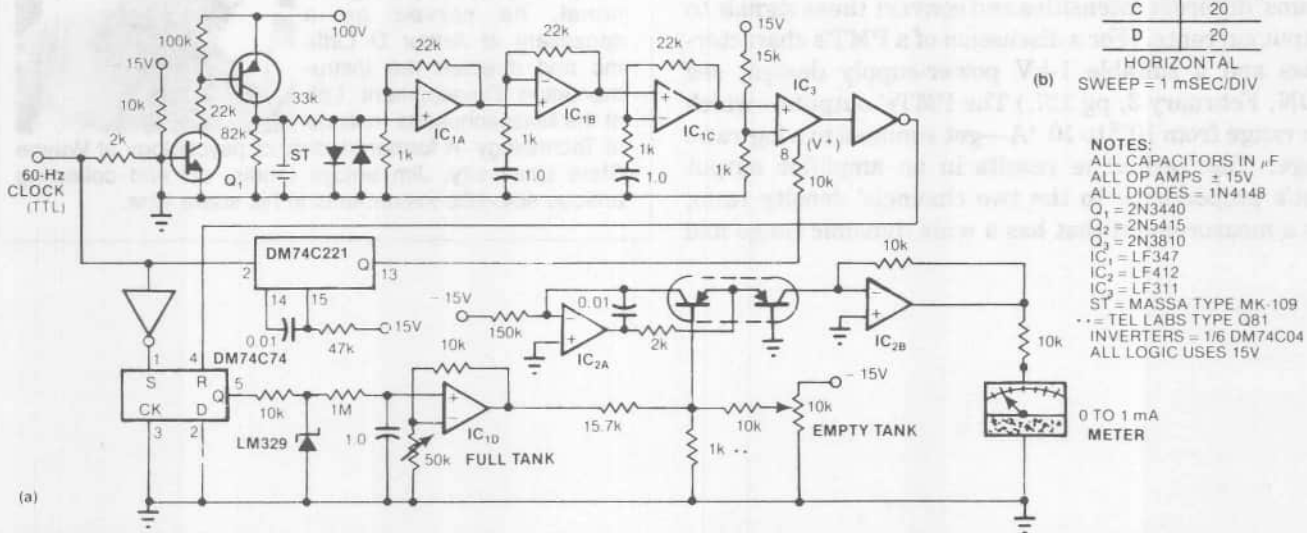

NOTES:
ALL CAPACITORS IN μF
ALL OP AMPS ± 15V
ALL DIODES = 1N4148
Q_1 = 2N3440
Q_2 = 2N5415
Q_3 = 2N3810
IC_1 = LF347
IC_2 = LF412
IC_3 = LF311
ST = MASSA TYPE MK-109
•• = TEL LABS TYPE Q81
INVERTERS = 1/6 DM74C04
ALL LOGIC USES 15V

Fig 3—A sonic transducer (ST) *gauges a fuel tank's contents by transmitting a signal and measuring the echo's return time. When the 60-Hz clock fires the transducer (trace **A**), the receiver saturates (trace **B**) before it's disabled by the 221's LOW output, trace **D**. (Trace **C** shows the time-measuring flip flop being set HIGH by the same clock pulse.) A few milliseconds later, the 221 times out, going HIGH **(D)** and allowing the receiver to detect the echo **(B)** and reset the timing flip flop **(C).***

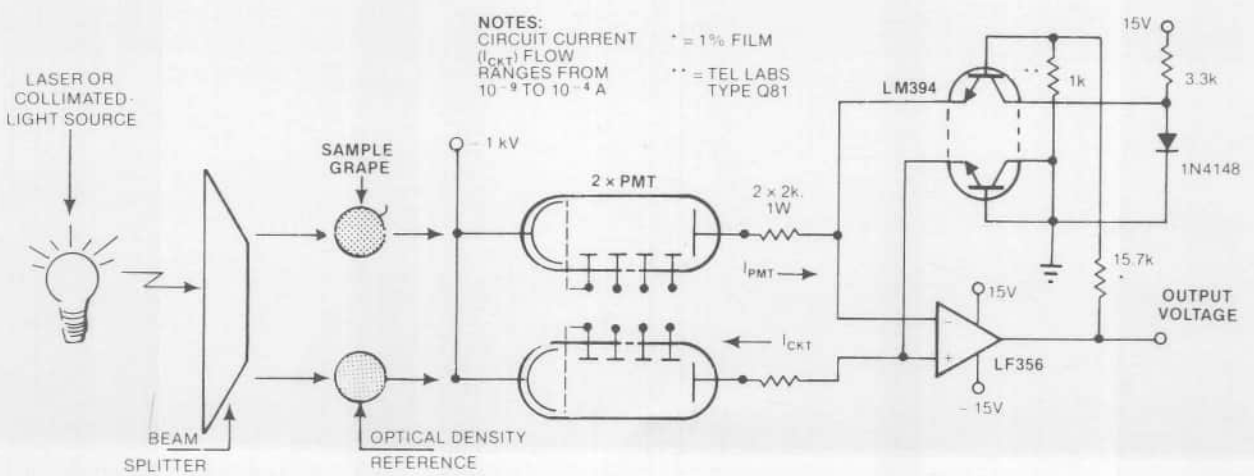

Fig 4—Photomultiplier tubes (PMTs) *determine a grape's ripeness by comparing its optical density with a reference. By using an active feedback, you can algebraically sum the PMTs' outputs in a log-ratio amplifier to yield accurate results over a 5-decade range.*

Photomultipliers determine grape ripeness, produce finer wines

and exponentiated via IC_{2A}, Q_3 and IC_{2B}. The result drives a 1-mA FS meter. The design's 1V/decade scale factor equates to a meter reading of 10% FS for an 80%-full tank; the meter's last 20% corresponds to the tank's last 2%.

Finer wines through science

Another example (**Fig 4**) demonstrates how logarithmic feedback networks can extend a photomultiplier tube's (PMT's) response range without employing complex current sources.

This design determines an object's optical density using photometric techniques. In it, a light source is optically split; one beam passes through a density reference, the other through the sample. (The sample in this case is a grape. The object of the test is to determine its ripeness.) The PMTs detect the light beams' different intensities and convert these signals to output currents. (For a discussion of a PMT's characteristics and a suitable 1-kV power-supply design, see EDN, February 3, pg 127.) The PMTs' outputs—which can range from 10^{-9} to 10^{-4}A—get summed in a log-ratio stage. This technique results in an amplifier output that's proportional to the two channels' density ratio; it's a measurement that has a wide dynamic range and isn't affected by variations in the light source's intensity. Theoretically, a less-than-perfect current-to-voltage conversion results because the log amp's inputs aren't at virtual ground. In fact, however, this error is insignificant because the PMTs' output impedance is very high. This simple circuit's most significant error results from the transistors' collectors operating at slightly different potentials. But for this application, you'll never taste the difference. **EDN**

Author's biography

Jim Williams, applications manager with National Semiconductor's Linear Applications Group (Santa Clara, CA), specializes in analog-circuit and instrumentation development. Before joining National, he served as a consultant at Arthur D Little Inc and directed the Instrumentation Development Lab at the Massachusetts Institute of Technology. A former student of psychology at Wayne State University, Jim enjoys tennis, art and collecting antique scientific instruments in his spare time.

Exploit D/A converters in unusual controller designs

More than just a data manipulator, a multiplying DAC simplifies designs such as scanner positioners, temperature regulators and electronic locks.

Jim Williams, National Semiconductor Corp

Employing multiplying digital-to-analog-converter (MDAC) ICs in other-than-standard data-handling tasks allows you to control many diverse—and difficult-to-interface—analog functions. MDACs such as the 12-bit DAC1218 and the 10-bit DAC1020 provide features that bring digital accuracy to familiar control chores involving temperature, voltage and vibration.

Digitally position mechanical scanners

Consider, for example, the use of these devices in the scanning-electrophoresis technique that biochemists employ to separate unidentified cells or molecular structures from each other. In one form of this process, a motor-driven scanner examines a sample suspended in a suitable liquid and contained within a glass or quartz tube approximately 1 ft long. A high voltage applied along the tube's length separates the cells according to their charge gradient, resulting in a series of bands within the tube where like cells collect. Photometrically scanning the tube's length, noting the bands' distances from a reference point and matching these locations against the potential's gradient, accomplishes cell identification.

The key to this technique lies in the scanning process:

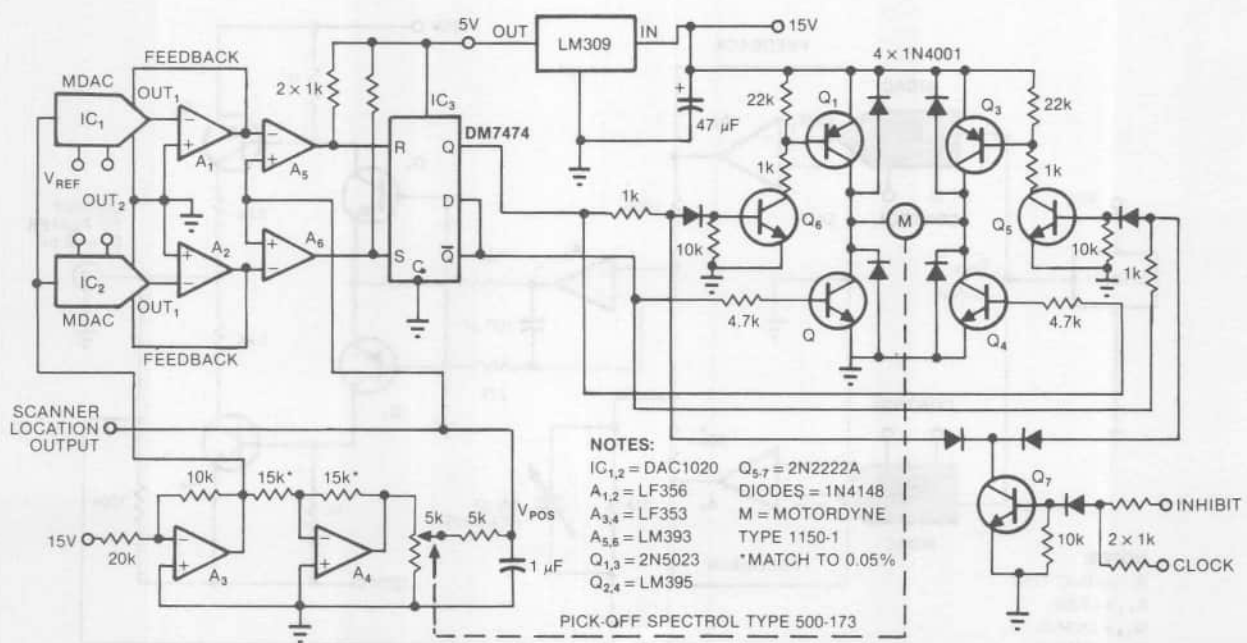

Fig 1—Digital words *determine a motor-driven scanner's excursion limits via a dual-MDAC-controlled transistor-bridge drive scheme. Two comparators (A_5, A_6) match a motor-position analog voltage (V_{POS}) with the MDAC's outputs and set or reset flip flop IC_3 accordingly. When the flip flop is set, for example, its Q output goes HIGH and turns transistors Q_1 and Q_4 on until V_{POS} is nulled.*

Digital-to-analog converters provide biochemical controls

Ideally, both the scanner's speed and the minimum and maximum scan length should be programmable. In Fig 1's approach, MDACs establish the scanner's travel limits via two sets of digital input codes. The scanner's motor drives a pick-off potentiometer, providing an analog voltage proportional to the scanner's position. This signal in turn feeds limit comparators A_5 and A_6, driving one of these device's outputs HIGH when either the high (A_5 and IC_1)- or low-position limit (A_6 and IC_2)

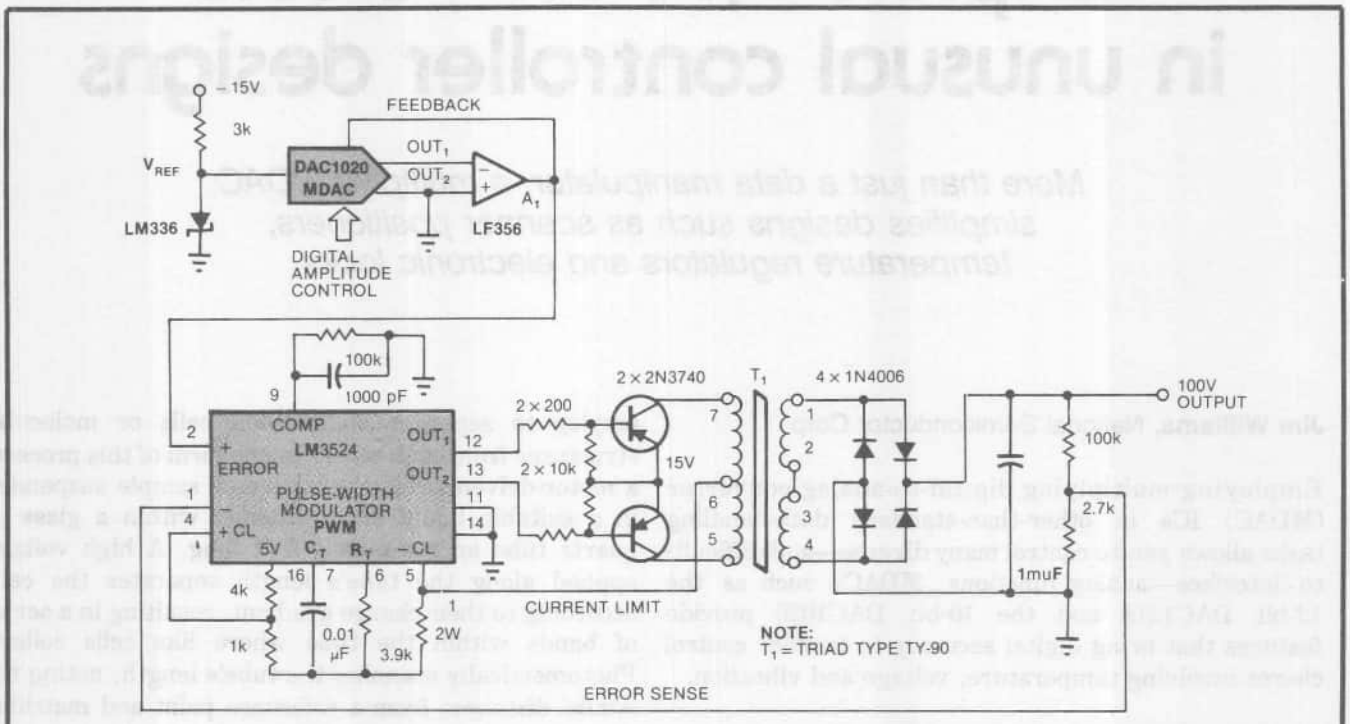

Fig 2—A settable output voltage *results when an MDAC controls a pulse-width modulator's input reference voltage. Overcurrent protection occurs when the voltage to the PWM's −CL input exceeds its +CL reference.*

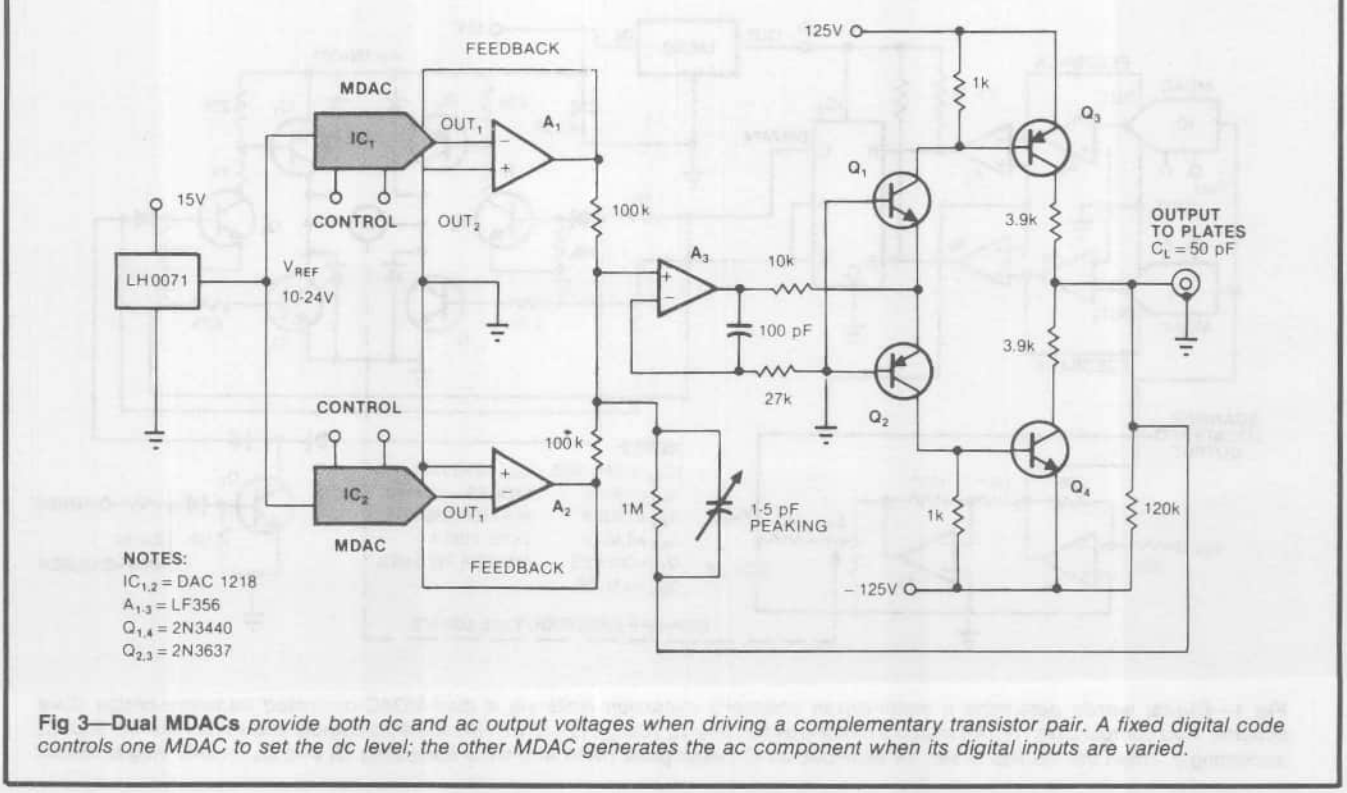

Fig 3—Dual MDACs *provide both dc and ac output voltages when driving a complementary transistor pair. A fixed digital code controls one MDAC to set the dc level; the other MDAC generates the ac component when its digital inputs are varied.*

is exceeded. (A_1 and A_2 serve as current-to-voltage converters, while A_3 and A_4 establish the feedback loop's reference voltages.)

When the scanner reaches a limit condition, these limit comparators set (S) or reset (R) flip flop IC_3; the resulting HIGH Q or $\overline{Q}$ output switches a transistor bridge on in a direction that reverses the motor's rotation. Thus, the scanner's motor bidirectionally runs the photometer head between the encoded scan limits.

Q_7 and its associated diodes control the motor's speed. When both Inhibit and Clock inputs are LOW, Q_7 is OFF and the flip flop's Q and $\overline{Q}$ signals can drive Q_5 and Q_6. However, if either Inhibit or Clock is HIGH, Q_7 turns on and shunts the drive signals to ground. You can employ a μC to generate all the scanner's control functions. For example, using a software-generated pulse-width-modulated signal as the clock allows you to dynamically alter the scanner's speed to run rapidly across distances where there aren't cell bands and slowly where there are. Similarly, you can use software to set the scan limits to home in on a cell-populated portion of the tube.

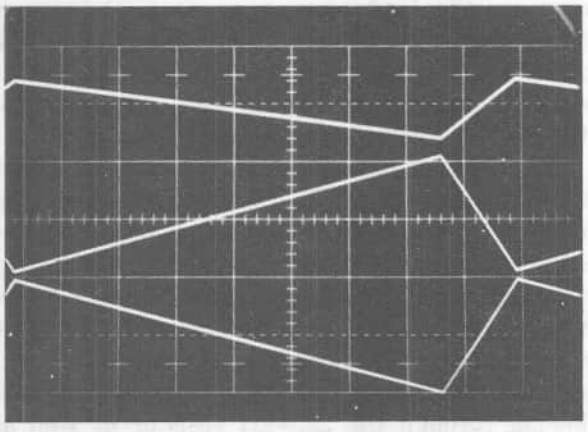

TRACE	VERTICAL	HORIZONTAL
TOP	10V/DIV	
MIDDLE	100V/DIV	50 μSEC/DIV
BOTTOM	100V/DIV	

Fig 4—An ac-driven MDAC *generates these CRT deflection voltages using the scheme shown in* ***Fig 3.*** *Buffer amplifier A_1's output (top) can be converted to a high-voltage complementary (middle) or in-phase equivalent (bottom) waveform.*

5V logic sets high-voltage levels

MDACs can control high-voltage sources as well as scanner positioners. Consider, for example, **Fig 2**'s circuit, which serves as a digitally controlled 15 to 100V supply suited to automatic-testing applications. This circuit couples a pulse-width-modulator (PWM)-driven push/pull voltage-converter stage with an MDAC in a feedback loop. The MDAC, in conjunction with A_1, establishes the PWM's setpoint voltage. The PWM in turn drives the transistors and—via the step-up transformer—converts the 15V to as much as 100V.

The transformer's square-wave output gets rectified, filtered and divided down by the resistor string. The resulting voltage level feeds back to the PWM's error amplifier, completing the control loop. You set the loop's gain and frequency characteristics with the 1000-pF/100-kΩ pair. Short-circuit protection results

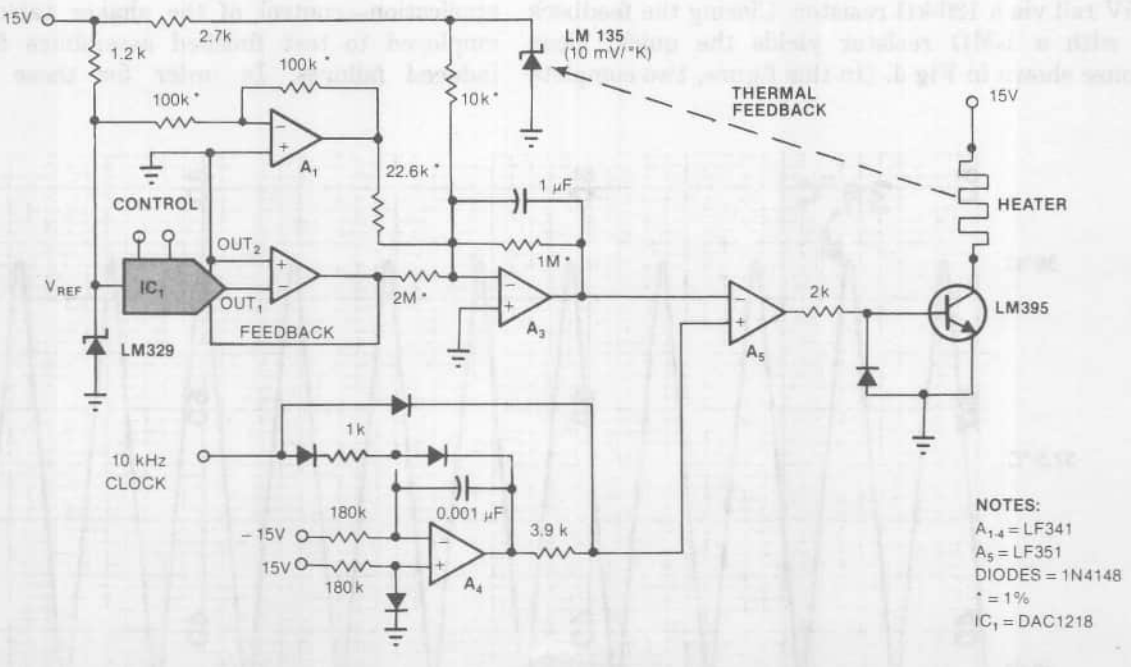

Fig 5—Precise temperature excursions *result when A_3 sums an MDAC-generated triangular waveform with A_1's fixed reference and the LM135's temperature-dependent signal. A_4 pulse-width-modulates the resulting error voltage and controls the heater's ON time.*

Set a shaker table's frequency with a D/A-converter IC

when the IR drop across the 1Ω resistor exceeds the 1V reference at the PWM's +CL input. (For a complete discussion of the PWM's functions, see EDN, September 2, pg 202.)

Although you can rapidly update the MDAC's output, the transformer's 20-kHz capability and the loop's time constants limit the design's bandwidth. In practice, though, you can modulate the MDAC's input at 250 Hz and still deliver a 100V sine wave into a 1-kΩ load.

Digitally modulate your CRT's plates

Another high-voltage requirement centers on modulating a CRT's deflection plates in electron-optics applications. In contrast to the previous high-voltage circuit, this design operates at greater bandwidths but has a low current-delivering capability. (Actually, this low-current limitation is not significant because the CRT's plates act like a very large resistor shunted by 50 pF.)

Fig 3's scheme uses two MDAC/op-amp pairs to generate the CRT's signals: One MDAC establishes the static (dc) bias; the second provides the dynamic (ac) drive signal (typically a ramp). A_3 sums these signals and feeds the result to the high-voltage stage, consisting of Q_1 through Q_4. This stage acts as an inverting, complementary, common-base-driven common-emitter amplifier with gain. And because the output-current requirements are low, you can avoid the usual crossover-distortion problems without complex compensation circuitry; merely tie the stage's output to the −125V rail via a 120-kΩ resistor. Closing the feedback loop with a 1-MΩ resistor yields the quick, clean response shown in **Fig 4.** (In this figure, two complete MDAC-driven amplifiers were used to produce the traces.) The top trace shows the ac signal created by digitally modulating IC_1's inputs; the middle and bottom traces depict the resulting high-voltage outputs.

MDACs regulate temperatures

MDACs also serve in temperature-regulating applications—such as those involving critical biochemical reactions occurring only within or at the edges of very specific (and often very narrow) temperature limits. **Fig 5**'s circuit, for example, employs an MDAC to regulate a heater and overcome the inability of standard temperature-control methods to provide both fine-grain resolution and long-term stability.

The basic temperature-control loop comprises an MDAC-controlled PWM (A_1 through A_5). Thermal feedback to the LM135 closes the loop; it varies the PWM's duty cycle to establish the controller's setpoint. Note that the PWM action results from A_5's comparing A_3's setpoint-equivalent output with the ramp output generated by the clock-driven integrator, A_4. A_3's output is in turn a function of the setpoint current flowing through the 22.6-kΩ resistor as well as the LM135's signal. (Amplifier A_3's 10-MΩ/1-μF feedback values limit the loop's response to 0.1 Hz.)

You control the temperature's excursions around the setpoint by modulating the MDAC's digital inputs with a slowly varying digitally encoded triangular waveform; the number of bits changed controls the temperature's span. **Fig 6**'s strip-chart recording demonstrates this design's advantages: Temperature can vary by ±1.5°C around a 37.5°C setpoint for many hours.

MDACs develop high-power audio signals

Now consider an MDAC's use in an audio-frequency application—control of the shaker tables frequently employed to test finished assemblies for vibration-induced failures. In order for these tests to be

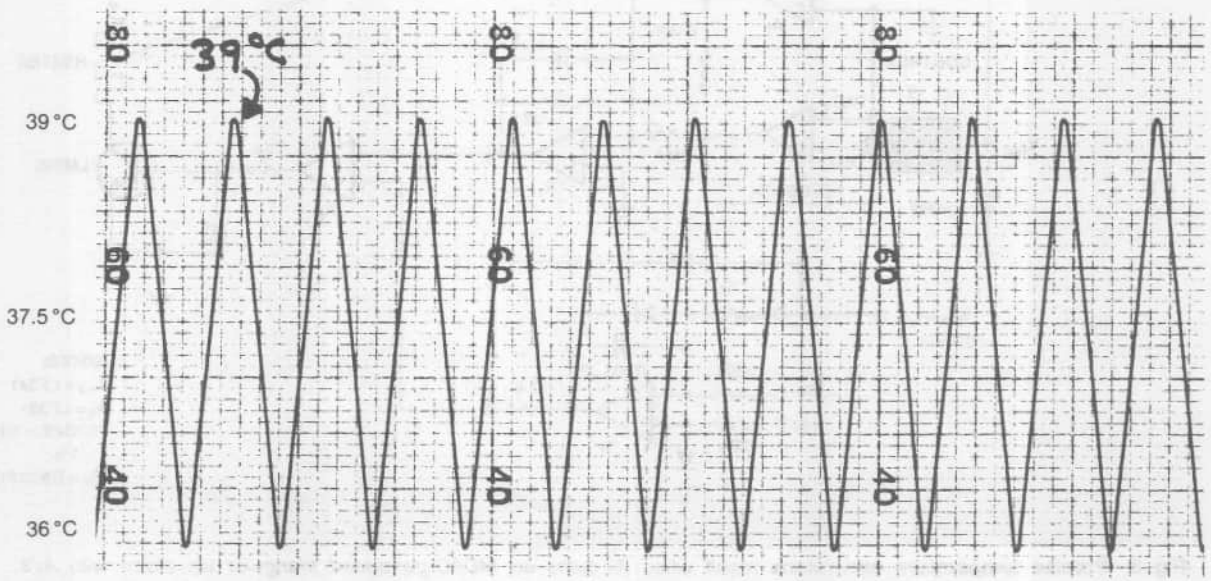

Fig 6—Long-term temperature control *is the result when* **Fig 5***'s design modulates the 37.5°C baseline setting via a triangular-wave-driven MDAC. The MDAC's digital input code controls the peak-to-peak oscillation amplitude.*

meaningful, the vibration patterns must be tightly controlled in terms of duration, frequency and amplitude. **Fig 7**'s dual-MDAC scheme can meet these requirements.

Frequency control results when MDAC IC_1 drives the integrator formed by A_1. This stage's output ramps until its 10-kΩ derived current just balances the feedback current at comparator A_2's + input. At this point, A_2's output changes state and forces the zener-diode network to furnish an equal-magnitude but opposite-polarity reference voltage. Because this now-inverted reference feeds both the MDAC and the comparator, the integrator generates a triangular waveform symmetrically centered on ground. Using this circuit technique, you can use 12 bits to encode the MDAC and synthesize a 1-Hz to 30-kHz output signal.

A sine wave results when the synthesized triangular signal feeds the dual npn/pnp stage; the logarithmic relationship between the LM394's collector current and its V_{BE} performs the smoothing function. You adjust the offset and wave-shape pots for low distortion.

The digital amplitude-control feature occurs in the

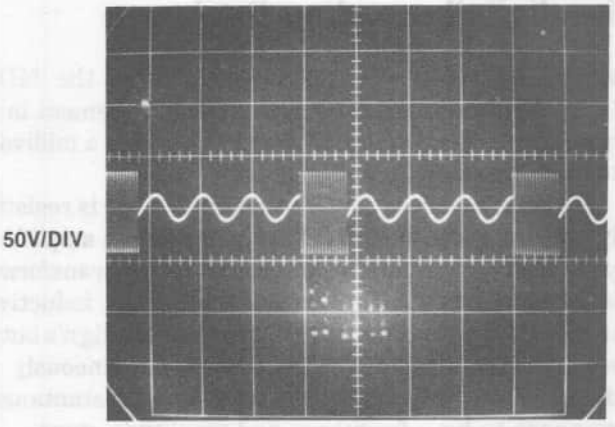

Fig 8—A signal's frequency or amplitude *is quickly changed by* **Fig 7***'s MDAC controllers. Using this technique, you can vary output frequency from 1 Hz to 30 kHz.*

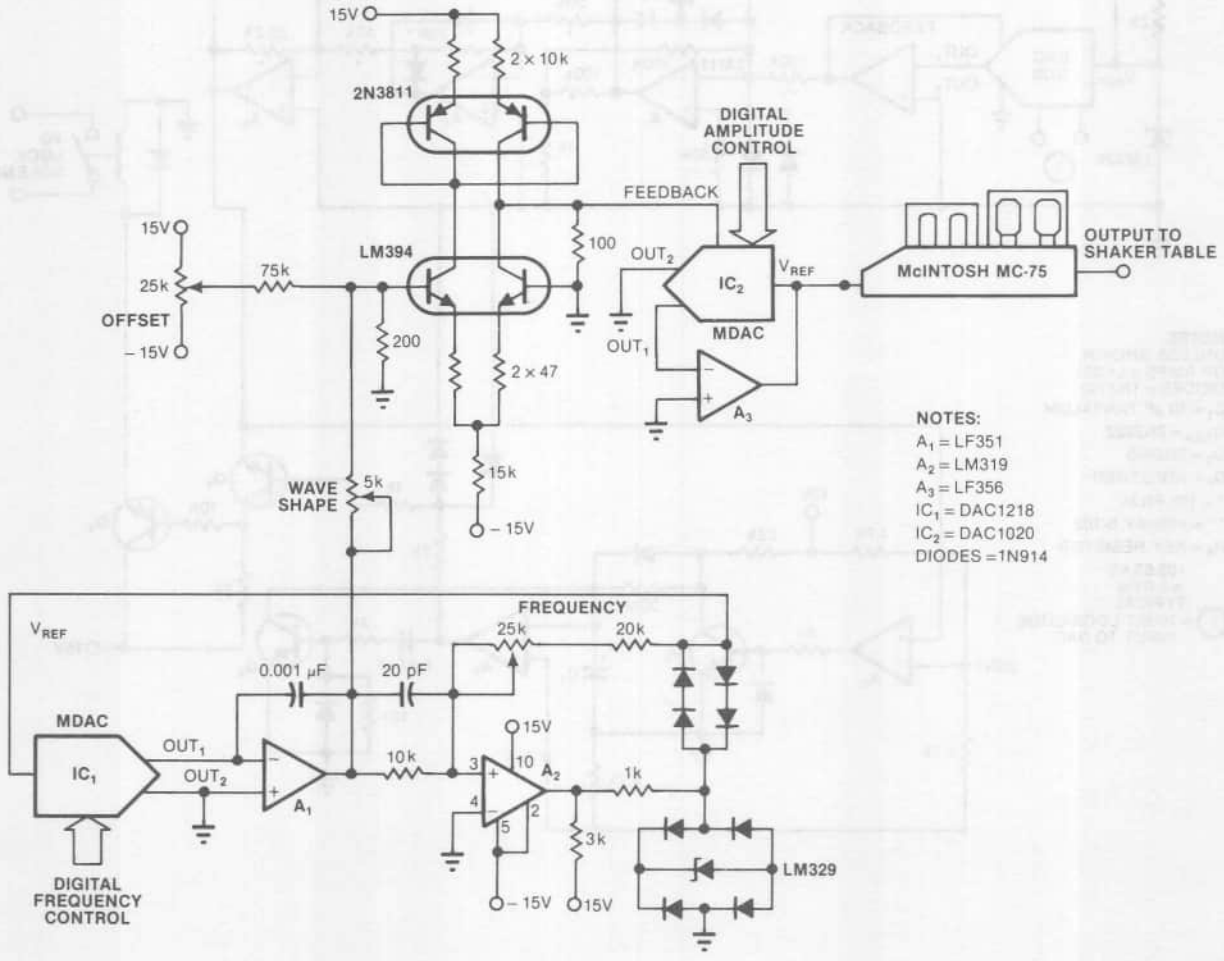

Fig 7—Digitally variable frequency and amplitude signals *arise when the triangular wave generated by IC_1 through A_2 is converted to a sine wave by the pnp/npn stage and modulated by MDAC IC_2. Both the frequency and amplitude functions can be fixed (via switches) or swept.*

Pick-proof electronic locks by digitally reading the key

associated MDAC/op-amp network. Here the MDAC (IC_2) operates as the programmable gain element in the op amp's feedback loop. This trick provides a millivolts-to-volts range at A_3's output pin.

Because a shaker table's input impedance is resistively low and inductively high, a vacuum-tube amplifier is your best choice for the power stage; its transformer-isolated output is immune to the table's inductively induced flyback spikes. **Fig 8** shows this design's output waveform when both MDACs are simultaneously updated. Note its clean and essentially instantaneous response to both frequency and amplitude steps.

Digital codes "pick-proof" a lock

Fig 9's circuit serves an unusual MDAC application: the programming of an electronically keyed combination lock. Because the inserted key is an 0.01% resistor, security is assured against all but the most determined and sophisticated thieves. If the key you insert isn't the correct one, the circuit knows it within 250 msec and ignores any further lock-opening attempts for 5 min. Decade-box- or potentiometer-equipped thieves thus don't have a chance.

When "key resistor" R_K has the correct value, the MDAC's output current precisely balances R_K's current at A_1's input and drives A_1's output to zero. The absolute-value stages (A_2 and A_3) sense this condition, and A_3's output, Q_1's emitter and A_4's + input also go to zero. And when A_4's input reaches zero, its output goes negative, Q_3 cuts off and C_1 starts charging toward the 15V supply level via the 22-kΩ/diode network. During this 250-msec charging time, A_5's HIGH output level turns the Q_1/Q_2 stage on and therefore opens the door's lock. When C_1 charges past 5V, A_5's output goes LOW and disables the lock again.

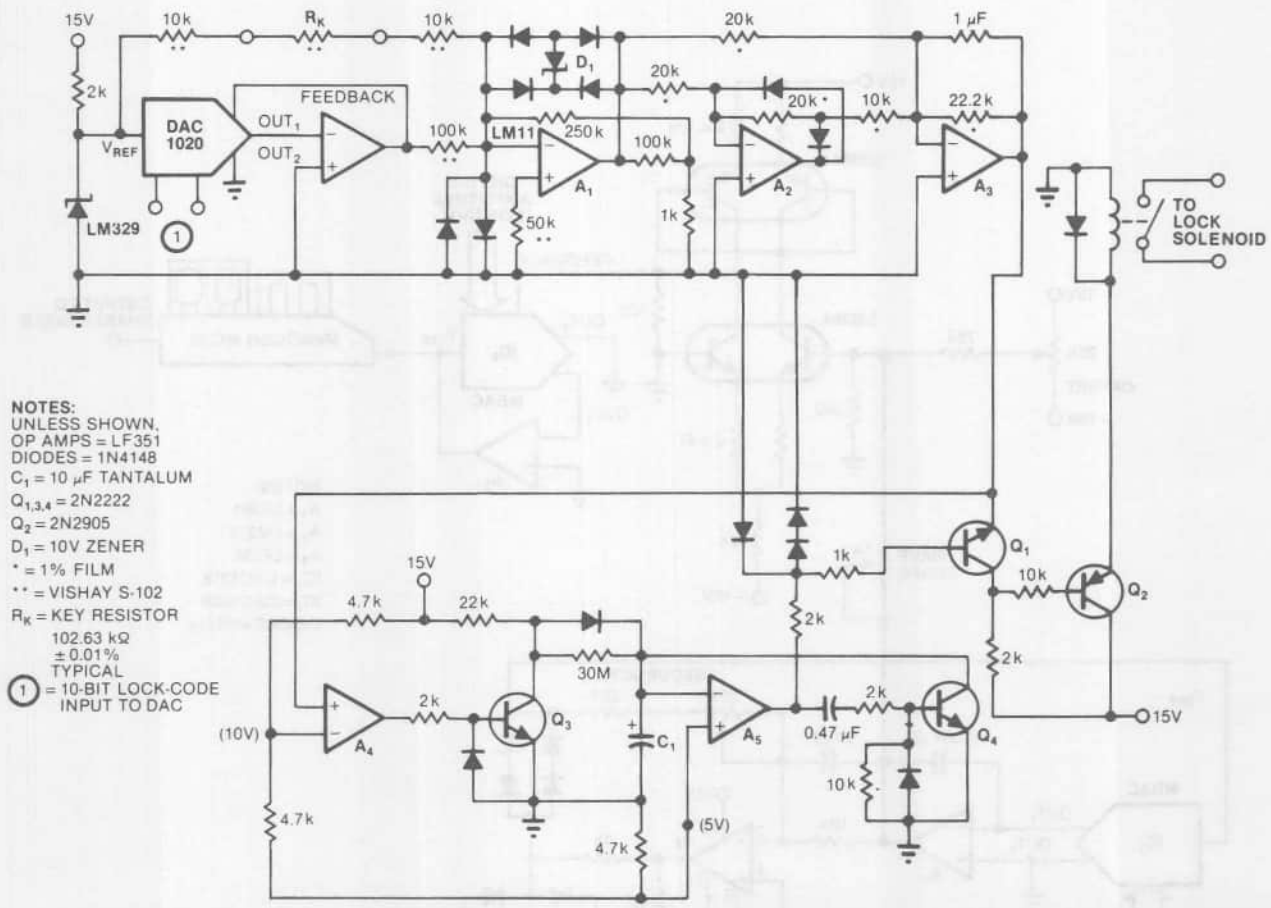

Fig 9—A virtually pick-proof electronic lock *employs an MDAC in a digital-code-to-resistor-value comparison loop. Resistor R_K serves as a key. When the inserted resistor's value isn't correct and accepted within 250 msec, the circuit inhibits another lock-opening attempt for 5 min.*

Pick-proof lock frustrates sophisticated thieves

If you try opening the lock with an illegal R_K, the absolute-value stages (A_2, A_3) don't settle to zero and Q_1 remains OFF. Under these conditions, it takes 5 min before C_1 discharges back down to 5V—via the 30-MΩ resistor—and is reset to 0V by Q_4.

This design discourages even the most sophisticated and/or frustrated thieves: Amplifier A_1's zener-diode bridge and input clamps prevent anyone from monitoring the summing junction's requirements or intentionally destroying the unit. And the 12-bit MDAC provides security via 4096 possible combinations. **EDN**

Piezoceramics plus fiber optics boost isolation voltages

Overcoming traditional magnetic-transformer drawbacks, a novel isolation-amplifier design hikes voltage-breakdown limits more than tenfold by incorporating a piezoceramic-based acoustic transformer and a fiber-optic link.

Jim Williams, National Semiconductor Corp

When standard parametric or isolation amplifiers don't adequately isolate or protect your analog measurement systems, the circuit design described in this article can help. Although typical isolation amplifiers achieve about a 2.5-kV max isolation voltage, this one can handle 20- to 100-kV breakdown limits. It incorporates a piezoceramic material structured as an acoustic transformer and a fiber-optic lightpipe.

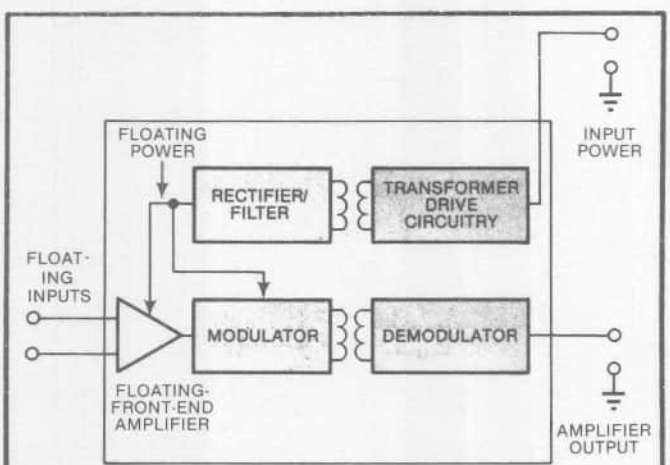

Fig 1—A traditional isolation amplifier *uses dual transformers to separate the input-signal line from the power and output-signal lines. This approach typically results in about a 2.5-kV max input-isolation voltage.*

Isolation amplifiers find use mainly in assuring safe and reliable analog measurements. They surmount the problems of high common-mode voltages in applications such as medical test instruments and completely isolate or interrupt ground loops or paths in equipment such as that used in industrial process-control systems.

Designing isolation amplifiers mandates careful attention to two key factors: isolating the power supply from the input-signal line and galvanically separating the input- and output-signal lines. The first half of the task generally involves the most effort.

Input isolation proves complex

Conventional isolation amplifiers employ a magnetic transformer to convey power to the circuit's floating front end (**Fig 1**). Although this transformer galvanically separates the power supply from the input terminals, it increases in size and cost when common-mode voltages exceed about 2.5 kV. Moreover, its leakage currents can total as much as 2 μA.

To separate the input- and output-signal lines, conventional isolation amplifiers modulate the floating front end's output onto a carrier signal. This signal traditionally passes via another magnetic transformer to the circuit's output terminals. Modulation schemes include pulse width, pulse amplitude and voltage to frequency. Here again, though, magnetic transformers become bulky and inefficient as common-mode voltages and leakage currents rise. And isolation limits depend

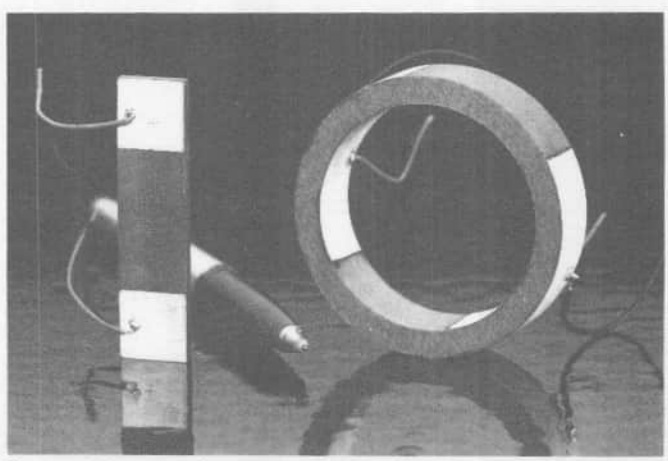

Fig 2—Able to perform as acoustic transformers, *piezoceramic materials come in various sizes and shapes, such as this thin bar and thick toroid (shown with a ballpoint pen for dimensional reference). Observe that two pairs of leads make input and output connections to each piece of piezoceramic material.*

Traditional isolation amplifiers employ magnetic transformers

on the transformer's breakdown rating.

Even when an optoisolator replaces the modulation transformer with a frequency- or light-intensity-coding approach, power requirements for operating the floating front end still require the power transformer. What's more, optoisolators are under excessive common-mode voltages.

Other methods for transmitting electrical energy with high isolation exist, such as using microwave devices and solar cells, but they prove expensive, inefficient and impractical. Batteries are an alternative power source, but they have maintenance and reliabiliy limitations.

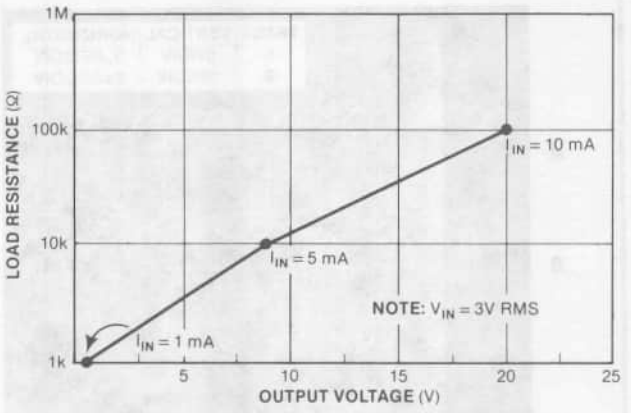

Fig 3—This typical load line *traces an acoustic transformer's performance at resonance. Note that for a constant 3V rms drive voltage and a varying 1- to 100-kΩ load resistance, the acoustic transformer draws up to 10 mA as its output voltage increases to 20V.*

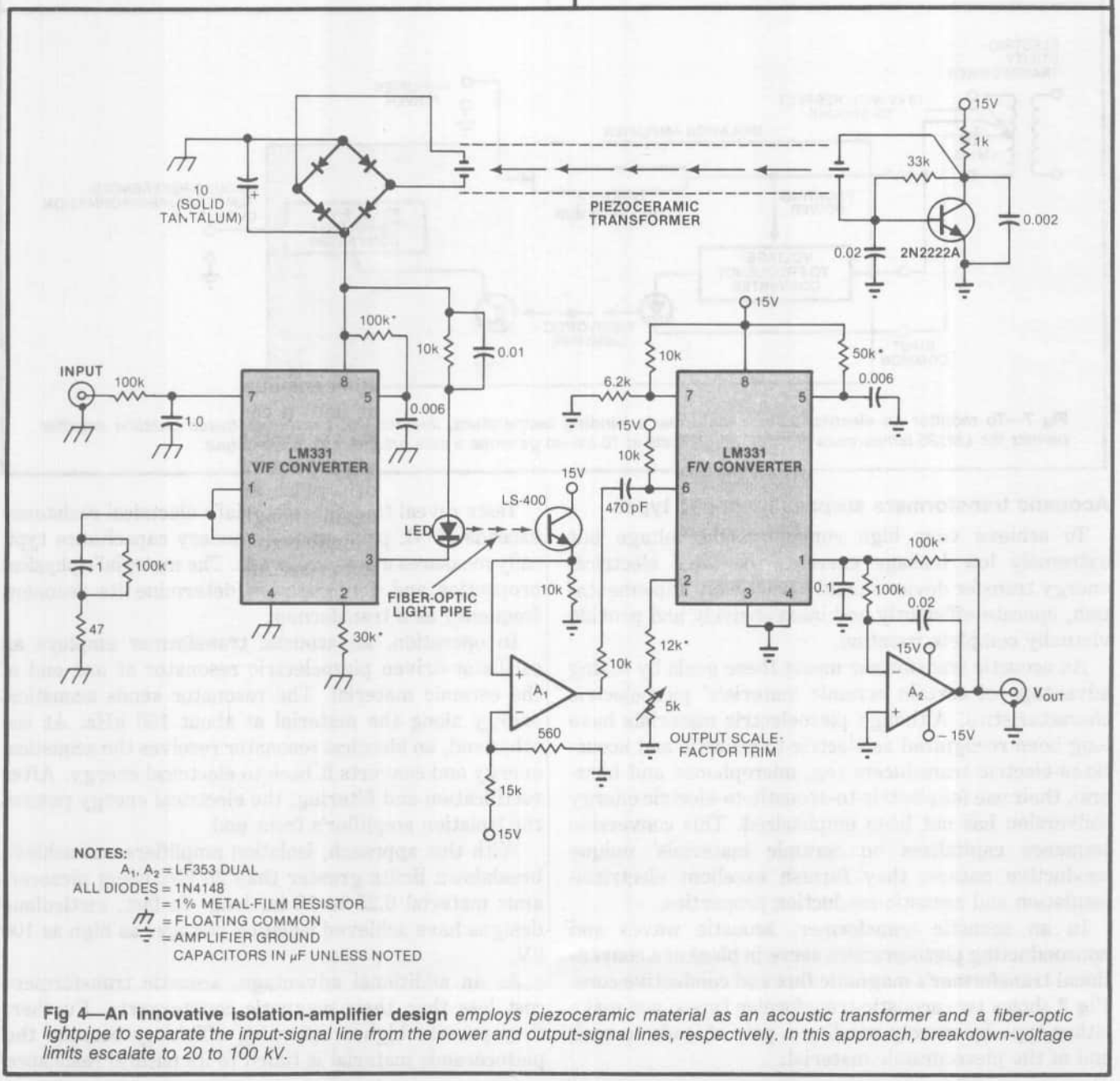

Fig 4—An innovative isolation-amplifier design *employs piezoceramic material as an acoustic transformer and a fiber-optic lightpipe to separate the input-signal line from the power and output-signal lines, respectively. In this approach, breakdown-voltage limits escalate to 20 to 100 kV.*

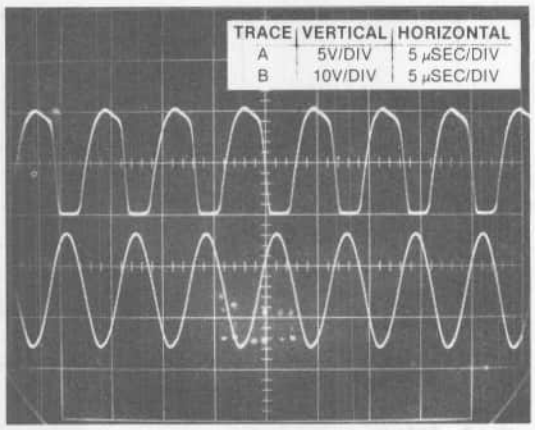

Fig 5—The 2N2222A transistor's output *(from **Fig 4**'s circuit) shows an irregularly shaped sine wave (trace **A**) delivered to the acoustic transformer's input. The transformer's high-Q properties cause it to filter and amplify the waveform into a smooth sinusoid **(B)** at its output.*

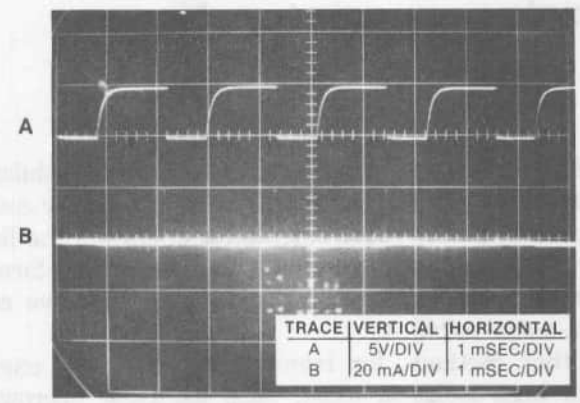

Fig 6—Trace A depicts the LM331 voltage-to-frequency converter's output *(from **Fig 4**'s circuit). This output drives the LED that couples to the fiber-optic lightpipe. Trace **B** indicates the LED's current waveform. Whenever the converter's output is LOW, the LED saves power by passing an extremely narrow (20 mA) light-encoded pulse.*

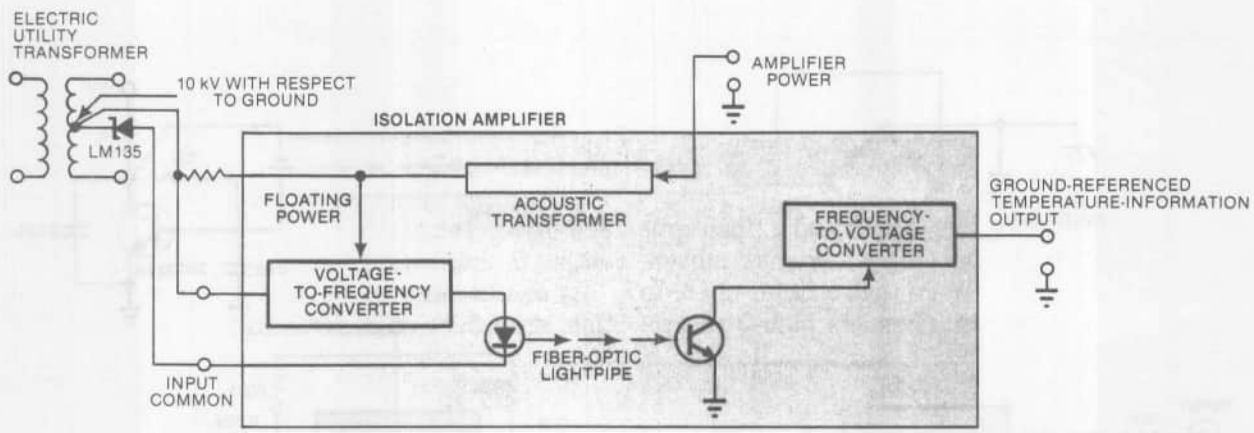

Fig 7—To monitor an electric-utility transformer's winding temperature, *this acoustic-transformer-based isolation amplifier permits the LM135 temperature sensor—which floats at 10 kV—to generate a safe ground-referenced output.*

Acoustic transformers surpass magnetic types

To achieve very high common-mode voltage but extremely low leakage current, the ideal electrical energy transfer device should permit easy implementation, operate efficiently and inexpensively and provide virtually complete isolation.

An acoustic transformer meets these goals by taking advantage of certain ceramic materials' piezoelectric characteristics. Although piezoelectric materials have long been recognized as electric-to-acoustic and acoustic-to-electric transducers (eg, microphones and buzzers), their use for electric-to-acoustic-to-electric energy conversion has not been emphasized. This conversion sequence capitalizes on ceramic materials' unique conductive nature; they furnish excellent electrical-insulation and acoustic-conduction properties.

In an acoustic transformer, acoustic waves and nonconducting piezoceramics serve in place of a conventional transformer's magnetic flux and conductive core. **Fig 2** shows two acoustic-transformer types; you make either type by merely bonding a pair of leads to each end of the piezoceramic material.

Tests reveal that this material's electrical resistance exceeds $10^{12}\Omega$; primary-to-secondary capacitance typically measures a few picofarads. The material's physical properties and configuration determine its resonant frequency as a transformer.

In operation, an acoustic transformer employs an oscillator-driven piezoelectric resonator at one end of the ceramic material. The resonator sends acoustical energy along the material at about 150 kHz. At the other end, an identical resonator receives the acoustical energy and converts it back to electrical energy. After rectification and filtering, the electrical energy powers the isolation amplifier's front end.

With this approach, isolation amplifiers can achieve breakdown limits greater than 20 kV, using piezoceramic material 0.25 to 12 in. long. In fact, meticulous designs have achieved isolation voltages as high as 100 kV.

As an additional advantage, acoustic transformers cost less than their magnetic counterparts. Further, they possess higher operating efficiency because the piezoceramic material is tuned to its natural resonance

An acoustic transformer isolates the power supply from the input

point.

Fig 3 depicts a typical acoustic transformer's output characteristics when driven at resonance. Note that the transformer's power-transfer efficiency can exceed 75%, depending on load conditions. Short-circuit output current for this device equals 35 mA.

Fiber optics upgrades input/output isolation

The other key design factor in designing isolation amplifiers—nearly total input-to-output line separation—is accomplished via fiber optics by stretching both lines further apart than an optoisolator can. This optical-encoding method works as it would in a typical optoisolator, but with an increased distance between transmitter and receiver yielding higher isolation voltages.

In practice, a light-emitting diode (LED) transmits optically encoded signals through a single-fiber cable to a photodiode receiver. The exact cable length depends on the particular circuit requirements.

Put it all together

Combining an acoustic transformer and a fiber-optic link in an isolation amplifier (**Fig 4**) extends conventional breakdown limits by more than a factor of 10. In this circuit, the acoustic transformer's high-Q characteristics allow self resonance in a manner similar to that of a quartz crystal. Resonance eliminates the need for a stable oscillator to drive the acoustic transformer.

To start operation, the 2N2222A transistor excites the piezoceramic transformer's primary (**Fig 5**). At the secondary, four diodes and a capacitor rectify and filter the transformer's electrical output. This output in turn energizes the LM331 V/F converter.

The converter transforms its amplitude-based input signal into a frequency-based output. This signal then drives an LED, whose output travels along a fiber-optic cable.

Each time the V/F converter's output goes LOW, a narrow (20-mA) spike passes through the LED via the 0.01-μF capacitor (**Fig 6**). This short duty cycle keeps the average current value small, minimizing power requirements.

At the receiver end, a photodiode detects the light-encoded signals. It in turn passes the signals to the LM331 for demodulation.

Amplifier accommodates varied uses

An acoustic-transformer/fiber-optic isolation amplifier finds use in diverse applications. In one example, an LM135 transducer tracks the winding temperature of an electric-utility transformer operating at 10 kV (**Fig 7**). The transducer's output biases the isolation amplifier's input. Temperature information at the amplifier's output is thus safely referenced to ground.

In another ground-referenced application, the isolation amplifier's high-common-mode voltage blocking

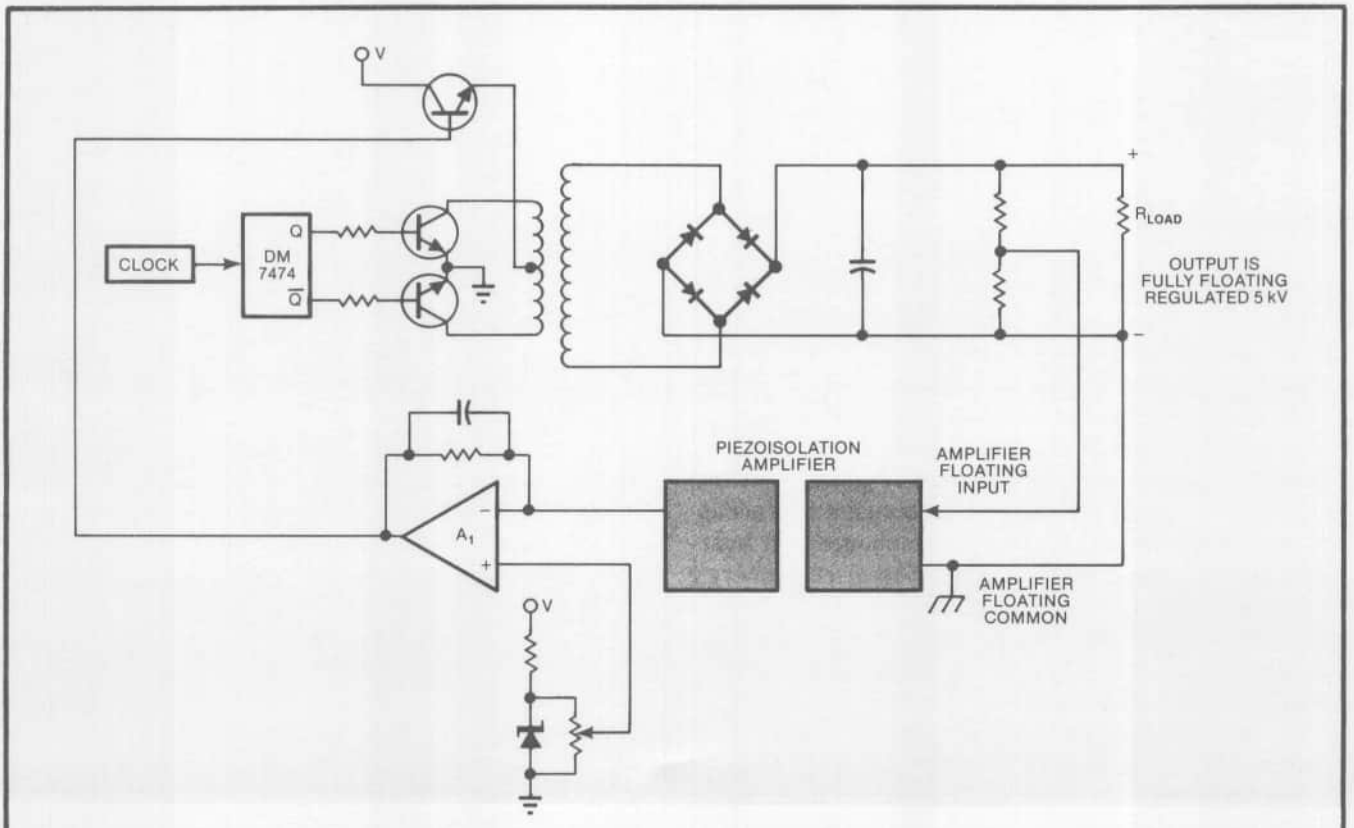

Fig 8—The piezoisolation amplifier *in this application provides a ground-referenced feedback path for the 5-kV regulated power supply. The power supply's output thus fully floats.*

A fiber-optic link galvanically separates output and input lines

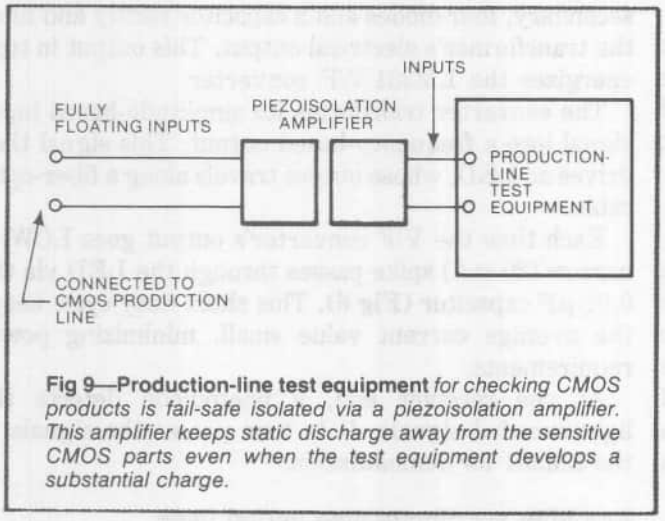

Fig 9—Production-line test equipment *for checking CMOS products is fail-safe isolated via a piezoisolation amplifier. This amplifier keeps static discharge away from the sensitive CMOS parts even when the test equipment develops a substantial charge.*

allows a 5-kV regulated power supply's output to fully float (**Fig 8**). Here, a push/pull dc/dc converter generates the high-voltage output. The isolation amplifier provides a ground-referenced output-feedback signal to op amp A_1, which controls the transformer's drive, completing the feedback loop.

For a fail-safe test application, an acoustic/fiber-optic amplifier isolates instrument inputs connected to CMOS ICs on a production line (**Fig 9**). This arrangement prevents static-discharge damage, even when the instruments have accumulated a substantial charge. **EDN**

References

Transducer Interfacing Handbook, Analog Devices Inc, Norwood, MA, 1980, pg 175.

Piezoceramic Catalog 761-01, Channel Industries Inc, Santa Barbara, CA, 1980.

Author's biography

Jim Williams, applications manager with National Semiconductor's Linear Applications Group (Santa Clara, CA), specializes in analog-circuit design and instrumentation development. Before joining the firm, he served as a consultant at Arthur D Little Inc and directed the Instrumentation Development Lab at the Massachusetts Institute of Technology. A former student of psychology at Wayne State University, Jim enjoys tennis, art and collecting antique scientific instruments in his spare time.

Transformers and optocouplers implement isolation techniques

Maintaining high precision can be a formidable task when you're taking measurements in industrial environments. Fortunately, there are ways to overcome this problem using readily available components.

Jim Williams, National Semiconductor Corp

High electrical-noise levels and excessive common-mode voltages complicate making safe, precise measurements in industrial environments. This article shows how to use transformers and optoisolators to isolate motors, transducers, converters or other real-world interfaces from control circuitry.

The conflicting requirements for high accuracy and total input-to-output isolation call for unusual design techniques. Typically, you use transformers and optoisolators to galvanically isolate the input terminals of a signal-conditioning amplifier from its output terminal. This technique breaks the common ground connection and eliminates noise and common-mode voltages.

A simple, isolated signal conditioner

Several examples demonstrate how to include these isolation devices in your circuits. In the first, a wide-band audio transformer permits safe, ground-referenced monitoring of a motor powered directly from a 115V ac line (**Fig 1a**). The floating amplifier's inputs connect across a brush-type motor. The R_1R_2 network and the transformer's turns ratio divide the motor voltage by 100 and simultaneously allow a ground-referenced amplifier output. The neon bulb

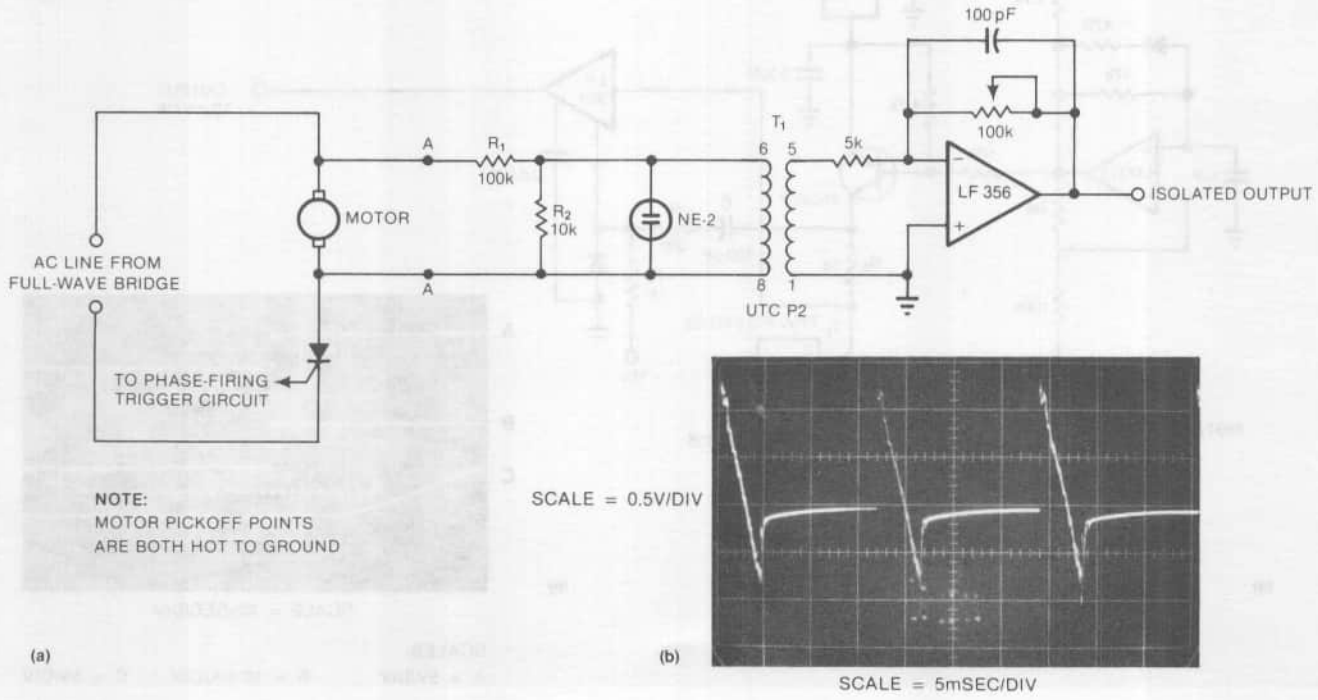

Fig 1—Safe ground-referenced monitoring *is possible using a wide-band audio transformer* ***(a).*** *The circuit's fast response* ***(b)*** *permits monitoring of SCR turn-on as well as motor-brush noise.*

Maintaining isolation is tricky when transducers need excitation

suppresses line transients, while the 10-kΩ pot in the amplifier's feedback loop trims the circuit for a precise 100:1 scale factor.

You must calibrate the network before connecting it to the motor. That procedure is simple—apply a 10V rms sine wave at points A-A and adjust the pot until the amplifier's output equals 100 mV rms. Despite the design's simplicity, though, network performance is impressive: Rise time measures roughly 10 μsec, full-power bandwidth spans 15 Hz to 45 kHz and the −3-dB point lies beyond 85 kHz.

Fig 1b illustrates the motor's waveform at the ground-referenced circuit output. The circuit's isolated wide-band response permits safe monitoring of the SCR's fast rise time as well as the motor's brush noise.

Isolating temperature measurements

A second example also uses an isolation transformer, this time to operate an LM135 temperature sensor in a fully floating fashion (**Fig 2a**). In this circuit, an LM311 generates a 100-μsec pulse (at approximately 20 Hz) that biases a pnp transistor. The voltage that develops across T_1's primary (trace A in **Fig 2b**) is a direct function of the secondary voltage established by the

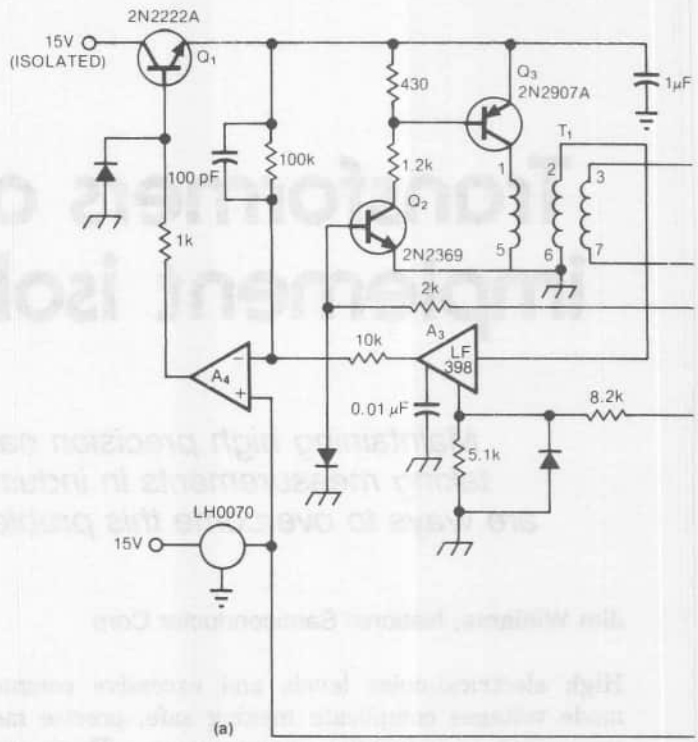

NOTES:
⏚ IS ISOLATED GROUND
T_1—TRW PC-SSO-32
T_2—UTC P2
DIODES ARE IN4148

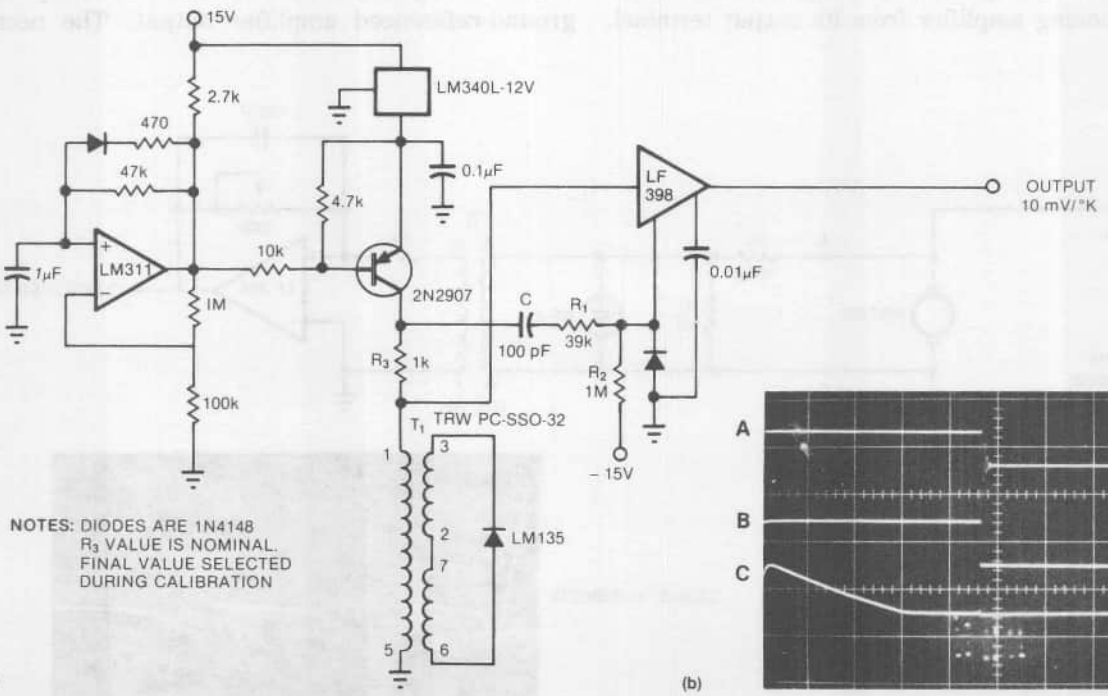

NOTES: DIODES ARE 1N4148
R_3 VALUE IS NOMINAL. FINAL VALUE SELECTED DURING CALIBRATION

SCALE = 20μSEC/DIV

SCALES:
A = 5V/DIV B = 10 mA/DIV C = 5V/DIV

Fig 2—Easily calibrated, *this scheme permits fully floating temperature sensing* ***(a).*** *Circuit design ensures that the sampling period doesn't end* ***(b)*** *until the LM135 sensor has settled.*

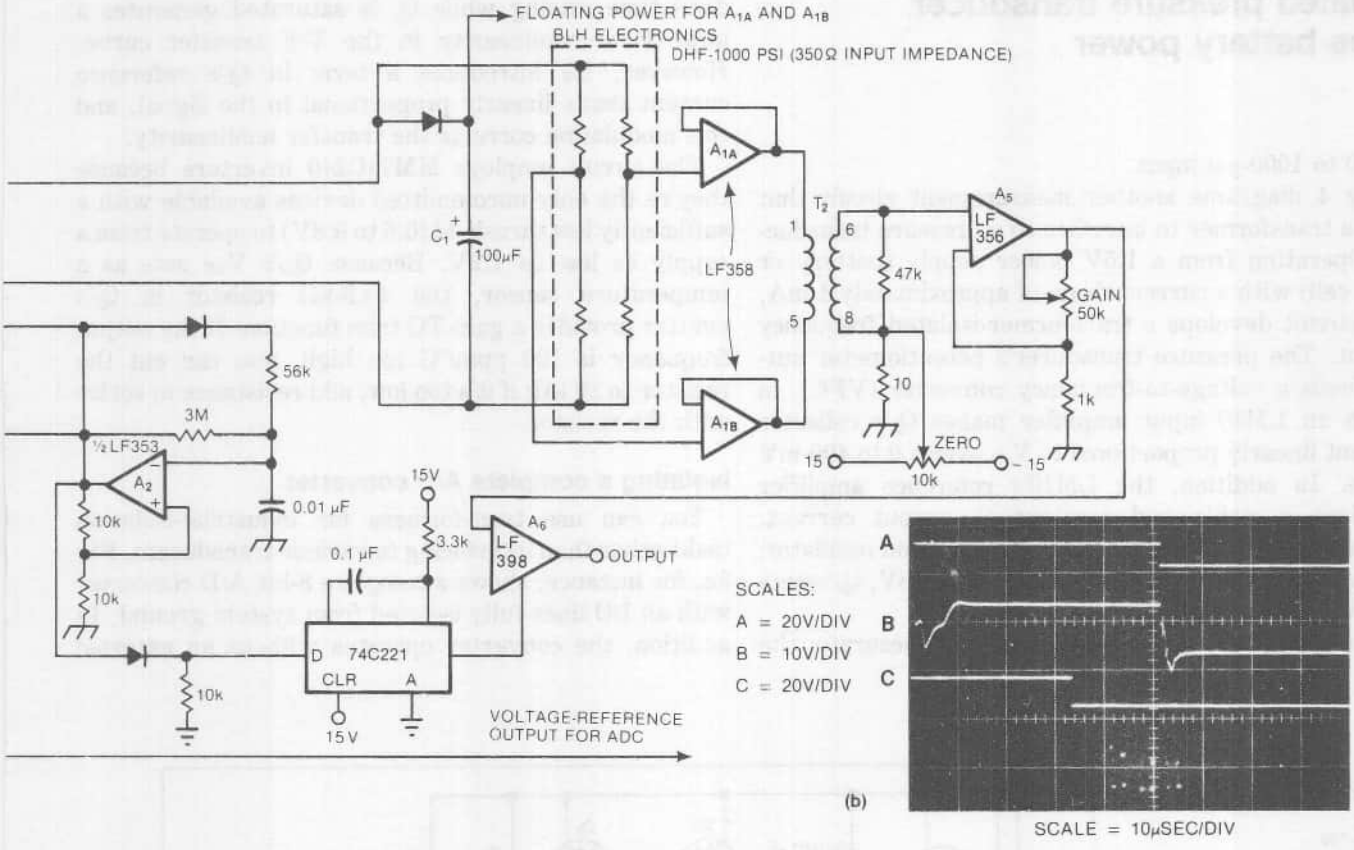

Fig 3—In addition to supplying floating drive *to the strain-gauge bridge, this network furnishes transducer output-signal amplification* ***(a)****. Because the Sample command—trace C in* ***(b)****—occurs while T_2's output is settled, network output is a dc representation of pressure-transducer output.*

LM135's clamp level. Of course, the voltage varies with the sensor's temperature reading in accordance with normal operation.

The LF398 sample/hold amplifier monitors the transformer's primary voltage and provides a dc output. The R_1R_2C network generates a trigger pulse for the LF398 that ensures that the sampling period doesn't terminate until after the LM135 settles. The LM340L −12V voltage regulator provides power-supply rejection.

To calibrate the circuit, first substitute an LM336 2.5V diode of known breakdown potential for the LM135. Then vary R_3 until circuit output equals the substitute diode's breakdown voltage. Replace the LM135 and the circuit's ready for use.

Pressure measurements present problems

Transformers also suit difficult isolation applications, such as those using strain gauges, where you must feed excitation power while maintaining total isolation from ground. This requirement arises, for example, in industrial-measurement situations when the transducer is physically connected to a structure that floats at a high common-mode voltage.

Fig 3a illustrates one way to solve such an isolation problem. A transformer (T_1) generating a pulse with a servo-controlled amplitude excites the strain bridge. For this pulse generation, the sampled output-pulse amplitude gets stored as a dc level, and this information goes to a feedback loop that controls the voltage applied to the output switch.

A_2 functions as an oscillator and simultaneously drives Q_2 and Q_3 and the LF398's (A_3) Sample pin. At the end of A_2's output pulse, A_3 outputs a dc level equal to the output pulse driving the strain bridge. T_1's dual secondary allows accurate magnetic sampling of the strain-bridge output pulse with no sacrifice in electrical isolation. A_4 compares A_3's output to the LH0070 10V reference, while Q_1's emitter provides the dc supply for the Q_2Q_3 switch.

This servo action develops constant-amplitude drive pulses (equal to the LH0070's reference output) for the strain-gauge transducer (trace A, **Fig 3b**). C_1 stores some of the pulse energy and powers the LM358 dual followers, which then unload the transducer's bridge output and drive T_2's primary. T_2's output amplitude (trace B, **Fig 3b**) represents the transducer's output.

After amplification, this potential goes to a sample/hold amplifier (A_6), and the 74C221 generates A_6's Sample command (trace C, **Fig 3b**). Because this command occurs during the settled portion of T_2's output pulse, A_6's output is a dc representation of the strain-gauge pressure transducer's amplified output.

As before, circuit calibration is simple: Insert a strain-bridge substitution box (BLH Model 625, for example) for the transducer and dial-in the respective values for zero and full-scale output (usually supplied with individual transducers). Then adjust the circuit's zero and gain pots until a 0 to 10V output corresponds

Isolated pressure transducer uses battery power

to a 0 to 1000-psi input.

Fig 4 diagrams another measurement circuit that uses a transformer to interface to a pressure transducer. Operating from a 1.5V power supply (battery or solar cell) with a current drain of approximately 1 mA, this circuit develops a transformer-isolated frequency output. The pressure transducer's potentiometer output feeds a voltage-to-frequency converter (VFC), in which an LM10 input amplifier makes Q_1's collector current linearly proportional to V_{IN} over a 0 to 400-mV range. In addition, the LM10's reference amplifier develops a stable and constant Q_2 output current. Transistors Q_3 through Q_{10} form a relaxation oscillator; every time the voltage across C_1 reaches 0.8V, Q_6 resets it to 0V differential.

Normally, this basic circuit isn't very accurate; the dead time arising while Q_6 is saturated generates a large (1%) nonlinearity in the V/F transfer curve. However, R_X introduces a term in Q_2's reference current that's linearly proportional to the signal, and this modulation corrects the transfer nonlinearity.

The circuit employs MM74C240 inverters because they're the only uncommitted devices available with a sufficiently low threshold (0.6 to 0.8V) to operate from a supply as low as 1.2V. Because Q_{12}'s V_{BE} acts as a temperature sensor, the 49.9-kΩ resistor in Q_2's emitter provides a gain-TC trim function: If the output frequency is 100 ppm/°C too high, you can cut the resistor to 20 kΩ; if it's too low, add resistance in series with the resistor.

Isolating a complete A/D converter

You can use transformers for industrial-isolation tasks other than interfacing to various transducers. **Fig 5a,** for instance, shows a complete 8-bit A/D converter with all I/O lines fully isolated from system ground. In addition, the converter operates without an external

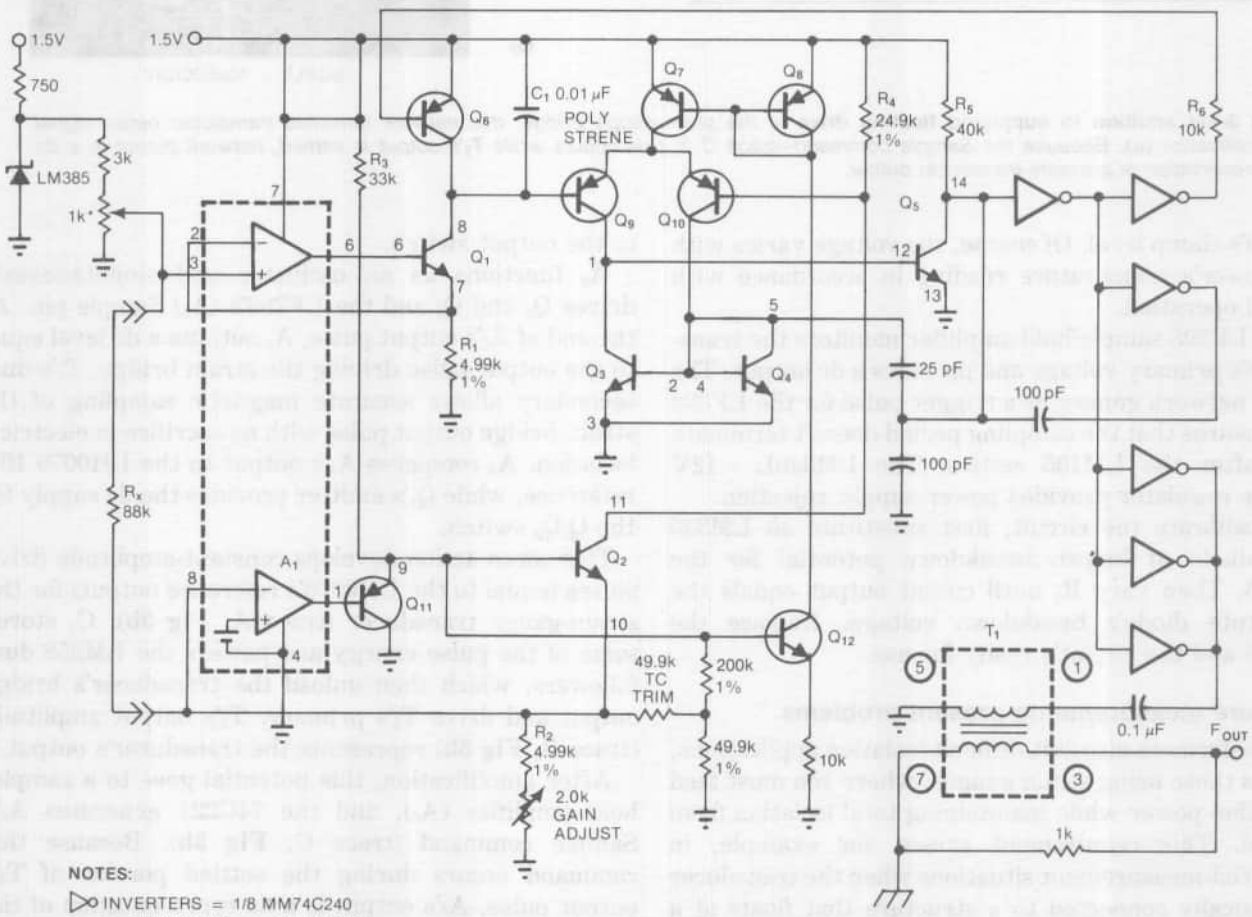

Fig 4—Capable of operating from battery or solar cell, *this pressure-measurement circuit has a fully isolated frequency output.*

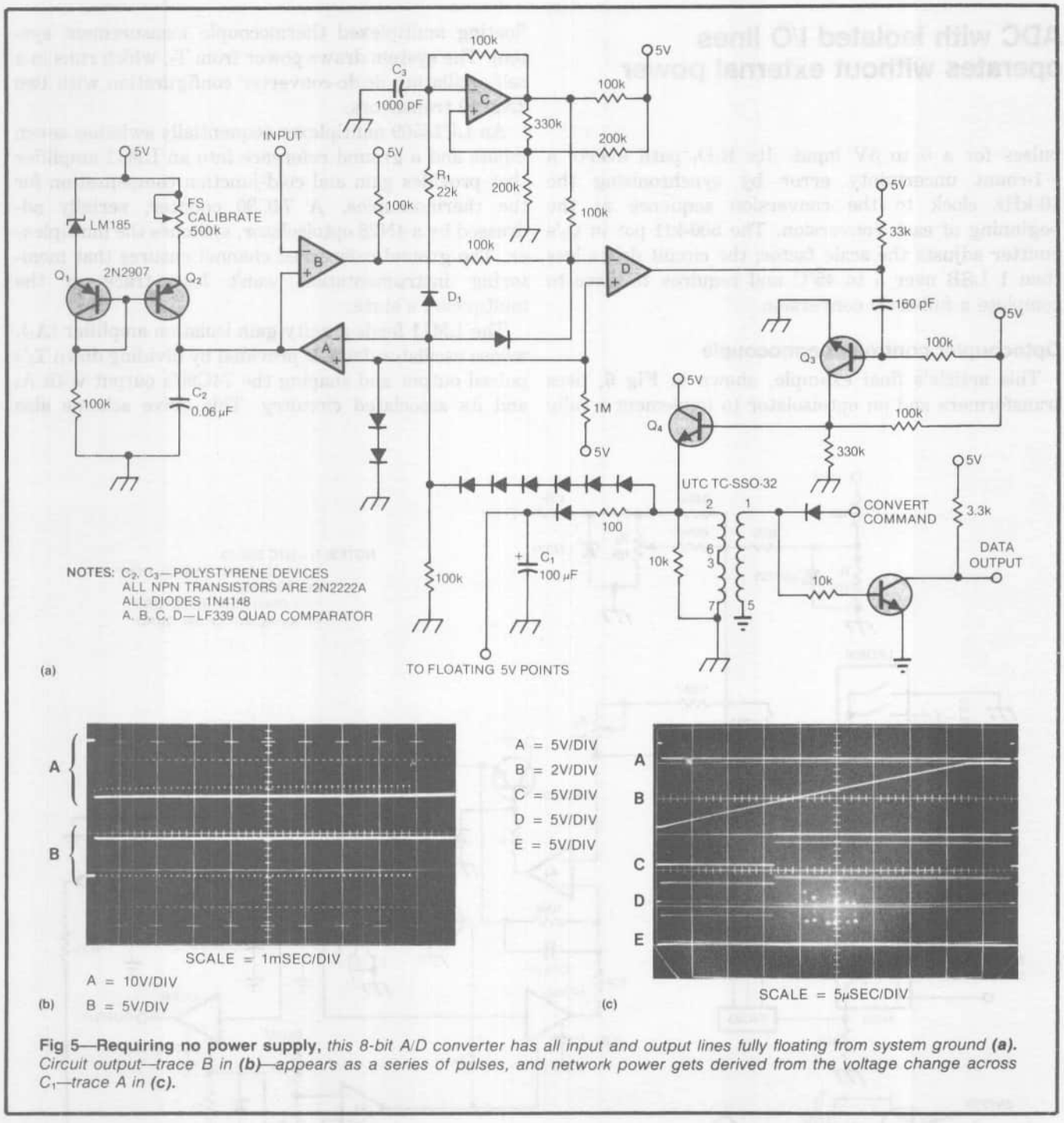

Fig 5—Requiring no power supply, *this 8-bit A/D converter has all input and output lines fully floating from system ground* ***(a).*** *Circuit output—trace B in* ***(b)****—appears as a series of pulses, and network power gets derived from the voltage change across* C_1*—trace A in* ***(c).***

power supply.

To initiate circuit operation, apply a pulse (trace A, **Fig 5b**) to the transformer's Convert input. This pulse simultaneously forces the Data Output line LOW (trace B, **Fig 5b**) and propagates across the isolation transformer. The secondary winding charges C_1 to 5V (trace A, **Fig 5c**)—the supply voltage for the floating ADC. This winding's voltage also starts the A/D conversion by biasing comparator A's inverting input LOW, and the biasing forces comparator A's output LOW, discharging C_2 (trace B, **Fig 5c**).

Simultaneously, the 100-kHz oscillator (trace D, **Fig 5c**) formed by comparator D and associated components gets forced LOW (trace E, **Fig 5c**) by two series resistor/diode combinations. Note the lack of oscillation while the Convert command pulse is HIGH. When that command goes LOW, the Q_1Q_2 current source charges C_2. During this period, comparator C's oscillator is enabled, and comparator D outputs a stream of 10-kHz clock pulses.

When the ramp voltage across C_2 (trace B, **Fig 5c**) exceeds the circuit's input, comparator B's output goes HIGH (trace C, **Fig 5c**), forcing comparator D LOW. The number of pulses that comparator D outputs is directly proportional to the input voltage. Q_3 and Q_4, used to modulate the data pulse stream back across the transformer, amplify these pulses. The diode string ensures that the data doesn't inadvertently trigger comparator A.

The design shown in **Fig 5a** produces 0 to 300 output

ADC with isolated I/O lines operates without external power

pulses for a 0 to 3V input. Its R_1D_1 path averts a +1-count uncertainty error by synchronizing the 10-kHz clock to the conversion sequence at the beginning of each conversion. The 500-kΩ pot in Q_2's emitter adjusts the scale factor; the circuit drifts less than 1 LSB over 5 to 45°C and requires 45 msec to complete a full-scale conversion.

Optocoupler controls thermocouple

This article's final example, shown in **Fig 6,** uses transformers and an optoisolator to implement a fully floating multiplexed thermocouple measurement system. The system draws power from T_2, which runs in a self-oscillating dc/dc-converter configuration with two 2N2219 transistors.

An LF13509 multiplexer sequentially switches seven inputs and a ground reference into an LM11 amplifier that provides gain and cold-junction compensation for the thermocouples. A 74C90 counter, serially addressed by a 4N28 optoisolator, switches the multiplexer. The ground-referenced channel ensures that monitoring instrumentation won't lose track of the multiplexer's state.

The LM11 feeds a unity-gain isolation amplifier (A_1), whose oscillator drive is provided by dividing down T_2's pulsed output and shaping the 74C90's output with A_4 and its associated circuitry. This drive scheme also

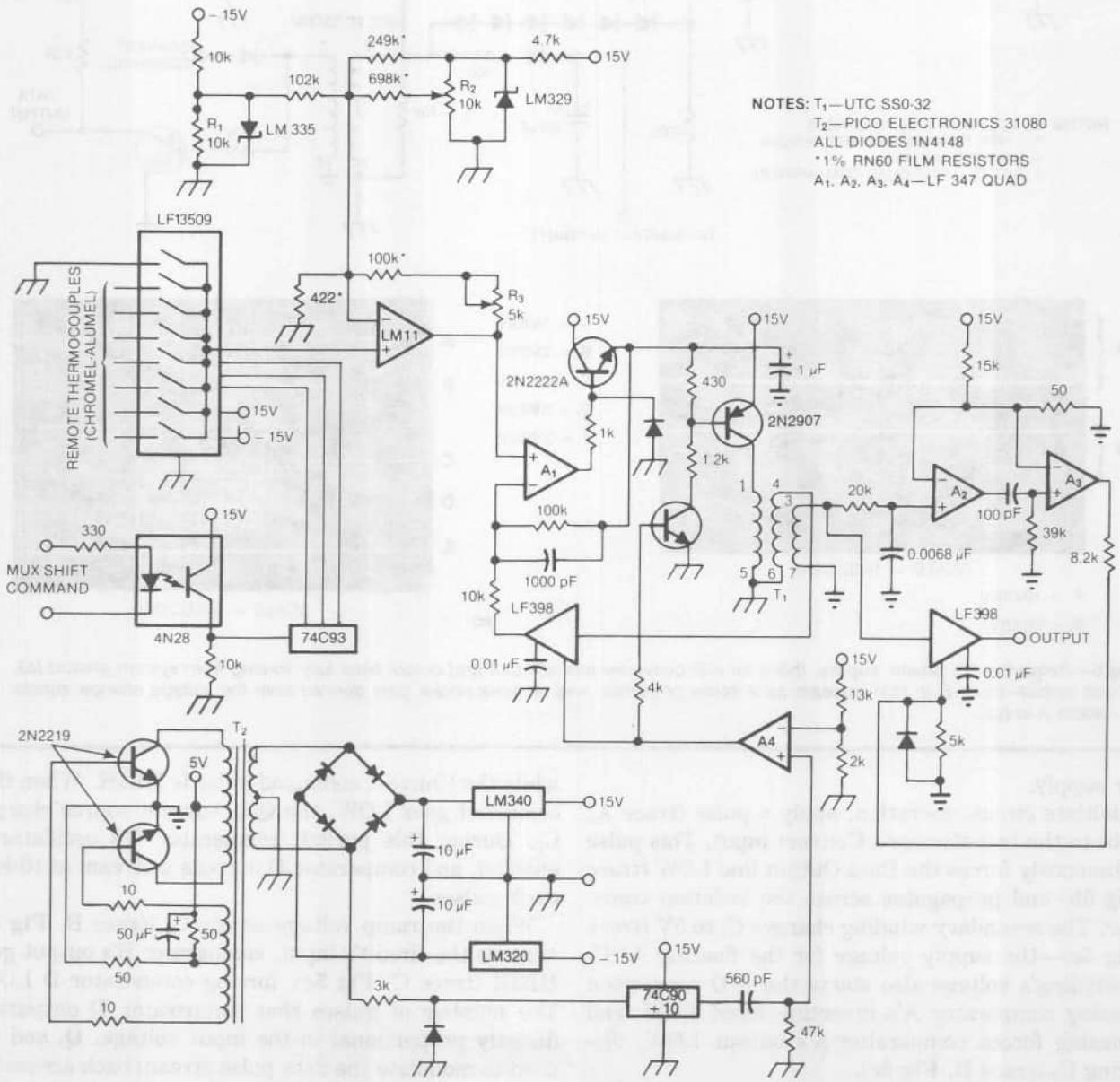

Fig 6—Supplying power to its floating system, *this thermocouple measurement system employs a multiplexer that sequentially switches seven inputs and a ground reference.*

Transformer, optoisolator combine in multiplexed thermocouple system

prevents unwanted interaction between the dc/dc converter and isolation amplifier.

The network develops a pulse across T_1's primary—pulse amplitude depends directly on the LM11's output. T_1's secondary feeds the pulse into an LF398 sample/hold amplifier. The trigger pulse for this amplifier is delayed to ensure that T_1 output sampling occurs well after settling.

Outputs from the LF398 and LM11 are identical. You can therefore monitor the fully floating thermocouple with grounded test equipment or computers. The most effective cold-junction compensation results when you hold thermocouple leads and LM335 isothermal.

Calibration for the circuit involves a 6-step procedure. First, adjust R_3 to set the LM11's gain at 245.7. Then short the noninverting input of the LM11 and LM329 to floating common, then adjust R_1 for a circuit output of 2.982V at 25°C. Next, remove the short across the LM329, then adjust R_2 for a circuit output of 246 mV at 25°C. Finally, remove the short from the LM11's input and the circuit is ready to use. **EDN**

Designer's Guide to: Temperature sensing

Part 1 of a 3-part tutorial on temperature explores the wide variety of sensors available, from basic to exotic, both analog and digital.

Jim Williams, Dept. of Nutrition and Food Science, Massachusetts Institute of Technology

Temperature plays a critical role in the performance of every electronic circuit. It's the one environmental parameter you can never ignore. Yet the moment you acknowledge its importance, temperature becomes fair game for systems that can sense, measure and control it. And that, fellow designers, is exactly what this 3-part series is all about.

This installment details the many types of sensors and transducers that convert heat into inputs for electronic circuits. Fundamentally, we can define temperature, as a statistical entity, as the number of molecular collisions in an environment per unit of time. All heat-sensing devices trace their performance to this basic physical fact.

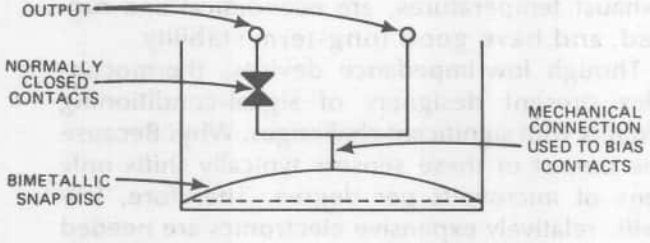

Fig. 1—Bimetallic disc snaps into the position shown by the dotted line when the ambient reaches the thermoswitch's transition temperature.

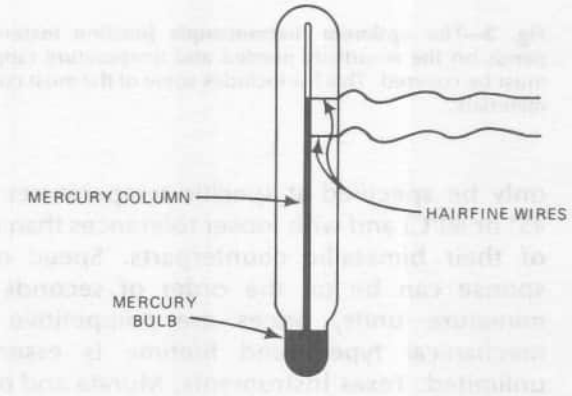

Fig. 2—Electrical contact is established when heat causes the mercury in this electrical output mercury thermometer to bridge both hairfine wires.

Thermostatic devices are a snap

Perhaps the most elementary component developed to convert temperature into an electrically measureable quantity is the bimetallic thermal switch. It uses metals with differing thermal coefficients of expansion to physically make or break an electrical contact at a preset temperature. Disc-shaped, bimetal elements provide snap action **(Fig. 1).**

Bimetallic thermal switches function from subzero temperatures to almost +300°C. Contacts

come in a variety of forms and can handle dry-circuit switching as well as currents beyond 15A. In addition, the hysteresis of the switching point can be specified.

Although inexpensive and reliable, bimetallic switches won't work in many situations because of their slow thermal response. Nevertheless, they still suit control applications such as crystal ovens and gyros, and find extensive use as temperature limit and override sensors. Manufacturers include Elmwood Sensors, Fenwal and Texas Instruments' Klixon Division.

Solid-state thermostatic devices take advantage of the exceedingly steep resistance curve of special ceramics. These materials are relatively unaffacted by temperature until that point where the resistance suddenly increases by orders of magnitude. Typically, solid-state thermostats can only be specified at specific temperatures (i.e., 45° or 80°C) and with looser tolerances than those of their bimetallic counterparts. Speed of response can be on the order of seconds with miniature units, prices are competitive with mechanical types, and lifetime is essentially unlimited. Texas Instruments, Murata and others sell these solid-state digital sensors.

JUNCTION MATERIALS	USEFUL TEMPERATURE RANGE (°C)	VOLTAGE SWING OVER RANGE
COPPER–CONSTANTAN	–270 TO + 600°C	25.0 mV
IRON–CONSTANTAN	–270 TO +1000°C	60.0 mV
CHROMEL–ALUMEL	–270 TO +1300°C	55.0 mV
CHROMEL–CONSTANTAN	–270 TO +1000°C	75.0 mV
PLATINUM 10%–RHODIUM/PLATINUM	0 TO +1550°C	16.0 mV
PLATINUM 13%–RHODIUM/PLATINUM	0 TO +1600°C	19.0 mV
PLATINUM 30%–RHODIUM/PLATINUM	+38 TO +1800°C	13.0 mV
PLATINEL 1813–PLATINEL 1503	0 TO +1300°C	51.0 mV
IRIDIUM–RHODIUM	+1400 TO +1850°C	2.5 mV
TUNGSTEN–RHENIUM	0 TO +2700°C	30.0 mV

Fig. 3—The optimum thermocouple junction material depends on the sensitivity needed and temperature range that must be covered. This list includes some of the most common materials.

Another generic relative of bimetallic thermoswitches, the electrical output mercury thermometer, is elegantly simple—just a glass-stem thermometer with very fine wires extending into the path of the mercury column **(Fig. 2).** Heat sensors of this type respond in 1-5 sec (at the trip point), have a sharply defined trip point with almost no hysteresis and boast nearly infinite life. Units with an absolute accuracy of 0.05°C are available, as are multiple and adjustable contact units.

Manufactured by P.S.G. Industries, thermometer-based thermoswitches make excellent choices for controlling ovens. For instance, they can control a thermodynamically properly designed crystal oven to 0.01°C stability to keep the crystal at its zero temperature-coefficient "turning point."

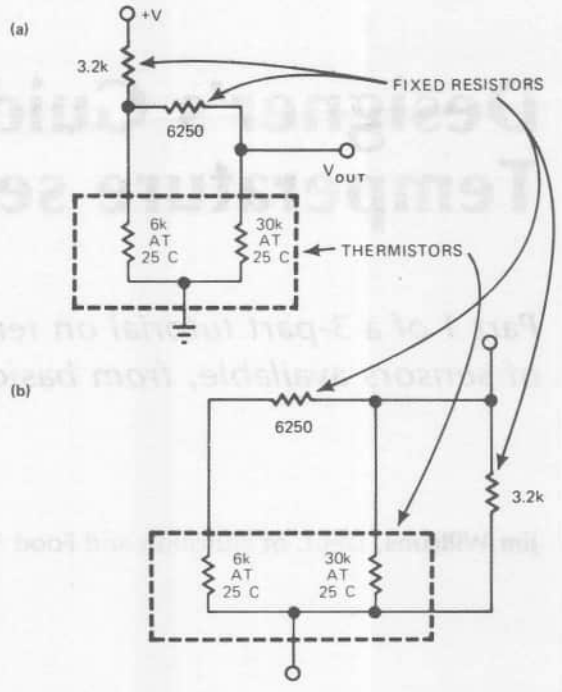

Fig. 4—Linear, accurate response can be obtained by combining two thermistors with fixed resistors. The penalty is decreased sensitivity. In **a,** the 3-terminal network functions as a temperature-dependent voltage source. In **b,** the same network is used in the 2-terminal mode to provide a shift in resistance that is linear with temperature.

Thermocouples handle wide temperature ranges

Thermocouples, a common form of a true analog-output temperature sensor, rely on the fact that junctions of dissimilar metals generate predictable low-level voltages as a function of temperature (Seeback effect). Of course, different combinations of metals produce junctions with varying characteristics **(Fig. 3).**

Because of their small size, thermocouples are fast devices and thus suit applications that emphasize speed of response. In addition, they function from cryogenic to well above jet-engine exhaust temperatures, are economical and rugged, and have good long-term stability.

Though low-impedance devices, thermocouples present designers of signal-conditioning circuits with significant challenges. Why? Because the output of these sensors typically shifts only tens of microvolts per degree. Therefore, low drift, relatively expensive electronics are needed to achieve resolutions better than 1°C.

Linearity of many thermocouple types is poor. Fortunately, however, the curves are predictable and repeatable, allowing designers to use either digital or analog linearization techniques.

The one serious drawback to thermocouples is that they require a reference to a known temperature for use in absolute temperature measurements; i.e., the circuitry must compare the output of the "signal" thermocouple with that of a similar "reference" thermocouple. Of course, the latter must be held at a known temperature.

Each signal thermocouple must have its own reference junction. Normally, all reference junctions are placed in the same constant temperature bath of 0.01°C (32.02°F), which is the triple point of water. "Black box" electronic equivalents of these triple-point baths are available from Omega, Acromag and others.

Every connection ("junction") between dissimilar metals represents a de-facto thermocouple, intended or not. Therefore, customary engineering practice in thermocouple cabling makes each signal wire (and all connections through which it passes) of the same metal as the side of the junction(s) to which it connects. Complex and expensive, these special cables and connectors run between the measuring thermocouple and reference junction.

It is worth noting that most of the world's thermocouples are junctions of solder and copper. These "thermocouples," usually unintentional and overlooked, can easily generate 20 times the offset drift of the low-drift amplifier in a precision preamp.

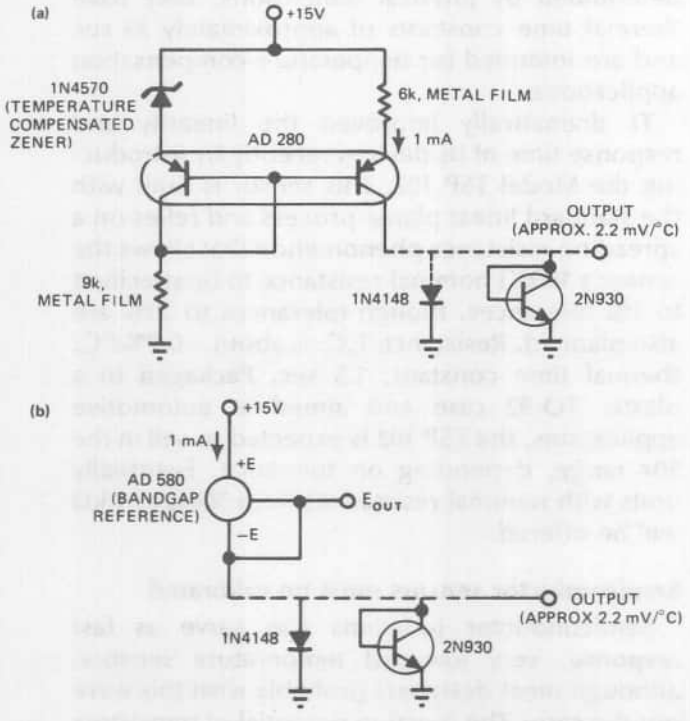

Fig. 5—Standard diodes and transistors can function as temperature sensors. The AD 820 transistor pair and associated components in **a** form a typical current source that can drive either diode or transistor sensors. For simplicity, these devices can be driven from voltage sources, but linearity decreases. An alternate current-source design, the band-gap reference circuit of **b** is extremely simple yet offers reasonably good performance.

Platinum sets the standard

Designers generally acknowledge platinum resistance wire as the standard for accuracy and repeatability in a temperature sensor. Some units have histories of years of agreement within 0.1 millidegree with the National Bureau of Standards calibration facilities. These generic cousins of wirewound resistors find heavy use in transfer-type measurements and provide linearity within several degrees over a 100° range.

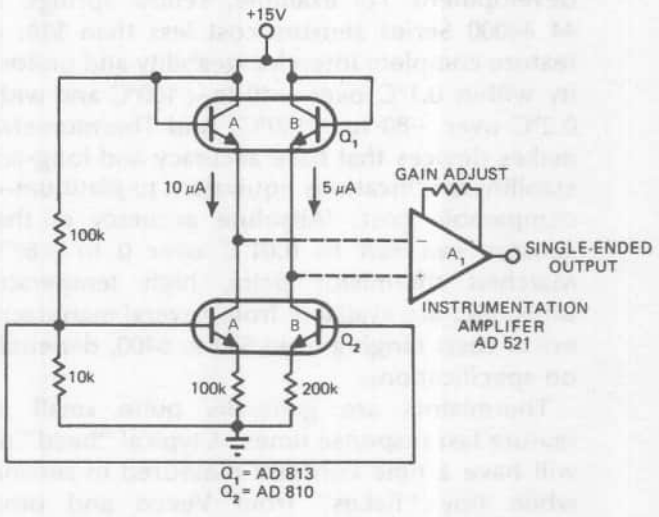

Fig. 6—In this practical current-ratio differential pair temperature sensor, dual transistor Q_2 provides currents of 10 and 5 μA through Q_{1A} and Q_{1B}, respectively. The difference between the V_{be} of Q_{1A} and that of Q_{1B} is a function highly linear and predictable with temperature. Instrumentation amplifier A_1 provides a single-ended output.

The absolute accuracy of platinum sensors can run to better than 0.01°C for standards-lab units. Resistance at 25°C ranges from tens to hundreds of ohms. Temperature coefficients are positive and typically run 0.5% of value/°C.

Because they are wirewound devices, platinum sensors tend to be large. However, versions about the size of 1/8W resistor are readily available.

Industrial versions of platinum sensors are reliable and retain much of the performance of premium units, yet they cost much less. A good industrial-grade sensor sells from $20-$100, while a *ne-plus-ultra* standards unit with a documented aging history can cost up to $1000.

Thermistors boast high sensitivities

Thermistors have the highest sensitivity of any common temperature transducer—at 25°C a typi-

cal unit shifts its resistance at a −5%/°C rate. The response curve is nonlinear, but predictable. Commercially available thermistors function over a range of −100 to +450°C and come in values from tens of ohms to megohms. Because of their high sensitivity, they frequently make the best choice in high-resolution measurement and control apparatus.

Designers often unjustly label thermistors as wild and unstable devices because of difficulties with early and some present commercial devices. But firms like Yellow Springs Instrument Co. and Thermometrics pursue serious research programs and have made great progress in thermistor development. For example, Yellow Springs' YSI 44 44000 Series sensors cost less than $10, yet feature complete interchangeability and uniformity within 0.1°C over −40 to +100°C and within 0.2°C over −80 to +150°C. And Thermometrics makes devices that have accuracy and long-term stability specifications equivalent to platinum—at comparable cost. (Absolute accuracy of these sensors can run to 0.01°C over 0 to +60°C.) Matched thermistor pairs, high temperature units, etc. are available from several manufacturers at costs ranging from $50 to $400, depending on specifications.

Thermistors are generally quite small and feature fast response times. A typical "bead" unit will have a time constant measured in seconds, while tiny "flakes" from Veeco and others respond in milliseconds.

Networks trade sensitivity for linearity

Manufacturers combine one or two thermistors in a single package with external fixed resistor shunts to produce sensor networks with highly linear response curves. Such networks are available over the −45 to +100°C range. One model, the Yellow Springs Instrument "Thermilinear" 44018, operates from 0 to +100°C with 0.15°C absolute accuracy and linearity. It costs about $15.

The penalty for the linearized response of composite thermistor/resistor networks is a drop of approximately an order of magnitude in sensitivity. These units can function as linearly temperature-dependent resistors or can operate in a potentiometric mode to produce an output voltage linear with temperature **(Fig. 4).** Composite beads containing two thermistors are not much larger than single thermistor units and have response times measured in seconds.

These thermistors think positive

A special class of thermistors, available from Texas Instruments and Pennsylvania Electronic Technology, has a positive 0.7%/°C temperature coefficient. TI's "Sensistors" are about the size of

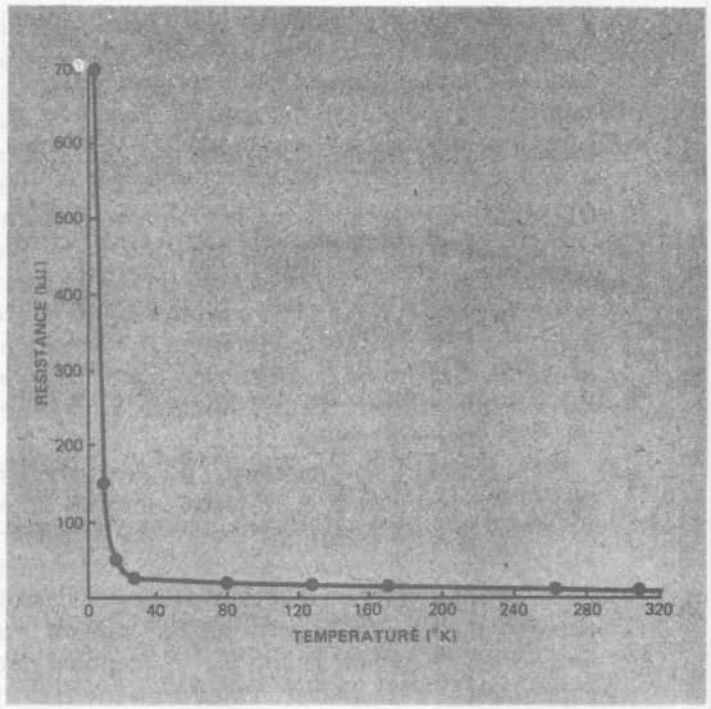

Fig. 7—Even a 1/4W resistor can be used to sense temperature. This curve was plotted for an 820Ω unit from Allen-Bradley.

1/4W resistors and are linear within 5° over −75 to +150°C. Bulk silicon devices with resistances determined by physical dimensions, they have thermal time constants of approximately 35 sec and are intended for temperature-compensation applications.

TI dramatically improved the linearity and response time of its devices recently by introducing the Model TSP 102. This sensor is built with the standard linear planar process and relies on a spreading resistance phenomenon that allows the sensor's 1000Ω nominal resistance to be specified to 1% tolerances, though tolerances to 20% are also planned. Resistance T.C. is about +0.7%/°C; thermal time constant, 1.5 sec. Packaged in a plastic TO-92 case and aimed at automotive applications, the TSP 102 is expected to sell in the 50¢ range, depending on tolerance. Eventually units with nominal resistances from 500Ω to 5 kΩ will be offered.

Semiconductor sensors must be calibrated

Semiconductor junctions can serve as fast response, very low-cost temperature sensors, although most designers probably wish this were not the case! The junction potential of transistors and diodes changes at about 2.2 mV/°C over a wide range of temperature. Linearity of within 2° is possible over −85 to +125°C with constant-current junction biasing techniques **(Fig. 5).** Source impedance is low and the output is a medium-level signal with 25 to 100 times the

voltage T.C. of a thermocouple.

Unfortunately, every semiconductor junction has its own initial offset and gain, so each individual device must be calibrated—a process that can easily outweigh the initial cost advantage. Recently, however, manufacturers have devised "clever" circuits to solve this problem. ECD Corp., for instance, uses diodes as sensors for a hand-held thermometer, yet achieves 0.5°C accuracy over −55 to +125°C with interchangeable probes.

The most sophisticated form of semiconductor sensor is the current-ratio differential pair **(Fig. 6).** Here transistor Q_{1A} is biased at higher collector current than Q_{1B}. The difference in V_{be}'s vs. temperature is theoretically predictable and extremely linear. Sensors based on this approach can afford >1°C accuracy over 300°C temperature ranges. National Semiconductor introduced an IC version of this circuit several years ago, the LX5600. It combines on chip, current-ratio differential pair and associated signal-conditioning electronics, and produces a scalable output voltage.

The highest performance IC version of the current-ratio differential pair sensor, Analog Devices' new Model AD 590, is a 2-terminal device that guarantees 1°C accuracy over −125 to +200°C and features a scaled current-source output. For remote sensing, a 5 to 15V supply can power the device down thousands of feet of wire, while the current output returns on another wire. The current output is scaled in degrees Kelvin (298.2 μA = 298.2°K), but other temperature scales are available by offsetting the output.

The AD 590 is an extremely low-noise device; preliminary studies indicate a noise level below (10^{-5})°C at 50°C. The sensor's TO-18 package provides reasonably fast thermal response, although other package designs (such as epoxy-coated or glass-passivated chips) may result in an extremely fast sensor. Sensitivity is about 0.3%/°C at 25°C.

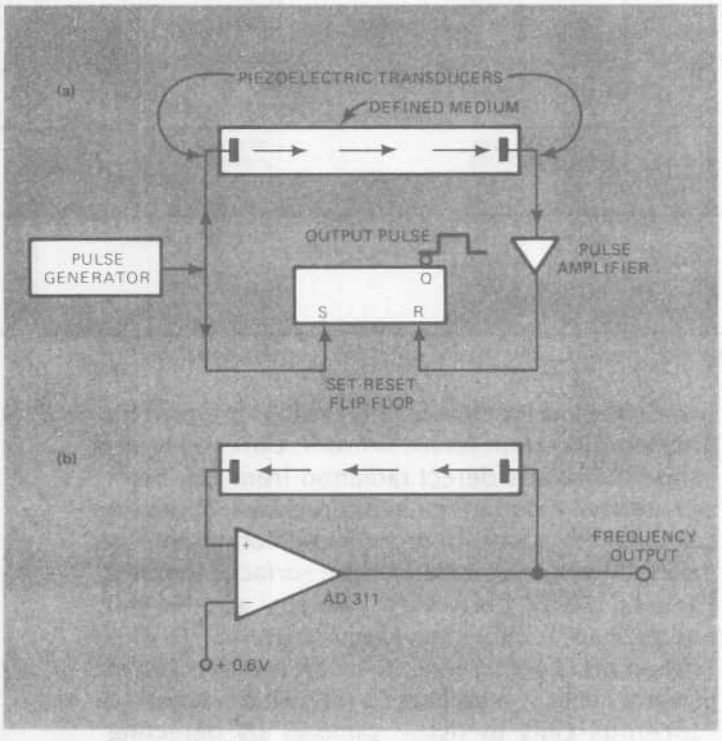

Fig. 8—In the acoustical thermometer diagrammed in **a** the pulse generator drives the "send" piezoelectric transducer, while simultaneously setting the output of the flip-flop to the ONE state. The sound wave propagates through the known medium and strikes the "receive" piezoelectric transducer, generating a small pulse. After amplification, this pulse resets the flip-flop to ZERO. Because the speed of sound varies with temperature in a predictable and reproducible manner, the temperature can be determined from the pulse width. In **b,** the acoustic thermometer is placed between the "+" input of a comparator and the output, causing an oscillation whose frequency varies with temperature.

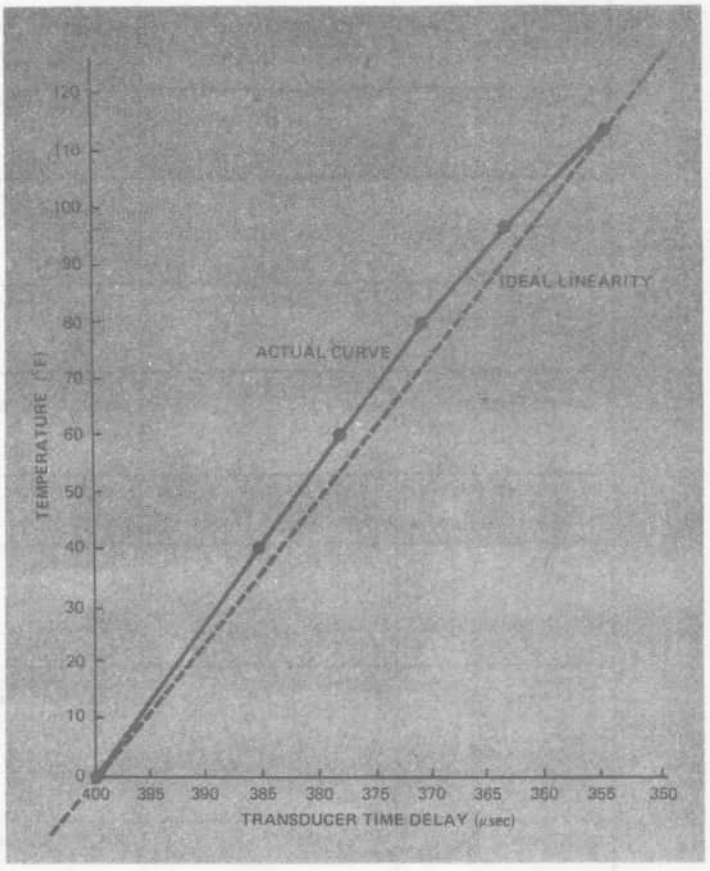

Fig. 9—A 3.6-in. tube filled with dry air and capped with piezoelectric sonic transducers produced this delay time plot.

With carbon resistors, you can go low

Standard carbon resistors are often used as cryogenic temperature sensors. Depending on the manufacturer and process control, units can be reasonably uniform from batch to batch. **Fig. 7** shows the response of a 1/4W Allan-Bradley resistor to a range of temperatures.

Carbon resistors can also provide inexpensive

TYPE	RANGE OF OPERATION	SENSITIVITY AT +25°C	ACCURACY	LINEARITY
THERMOSWITCHES & ELECTRICAL OUTPUT THERMOMETERS	−25 TO +265°C FOR BIMETALLICS; −35 TO +390°C FOR THERMOMETERS	HYSTERESIS AS LOW AS ±1°C IN BIMETALLIC UNITS. NO HYSTERESIS IN THERMOMETER TYPES	AS GOOD AS ±0.05°C FOR THERMOMETERS; ±2° FOR BIMETALLICS	NOT APPLICABLE
THERMOCOUPLES (ALL TYPES)	−270 TO +1800°C	TYPICALLY 1%/°C	±0.5°C WITH REFERENCE	POOR
THERMISTORS AND THERMISTOR COMPOSITES	−100 TO +450°C	−5%/°C FOR THERMISTORS; −0.5%/°C FOR LINEARIZED UNITS	±0.1°C STANDARD FROM −40 TO +100°C; ±0.01°C FROM 0 TO +60°C AVAILABLE	±0.2°C FOR LINEARIZED COMPOSITE UNITS OVER 100°C RANGES
PLATINUM RESISTANCE WIRE	−200 TO +900°C	APPROXIMATELY +0.5%/°C	±0.1°C READILY AVAILABLE; ±0.01°C IN PRECISION STANDARDS—LAB UNITS	NEARLY LINEAR OVER LARGE SPANS; TYPICALLY WITHIN 1° OVER 200°C RANGES
DIODES & TRANSISTORS	−250 TO +175°C	−2.2 μV/°C (APPROX. −0.37%/°C)	±2 TO ±5°C OVER −85 TO +125°C	WITHIN 5% OVER OPERATING RANGE
INTEGRATED CIRCUIT (CURRENT RATIO DIFFERENTIAL PAIR)	−125 TO +200°C FOR AD 590; −85 TO +125°C FOR OTHERS	0.4%/°C TYPICAL	±1° OVER −125 TO +200°C FOR AD 290	WITHIN 1° FOR TYPE AD 290 (0.2° FROM 0 TO +70°C)
QUARTZ CRYSTALS	−80 TO +250°C	0.0035%/°C	±0.03°C ACHIEVEABLE	0.01° ACHIEVABLE OVER 100°C RANGES
CARBON RESISTORS	−250 TO +200°C	0.05%/°C (VARIES WITH MANUFACTURER AND POWER RATING); 300%/°C AT CRYOGENIC TEMPERATURES	VERY POOR	POOR OVER LARGE RANGE; AS GOOD AS 5°C OVER 0 TO +75°C; WILDLY NON-LINEAR AT CRYOGENIC TEMPERATURES
INFRARED	0 TO +3500°C	NOT APPLICABLE	±0.4% FOR HIGH QUALITY UNITS; ±5 TO ±10% FOR LOW COST UNITS	POOR
ACOUSTIC THERMOMETERS	−250 TO +4000°C	0.05%/°C (DRY AIR)	AS GOOD AS ±0.01°C OVER +10 TO +100°C	WITHIN 2° FROM +10 TO +100°C
PYROELECTRIC	−270 TO +200°C	20V/1 STEP	NOT APPLICABLE	NOT APPLICABLE

Fig. 10—To help you select the temperature sensor that best meets your needs, this chart summarizes the important characteristics of the most common types.

low-order temperature compensation in circuitry. However, note that a significant difference exists between the T.C.'s of various brands and wattage sizes. Further, resistor manufacturers will not likely guarantee any curve with temperature. Generally speaking, a standard 1/2W resistor will provide an average of −500 ppm/°C from 0 to +100°C.

Special sensors for special problems

Under certain conditions, the standard temperature sensors previously described do not provide the necessary characteristics to make a measurement. Fortunately, a number of exotic sensors have been developed to meet special needs. We will now describe four of the most interesting types.

IR sensors take a "hands-off" approach

A number of applications require a noncontact heat measurement—a job easily handled by infrared (IR) temperature sensors. Extremely sensitive, IR sensors detect radiation from an object or surface. Combined with precision optics in satellites that study environmental conditions on earth, they can determine ocean surface temperature to 0.5°C precision. And in a "thermal microscope" under development at M.I.T.'s Nutrition and Food Science Instrumentation Lab, IR sensors allow researchers to follow the spread of cancerous cells in tissue samples by detecting 0.01°C temperature differences in the tissue. This same instrument could serve to quantitatively measure thermal gradients in a power transistor or integrated circuit. Key to its performance is an Indium-Antimonide detector cooled by liquid nitrogen to obtain low noise.

High-performance IR sensors have unit costs ranging from hundreds to thousands of dollars. Further, they usually require complex and expen-

	SPEED IN STIRRED OIL	SIZE	PACKAGE	COST	COMMENTS
	5 TO 30 SEC FOR BIMETALLIC TYPES; 1 TO 5 SEC FOR MERCURY TYPE (AT THE TRIP POINT)	BIMETALLIC UNITS TYPICALLY ARE 3/32 x 3/4 x 1/4 IN.; THERMOMETERS CAN BE AS SMALL AS 0.1 IN. DIA. x 1 IN. LONG	BIMETALLIC–METAL, GLASS, CERAMIC, PLASTIC. THERMOMETER–GLASS	$1 TO $85	BIMETALLIC UNITS INEXPENSIVE. THERMOMETERS COME IN CALIBRATED ADJUSTABLE TYPES IF DESIRED.
	TYPICALLY 1 SEC; SOME TYPES ARE FASTER	0.02 IN. BEAD TYPICAL; 0.0005 IN. UNITS ARE AVAILABLE	METALLIC BEAD	$1 TO $50 DEPENDING ON TYPE AND SPECIFICATIONS	REQUIRES REFERENCE. LOW LEVEL OUTPUT REQUIRES STABLE SIGNAL CONDITIONING COMPONENTS.
	1 TO 10 SEC IS STANDARD; 3 TO 100 mSEC TYPES ARE AVAILABLE	BEADS CAN BE AS SMALL AS 0.005 IN., BUT 0.04 TO 0.1 IN. IS TYPICAL; "FLAKE" TYPES ARE ONLY 0.001 IN. THICK	GLASS, EPOLY, TEFLON ENCAPSULATED, METAL HOUSING, ETC.	$2 TO $10 FOR STANDARD UNITS; $10 TO $350 FOR HIGH PRECISION TYPES AND SPECIALS	HIGHEST TEMPERATURE SENSITIVITY OF ANY COMON SENSOR. SPECIAL UNITS REQUIRED FOR LONG TERM STABILITY ABOVE +100°C.
	TYPICALLY SEVERAL SECONDS	1/8 TO 1/4 IN. TYPICAL; SMALLER SIZES AVAILABLE	GLASS, EPOXY, CERAMIC, TEFLON, METAL, ETC.	$25 TO $1000, DEPENDING ON SPECS; MOST INDUSTRIAL TYPES BELOW $100	SETS STANDARD FOR STABILITY OVER LONG TERM. HAS WIDER TEMP. RANGE THAN THERMISTOR, BUT LOWER SENSITIVITY.
	1 TO 10 SEC IS STANDARD; SMALL DIODE PACKAGES PERMIT SPEEDS IN mSEC RANGE	STANDARD DIODE AND TRANSISTOR CASE SIZES. GLASS PASSIVATED CHIPS PERMIT EXTREMELY SMALL SIZES	GLASS, METAL	BELOW 50¢	REQUIRE INDIVIDUAL CALIBRATION. MUST BE DRIVEN FROM CURRENT SOURCE FOR OPTIMUM PERFORMANCE. EXTREMELY INEXPENSIVE.
	SEVERAL SECONDS	TO-18 TRANSISTOR PACKAGE SIZE; ALSO MINI-DIP	METAL, PLASTIC	$2 TO $10	AD 590 IS A 2-TERMINAL CURRENT-OUTPUT DEVICE.
	2 TO 5 SEC ACHIEVABLE	AS SMALL AS 0.5 IN. DIA. x 0.75 IN. LONG	GLASS, METAL	$75 TO $350	NOT READILY AVAILABLE COMMERCIALLY. REQUIRES SIGNIFICANT SIGNAL CONDITIONING. PARASITICS IN CABLES PRESENT PROBLEMS. EXCELLENT LINEARITY AND ACCURACY.
	3 TO 10 SEC	1/4W, 1/2W RESISTOR SIZES	TYPICAL RESISTOR PACKAGE	5¢	WILL PROVIDE SECOND ORDER TEMP. COMPENSATION FOR CIRCUITS. INEXPENSIVE CRYOGENIC SENSOR. WHILE UNIT-TO-UNIT UNIFORMITY IN A GIVEN BATCH MAY BE GOOD, MANUFACTURERS WILL NOT GUARANTEE SPECS.
	LESS THAN 1 SEC	THERMISTOR TYPE SENSORS TYPICALLY 0.01 IN. FLAKE; SOPHISTICATED UNITS AS LARGE AS 12 x 3 IN., INCLUDING LIQUID NITROGEN DEWAR FLASK, ETC.	GLASS	$10 TO $2500	NON-CONTACT TEMP. SENSOR. SOPHISTICATED SENSORS REQUIRE EXPENSIVE SUPPORT OPTICS AND ELECTRONICS.
	< 1 mSEC UNDER IDEAL CONDITIONS. TYPICALLY SEVERAL SECONDS	TYPICALLY 1.5 x 0.25 IN.	SOME TYPES HAVE NO PACKAGE; OTHERS USE METAL, GLASS, CERAMIC, QUARTZ, ETC.	$5 TO $1000, DEPENDING ON DESIRED PERFORMANCE	NOT COMMERCIALLY AVAILABLE. HIGH PERFORMANCE TYPES REQUIRE FULL DESIGN OF TRANSDUCERS AND PACKAGE.
	TYPICALLY 10 SEC TO 1 MINUTE	0.75 IN. DIA. DISC IS TYPICAL	CERAMIC	$10	HIGHEST GAIN TEMP. SENSOR KNOWN, BUT SENSES RATE OF CHANGE ONLY. NO OUTPUT FOR CONSTANT TEMP. A TRUE AC COUPLED DEVICE. OUTPUT IMPEDANCE IS $10^{12}\Omega$.

sive optics, cooling equipment and signal-conditioning electronics.

The manufacture of IR sensing devices is a specialized, difficult art, and elements of witchcraft seem necessary to produce high-performance devices. Santa Barbara Research Corp. and Barnes Engineering number among the leading innovators in this field.

Acoustic thermometers go to extremes

Acoustic thermometers operate on the principle that the speed of sound varies with temperature in a medium in a highly predictable and reproducible manner over temperatures ranging from cryogenic to thousands of degrees. These devices usually operate as either clocked systems or oscillators **(Fig. 8).** In both modes, the sensor effects a temperature-dependent delay line.

Acoustic sensors function at temperature extremes that other sensors cannot tolerate. Linearity is good over small ranges, but over extremely wide dynamic ranges or for precision work, the output must be linearized by digital methods.

An acoustic thermometer composed of a 3.6-in. dry-air-filled tube with piezoelectric sonic transducers produced the data in **Fig. 9.** Precise acoustic thermometers require considerable engineering to compensate for temperature errors in the sonic transducers, thermal expansion effects in the tube walls and wave dispersion inside the device. Acoustic thermometers are not available commercially, although a number of experimental designs have been published. They can be made as small as 1/8×1/4 in. with time constants of 0.5 to 15 sec.

Pyroelectrics measure minute changes

Pyroelectric materials boast the highest sensitivity of any known sensor. Pyroelectric thermometers consist of crystalline solids that respond to

the time derivative of temperature (Δtemperature/Δtime). One typical unit can produce a 20V peak pulse for a 1°C step change, and temperature rate deltas as small as 60 nanodegrees/sec have been measured with devices of this type.

Unfortunately, pyroelectric sensors are relatively unknown and commercial versions are not readily available. Their output impedance is around $10^{12}\Omega$, so high-performance FET or varactor-bridge input amplifiers must be used for signal conditioning. Since they are extraordinarily high-gain ac devices, pyroelectrics hold promise as detectors for low-level micro-calorimetry.

Quartz crystals—results worth the effort

The resonant frequency of quartz crystals changes with temperature. However, even inexpensive crystals have a temperature coefficient of only 1 ppm/°C. To get higher sensitivities, the "LC" cut was devised to raise the temperature coefficient to 35 ppm/°C over −80 to +250°C. This is still low sensitivity, but the availability of crystal time bases with 1×10^{-9} stability means that temperature shifts of (10^{-4})°C can be observed. Hewlett-Packard's Model 2801A thermometer uses this type of sensor.

The problems involved in designing around quartz crystals as temperature sensors are formidable: Many crystal manufacturers do not even want to make the "LC" cut. Capacitance shifts in the cable can easily cause erratic operation and incorrect readings. And a precision time base that's difficult to make and expensive to buy is required for high-resolution work. For the latter two reasons quartz sensors usually require dedicated cables and sometimes include the oscillator circuit in the cable.

On the positive side—as would be expected of quartz—long-term stability, accuracy and linearity characteristics are all excellent.

More to come....

Fig. 10 summarizes the key characteristics of all temperature sensors discussed in this article.

Part 2 of this series will appear in our May 20, 1977 issue. It will match specific signal-conditioning circuits with popular temperature-sensor types, as well as provide practical design hints and typical performance details. **Part 3,** scheduled to appear in our June 20, 1977 issue, will describe the application of measurement schemes to temperature controllers, including one capable of very spectacular performance. □

Bibliography

1. "Theory and Properties of Thermocouple Elements," American Society for Testing and Materials.

2. "Use of Thermocouples in Temperature Measurement," American Society for Testing and Materials.

*3. Anderson, "Stability of Platinum Resistance Thermometers," National Bureau of Standards. **

*4. Anderson, "Carbon Resistance Thermometry," Univ. of Illinois. **

*5. Benjaminson and Rowland, "Development of the Quartz Crystal Resonator as a Temperature Sensor," Hewlett-Packard Co. **

*6. Carr, "An Evaluation of Industrial Platinum Thermometers," Oak Ridge National Lab. **

*7. Darling and Selman, "Effects of Environment on Performance of Noble Metal Thermocouples," Johnson, Matthey and Co., Wembley, England. **

*8. Dutt, "Practical Applications of Platinum Resistance Thermometers," Rosemont Engineering Co. **

*9. Howard, "Error Accumulation in Thermocouple Thermometry," Boeing Co. **

*10. Lang, "The Pyroelectric Thermometer: A Sensor for Measuring Extremely Small Temperature Changes or Rates of Change," McGill Univ., Toronto. **

*11. Lynnworth and Carnevale, "Ultra-sonic Thermometry Using Pulse Techniques," Panametrics. **

*12. Sapoff, "Thermistors for Biomedical Use," Thermometrics, Edison, NJ. **

*13. Schlosser and Munnings, "Survey of Thermometric Characteristics of Recently Produced Allan Bradlen/Ohmite Resistors," Univ. of Toronto. **

*14. Starr and Wang, "Thermocouples and Extension Wires," Wilbur Drive Co., Newark, NJ. **

15. Timko, M.P., "A Two Terminal IC Temperature Transducer," IEEE Journal of Solid State Circuits, Volume SC 11, #6 Dec., 1976.

*16. Trolander, Harruff and Case, "Reproducibility, Stability and Linearization of Thermistor Resistance Thermometers," Yellow Springs Instrument Co. **

*17. Verster, "The Silicon Transistor as a Temperature Sensor," Council for Scientific and Industrial Research, Pretoria, South Africa. **

**Available through the Instrument Society of America. Presented at the Fifth International Symposium on Temperature, Washington, DC, 1971.*

Exotic-transducer interfacing calls for proven techniques

Measuring fundamental physical phenomena involves designing circuitry that conditions sensor output signals. This conclusion of a 2-part series looks at schemes for detecting acceleration and magnetic fields.

Jim Williams, National Semiconductor Corp

Whether your measurement applications involve sensing a disturbance in the earth's magnetic field or monitoring acceleration, you can often employ building-block approaches to sensor-interface-circuit designs. These signal-conditioning techniques meet the interfacing requirements of such devices as piezoelectric and pendulous accelerometers, linear variable differential transformers, rate gyros and flux-gate transducers.

Charge-sensitive op amp detects g-force signal

Consider, for example, the piezoelectric accelerometer, a device employing a mass-loaded ceramic or quartz element that generates an output charge proportional to its acceleration. You can ascertain an impact level's frequency and amplitude characteristics if you combine the device with **Fig 1**'s interfacing electronics—a signal-conversion stage that employs a charge-sensitive, very-low-input-bias-current op amp with a capacitive feedback element to furnish a V/g output. (The $10^{11}\Omega$ resistor establishes the circuit's dc stability; the variable capacitor sets the stage's charge-to-voltage conversion sensitivity.)

In the **Fig 1** configuration, the accelerometer looks directly into the op amp's ground-potential summing junction. The resulting lack of voltage differential between the interconnecting cable's center conductor and shield eliminates capacitive loading and therefore prevents signal rise-time degradation. Thus, you can use long cable runs between the transducer and its amplifier. (However, employ cable that's spec'd for low triboelectric-charge effects.)

Fig 1's scope photo illustrates this design's operation. It depicts the results of mounting an accelerometer on a standard hand-held voltmeter and dropping the combination on the floor. The trace represents an initial shock level of nearly 1000g and three lower amplitude aftershocks. In other words, the 8-oz voltmeter "weighed" 500 lbs during the impact.

Although piezoelectric transducers are suitable for measuring peak or instantaneous accelerations, the force-balanced pendulous accelerometer (**Fig 2**) better suits monitoring a constant acceleration. This device is basically a transformer with a pivoted, movable core. Two of the transformer's windings—the pick-off drive and sense coils—determine the core's position; the remaining two control the core's position. Additional internal elements include two temperature sensors: One merely monitors the device's operating temperature; the other works with the heater element to stabilize that temperature. (Temperature control is needed because the viscous-damped pendulum uses dampening fluid with temperature-sensitive viscosity.)

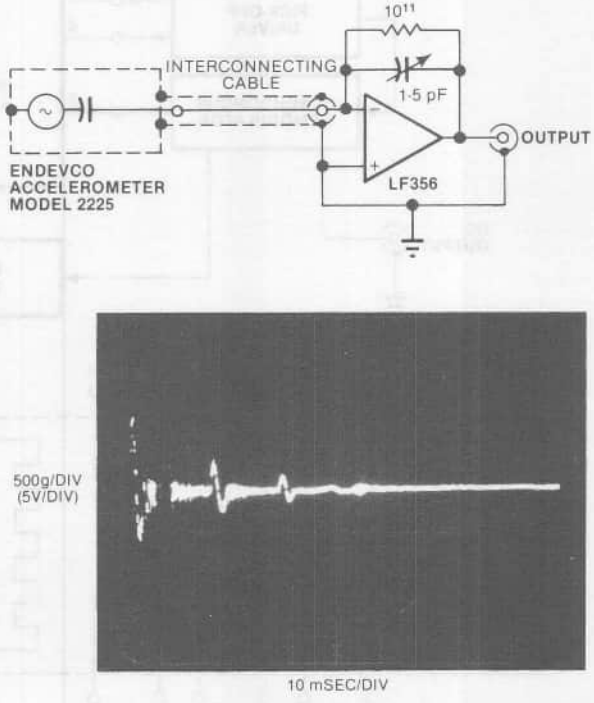

Fig 1—Piezoelectric accelerometers *generate an output charge that's proportional to a sensed shock level. By using a charge-to-voltage converting op amp, you can monitor fast, high-level impacts like the 1000g force represented by the scope trace.*

Some sensors detect movement by not moving

Fig 2's block diagram depicts how you can meet the sensor's circuit requirements. When excited, the pick-off drive coil generates a field that couples to the sense coil via the transducer's core. When an accelerative force tries to move the core, the sense coil's changed output creates an error signal that can be synchronously demodulated and reapplied to the torque winding in a way that maintains the core's original position. You can determine the accelerative force's magnitude by measuring the torque driver's corrective-current level. And because the signal is synchronously demodulated, you can also determine the direction along the pendulum's sensitive axis in which the force occurred. Note that because the torque coil can only attract the pendulum, a separate bias coil must provide a constant force for the torque coil to work against. These combined actions prevent the pendulum from moving, and as a result, the pendulous accelerometer's accuracy, linearity and dynamic range are very high.

Fig 3 details the circuits represented by **Fig 2**'s block diagram. Op amp A_{1A} and its booster stage generate the bias coil's current by sensing the signal developed across a resistor and comparing it with a reference voltage in a closed-loop configuration. A transistor phase-shift oscillator combines with another op amp (A_{1B}) and its driver to provide the pick-off drive coil's excitation. Here, too, a current-monitoring resistor furnishes the loop's error signal. Oscillator amplitude stabilization results from the combined actions of op amps A_{1C} through A_{2A}; the error signal is amplified, rectified, filtered and employed as the oscillator's supply voltage.

A_{2C} through A_{3B}'s booster stages process the sense coil's error signal. The booster's high-level dc output drives the torque coil and thus completes the pendulum-correcting feedback loop. The error signal's synchronous demodulation occurs because of A_{2B} and its associated FET. In this configuration, the oscillator's signal drives the op amp (and thus the FET) in an OFF/ON switching fashion. When the FET is OFF, A_{2D}'s + input sees the error signal; when the FET is ON, the − input is operational. Thus, A_{2D}'s gain changes from + to − synchronously with the sense coil's error signal, yielding a dc voltage whose amplitude and polarity completely define the pendulum's magnitude and direction. You calibrate this circuit by loading the accelerometer to at least one-half its sensing range and adjusting the phase trimmer for a maximum dc output level.

The remaining circuits—A_3 and the LM395—form the temperature-control loop. The temperature sensor's output (pin 9) forms one leg of a 4-resistor bridge. At the control temperature of 180°F, the sensor's

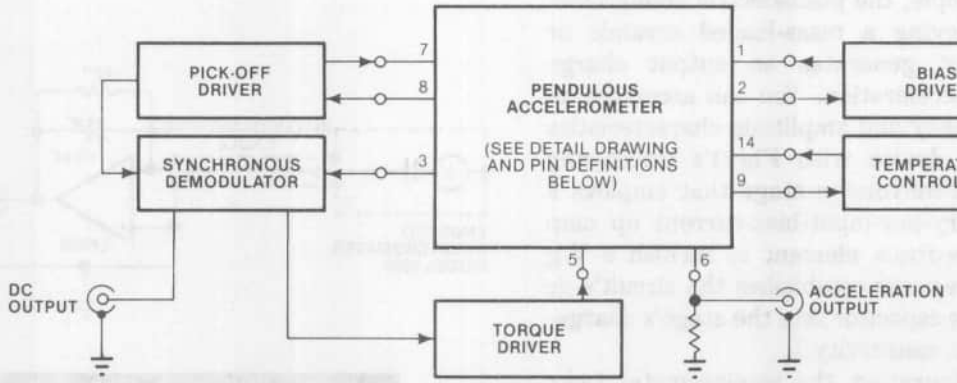

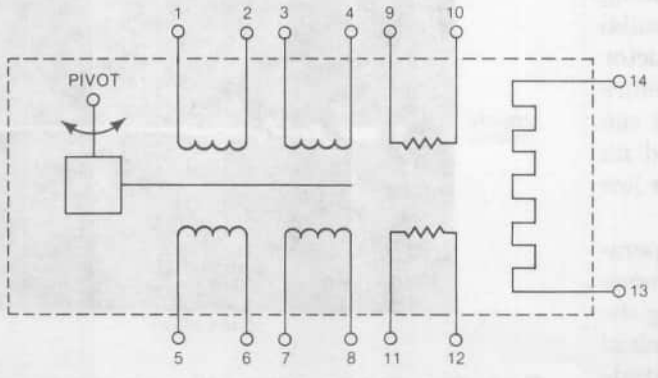

PIN	FUNCTION	LEAD COLOR
1	BIAS	RED
2		ORN
3	PICK-OFF SENSE	WHT-BRN
4		WHT-BRN
5	TORQUE	GREY
6		PURPLE
7	PICK-OFF DRIVE	WHT-GRN
8		RED-WHT
9	TEMPERATURE SENSE	BLUE
10		GRN
11	TEMPERATURE MONITOR	WHT-YEL
12		WHT-BLU
13	HEATER	BLK
14		BRN

Fig 2—Pendulous accelerometers *detect an external force by synchronously detecting the error signal generated when the transformer's core attempts to move. This error signal gets amplified and reapplied via the torque coil to counterbalance the core's movement; the correcting current's magnitude represents the applied force.*

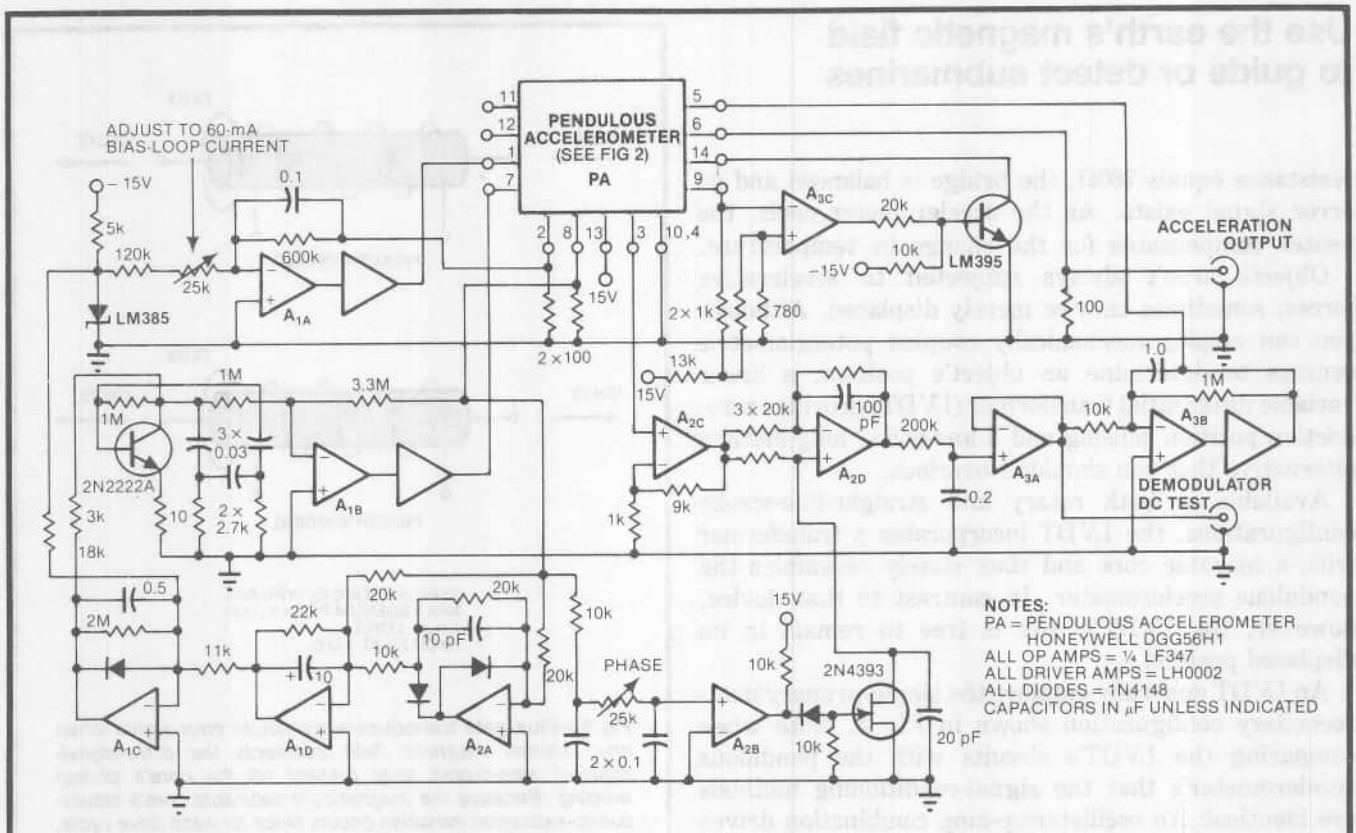

Fig 3—A transistor oscillator *generates the pick-off drive coil's signal used by* ***Fig 2****'s accelerometer. The drive coil's signal feeds back to the oscillator, its stabilization stages (A_{1C} through A_{2A}) and the A_{2B}/FET synchronous-demodulator network. The force-induced error signal gets amplified by A_{2C}, demodulated by A_{2D}, and filtered and amplified by A_{3A}, A_{3B} and the power-booster stage before being returned to the displacement-correcting torque coil.*

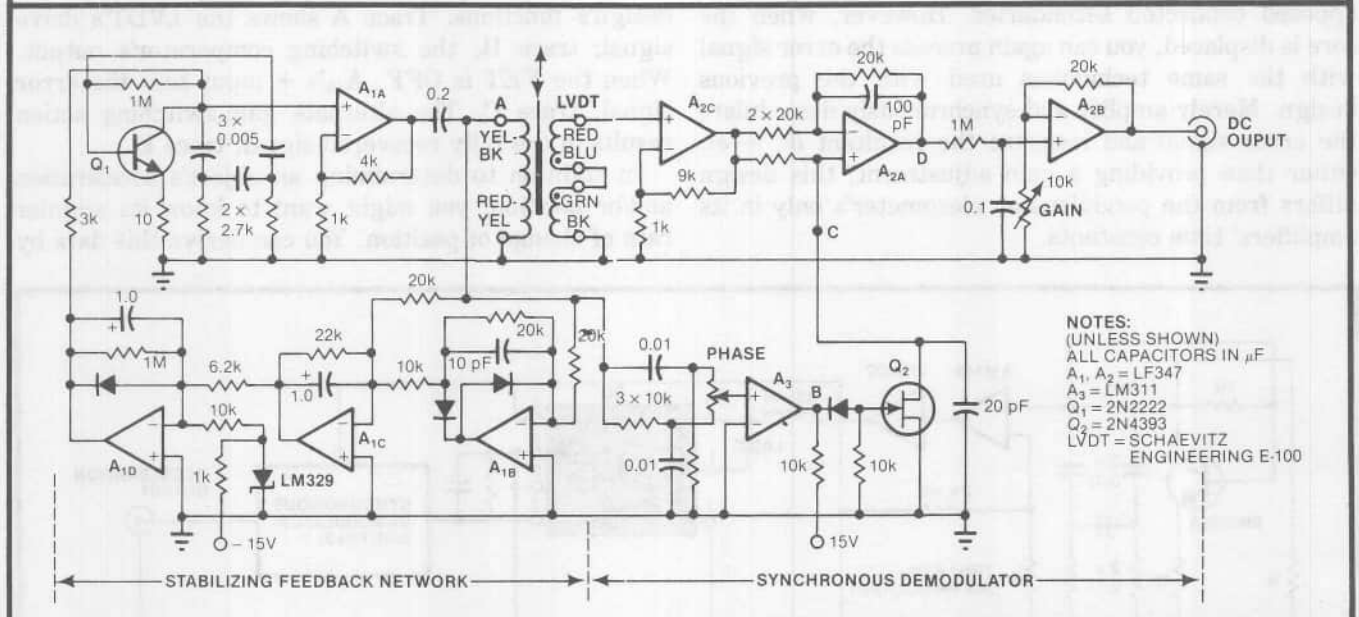

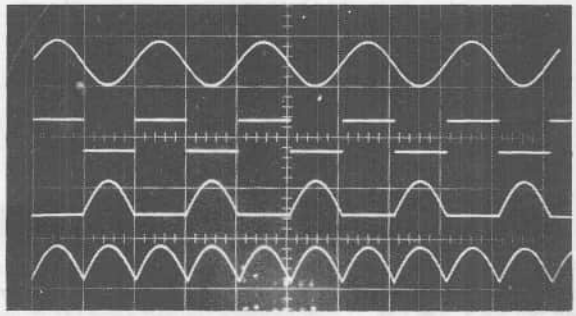

Fig 4—Linear variable differential transformers (LVDTs) *sense a movable core's displacement to determine an object's position. In common with* ***Fig 3****'s pendulous-accelerometer design, the LVDT's signal-conditioning scheme employs an amplitude-stabilized oscillator as an excitation source and a synchronously demodulated error amplifier. The scope photo depicts the circuit's wave shapes at the labeled circuit nodes.*

Use the earth's magnetic field to guide or detect submarines

resistance equals 780Ω, the bridge is balanced and no error signal exists. As the accelerometer cools, the heater compensates for the change in temperature.

Objects aren't always subjected to accelerative forces; sometimes they're merely displaced. Although you can employ mechanically coupled potentiometric sensors to determine an object's position, a linear variable differential transformer (LVDT) provides zero-friction position sensing and a low-noise, long-lifetime alternative that you shouldn't overlook.

Available in both rotary and straight-line-stroke configurations, the LVDT incorporates a transformer with a movable core and thus closely resembles the pendulous accelerometer. In contrast to that device, however, the LVDT's core is free to remain in its displaced position.

An LVDT generally employs the single-primary/dual-secondary configuration shown in **Fig 4.** Note when comparing the LVDT's circuits with the pendulous accelerometer's that the signal-conditioning methods are identical: An oscillator/op-amp combination drives the transducer, and the same stabilization methods apply. When the LVDT's core is in its magnetic (and usually also its geometric) center, a null condition exists, and no error signal results from the series-opposed connected secondaries. However, when the core is displaced, you can again process the error signal with the same techniques used with the previous design. Merely amplify and synchronously demodulate the error signal and measure the resultant dc level. Other than providing a gain adjustment, this design differs from the pendulous accelerometer's only in its amplifiers' time constants.

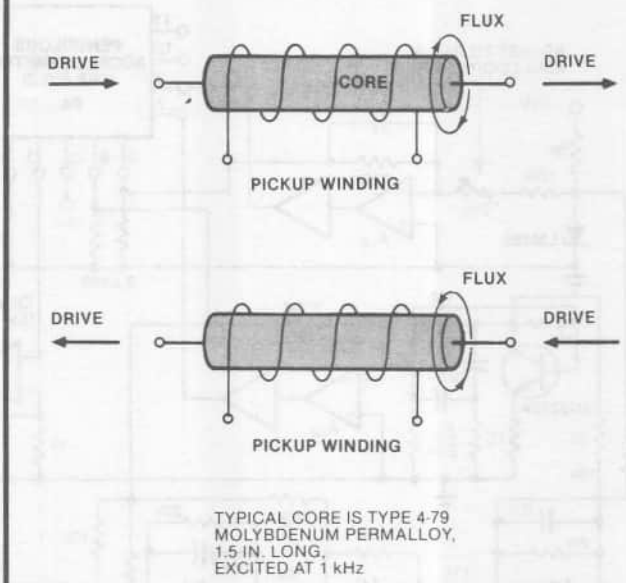

Fig 6—Flux-gate transducers *furnish an error signal when any external magnetic field intersects the drive-signal-induced zero-output level present on the core's pickup winding. Because the magnetically saturable core's saturation-to-saturation transition occurs twice for each drive cycle, the output error signal's frequency is twice the input's.*

Fig 4's accompanying waveforms demonstrate the design's functions. Trace **A** shows the LVDT's drive signal; trace **B**, the switching comparator's output. When the FET is OFF, A_{2A}'s + input sees the error signal, trace **C**. The alternate gain-switching action results in the fully recovered signal, trace **D.**

In addition to determining an object's acceleration and/or position, you might want to know its angular rate of change of position. You can derive this data by

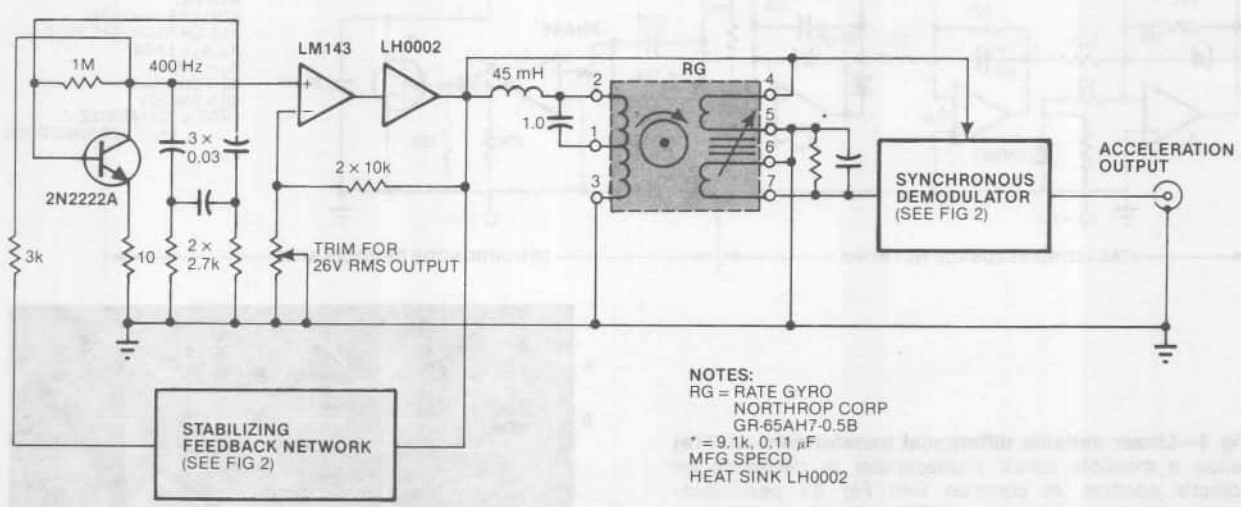

Fig 5—Rate gyros *track angular displacement by detecting the unbalanced error signal that occurs when a rotating (but positionally captive) flywheel attempts to resist a displacement. This action disturbs the flux balance that exists between pin 4's pick-off drive coil and pin 5's sense coil. A synchronous demodulator feeds the result to the outside world.*

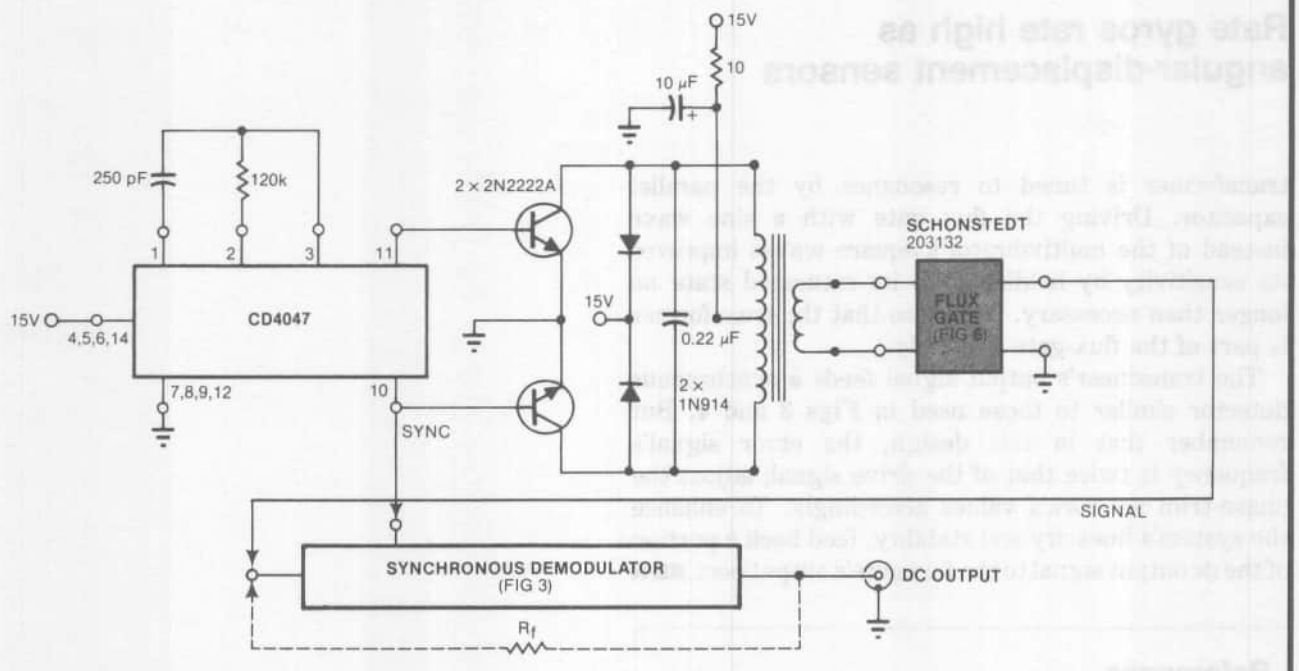

Fig 7—An RC-timed multivibrator *provides the complementary drive signals for the push/pull transistor-operated sine-wave source that excites* **Fig 6***'s flux-gate sensor. Induced by an unknown external magnetic field, the gate's field-proportional output signal is processed by a synchronous detector. By feeding back a portion of the dc output signal, you can enhance the system's dynamic range and linearity.*

time-differentiating a pendulous accelerometer's error signal. But employing a rate gyro yields a cleaner design.

Rate gyros, like the aforementioned transducers, sense a force by electrically sensing an unbalanced condition. Unlike standard gyros, which are unrestrained and thus can maintain their position when moved, the rate gyro is held captive in its gimbals and thus must track any positional changes. If the gyro's flywheel is electrically driven and the unit is equipped with a pick-off drive- and sense-coil scheme, you can employ signal-conditioning circuits like those used in the previous design examples.

The gyro's flywheel drive circuits (**Fig 5**) use the now-familiar stabilized-oscillator design—the only difference here is the required 26V rms signal level. This same signal also feeds the pick-off drive coil to provide a reference signal for the sense coil. So long as the gyro's platform remains stationary, no error signal is generated. Any angular motion, however, disturbs the flywheel's positional stability and upsets the field coupling the pick-off drive and sense coils. You process the error signal via a synchronous demodulator.

Use the earth as a signal source

Whereas LVDTs, rate gyros and pendulous accelerometers all employ an internally generated magnetic field to sense a force, the magnetic field itself is sometimes the force of interest. For these applications, consider using flux-gate transducers; they're far more sensitive than Hall-effect devices.

A flux-gate transducer converts an external magnetic field (such as the earth's) into an electrical signal. As such, it's useful in metal detectors (including submarine-hunting gear), electronic compasses or similar applications where measuring the strength of—or a locally caused disturbance in—the earth's magnetic field is of interest. These devices can detect variations to within 1 gamma (10 μOe).

Although many flux-gate configurations exist, the simplest is the form shown in **Fig 6.** In this version, a cylindrical piece of easily saturated ferrous material is first saturated in, say, a clockwise direction and then in a counterclockwise direction by an alternating axial current. While the material is between its saturation extremes, it maintains a certain average permeability, but while saturated, this permeability (μ=dB/dH) equals 1; ie, an increase in driving field (H) produces the same increase in flux (B).

Note that if no external magnetic-field component exists along the cylinder's axis, the flux change seen by the unit's pickup winding equals zero because the excitation flux is normal to the winding's axis. If, on the other hand, an external field is present, each time the material switches from one saturation extreme to the other, it generates an output pulse on the pickup winding. This pulse is a function of the material's permeability and proportional to the external magnetic field's strength. And because the saturation-to-saturation transition occurs twice for each excitation period, the output signal's frequency is twice that of the drive signal.

In **Fig 7**'s design, an RC-timed multivibrator provides the complementary signals that push/pull-drive the transformer-coupled transistors. (Note that the

transformer is tuned to resonance by the parallel capacitor. Driving the flux gate with a sine wave instead of the multivibrator's square waves improves its sensitivity by holding it in its saturated state no longer than necessary. Note also that the transformer is part of the flux-gate assembly.)

The transducer's output signal feeds a synchronous detector similar to those used in **Figs 3** and **4.** But remember that in this design, the error signal's frequency is twice that of the drive signal; adjust the phase-trim network's values accordingly. To enhance the system's linearity and stability, feed back a portion of the dc output signal to the flux gate's output port. **EDN**

References

1. *RCA Photomultiplier Handbook,* RCA Electro-Optics Div, Lancaster, PA.
2. Lange, S B, "The pyroelectric thermometer: A sensor for measuring extremely small temperatures." McGill University, *1971 International Symposium on Temperature,* Washington, DC.
3. "A User's Guide to Pyroelectric Detection," *Electro-Optical Systems,* November 1978.
4. *Pyroelectric Detectors and Detection Systems,* Laser Precision Corp, Utica, NY.
5. *Multiplier Application Guide,* "Acoustic Thermometer," pg 11, Analog Devices Inc, Norwood, MA.
6. *Ultrasonic Thermometry Using Pulse Techniques,* Lynnwood and Carnevale Corp, Waltham, MA.
7. *Handbook of Measurement and Control,* Schaevitz Engineering, Pennsauken, NJ.
8. Geyer, William, "Self-balancing Flux Gate Magnetometers," *AIEE Transactions on Communications and Electronics,* Vol 77, May 1958.
9. Morris, H D, "A Low Cost Precision Inertial Grade Accelerometer," Systron Donner, *DGON Symposium on Gyro Technology,* 1976.
10. *Short Form Catalog,* Endevco Corp, San Juan Capistrano, CA.
11. *Ultrasonic Transducers,* Bulletin 31, MK109, Massa Corp, Hingham, MA.

Acknowledgements

The author gratefully acknowledges the following organizations, which provided transducers, literature and/or advice: Hewlett-Packard Co, Optoelectronics Div; Honeywell Inc, Avionics Div; Laser Precision Corp; Shonstedt Instrument Co; Schaevitz Engineering Co; Northrop Corp, Precision Products Div; RCA Electro-Optics Div; Lancaster Radiology Associates.

Increase your design options with analog-MUX ICs

Useful for more than commutating analog signals in data-acquisition systems, multiplexer ICs can also provide alternative and often superior solutions to many design problems. Applications range from servo positioning to waveform synthesis.

Jim Williams, National Semiconductor Corp

An analog data-multiplexer (MUX) IC's capabilities provide you with an additional tool for solving a range of diverse design problems. These features—fast multipole switching, high input-to-output isolation and direct digital interfacing—allow you to achieve some interesting and useful circuit realizations.

The design shown in **Fig 1,** for example, uses an 8-pole MUX in an arrangement that permits setting a servomotor in any of eight predetermined positions. You can preset these positions—via potentiometers R_1

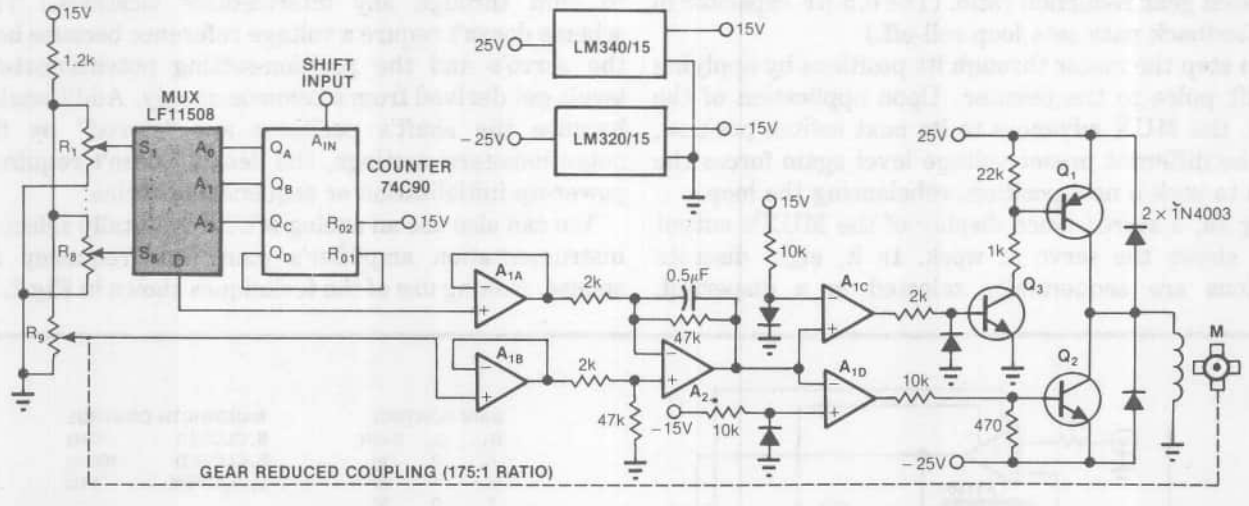

NOTES:
A_1 = LF444
A_2 = LF441
UNMARKED DIODES = 1N4148
Q_1 = 2N5023
Q_2 = LM395
Q_3 = 2N2222
R_1-R_8 = 50k
R_9 = SPECTROL 500-173, 5k
M = MOTORDYNE 1150-1

(a)

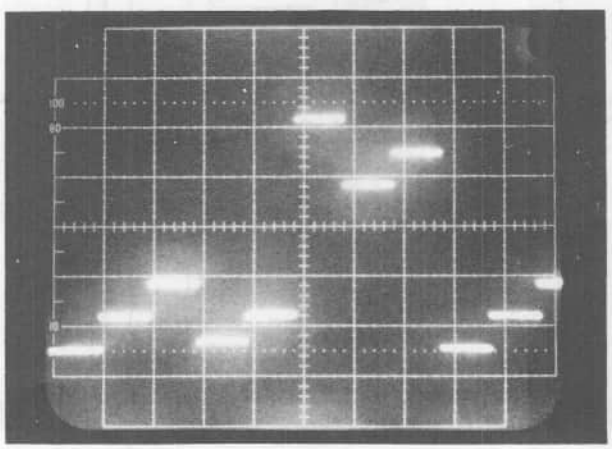

VERTICAL 2V/DIV
HORIZONTAL 200 mSEC/DIV

(b)

Fig 1—A servomotor's shaft position *settles into one of eight MUX-selected locations when a motor-driven potentiometer (R_9) balances out the addressed potentiometers' (R_{1-8}) preset level* **(a).** *Driven by a Shift pulse* **(b),** *the counter sequentially selects—via the MUX—each reference voltage.*

Analog-multiplexer ICs steer servomotors to random positions

through R_8—and then sequentially home the motor in. And because the drive circuits are complementary, the motor can run bidirectionally.

Assume power has just been applied and the counter's output is 0000. This all-ZERO input to the MUX closes its first switch (S_1) and feeds R_1's wiper voltage into the feedback loop. The potential difference between R_1's output and the servo potentiometer's (R_9) gets amplified by A_{1A} and A_{1B} and fed to A_2. This stage algebraically sums the signals and drives A_{1C} and A_{1D}, amplifiers configured as a dual limit comparator with deadband. Depending on A_2's output polarity, the appropriate comparator outputs a high-level voltage and turns its associated driver on. This action in turn drives the motor in the direction necessary to force a null at A_2's output. When that output falls within the diode-generated 0.6V deadband, both comparators' outputs drop LOW, and the motor stops.

A_2 operates at a gain of 30 and thus provides adequate sensitivity for precise positioning. Good loop dynamics result from using ±25V supplies and the indicated gear reduction ratio. (The 0.5-μF capacitor in A_2's feedback path sets loop roll-off.)

You step the motor through its positions by applying a Shift pulse to the counter. Upon application of the pulse, the MUX advances to its next switch position, and the different preset voltage level again forces the servo to seek a new position, rebalancing the loop.

Fig 1b, a stored-trace display of the MUX's output port, shows the servo at work. In it, eight discrete positions are sequentially selected in a dispersed, nonmonotone fashion. (Note how you can attain any desired positioning sequence without requiring the loop to hunt through any intermediate locations.) This scheme doesn't requre a voltage reference because both the servo's and the position-setting potentiometers' levels get derived from a common supply. Additionally, because the shaft's positions are "stored" by the potentiometers' settings, the design doesn't require a power-up initialization or sequencing routine.

You can also use an analog MUX to digitally select an instrumentation amplifier's gain and frequency response, making use of the techniques shown in **Fig 2.** In

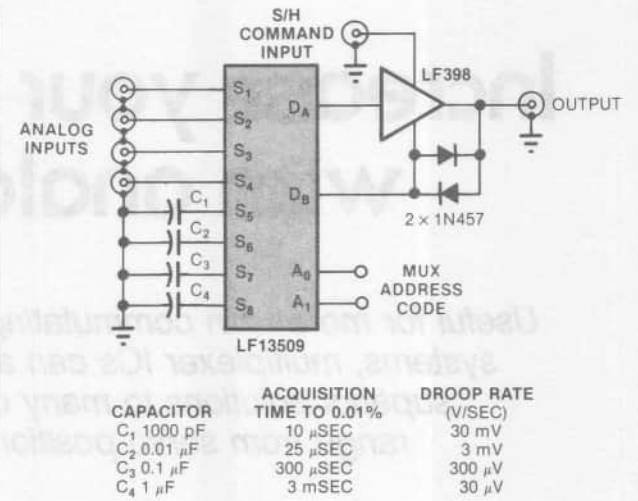

CAPACITOR	ACQUISITION TIME TO 0.01%	DROOP RATE (V/SEC)
C_1 1000 pF	10 μSEC	30 mV
C_2 0.01 μF	25 μSEC	3 mV
C_3 0.1 μF	300 μSEC	300 μV
C_4 1 μF	3 mSEC	30 μV

Fig 3—A multiplexer selects this sample/hold amplifier's 1-of-4 inputs *and its acquisition time. Requiring only a 2-bit address, the 4-channel MUX can apply any hold capacitor to any input signal.*

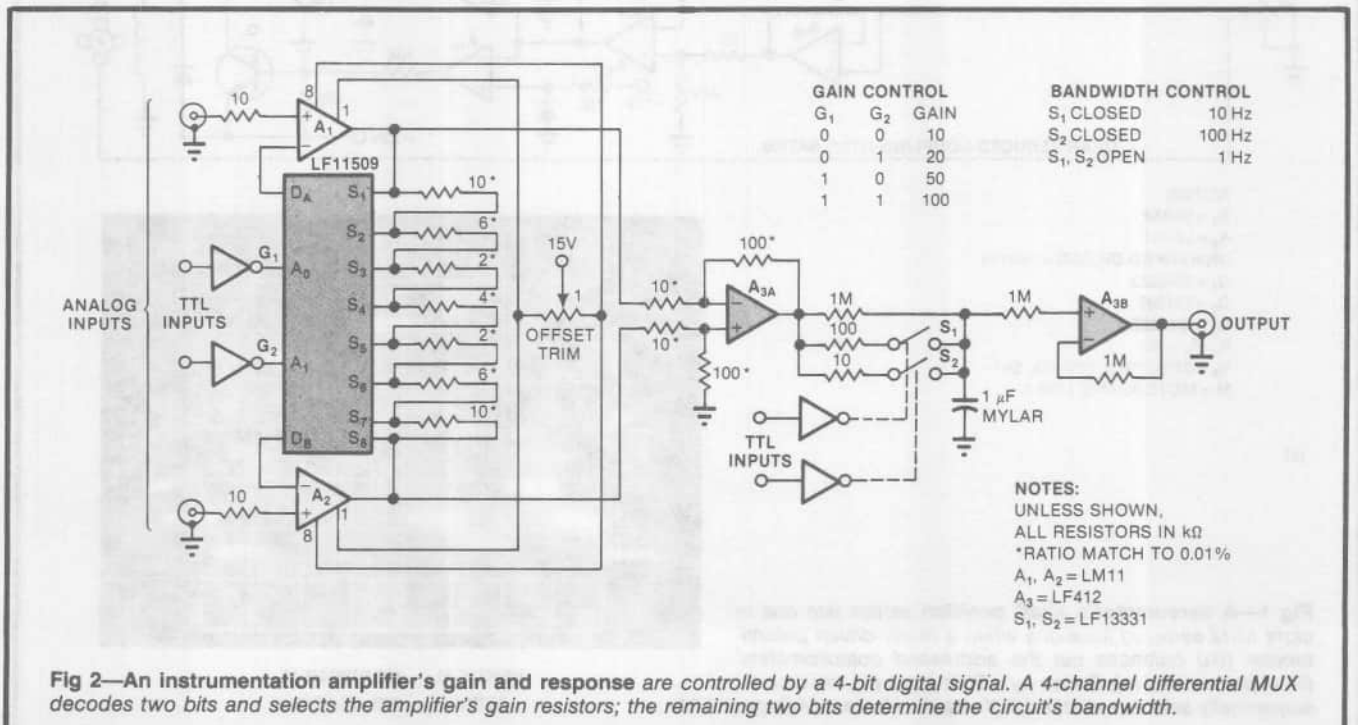

Fig 2—An instrumentation amplifier's gain and response *are controlled by a 4-bit digital signal. A 4-channel differential MUX decodes two bits and selects the amplifier's gain resistors; the remaining two bits determine the circuit's bandwidth.*

this approach, a 4-channel differentially switched MUX selects the feedback resistors for the design's input stages, A_1 and A_2. These stages' differential outputs get summed and amplified at a gain of 10 by A_{3A}. The resultant single-ended signal feeds an RC low-pass network consisting of 1-of-3 switch-selected resistors and a 1-μF capacitor. The final stage (A_{3B}) functions as an output buffer.

Thus, with a 4-bit digital signal, you can determine the amplifier's gain and response; two bits set the gain and the remaining two set the response as shown in **Fig 2**'s tables. You can realize true instrumentation-amplifier performance by using LM11s for A_1 and A_2; circuit drift then remains within 2 μV/°C, and you can achieve a CMRR of 100 dB with 0.01% resistor matching.

MUX a S/H amplifier for variable performance

Another analog-MUX application occurs when you're using sample-and-hold (S/H) amplifiers, which are usually constrained to processing a single input signal over a limited range of acquisition times and droop rates. The MUX-based design shown in **Fig 3** not only accepts any of four inputs, it also provides a wide range of acquisition and droop options.

This approach employs a 4-channel differential MUX to sort out the input and hold-capacitor options; half of the MUX selects the desired input, and the other half determines the in-circuit hold capacitor's value. Because any address code simultaneously selects the corresponding switches in both halves of the MUX, you can use any desired hold capacitance for any input.

A flash sampler captures single events

Fig 4a illustrates a technique for using analog MUXs for capturing single-shot or low-repetition-rate waveforms and then repetitively displaying the signal on an oscilloscope. It doesn't require a pretrigger signal because the input signal itself initiates the sampler

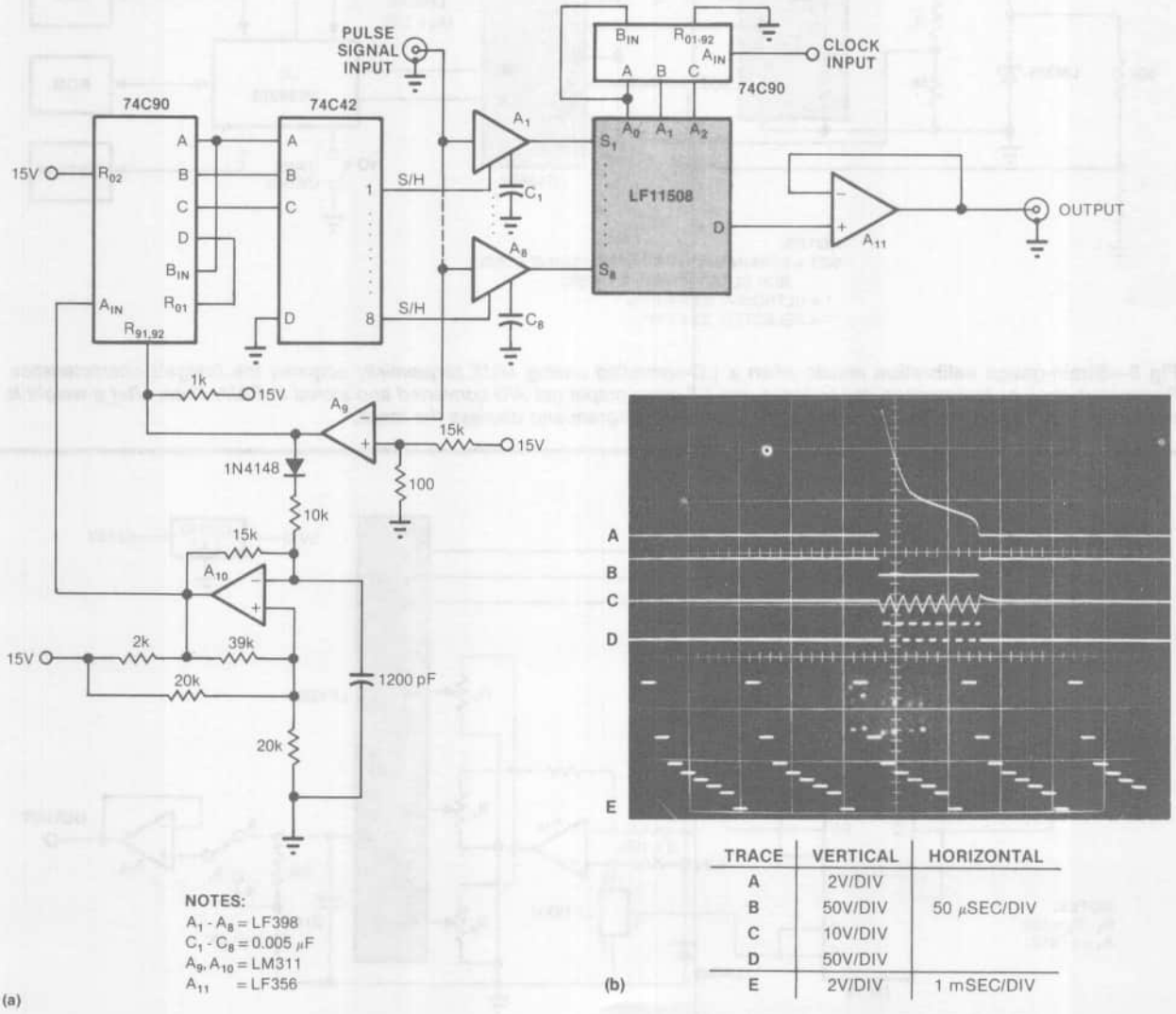

TRACE	VERTICAL	HORIZONTAL
A	2V/DIV	
B	50V/DIV	50 μSEC/DIV
C	10V/DIV	
D	50V/DIV	
E	2V/DIV	1 mSEC/DIV

Fig 4—This flash-sampler design (a) *captures single-event signals and provides an instant and repetitive scope display. An incoming signal (**(b)**, trace **A**) triggers A_9 **(B)**, resets the counter and starts the oscillator A_{10} **(C)**. A_{10}'s output **(D)** drives the counter that sequentially addresses the sampling amplifiers, A_1 through A_8. A clocked counter then steps through the MUX's switches and reconstructs the sampled input **(E)**.*

An analog flash converter can provide an instant signal replay

string. And because the circuit's output is independently clocked, you can vary the scope's display rate to suit your requirements.

An incoming signal (**Fig 4b**, trace **A**) triggers comparator A_9 LOW, as shown by trace **B**. This action allows A_{10}'s 15-kΩ/1200-pF combination to start charging (**C**); as a result, A_{10} outputs a pulse train (**D**). Advanced in count by these pulses, the counter's BCD-encoded output gets decoded by the 74C42 and is used to sequentially drive the eight paralleled sample/hold amps (A_1 through A_8). In this manner, each S/H stage acquires a fraction of the input signal.

When the input signal ceases, A_9's output again goes HIGH, A_{10} no longer generates pulses and the sampling procedure stops. To display the stored waveform, enable the clock input to the MUX-controlling counter. The counter's outputs sequentially address the MUX's switches, and stored signal segments go to the output buffer (A_{11}). Trace **E** demonstrates how you can repetitively display the reconstructed waveform at a rate governed by the clock's frequency.

A μC-driven MUX calibrates strain gauges

Fig 5's design shows how you can use a MUX to realize an autocalibration arrangement that eliminates

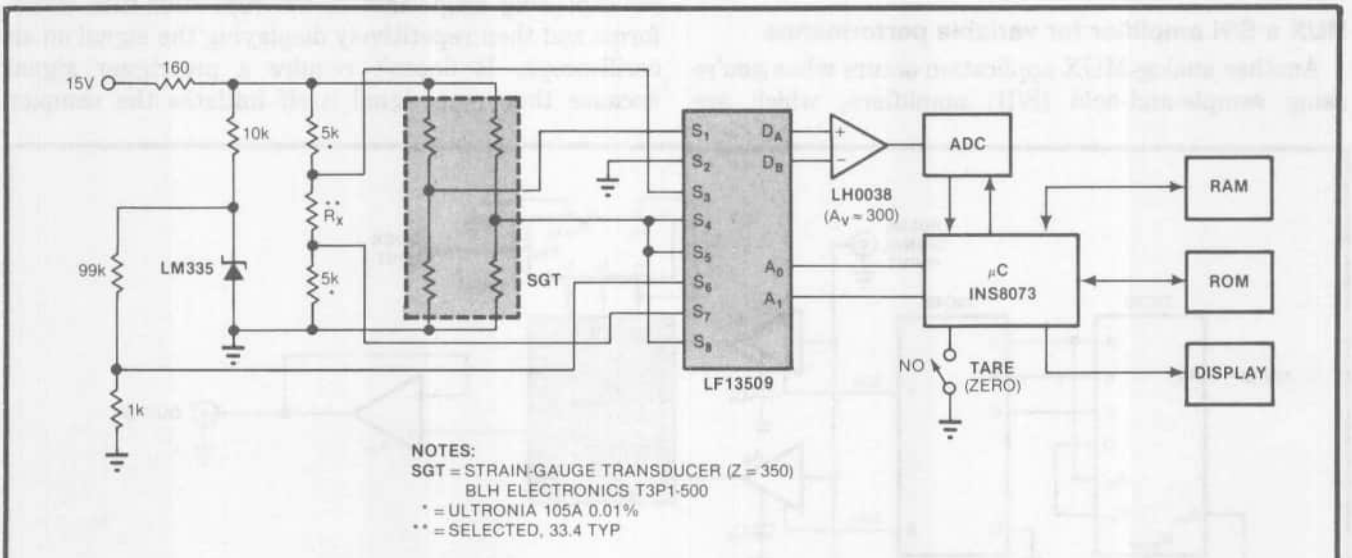

Fig 5—Strain-gauge calibration *results when a μC-controlled analog MUX sequentially acquires the bridge's characteristics. Parameters such as temperature dependence and full-scale output get A/D converted and stored in RAM. Then, after a weight is measured and converted, the μC runs a correction-factor program and displays the result.*

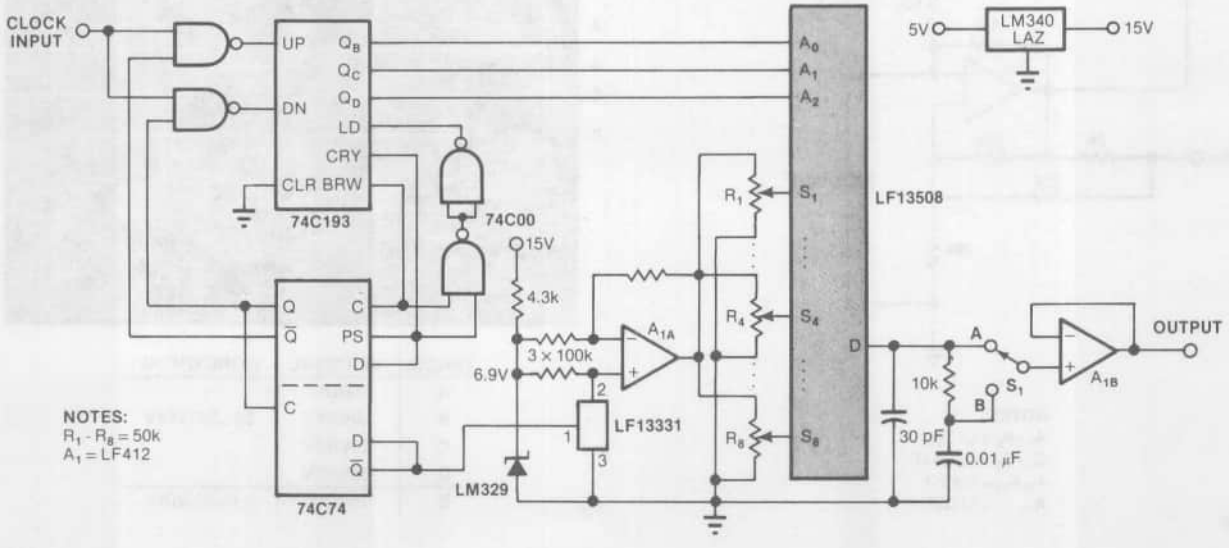

Fig 6—A programmable waveform *is created when a counter-driven 8-channel MUX samples preset potentiometers. When clocked, the counter counts up and then down and in the process switches the amplifier's input between 6.9V and ground. This action permits the amplifier to synthesize both the positive- and negative-going portions of the waveform, as shown in* ***Fig 7.***

almost all of the errors inherent in strain-gauge load-cell transducer measurements. Errors arising from drift over time and temperature are cancelled, and you can interchange transducers without having to rezero or recalibrate the circuit's gain. This design performs four separate operations to determine the factors necessary for correcting transducer output.

The measurement cycle commences when the μC switches the MUX into position 1. This action connects the strain gauge's output to the instrumentation amplifier. After amplification, the analog signal gets converted to a digital equivalent and stored in the RAM. When advanced to position 2, the MUX acquires the output of the load-cell-mounted LM335 temperature sensor. This value is also amplified, converted and stored in memory. (Note that the LM335's high output must be divided to prevent saturating the amplifier.)

The load cell's precise full-scale output voltage gets acquired when the MUX is in position 3 and connected to R_X, the cell-mounted resistor. By making this data inherently available with each cell, the system can ascertain (and correct for) the cell's gain slope. This capability eliminates the need for recalibration whenever you change cells. Position 4 provides the system with an electrical zero by connecting both of the amplifier's inputs to the bridge's common-mode point.

Physical-zero information (ie, tare (container) weight) is fed to the μC when you operate the pushbutton with no load on the cell. (You must perform this operation only when the system is turned on or after a different cell has been connected.) The system's memory then holds values for zero, the loaded bridge's output, its full-scale output and its temperature. Additionally, a tare-weight value has been determined. Using this data, the μC's program can calculate the strain gauge's precise loading regardless of drifts or the cells' individual gain-slope characteristics.

The temperature information provides a first-order correction factor for the relatively small effect that ambient temperature has on gain slope and zero. The bridge's voltage needn't be stabilized because it's common to the gain-calibration string and therefore ratiometrically cancels. In fact, the system's stability is governed solely by the stability of the gain-calibration string's resistors. MUX-controlled systems of this type achieve repeatability of one part in 20,000 in industrial environments.

Switched resistors generate waveforms

Fig 6 diagrams how you can use an 8-channel MUX to generate a 32-piece approximation of any desired waveform—a sine wave demonstrates the approach. When clocked, the logic circuits combine to force the MUX to count up to eight. (The counter's Up/Down control inputs appear as traces **A** and **B** in **Fig 7**'s top photo.) When this operation is completed, the MUX counts down to zero and resamples the potentiometers' settings in the process. These two cycles create the positive half of the output's waveform.

The logic next inverts the potentiometers' voltage by

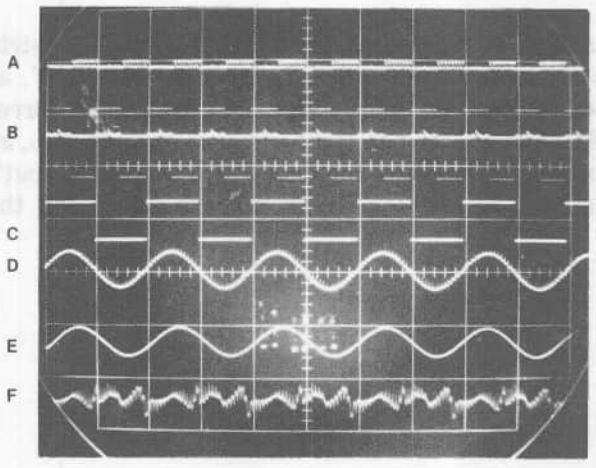

TRACE	VERTICAL	HORIZONTAL
A	5V/DIV	
B	5V/DIV	
C	20V/DIV	500 μSEC/DIV
D	20V/DIV	
E	20V/DIV	
F	0.5V/DIV	

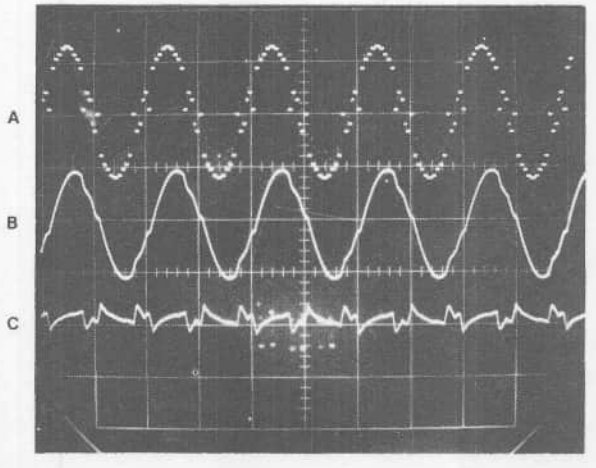

TRACE	VERTICAL	HORIZONTAL
A	5V/DIV	
B	5V/DIV	500 μSEC/DIV
C	0.5V/DIV	

Fig 7—Waveform synthesis *proceeds when* ***Fig 6****'s counter cycles through its first up/down sequence (top, traces* ***A*** *and* ***B****). After this sequence, the D flip flop's Q output drives the amplifier's input (and therefore its output) LOW* ***(C)****. The counter/MUX combination recycles through the up/down sequence and creates the negative half of the waveform. The unfiltered* ***(D)*** *and filtered* ***(E)*** *outputs indicate how well a sine wave can be synthesized. This 32-step approximation results in a distortion level of less than 0.5%* ***(F)****. The bottom photo depicts how you can intentionally distort a waveform: The unfiltered* ***(A)*** *and filtered* ***(B)*** *outputs indicate that trace* ***C****'s 7% distortion is easily achieved.*

MUXing a strain-gauge bridge relieves recalibration pains

grounding A_{1A}'s + input via an LF1331 FET switch. This action forces the amplifier's output to −6.9V, as shown by trace **C**. Concurrently, the logic again forces the MUX to count up to eight and back down to zero, an action that synthesizes the negative half of the output's waveform. At the conclusion of these 32 counts, the logic resets, A_{1A}'s output switches to a 6.9V level and the entire cycle repeats.

When appropriately set, the potentiometers can provide the correct levels for synthesizing a sine wave, as shown by trace **D**. When filtered, this signal (**E**) contains less than 0.5% distortion (**F**). As the bottom photo in **Fig 7** shows, you can intentionally distort the output by resetting the potentiometers. Trace **A** displays the 32-piece approximation of the distorted signal, and **B** shows the filtered version. A distortion analyzer's output signal (**C**) indicates a 7% distortion level. **EDN**

Interface nonstandard sensors using standard circuit methods

Try these designs to interface such sensors as photomultiplier tubes and ultrasonic devices to your measurement system.

Jim Williams, National Semiconductor Corp

Although a transducer might be exotic, its interfacing and signal-conditioning circuitry can be simple, as this first article in a 2-part series shows. The designs presented here, all of which have been built and tested, illustrate several useful interfacing techniques for sophisticated transducers, expanding on the somewhat sketchy data sheets often characterizing the devices.

Use electrons to find photons

The first design uses perhaps the most versatile light detector available—the photomultiplier tube (PMT). In addition to single-photon-detection capability, these sensors provide subnanosecond rise times, bandwidths approaching 1 GHz and response linearity better than 10^7. PMTs furnish low noise, stable performance and long life because they don't employ a filament-heated cathode as the electron source; instead, they employ a photosensitive cathode, a focusing electrode, 10 amplifying dynode stages and an electron-collecting anode.

In operation, a PMT's photocathode emits electrons when struck by a photon. The more positively biased focus electrode (**Fig 1**) collects and beams these electrons toward the first dynode, where the particles generate additional electrons via impingement-induced

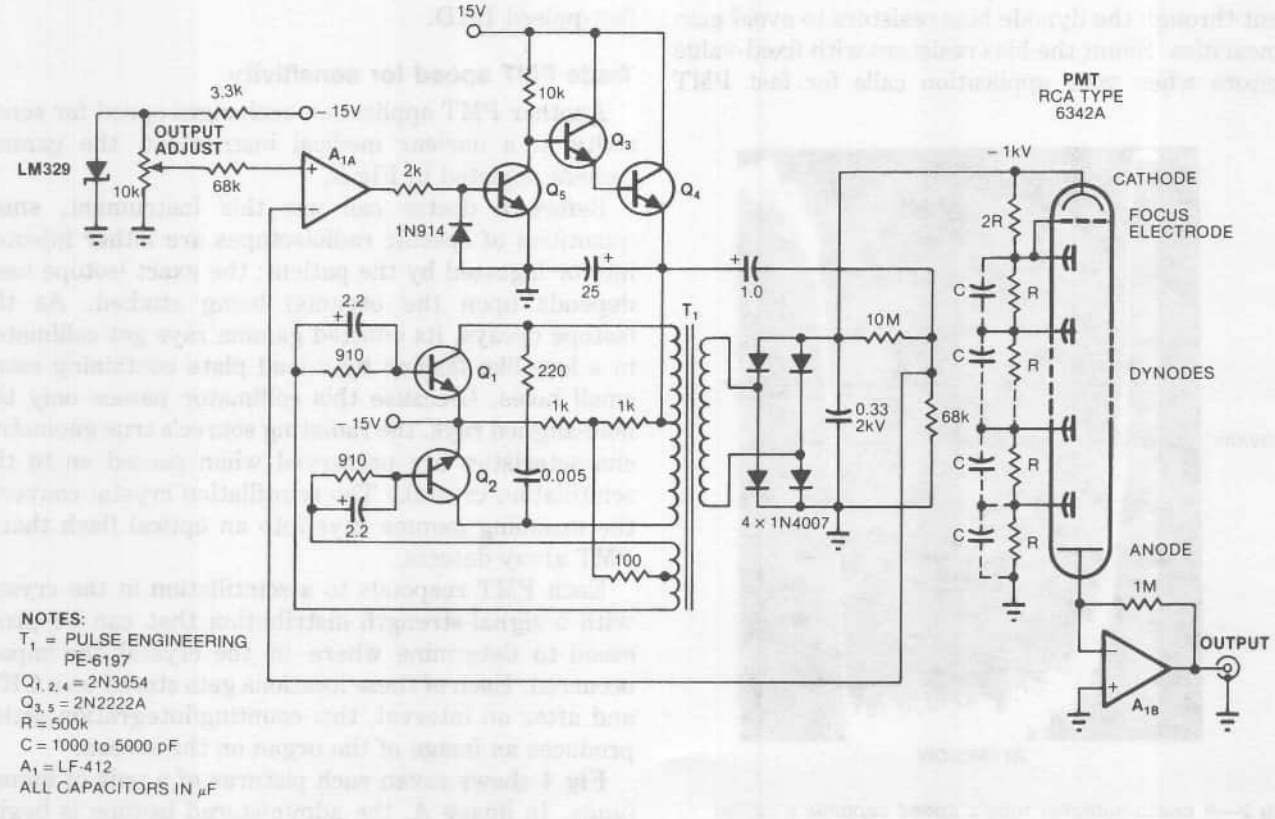

Fig 1—Photomultiplier-tube power-supply designs *must be stable and accurate but not complex. In this scheme, a closed-loop feedback-amplifier network—consisting of A_{1A} and Q_3 through Q_5—compares a portion of the dc/dc converter's output voltage with an adjustable reference level. The error-correcting result appears at Q_4's emitter as a varying converter-supply voltage.*

Phototube-based designs look into you with gamma-ray sources

secondary emission. Then, because the second dynode is even more positively biased, the now-larger electron cloud bombards this dynode's surface and again multiplies in density. In this fashion, several cascaded dynodes (10 in this example) can achieve an overall current gain spanning 10^6 to 10^8. The final dynode's electrons are collected by the anode, which functions as a nearly ideal current source.

To satisfy the PMT's requirements, you must provide both a stable high-voltage bias supply and a low-noise current-to-voltage conversion stage at the anode's output. The design shown in **Fig 1** employs a closed-loop stabilized dc/dc converter to generate the required 1-kV PMT bias supply. An op amp (A_{1A}) compares the LM329-derived reference voltage with a sample of the high-voltage stage's output and sets Q_3 through Q_5's output accordingly. This regulated voltage in turn supplies the converter's drivers (Q_1 and Q_2) and, via T_1's step-up action, the circuit's high-voltage output.

In general, a PMT supply's regulation should be at least 10 times greater than the measurement's required gain stability. (This requirement arises from the PMT's gain-slope vs applied-high-voltage relationship.) Additionally, the supply must be able to source a current at least 10 times that needed by the PMT. This specification stems from the necessity to bleed that much extra current through the dynode bias resistors to avoid gain nonlinearities. Shunt the bias resistors with fixed-value capacitors when your application calls for fast PMT response—they supply the peak transient currents required by a fast-acting PMT.

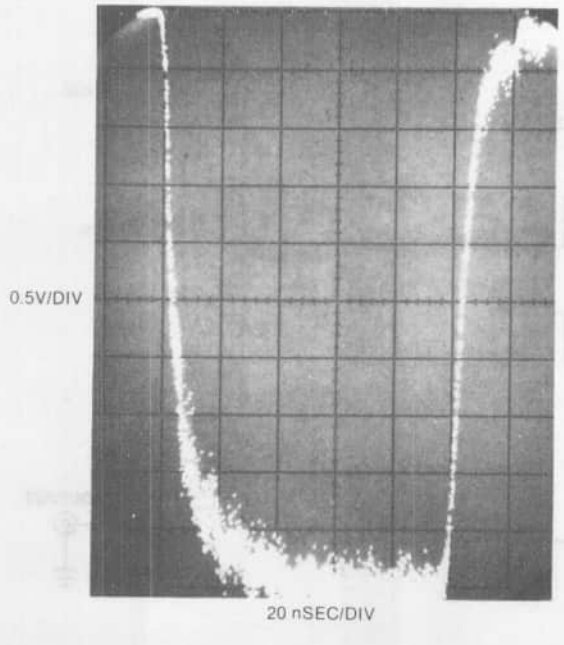

Fig 2—A photomultiplier tube's speed *captures a pulsed LED's optical-output rise and fall times. To realize the PMT's maximum speed capabilities, you might have to incorporate the dynode-shunting capacitors shown in* ***Fig 1.***

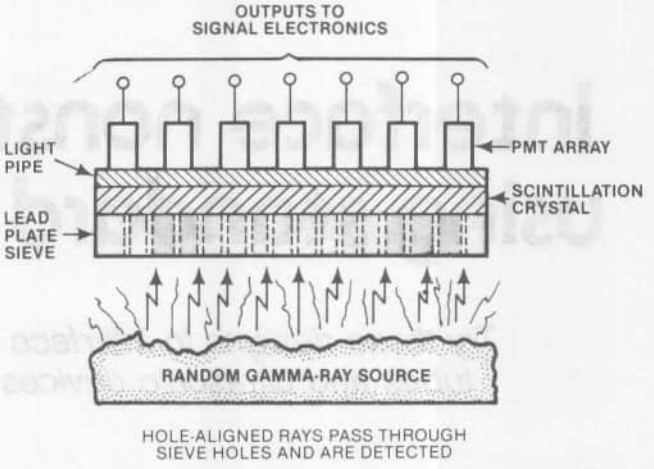

Fig 3—A gamma-ray camera *results when the collimating action of a lead-plate sieve allows only image-related rays to impinge upon a scintillation crystal. A photomultiplier-tube array detects and converts the output into usable signals.*

Although **Fig 1** shows how you can employ op amp A_{1B} as the PMT's current-to-voltage converter, **Fig 2**'s remarkable photo was taken with a high-speed PMT directly feeding the 50Ω input of a 1-GHz-bandwidth sampling scope. This photo demonstrates the PMT's combination of high speed and high sensitivity by capturing the actual (inverted) rise and fall times of a fast-pulsed LED.

Trade PMT speed for sensitivity

Another PMT application exchanges speed for sensitivity in a nuclear medical instrument, the gamma camera depicted in **Fig 3.**

Before a doctor can use this instrument, small quantities of specific radioisotopes are either injected into or ingested by the patient; the exact isotope used depends upon the organ(s) being studied. As the isotope decays, its emitted gamma rays get collimated in a lens-like fashion by a lead plate containing many small holes. (Because this collimator passes only the hole-aligned rays, the radiating source's true geometric characteristics are preserved when passed on to the scintillation crystal.) The scintillation crystal converts the incoming gamma rays into an optical flash that a PMT array detects.

Each PMT responds to a scintillation in the crystal with a signal-strength distribution that can be processed to determine where in the crystal the impact occurred. Each of these locations gets stored on a CRT, and after an interval, this counting/integration action produces an image of the organ on the screen.

Fig 4 shows seven such pictures of a pair of human lungs. In image **A,** the administered isotope is beginning to collect in the lungs, and **B** shows saturation. Images **C** through **G**—taken at 30-sec intervals—depict the isotope's progressive decay. (Healthy lungs are

usually clear after 120 sec. This patient, however, shows evidence of an obstructive pulmonary disease; congestion is especially pronounced in the lower part of the right lung.)

The next design uses another type of light detector—a pyroelectric unit. These ceramic-based devices provide extraordinary sensitivity that spans microwatts to watts—with excellent linearity (flat from ultraviolet through the far IR bands). They also achieve subnanosecond response times and don't need cooling—they operate at room temperature.

Why, if they're so good, aren't these devices used more often? Probably because they don't respond to dc inputs and provide signals that are difficult to condition.

For signal-conditioning purposes, you can model a pyroelectric sensor either as a voltage source in series with a capacitor (**Figs 5a, b**) or as a capacitively shunted current source (**Fig 5c**). And because the unit has no resistive component, no Johnson noise arises.

If you're detecting fast, high-energy light pulses, consider **Fig 5a**'s simple solution. Here, the pyroelectric detector directly feeds a high-speed scope. **Fig 5b** shows how to interface to the device a slower detector for lower speed applications; the 1-MΩ resistor correctly terminates the sensor, and the low-input-bias FET op amp provides the required isolation. When the required response time exceeds several milliseconds, you can employ a light chopper between the signal source and the sensor. When chopped, the output signal appears as an amplitude-modulated carrier

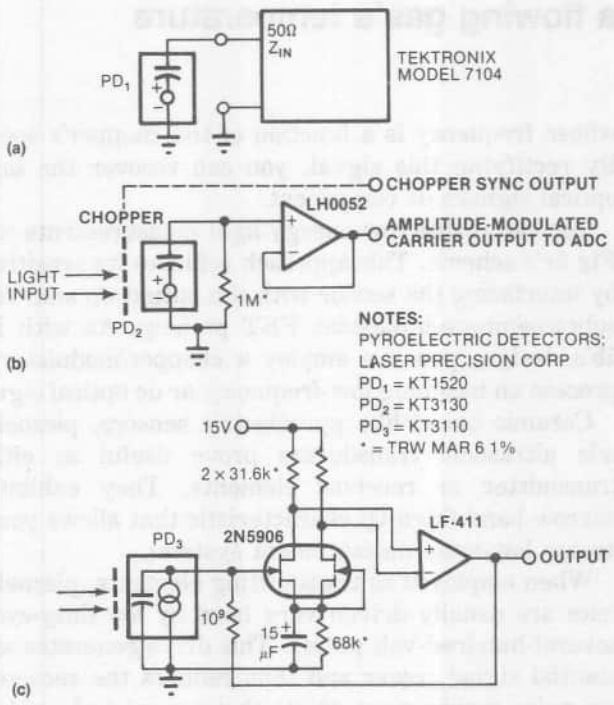

Fig 5—Pyroelectric detectors *can be modeled as series voltage-source/capacitor combinations, (**(a)** and **(b)**) or as a capacitively shunted current source **(c)**. But because neither version responds to dc inputs, you need special signal-conditioning circuits. Fast-pulse detection is accomplished in **(a)** by directly driving a scope's 50Ω input port. Slowly changing optical signals are best handled by the chopper techniques shown in **(b)** and **(c)**.*

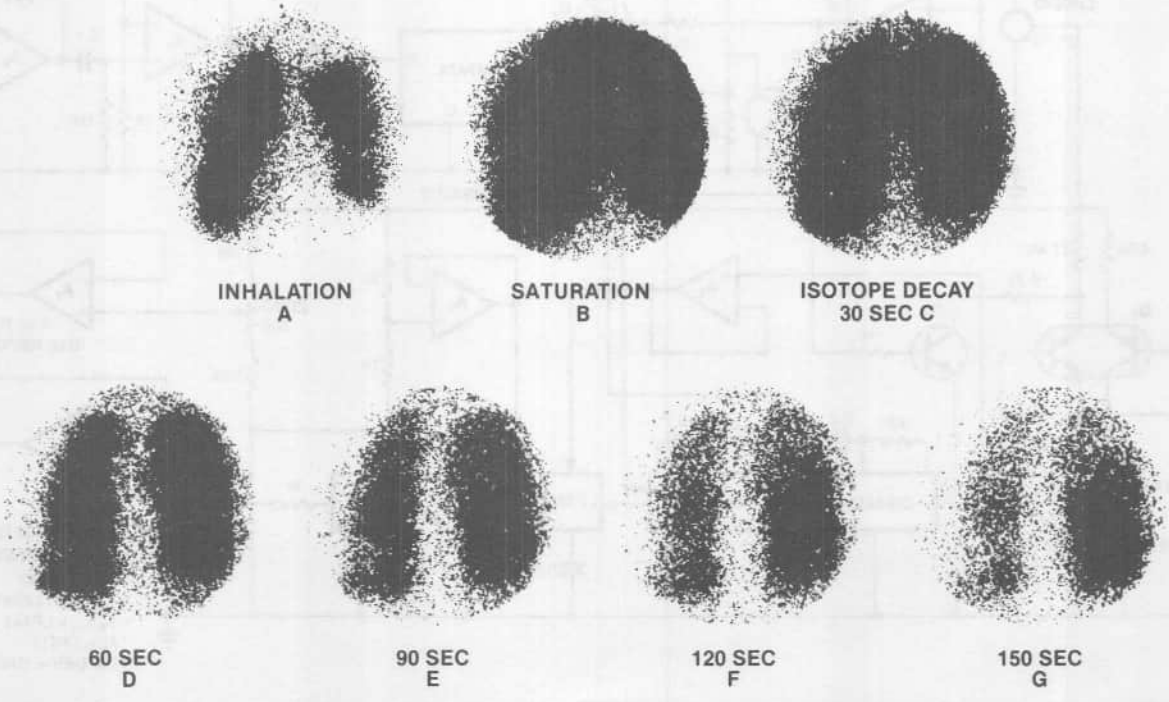

Fig 4—Congestion in human lungs *is revealed by this series of gamma-camera images. Image **A** depicts how a selective radioisotope starts concentrating in the lungs, with saturation occurring in **B**. Images **C** through **G**—taken at 30-sec intervals—disclose how the radioisotope decays with time. Healthy lungs clear within 120 sec (image **F**). This patient, however, shows obstructive pulmonary problems in the lower part of his right lung (**G**) even after 150 sec.*

Use ultrasonic signals to find a flowing gas's temperature

whose frequency is a function of the chopper's speed. By rectifying this signal, you can recover the input optical signal's dc component.

You can realize low-energy light measurements with **Fig 5c**'s scheme. This approach achieves its sensitivity by interfacing the sensor with the output op amp via a subpicoampere-input-bias FET preamp. As with **Fig 5b**'s design, you can employ a chopper/modulator to process an incoming low-frequency or dc optical signal.

Ceramic based like pyroelectric sensors, piezoelectric ultrasonic transducers prove useful as either transmitter or receiver elements. They exhibit a narrow-band (high-Q) characteristic that allows you to design low-noise measurement systems.

When employed as transmitting elements, piezoelectrics are usually driven very hard by low-duty-cycle, several-hundred-volt pulses. This drive generates substantial signal power and thus reduces the receiver's low noise requirement. (Note that you might be able to employ the same transducer as both a transmitter and receiver in some applications.)

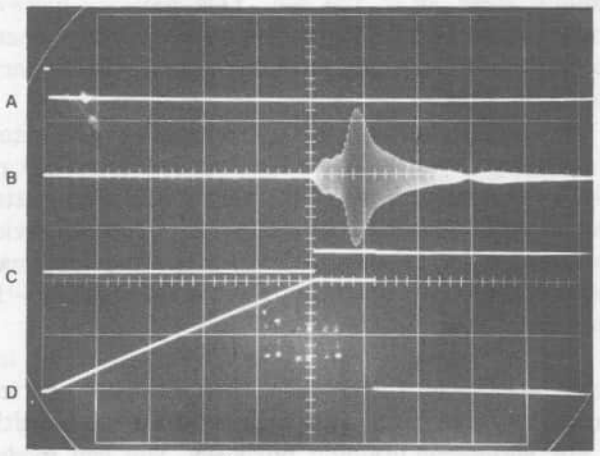

TRACE	VERTICAL	HORIZONTAL
A	30V/DIV	
B	10V/DIV	500 nSEC/DIV
C	10V/DIV	
D	2V/DIV	

Fig 7—Gas-temperature measurements *commence when* ***Fig 6****'s* A_1 *pulses the ultrasonic transmitter (trace* ***A****). This action also sets a flip flop's Q output LOW (trace* ***C****) and starts the capacitance charging cycle (trace* ***D****). When the sonic pulse is detected (trace* ***B****), the flip flop resets HIGH and terminates the charge cycle. The capacitor's voltage is then a convertible function of the gas's temperature.*

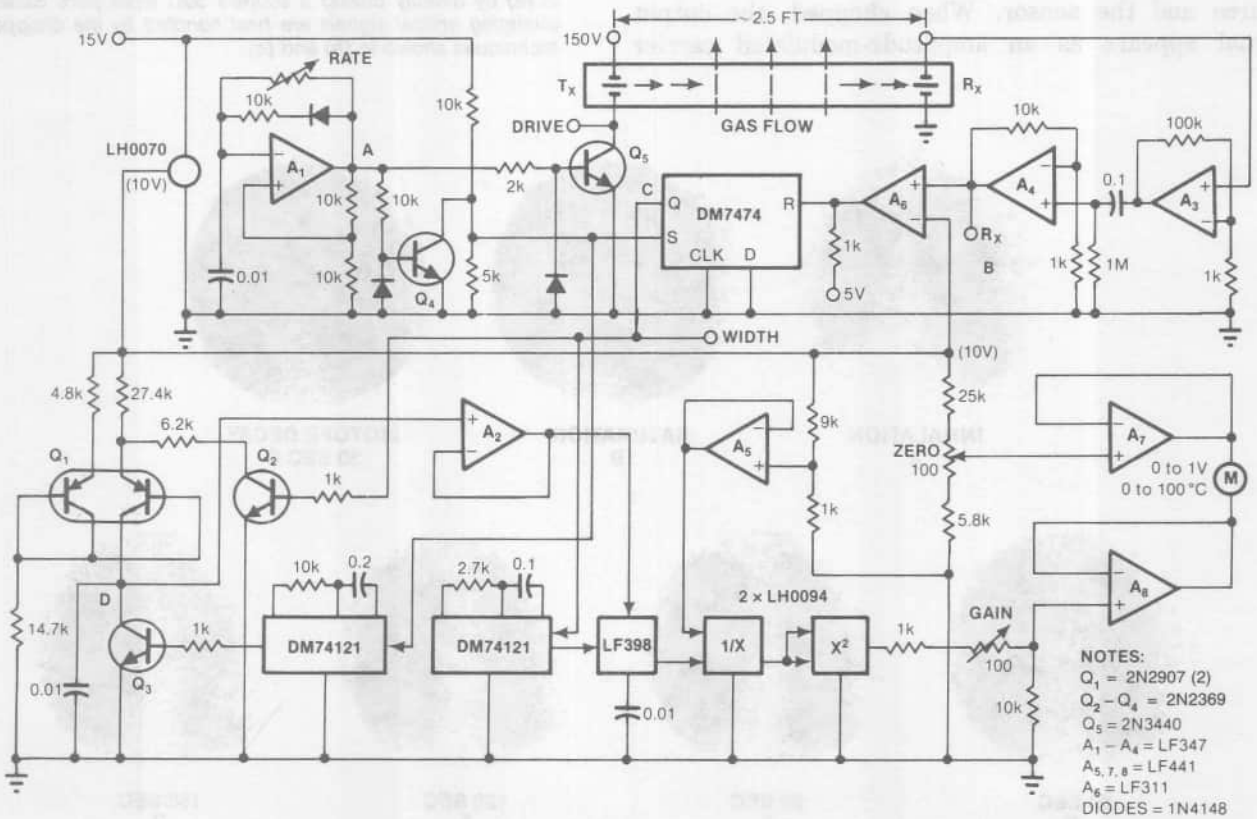

Fig 6—A gas's temperature *is determined by its sonic-propagation characteristics in this design.* A_1 *pulses an ultrasonic-wave transmitting transducer (*T_X*) and simultaneously enables the* Q_1*-based capacitance-charging constant-current source via a flip flop's Q output. At a later, gas-temperature-dependent time, receiver transducer* R_X *detects the pulse and stops the charging cycle. Because the capacitor's voltage is a function of the sonic travel time (and thus the gas's temperature), it can be sampled, linearized and used to drive a direct-reading temperature indicator. (Points marked with boldface letters correspond to* ***Fig 7****'s traces.)*

In contrast to an ultrasonic transducer's usual camera-focusing, intrusion-alarm or liquid-level-sensing applications, **Fig 6**'s circuit permits its use for difficult thermal measurements. The technique employed resembles one that measures high-speed temperature shifts in a gaseous medium. Unlike most other temperature-measuring schemes, though, it doesn't require that the sensor come into thermal equilibrium with the measured material. Instead, it finds the medium's temperature by determining the medium's ultrasonic-propagation characteristics. Thus, the circuit's response times are very short, and the measurement is noninvasive. As an example of this principle, you can find the absolute temperature (T) of dry air by using the equation

$$T = C^2 \times 273/(331.5)^2$$

where C=a sound wave's speed in the medium, measured in metres per second.

Obviously, then, if you can identify the gaseous medium and know its temperature-dependent characteristics, you can determine its temperature using only the ultrasonic signal's propagation time. And by using high-Q transducers, you can achieve a noise-filtering feature that ignores medium-generated noise.

The traces in **Fig 7** (corresponding to the points marked in **Fig 6**'s circuit) illustrate how the scheme operates. Amp A_1 periodically generates a pulse (trace **A**) that drives a 40-kHz transmitter transducer (T_X) on via Q_5. This same trigger pulse turns on Q_4 and sets a flip flop LOW (trace **C**). After a time interval

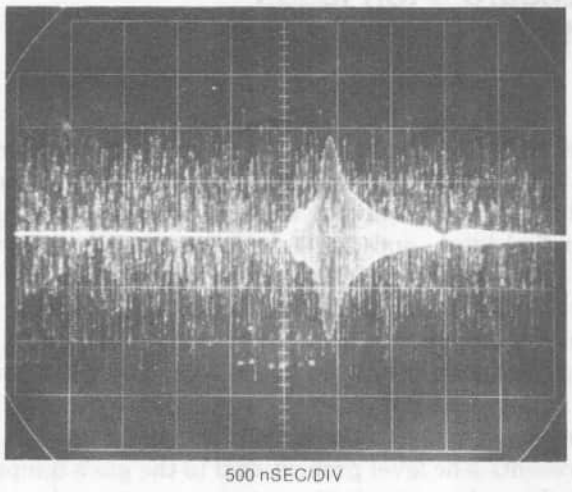

Fig 8—The noise-filtering property *of a high-Q ultrasonic transducer permits amplifying the desired signal (the same as* ***Fig 7****'s trace* ***B****) even though it's buried in an excess noise level of 100 dB.*

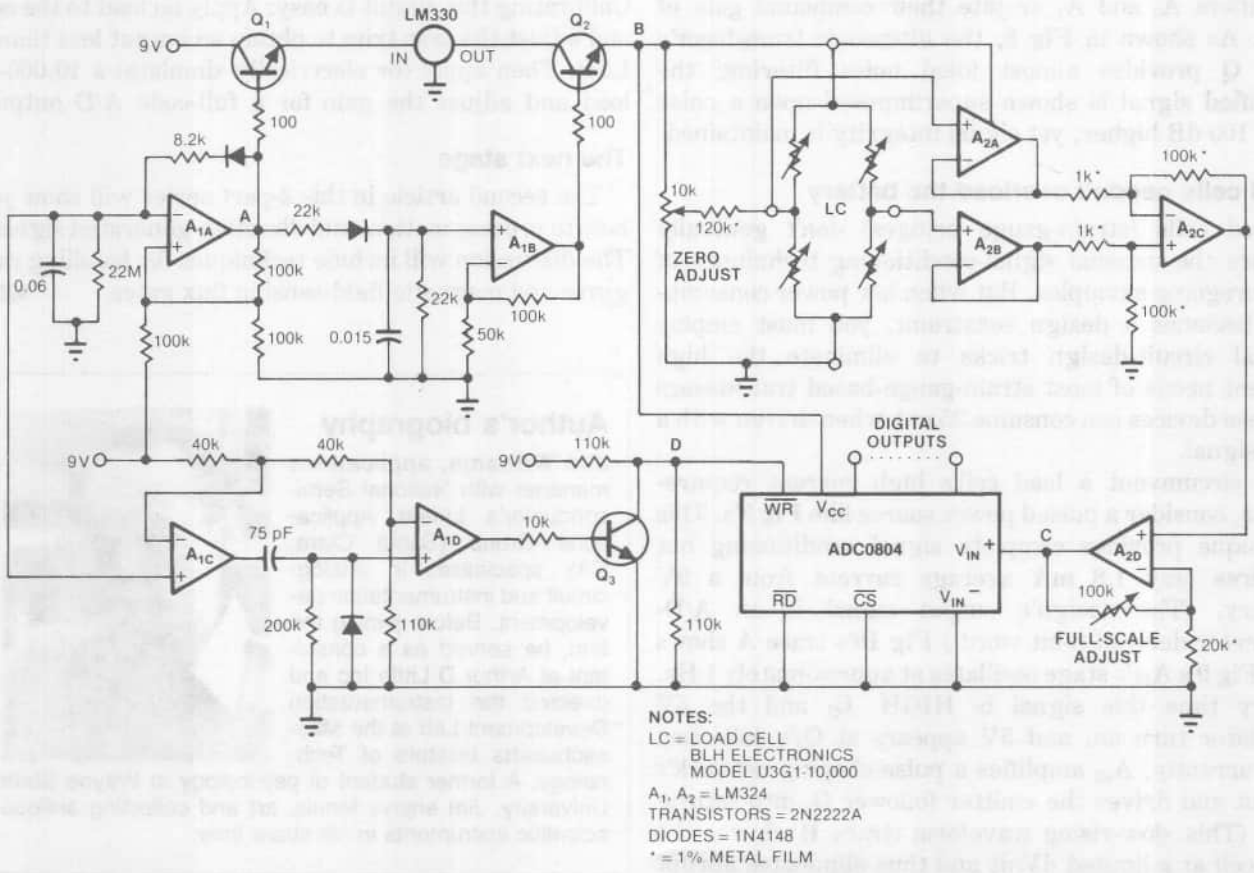

Fig 9—Pulse-powering a load cell (LC) *and its signal-conditioning electronics reduces current requirements from more than 35 mA to 1.8 mA. A_{1A} and A_{1B} gate voltage followers Q_1 and Q_2 to provide the load cell, its amplifiers (A_{2A} through A_{2D}) and an A/D converter with a 5V supply level. A delayed trigger—created by $A_{1C,D}$ and Q_3—operates the converter after the cell's amplified output stabilizes.*

Measure 5-ton loads with a 16-mW supply

determined by the distance between the transducers and the gas's temperature, the sonic signal pulse arrives at the receiving element, R_X, where it gets amplified by A_3 and A_4. (A_4's output appears as trace **B**.) This amplified signal triggers A_6 and resets the flip flop HIGH. During the flip flop's LOW period, the current source formed by Q_1 charges the 0.01-μF capacitor (trace **D**). Then, when a received pulse resets the flip flop HIGH, Q_2 comes on and in turn shuts off the current source. Voltage follower A_2's output then represents a dc level proportional to the gas's temperature-dependent transit time.

After being triggered by the flip flop's Q transition, a one-shot times out and causes the LF398 S/H stage to sample A_2's output. The S/H's output feeds a pair of multifunction LH0094 nonlinear converters arranged to linearize the sound-speed-vs-temperature relationship. This level, further processed by bridge amplifiers A_7 and A_8, then drives a directly indicating temperature-calibrated voltmeter. When A_1 issues its next pulse, a one-shot times out, Q_3 discharges the capacitor and the cycle repeats.

Note that you need no bandwidth limiting in receiver amplifiers A_3 and A_4 despite their compound gain of 1000. As shown in **Fig 8**, the ultrasonic transducer's high Q provides almost ideal noise filtering; the amplified signal is shown superimposed upon a noise level 100 dB higher, yet signal integrity is maintained.

Load cells needn't overload the battery

Load cells (strain-gauge bridges) don't generally require the unusual signal-conditioning techniques of the foregoing examples. But when low power consumption becomes a design constraint, you must employ special circuit-design tricks to eliminate the high current needs of most strain-gauge-based transducers —these devices can consume 35 mA when driven with a 10V signal.

To circumvent a load cell's high current requirements, consider a pulsed power source like **Fig 9**'s. This technique provides complete signal conditioning but requires only 1.8 mA average current from a 9V battery. (The design's output signal is an A/D-converter-derived 8-bit word.) **Fig 10**'s trace **A** shows how **Fig 9**'s A_{1A}'s stage oscillates at approximately 1 Hz. Every time this signal is HIGH, Q_1 and the 5V regulator turn on, and 5V appears at Q_2's collector. Concurrently, A_{1B} amplifies a pulse-shaping network's output and drives the emitter follower Q_2 into saturation. (This slow-rising waveform (trace **B**) drives the load cell at a limited dV/dt and thus eliminates abrupt step-drive-induced bridge changes over time.)

A differential-input, single-ended output-amplifier network processes the bridge's signal, which it feeds to the A/D converter (trace **C**). An $A_{1C,D}$-generated delay pulse (trace **D**) triggers the conversion when A_{2D}'s output is stable. In this fashion, the circuit realizes considerable power savings—the bridge, its conditioning stages and the A/D converter are all pulsed. Calibrating this circuit is easy: Apply no load to the cell and adjust the zero trim to obtain an output less than 1 LSB. Then apply (or electrically simulate) a 10,000-lb load and adjust the gain for a full-code A/D output.

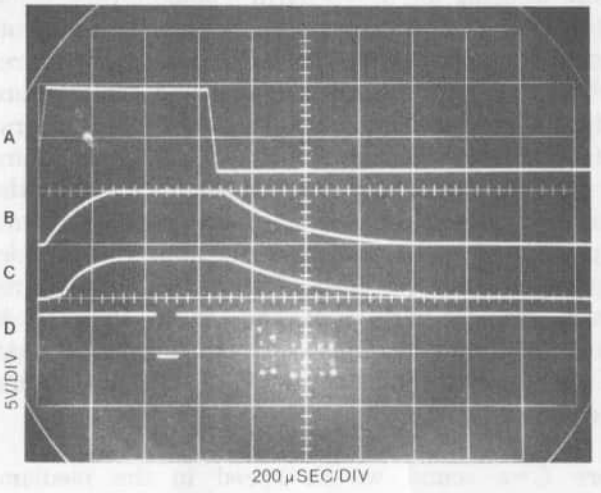

Fig 10—A 650-μsec signal (A) *initiates Fig 9's pulse-powered load-cell-based measurement scheme. This signal, after being shaped by A_{1B} and Q_2 (trace **B**), drives the load cell (LC) and its conditioning stages and supplies the A/D converter with power. After the cell output-amplifier's signal stabilizes (trace **C**), the $A_{1C,D}$-generated delay pulse (trace **D**) triggers the data converter.*

The next stage

The second article in this 2-part series will show you how to process motion- and direction-generated signals. The discussion will include techniques for handling rate gyros and magnetic-field-sensing flux gates. **EDN**

Author's biography

Jim Williams, applications manager with National Semiconductor's Linear Applications Group (Santa Clara, CA), specializes in analog-circuit and instrumentation development. Before joining the firm, he served as a consultant at Arthur D Little Inc and directed the Instrumentation Development Lab at the Massachusetts Institute of Technology. A former student of psychology at Wayne State University, Jim enjoys tennis, art and collecting antique scientific instruments in his spare time.

Conversion techniques adapt voltages to your needs

Different parts of your system often need specialized voltages. A variety of conversion techniques can help you obtain these voltages from the main supply.

Jim Williams, National Semiconductor Corp

Need more than one voltage in a single-supply system design? You can tailor the main system supply by using a variety of techniques; understanding how each works lets you choose the one most appropriate to producing the levels—and characteristics—you need.

Analog circuits need ±15V

Specifically, note that if you have a 5V logic rail available in your system but need ±15V, it's easy to construct a dc/dc converter with an oscillator, a transformer and a rectifier circuit. However, most dc/dc converters suffer from large noise spikes generated by the fast-switching oscillator. So if the analog circuitry is especially sensitive to power-supply noise, you can eliminate or minimize the switching noise by using an interrupt-driven converter or a full-duty-cycle, low-noise converter.

Fig 1 shows an interrupt-driven circuit. The LM3524 switching regulator runs open-loop; its Q_1-Q_2 output pair drives the step-up transformer. Unlike a standard

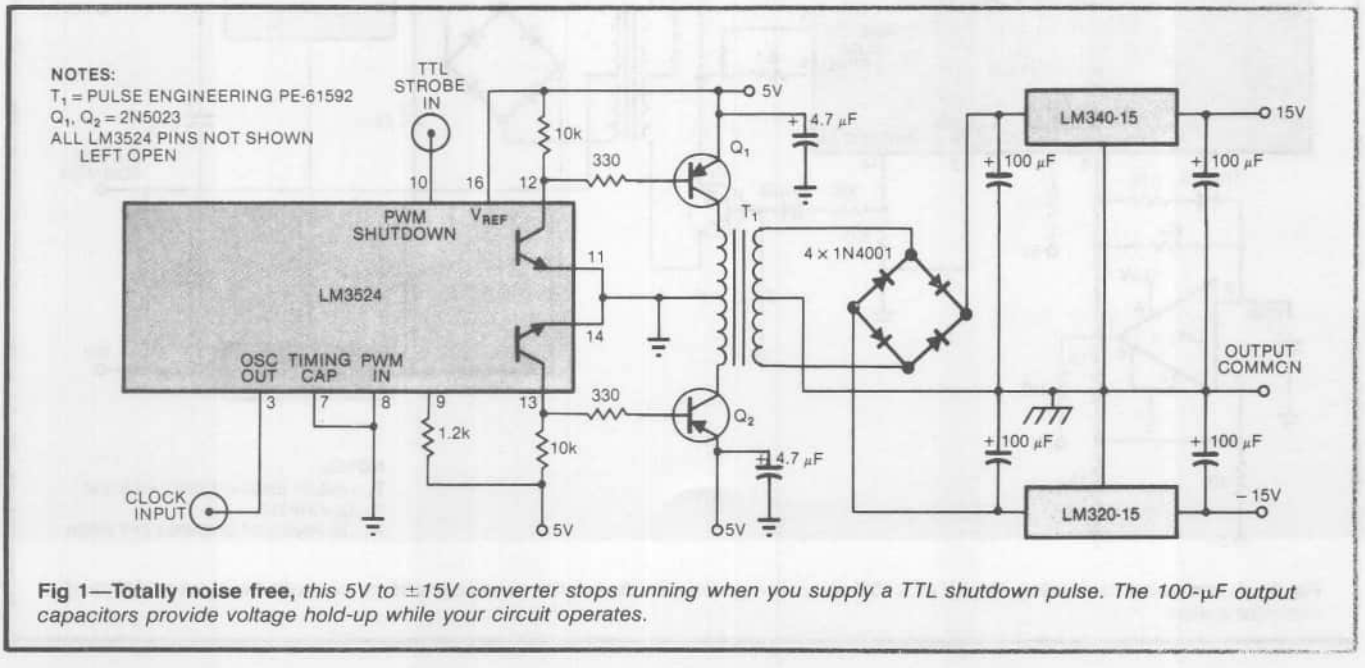

Fig 1—Totally noise free, *this 5V to ±15V converter stops running when you supply a TTL shutdown pulse. The 100-µF output capacitors provide voltage hold-up while your circuit operates.*

Interrupt switching for noise-free operation

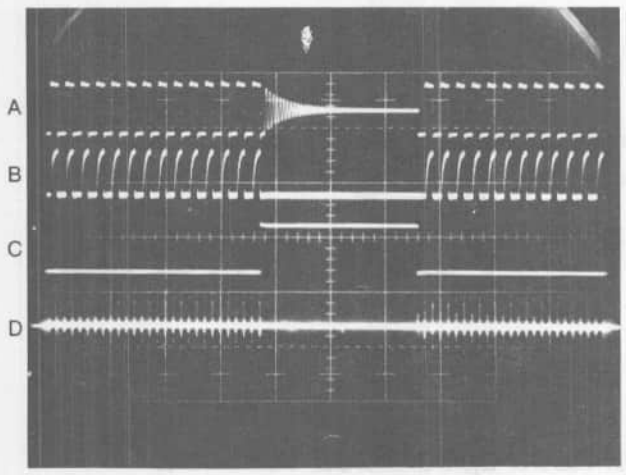

TRACE	VERTICAL	HORIZONTAL
A	10V/DIV	200 μSEC/DIV
B	1A/DIV	200 μSEC/DIV
C	5V/DIV	200 μSEC/DIV
D	20 mV/DIV (AC COUPLED)	200 μSEC/DIV

Fig 2—The center portion *of this scope photo shows the drop in output noise (trace D) that occurs when* ***Fig 1****'s converter shuts down.*

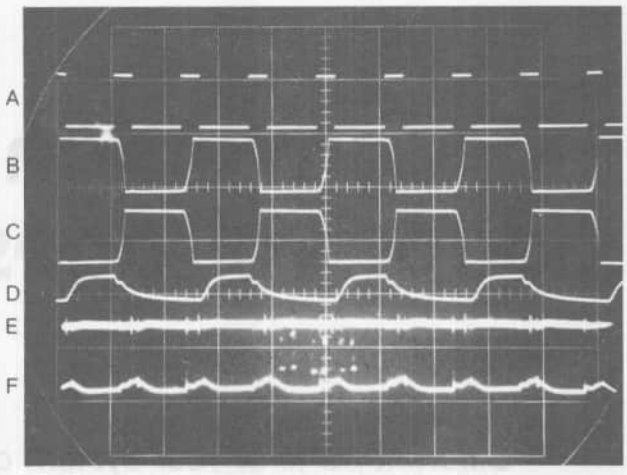

TRACE	VERTICAL	HORIZONTAL
A	5V/DIV	20 μSEC/DIV
B	10V/DIV	20 μSEC/DIV
C	10V/DIV	20 μSEC/DIV
D	500 mA/DIV	20 μSEC/DIV
E	2 mV/DIV (AC COUPLED)	20 μSEC/DIV
F	100 mV/DIV	20 μSEC/DIV

Fig 4—Barely discernible spikiness *is visible in the output (trace E) of* ***Fig 3****'s low-noise converter.*

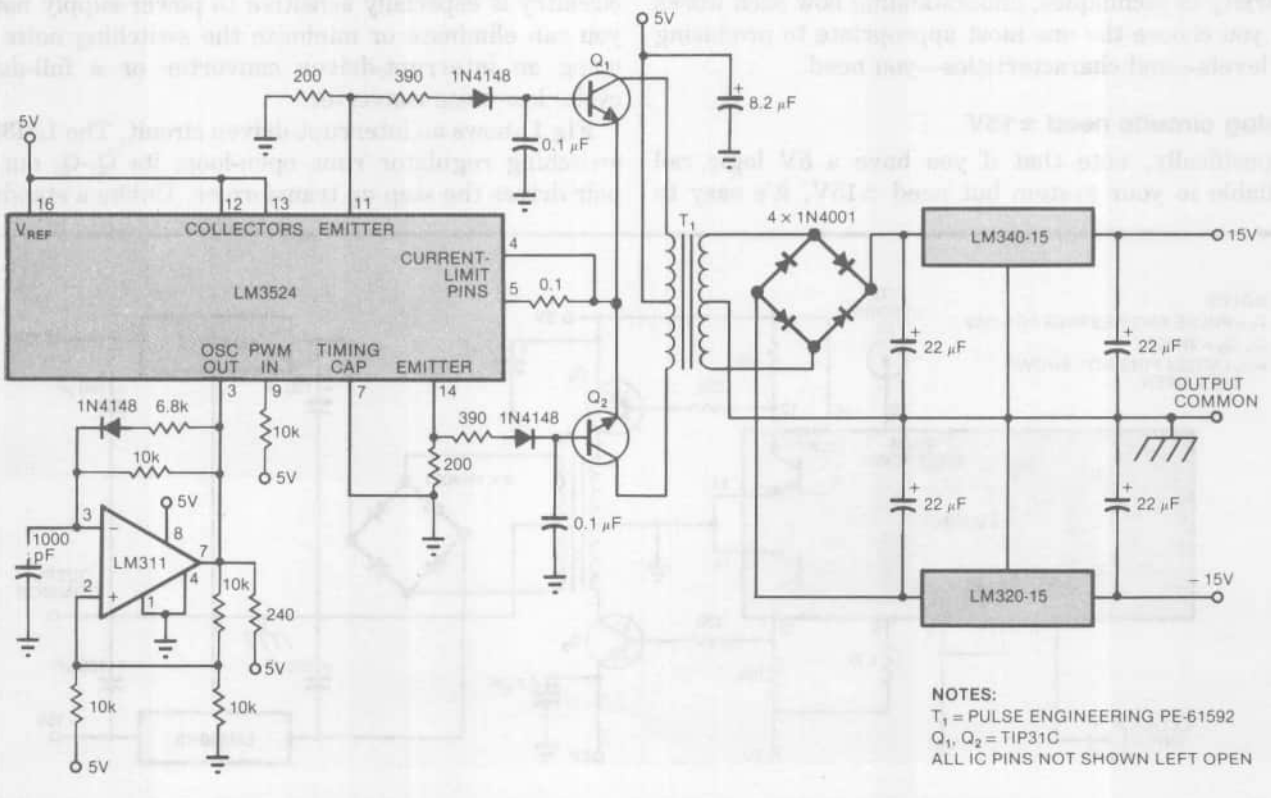

NOTES:
T_1 = PULSE ENGINEERING PE-61592
Q_1, Q_2 = TIP31C
ALL IC PINS NOT SHOWN LEFT OPEN

Fig 3—A low-noise converter, *this 5V to ±15V circuit runs continuously, but the output transistors' controlled turn-on and turn-off minimize spikes.*

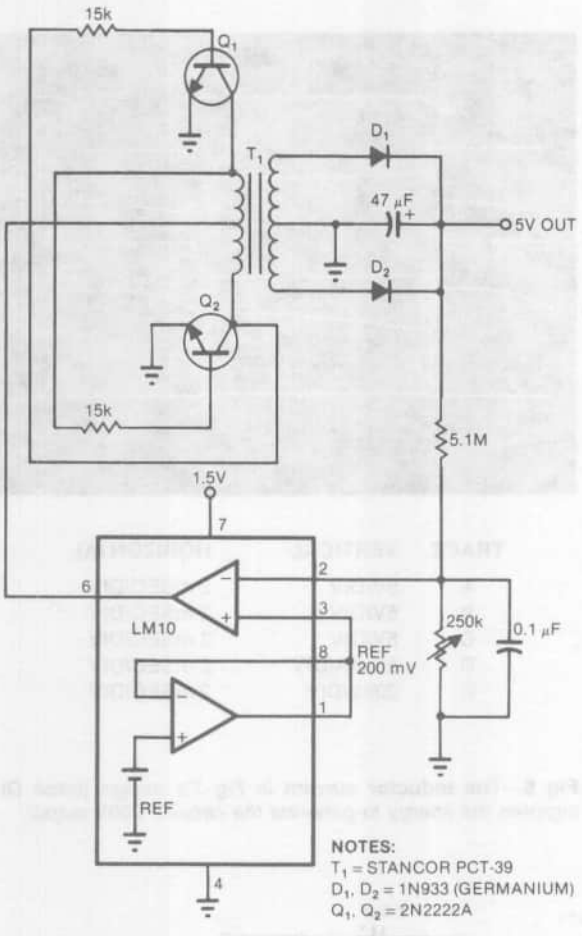

Fig 5—Powered by a 1.5V battery, *this 5V-output design can drive low-power circuitry for months from one cell.*

dc/dc converter, this circuit uses an external clocked oscillator, allowing you to synchronize the converter to the host system. To use this feature, you disable the LM3524's internal oscillator by grounding the capacitor timing pin and apply the system clock to the oscillator output, yielding a 50% switching duty cycle.

To obtain a noise-free ±15V output for a critical circuit operation such as an A/D conversion or a sample/hold acquisition, interrupt the switching by applying a TTL-level pulse to the LM3524's shutdown pin. This action stops the converter, leaving the large output capacitors as a virtually noiseless dc source to power the output regulators.

Fig 2 details the circuit's performance; traces A and B show Q_1's voltage and current waveforms, respectively (Q_2's waveforms are similar). Trace D depicts the 15V output line (the −15V line is similar): The noise pulses caused by the switching circuitry are clearly visible. When the interrupt pulse is applied (trace C), the noise disappears. The large output filter capacitors provide adequate ±15V holdup time for the critical operation required while the interrupt pulse is HIGH.

Don't interrupt—just quiet down

If you need a 5V to ±15V converter with low (but not necessarily zero) noise, consider the continuously running circuit shown in **Fig 3.** Here, the LM311 multivibrator clocks the LM3524 (**Fig 4,** trace A), whose internal oscillator is again disabled by grounding the timing-capacitor pin. While the LM311's output is HIGH, the LM3524 cuts the drive to Q_1 and Q_2, helping to minimize switching noise.

The main contributor to low-noise performance is the base-drive slowdown network used with Q_1 and Q_2: The 390Ω/0.1-μF time constant slows turn-on, and the diode forces base-emitter charge trapping to delay turn-off.

The effect of these components is evident in the Q_1-Q_2 collector-voltage waveforms (**Fig 4,** traces B and C) and Q_2's current waveform (**Fig 4,** trace D). Note that the LM311's long ON time permits no current to flow in Q_2 until well after Q_1 has turned off. Moreover, the current's rise and fall times are smoothly controlled and long, unlike those of the more common fast-switching converters. Therefore, very little harmonic content appears in the transformer drive, so converter output noise (**Fig 4,** trace E) is exceptionally low. In addition,

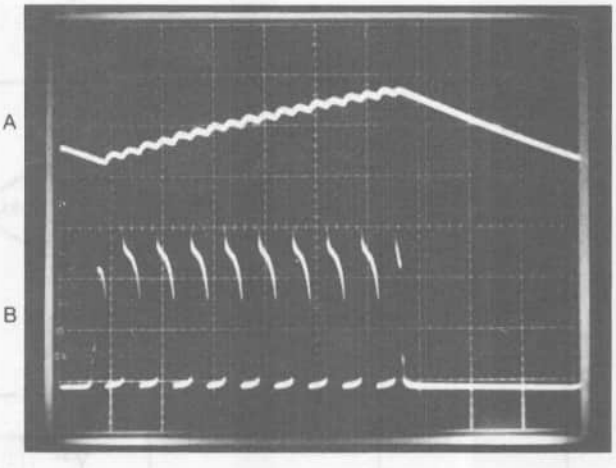

TRACE	VERTICAL	HORIZONTAL
A	0.1V/DIV (AC COUPLED)	10 mSEC/DIV
B	1V/DIV	10 mSEC/DIV

Fig 6—The on-demand operation *of* ***Fig 5****'s 1.5V to 5V converter is evident in this scope photo. The converter turns on when the output drops to approximately 4.93V and off when it rises to roughly 5.07V.*

Power CMOS ICs for months with one D cell

the disturbance to the 5V rail (**Fig 4**, trace F) is small compared with standard designs.

This circuit's low noise comes at the expense of efficiency and available output power, though: During the slow base transitions, Q_1 and Q_2 dissipate power, reducing efficiency to about 50% and available output to approximately 50 mA. Heat-sinking Q_1 and Q_2 won't help, either, because it involves the risk of secondary breakdown. The circuit is, however, short-circuit protected by the 0.1Ω emitter resistor and the LM3524's current-limiting circuitry.

Power circuits from a battery

What if your basic system supply is a battery? The circuit depicted in **Fig 5** supplies 5V from a 1.5V source—such as a battery, saltwater cells or a solar-cell stack. With 125-μA load current (typically 20 CMOS ICs), it runs for 3 months on one D cell.

The circuit is unusual because the amount of time required for Q_1 and Q_2 to drive the transformer is directly related to the load resistance. The LM10 op-amp/reference IC compares the converter's output with its own internal 200-mV reference via the 5.1-MΩ/250-kΩ voltage divider. Whenever the converter's output drops below 5V, the LM10 output goes HIGH, driving the Q_1-Q_2-T_1 oscillator circuit. The rectified transformer output then charges the 47-μF

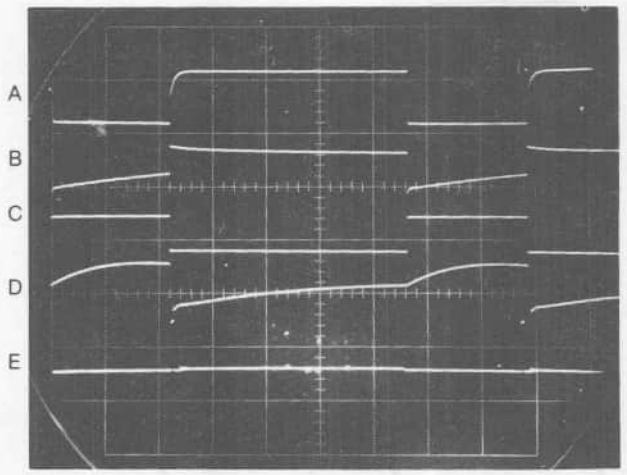

TRACE	VERTICAL	HORIZONTAL
A	5V/DIV	2 mSEC/DIV
B	5V/DIV	2 mSEC/DIV
C	5V/DIV	2 mSEC/DIV
D	50 mA/DIV	2 mSEC/DIV
E	200V/DIV	2 mSEC/DIV

Fig 8—The inductor current *in* ***Fig 7****'s design (trace D) supplies the energy to generate the circuit's 200V output.*

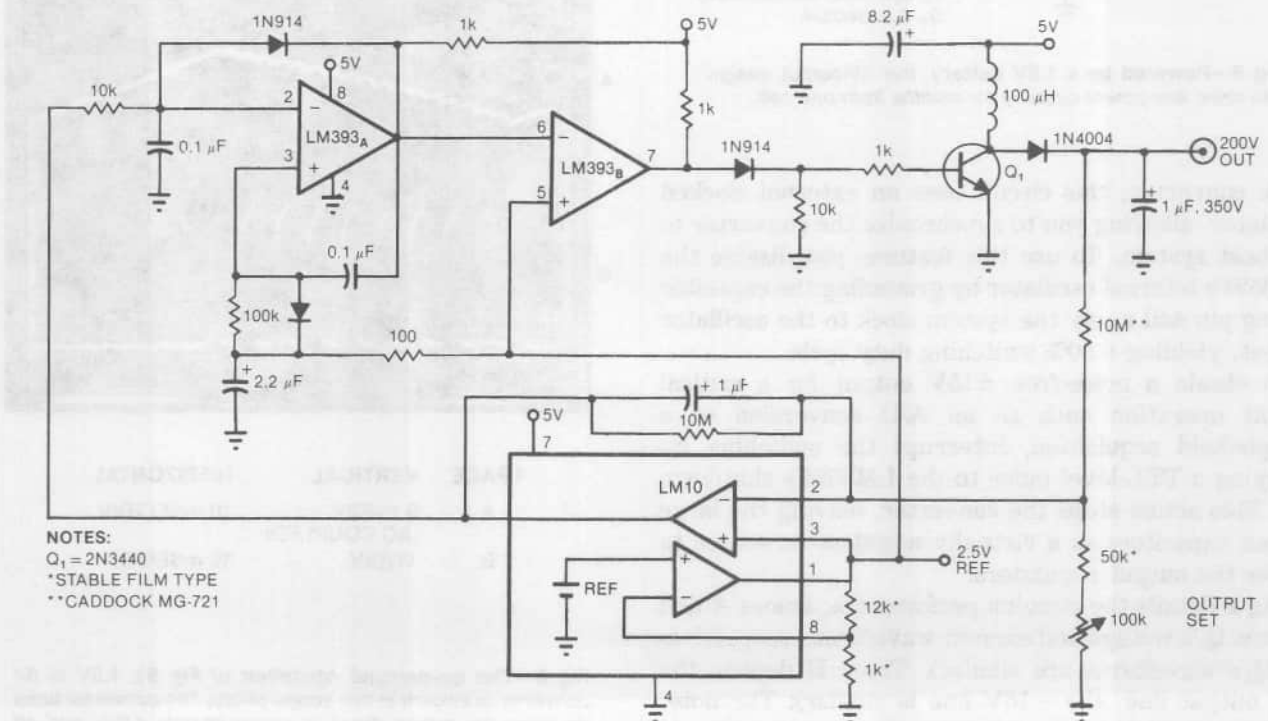

Fig 7—A 40-fold multiplication *of the 5V supply results with this flyback-type converter. It furnishes 200V into a 500-μA load.*

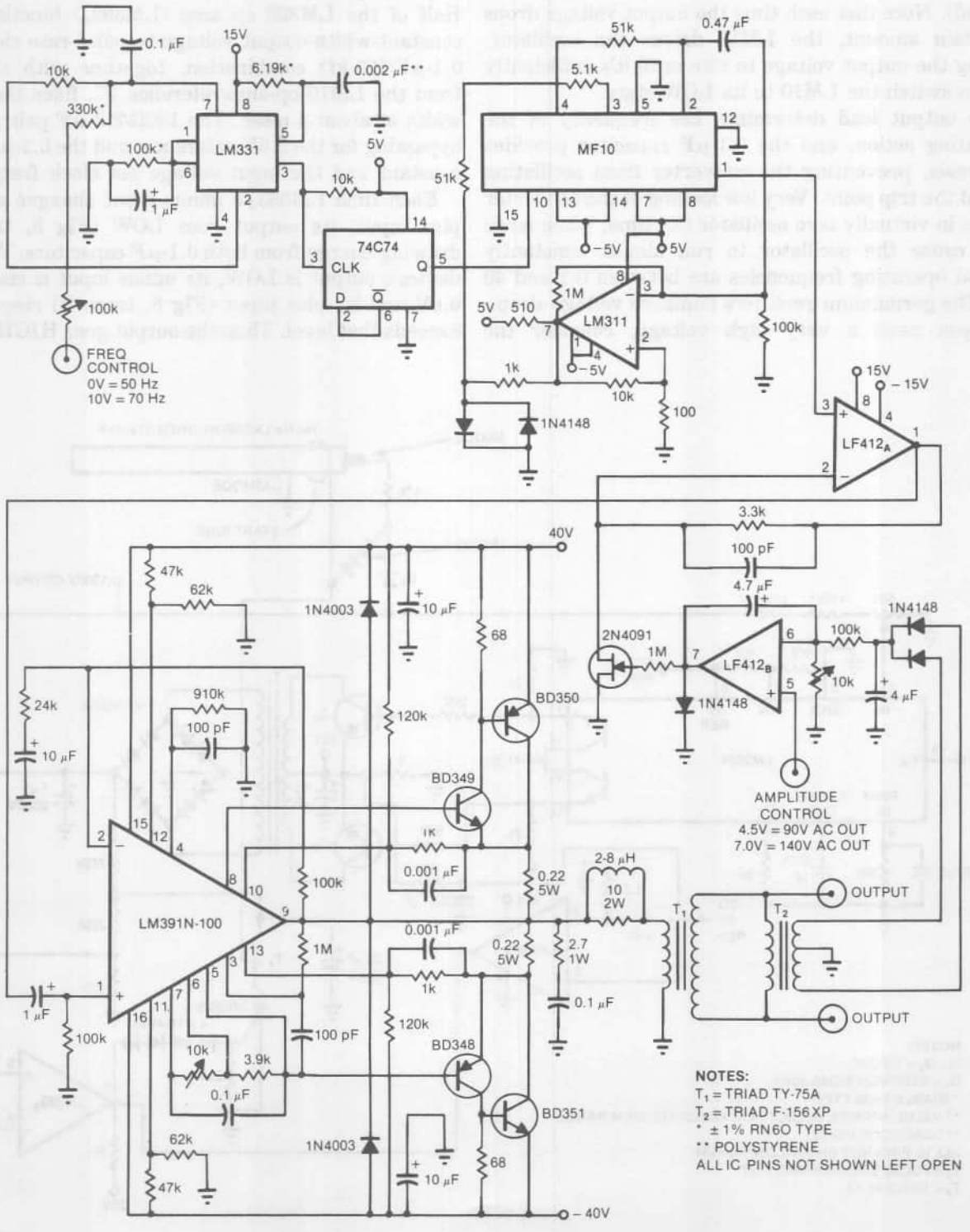

Fig 9—Test line-operated devices *with this variable-voltage and -frequency converter. From a 40V dc input, you can get 90 to 140V ac at 50 to 70 Hz.*

Use a flyback circuit to obtain high voltages

capacitor to a value high enough to cause the LM10 output to go LOW, thereby cutting off the oscillation.

In **Fig 6**, trace B shows the collector voltage of Q_1; trace A shows the converter's output voltage (ac coupled). Note that each time the output voltage drops a certain amount, the LM10 drives the oscillator, causing the output voltage to rise until it's sufficiently high to switch the LM10 to its LOW state.

The output load determines the frequency of the regulating action, and the 0.1-μF capacitor provides hysteresis, preventing the converter from oscillating around the trip point. Very low loading of the converter results in virtually zero oscillator ON time, while large loads cause the oscillator to run almost constantly (typical operating frequencies are between 0.1 and 40 Hz). The germanium rectifiers minimize voltage drop.

If you need a very high voltage, consider the flyback-type converter shown in **Fig 7.** It generates 200V (regulated) into a 500-μA load from a 5V supply and thus serves applications such as gas-discharge displays, piezoelectric transducers and strobe lamps. Half of the LM393 op amp ($LM393_A$) functions as a constant-width-output voltage-to-pulse-rate clock. The 0.1-μF/100-kΩ combination, together with the 2.5V from the LM10 op-amp/reference IC, fixes the output width at about 4 msec. The 100Ω/2.2-μF pair provides bypassing for the 2.5V reference, and the 0.1-μF/10-kΩ constant and the input voltage set clock frequency.

Each time $LM393_A$'s minus input charges above its plus input, its output goes LOW (**Fig 8**, trace A), drawing charge from both 0.1-μF capacitors. When the device's output is LOW, its minus input is clamped at 0.6V and its plus input (**Fig 8**, trace B) rises until it exceeds that level. Then the output goes HIGH, ending

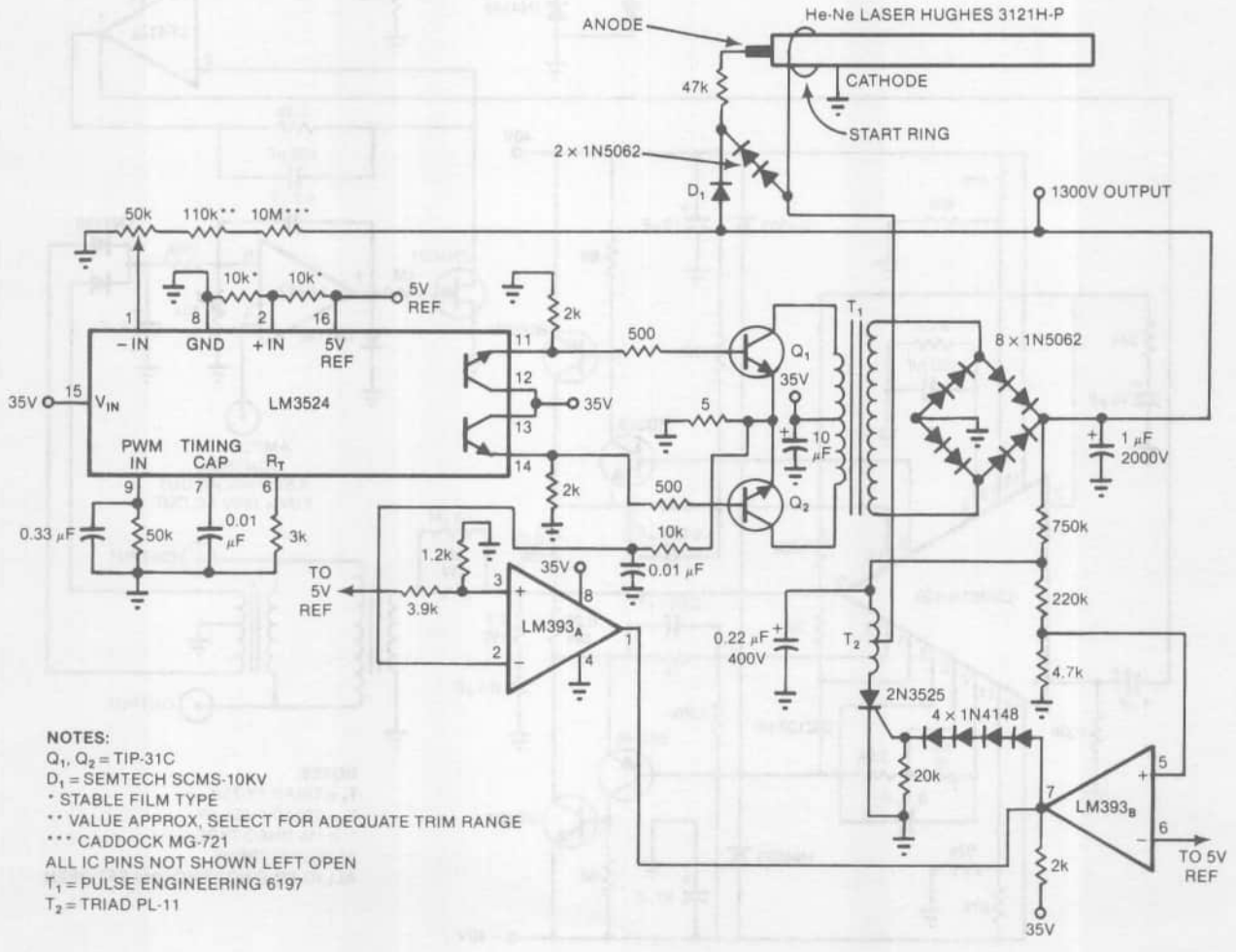

Fig 10—Start and run a laser *with this 35V to 1300V converter. It furnishes an 8000V pulse that repeats as often as needed until the laser starts.*

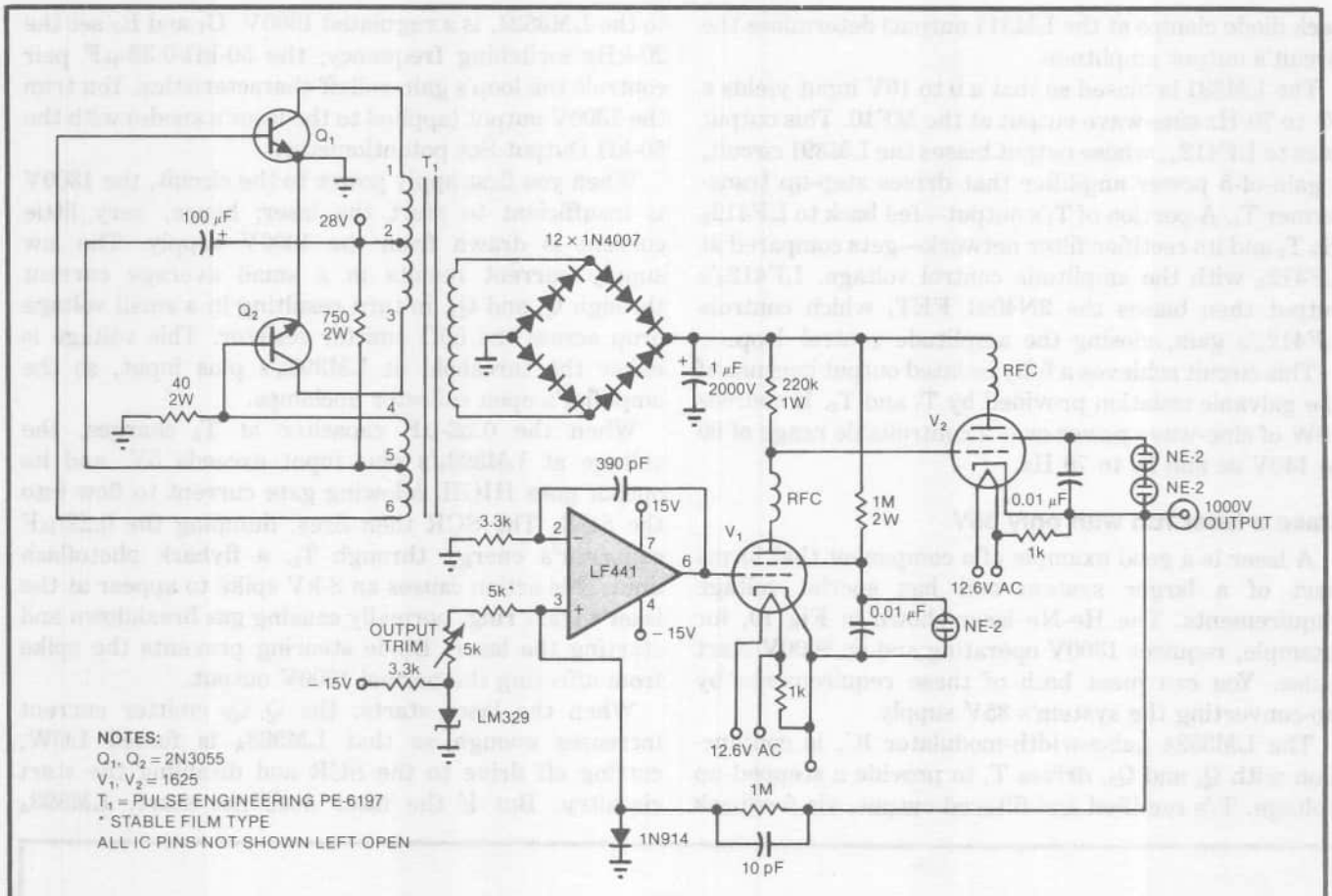

Fig 11—Using tried-and-true technology, *this ±15V to 1000V hybrid-semiconductor/vacuum-tube converter incorporates inexpensive components and is very forgiving of overloads.*

the timing cycle and reinitializing the entire process. The 1N914 diode prevents a differentiated positive response at $LM393_A$'s plus input, allowing the circuit to recover quickly for the next cycle.

$LM393_B$, meanwhile, inverts the clock's output and drives Q_1. When this op amp's output goes HIGH (**Fig 8**, trace C), Q_1 turns on, its collector current rises (**Fig 8**, trace D) and the 100-µH inductor stores energy. *(Ed Note: The current probe is ac coupled—the long tail is actually flat.)* When $LM393_B$'s output goes LOW, the magnetic field in the inductor collapses and Q_1's collector voltage rises to about 200V (**Fig 8**, trace E). This high-voltage spike gets clamped and stored by the 1N4004/1-µF combination at the circuit's output.

The LM10 compares a divided-down portion of the output with its 2.5V internal reference. The difference voltage at the LM10 output then closes the loop at $LM393_A$'s clock. The 10-MΩ/1-µF feedback components set loop gain and frequency compensation.

Vary voltage, frequency with ac line converter

If you must generate a variable-frequency and -amplitude ac supply from a 40V source, consider **Fig 9**'s circuit. This arrangement is ideal for testing 115V ac, 60-Hz line-powered loads for sensitivity to amplitude and frequency variations. The frequency of its sinusoidal output is voltage controllable from 50 to 90 Hz; output amplitude is also voltage controllable over a 90 to 140V ac range.

In the circuit, the LM331 V/F converter and flip flop form a voltage-controlled square-wave clock that drives the MF10 filter. That device, together with an LM311 comparator, forms a resonator that generates stable-amplitude sine outputs without using AGC circuitry. The MF10 operates as a Q-of-10 bandpass filter that rings at its resonant frequency in response to a step input. The LM311, upon receipt of this ringing signal, creates a square-wave input signal for the bandpass to regenerate the oscillation.

The bandpass output is the filtered fundamental frequency of a 50%-duty cycle square wave. The clock controls the filter's center frequency, in turn setting the oscillation frequency. The peak-to-peak swing of the MF10's square-wave input (defined by the back-to-

Build an isolated ac supply using a bandpass-filter IC

back diode clamps at the LM311 output) determines the circuit's output amplitude.

The LM331 is biased so that a 0 to 10V input yields a 50- to 70-Hz sine-wave output at the MF10. This output goes to $LF412_A$, whose output biases the LM391 circuit, a gain-of-5 power amplifier that drives step-up transformer T_1. A portion of T_1's output—fed back to $LF412_B$ via T_2 and its rectifier/filter network—gets compared at $LF412_B$ with the amplitude control voltage. $LF412_B$'s output then biases the 2N4091 FET, which controls $LF412_A$'s gain, closing the amplitude control loop.

This circuit achieves a fully isolated output because of the galvanic isolation provided by T_1 and T_2. It sources 10W of sine-wave power over a controllable range of 90 to 140V ac and 50 to 70 Hz.

Make a laser run with only 35V

A laser is a good example of a component that forms part of a larger system and has special voltage requirements. The He-Ne laser shown in **Fig 10,** for example, requires 1300V operating and an 8000V start pulse. You can meet both of these requirements by up-converting the system's 35V supply.

The LM3524 pulse-width-modulator IC, in conjunction with Q_1 and Q_2, drives T_1 to provide a stepped-up voltage. T_1's rectified and filtered output, via feedback to the LM3524, is a regulated 1300V. C_T and R_T set the 20-kHz switching frequency; the 50-kΩ/0.33-μF pair controls the loop's gain-rolloff characteristics. You trim the 1300V output (applied to the laser's anode) with the 50-kΩ Output Set potentiometer.

When you first apply power to the circuit, the 1300V is insufficient to start the laser; hence, very little current is drawn from the 1300V supply. The low supply current results in a small average current through Q_1 and Q_2, in turn resulting in a small voltage drop across the 50Ω emitter resistor. This voltage is below the threshold at $LM393_A$'s plus input, so the amplifier's open collector unclamps.

When the 0.22-μF capacitor at T_2 charges, the voltage at $LM393_B$'s plus input exceeds 5V, and its output goes HIGH, allowing gate current to flow into the SCR. The SCR then fires, dumping the 0.22-μF capacitor's energy through T_2, a flyback photoflash unit. This action causes an 8-kV spike to appear at the laser's start ring, normally causing gas breakdown and starting the laser. Diode steering prevents the spike from affecting the normal 1300V output.

When the laser starts, the Q_1-Q_2 emitter current increases enough so that $LM393_A$ is forced LOW, cutting off drive to the SCR and disabling the start circuitry. But if the laser does not start, $LM393_A$

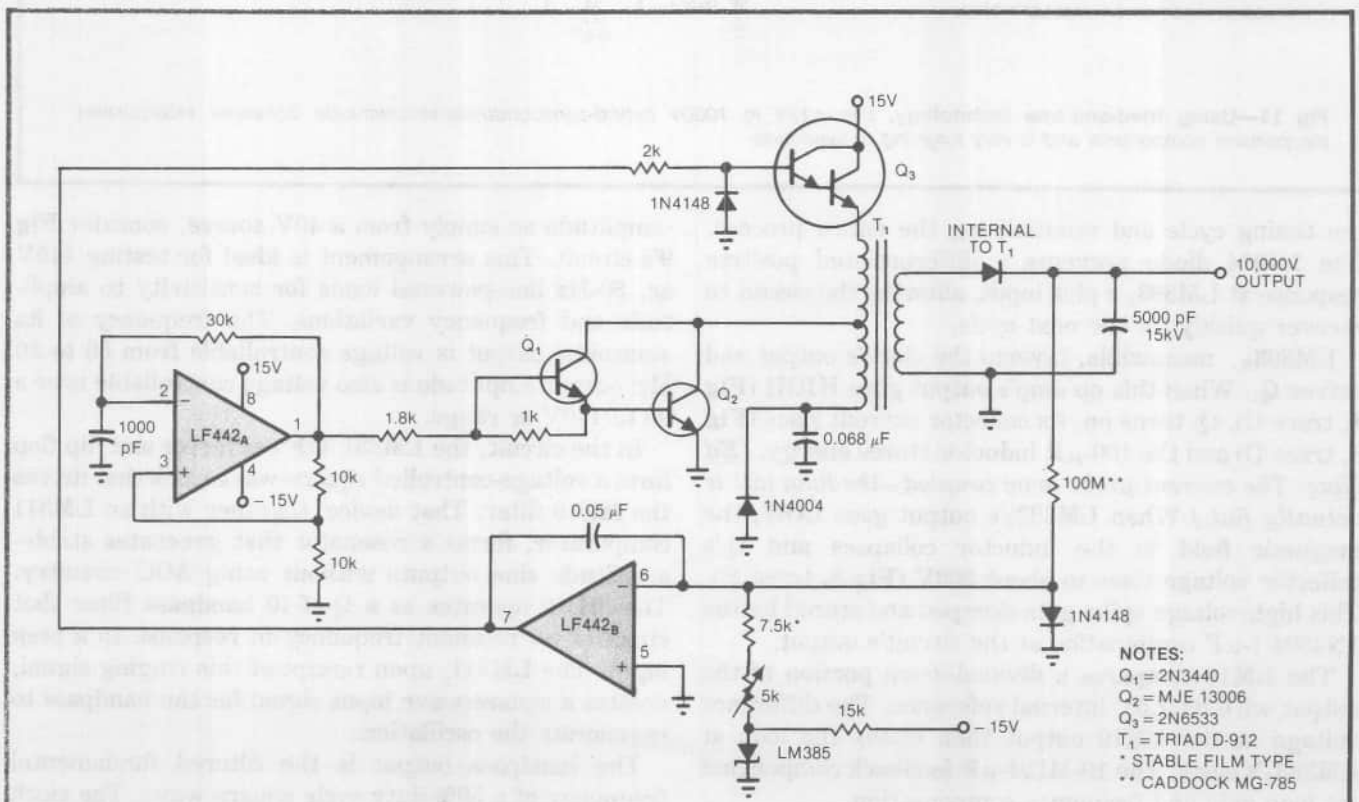

Fig 12—Accelerate electrons in a CRT *with this ±15V to 10-kV flyback-type converter; its servo loop ensures output stability.*

Meet lasers' special needs with a PWM IC

remains unclamped. When the 0.22-μF capacitor charges fully, LM393$_B$'s plus input exceeds 5V, and the SCR again drives T_2, producing the 8-kV start pulse. This action continues until the laser runs.

Don't write off vacuum tubes

Fig 10's laser supply achieves its 1300V output through servo control around a transformer. A potential problem with this type of converter is that its transient response is limited by the modulation frequency applied to the transformer. The best way to avoid the problem is to regulate with a series-pass

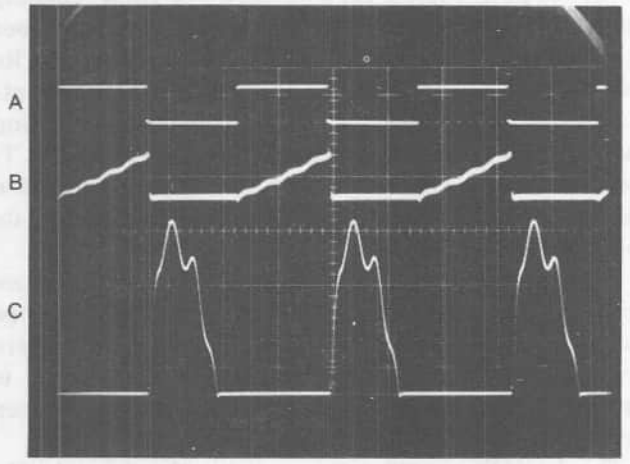

TRACE	VERTICAL	HORIZONTAL
A	50V/DIV	20 μSEC/DIV
B	4A/DIV	20 μSEC/DIV
C	50V/DIV	20 μSEC/DIV

Fig 13—Magnetic-field collapse *in* ***Fig 12****'s T_1 primary produces the high Q_2 collector-voltage pulses in trace C.*

element on the transformer's high-voltage side. But this action usually implies the use of expensive high-voltage transistors and a substantial amount of protective circuitry. **Fig 11** shows a converter that deals with these problems. It's inexpensive, provides the fast transient response of a series regulator and requires no output protection. Moreover, it withstands short circuits and output-current or -voltage reversals arising from reactive loads.

The self-exciting dc/dc converter composed of T_1, Q_1, Q_2 and their associated components generates the unregulated high voltage from a 28V supply. This converter's rectified and filtered output is applied to the plates of the two 1625 vacuum tubes, which are configured in a common-cathode-driven cathode-

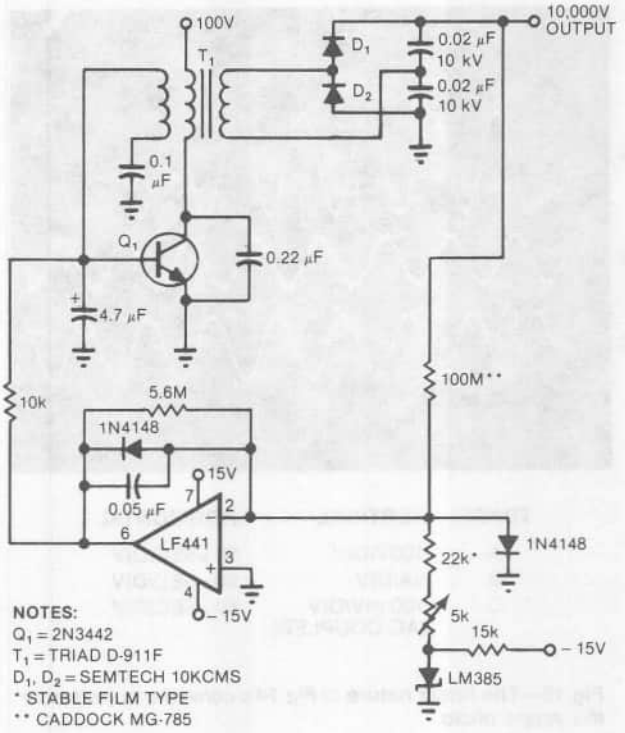

Fig 14—Using sinusoidal signals, *this converter supplies 10 kV with no radiated noise or spikiness.*

follower arrangement, with NE-2 neon-lamp screen-to-cathode clamps. Feedback from V_2 to the LF441 provides overall loop stabilization. The 390-pF/3.3-kΩ pair provides local rolloff at the LF441; overall compensation comes from the 10-pF/1-MΩ network. The 1N914 prevents capacitively coupled transients from appearing at the LF441's input.

Set the output voltage with the 5-kΩ potentiometer at the LM329 reference. The power-handling capability of T_1 limits the circuit's output to 10W at 1000V—a chore that V_2 can perform effortlessly. If you anticipate extended (greater than 5 min) short circuits at the output, consider fusing V_2's plate circuit.

Multiply ±15V for voltage-hungry CRTs

In data-terminal designs, you must often convert the supply rails to the high voltage needed for CRT electron-beam acceleration. You can use a flyback approach for this task, but for more demanding applications (such as oscilloscopes), you might have to use a sine-wave conversion technique. So consider examples of conversion circuits that use each method.

In **Fig 12**'s flyback circuit, LF442$_A$ functions as an oscillator whose output (**Fig 13**, trace A) drives the Q_1-Q_2 Darlington pair. When the output is HIGH, Q_1 and Q_2 conduct and the current through T_1's primary

Use vacuum tubes for a low-cost high-voltage supply

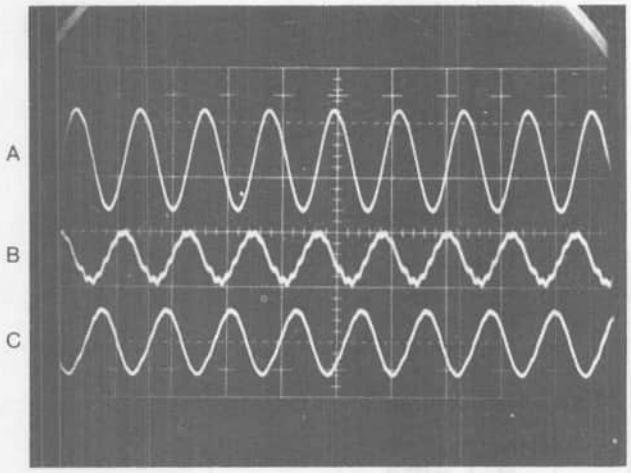

TRACE	VERTICAL	HORIZONTAL
A	100V/DIV	50 μSEC/DIV
B	5A/DIV	50 μSEC/DIV
C	100 mV/DIV (AC COUPLED)	50 μSEC/DIV

Fig 15—The linear nature *of* ***Fig 14****'s converter is evident in this scope photo.*

builds up (**Fig 13,** trace B). When $LF442_A$ goes LOW, however, the field in T_1's primary collapses and a large flyback voltage appears at Q_2's collector (**Fig 13,** trace C). This field collapse also appears at T_1's secondary and produces a very-high-voltage output, which is rectified and filtered and fed back to $LF442_B$ via a divider. $LF442_B$'s output then servo-controls Q_3, which determines the amount of drive available to T_1. The 0.05-μF capacitor provides stable loop compensation; the LM385 and the 5-kΩ pot set the output voltage.

Although effective, this circuit produces unavoidable radiated noise and supply spiking—which some sensitive data terminals and oscilloscopes can't tolerate. **Fig 14**'s sine-wave-based high-voltage converter eliminates these problems.

When you apply power to this circuit, the LM385 reference pulls the LF441's minus input LOW, causing the LF441's output to rise. This action in turn causes Q_1's collector voltage to drop (**Fig 15,** trace A) and its collector current to rise (**Fig 15,** trace B). Concurrently, the 0.1-μF capacitor in T_1's feedback winding charges to a negative voltage. When the current in T_1 stops building, T_1's feedback winding pulls Q_1's base negative (**Fig 15,** trace C), cutting off Q_1 and causing its collector voltage to rise.

When the voltage on the 0.1-μF capacitor becomes positive, Q_1 starts to conduct, its collector voltage drops and the cycle repeats. The 0.22- and 4.7-μF capacitors provide stabilization, and the high-voltage output is current-summed with the LM385's negative reference current at the LF441 servo amplifier.

The LF441's output servo-controls the drive to Q_1,

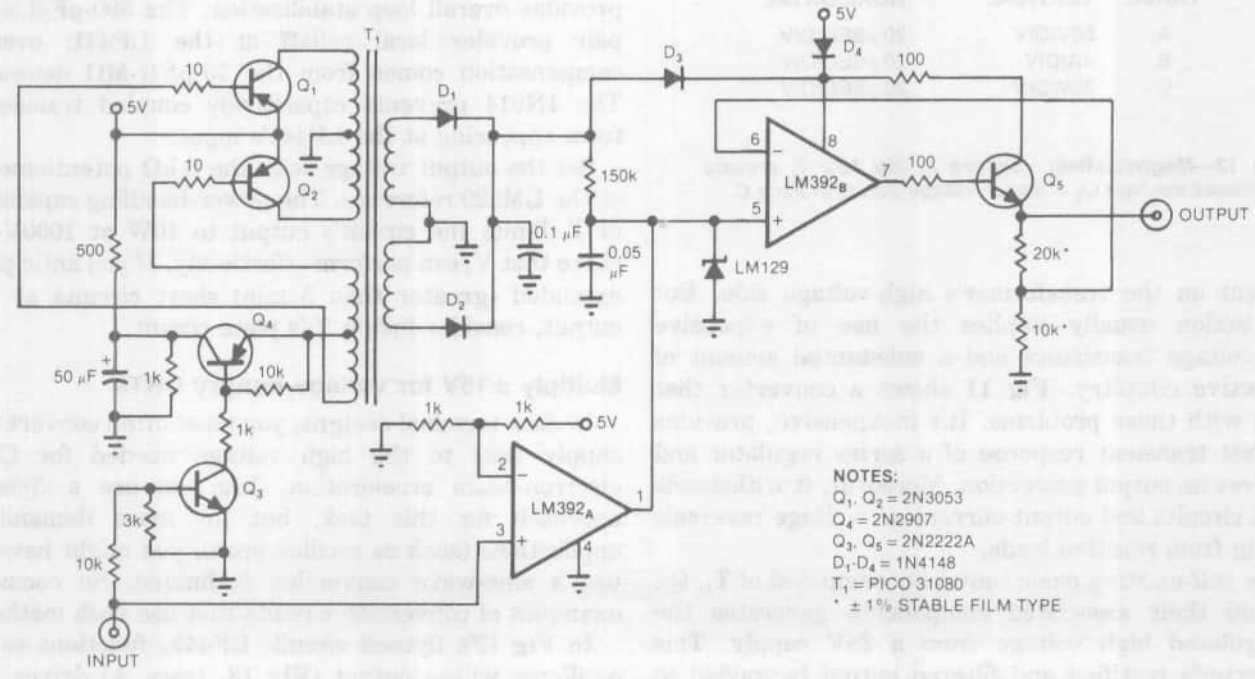

Fig 16—Memories are made of this—*a converter that supplies the 21V pulses for EEPROM programming. It achieves controlled rise time; you determine the pulse's width with a TTL command.*

Generate EPROM-programming pulses from the 5V rail

closing the feedback loop around the transformer. Because the transformer isn't used in the flyback mode, the voltage step-up ratio is smaller than in **Fig 12**'s design, so you need higher initial input voltages. Alternatively, you could use a voltage-doubler network at the transformer output.

An easy way to power memory programming

What about the voltage required by programmable memories? Widely used EEPROM types such as the 2816 require controlled-rise-time 21V pulses for programming. **Fig 16** shows a converter that generates the necessary high-voltage pulses from the 5V rail.

T_1, in conjunction with Q_1 and Q_2, forms a self-driven 5 to 30V dc/dc converter. Q_3 and Q_4 serve as a strobe for this converter, allowing it to draw power and run only when a TTL signal is present at the circuit's input. When you apply a signal to the input (**Fig 17,** trace A), the Q_3-Q_4 pair conducts, biasing Q_1 and Q_2 so the converter runs (Q_2's collector waveform appears in **Fig 17,** trace B). The converter's output (**Fig 17,** trace C) is very lightly filtered by the 0.1-μF capacitor, allowing it to rise quickly. This output charges the 0.05-μF/150-kΩ combination.

The gain-of-3 $LM392_B$ amplifies the 0.05-μF capacitor voltage; Q_5 serves as an output-current booster. As the 0.05-μF capacitor charges, Q_5's emitter voltage rises, providing the leading edge of the programming pulse (**Fig 17,** trace D). When the capacitor voltage reaches 7V, the LM129 clamps, charging ceases and the output remains at 21V.

When you switch the TTL input pulse LOW, the $LM392_A$'s open-collector output clamps LOW, discharging the 0.05-μF capacitor and readying the circuit for the next pulse. You can satisfy any EEPROM's programming requirement by varying the gain of $LM392_B$, the time constant at its input or the zener clamp across the 0.05-μF capacitor. **EDN**

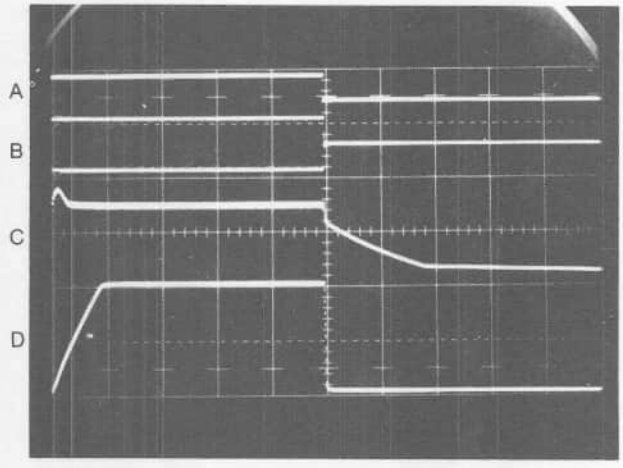

TRACE	VERTICAL	HORIZONTAL
A	10V/DIV	2 mSEC/DIV
B	10V/DIV	2 mSEC/DIV
C	20V/DIV	2 mSEC/DIV
D	10V/DIV	2 mSEC/DIV

Fig 17—The programming pulse *of* ***Fig 16****'s circuit appears in trace D. Note the cleanly rising leading edge.*

Author's biography

Jim Williams, now a consultant, was applications manager in National Semiconductor's Linear Applications Group (Santa Clara, CA), specializing in analog-circuit and instrumentation development, when he wrote this article. Before joining the firm, he served as a consultant at Arthur D Little Inc and directed the Instrumentation Development Lab at the Massachusetts Institute of Technology. A former student of psychology at Wayne State University, Jim enjoys tennis, art and collecting antique scientific instruments in his spare time.

References

1. Tektronix Inc, *CRT Circuit,* Operating Manual 453, pgs 3-16.
2. Regan, Tim, *Introducing the MF10,* Application Note, National Semiconductor Corp, Santa Clara, CA.
3. John Fluke Mfg Co, *Operating Manual—Model 415B High Voltage Supply.*
4. Kepco Inc, *Operating Manual—Model BHK-2000-01M.*
5. Williams, Jim, "Design dc/dc converters to catch noise at the source," *Electronic Design,* October 15, 1981, pgs 229-234.

Heavy-duty power supply regulates either voltage, current or power

By combining switching and series-pass techniques, this high-voltage supply's designer achieved 0.01% regulation at power levels to 100W.

James M. Williams, Teledyne Philbrick

Regulated high-voltage power supplies, while common, generally offer only constant-current and constant-voltage modes of operation. This one adds a constant-power (EI product) mode.

Careful circuit design permitted fitting the unit's 100W capability into an unventilated rack-mount chassis measuring only 3-1/2×14×19 inches. Also, no high-voltage semiconductors (except diodes) are employed in it. Voltage output is 50 to 1000V at up to 100W, with better than 0.01% regulation. In the current mode, the unit delivers a maximum of 100 mA with 0.01% stability. Finally, when regulating power (EI), the output supplies up to 100W with 0.01% stability.

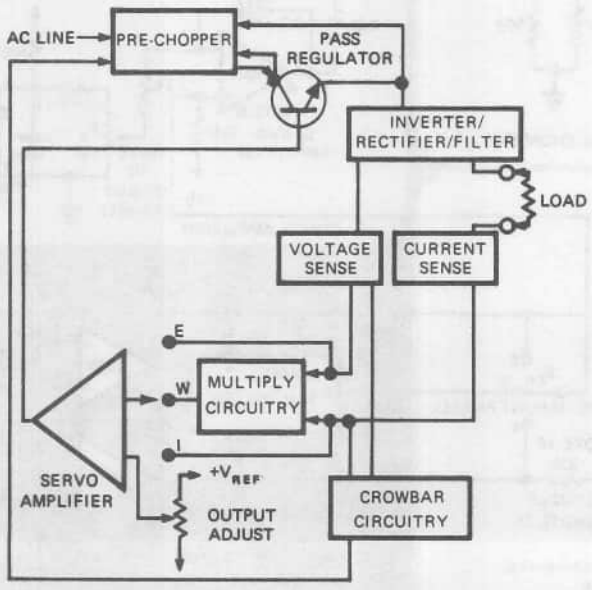

Fig. 1—Functional diagram of the 3-mode HV power supply.

Regulator + converter = amplifier

Both switching and series-pass regulation techniques are used (**Fig. 1**). The instrument functions by controlling the input power to a toroidal dc-to-dc inverter with a FET-input operational (servo) amplifier. One of the amplifier's inputs is referenced to a precision variable voltage. The other input is connected, through suitable circuitry, to the rectified and filtered output of the inverter.

Considered as a unit, the pass regulator and converter function as an amplifier within the servo amplifier's feedback loop. When feedback is taken from the "voltage sense" network, a constant-voltage output is produced. Taking it from the "current sense" network results in a constant current through the load. Lastly, when inputs from the voltage-sensing and current-sensing networks are multiplied by the multiplier circuitry, the load receives constant power.

The pre-chopper maintains a small fixed voltage across the pass regulator regardless of inverter output setting. It does this by synchronously chopping the 120-Hz peaks from a full-wave rectifier in a manner similar to a lamp dimmer. This limits the pass regulator dissipation to an acceptable level. Had it not been done, dissipation would have been excessive, especially at low-voltage output settings.

Crowbarring prevents overload by shutting down the supply when it senses either too much current flowing in the load or a load dropout.

A Cook's tour of the circuit

Details of the circuit will now be discussed with

the aid of a detailed schematic (**Fig. 2**). Looking at the SERVO AMPLIFIER section, reference stability results from using a 1N944B temperature-compensated zener diode (D_7) with its output scaled to 10.000V across the Kelvin-Varley potentiometer. The potentiometer's output biases the 1023 FET amplifier A_1, which functions as a precision servo amplifier. Its 20-pA bias current insures negligible loading error on the potentiometer. A_1's output drives the Q_6/Q_7 pair, a 2N2102 - 2N3442 Darlington pass regulator, via the 2N2102 pull-down transistor Q_5. Q_7's collector is supplied dc power from the output of the pre-chopper, which will be described later. Q_7's emitter drives the toroid transformer, T_1.

The wide dynamic range of the inverter is due to the 2N2528 transistors (Q_8, Q_9) that feature low saturation voltages, good beta linearity and reasonable speed. They permit the inverter to run at low output voltages with no resultant sacrifice in performance at high output potentials. Output of the transformer is rectified by a full-wave bridge employing two 1N5061's in each leg. The stacking

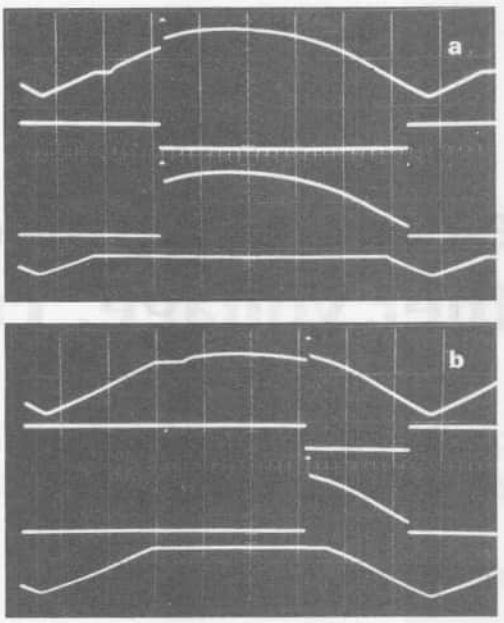

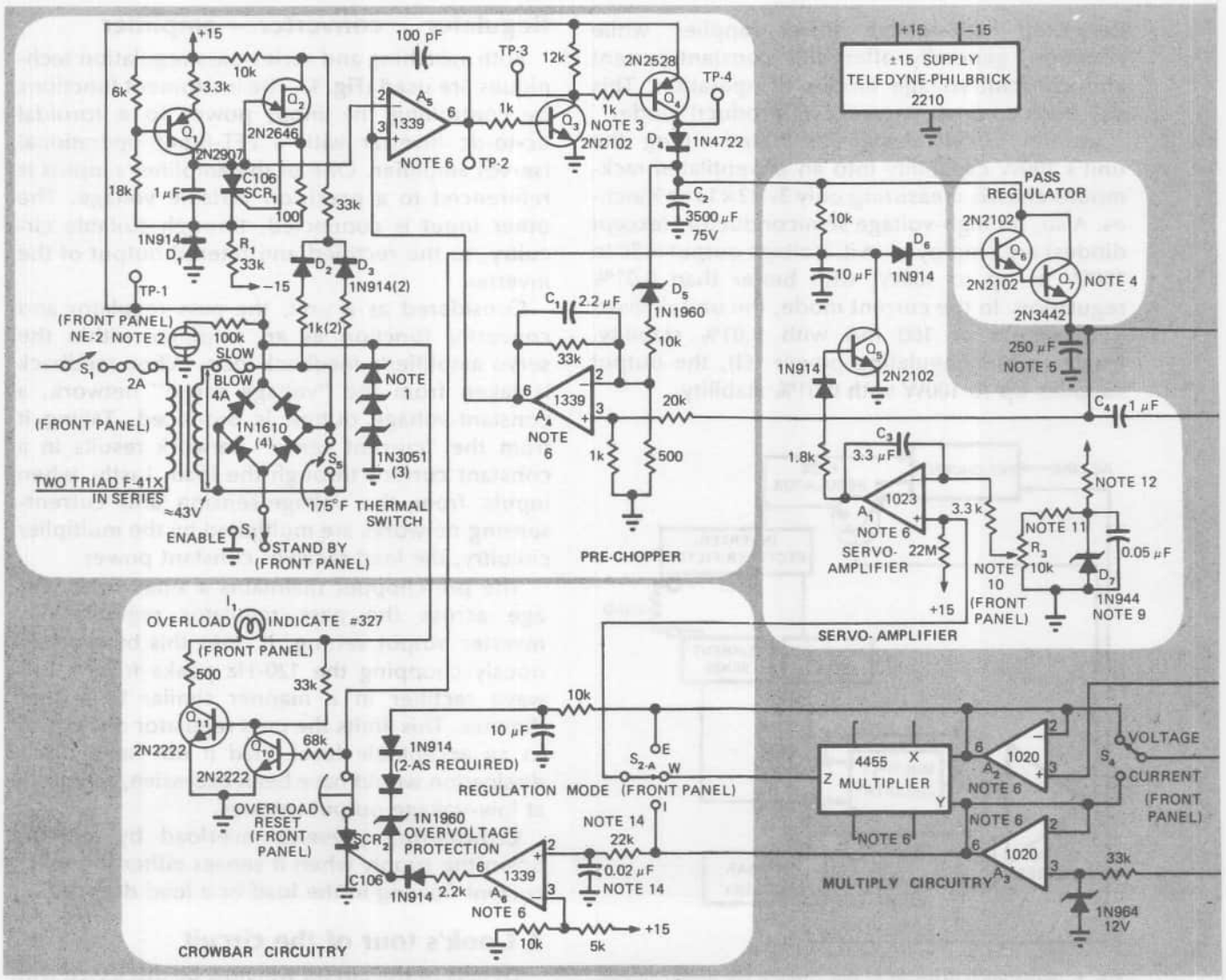

◀ **Fig. 3—Pre-chopper waveforms** at 4.2W output (**a**), and 42W output (**b**) (taken with a 15 kΩ load on the supply output). Scope traces shown are at 50V/div. and 1 msec/div. In each picture the top waveform, taken at TP_1, shows the 120-Hz output of the full-wave bridge. Note the spike created by flyback effect in the power transformer when the pre-chopper allows it to "let go." Spike amplitude would normally be about 150V, but the series string of three 30V zeners (1N3051) clips it to 90V. The second waveform, present at TP_2, is that at the output of pulse-width modulator A_5. The third waveform, taken at Q_3's collector (TP_3), shows how much of the 120-Hz waveform is not being utilized. At the bottom is the waveform present at TP_4. The 1N4722 diode (D_4) prevents Q_4 from becoming reverse biased when the dc voltage on C_2 is greater than that on Q_4's emitter.

allows use of diodes rated at only 800V. Filtering, provided by the 1-μF capacitor, is adequate for the square-wave output.

Higher is better

Voltage feedback is derived by a 99 to 1 division of the filtered output. The current-feedback signal, on the other hand, is split into four separate switch-selectable ranges. This promotes ease of setting and keeps the current-feedback signal at high levels—and therefore easy to work with. The "shorting-switch" selection scheme insures feedback even during the switching operation.

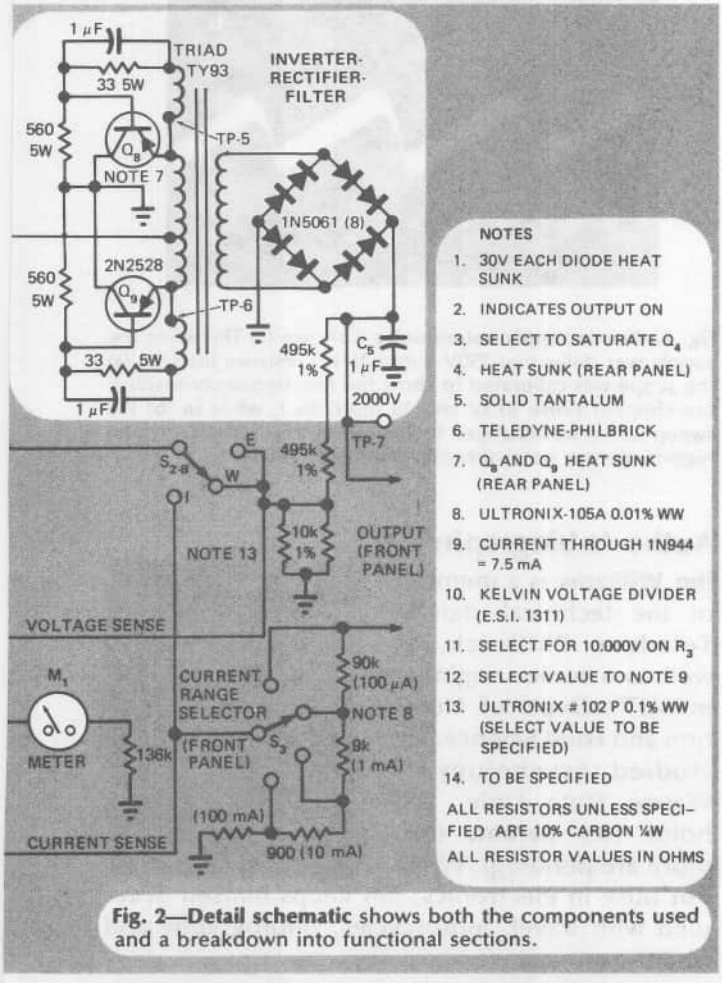

Fig. 2—Detail schematic shows both the components used and a breakdown into functional sections.

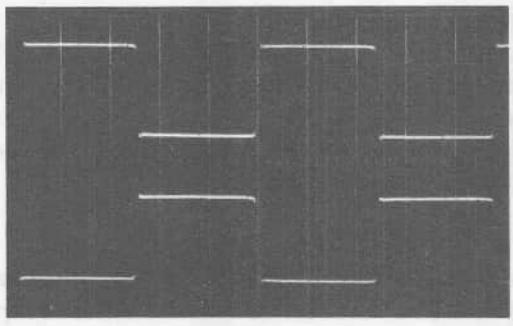

Fig. 4—Inverter waveforms taken at TP_5 and TP_6 (the emitters of Q_8 and Q_9). Scope was set at 50V/div. and 50 μsec/div. Despite the high currents, the combination of suitable transistors and a well-designed transformer obviously yields clean waveforms containing a minimum of ringing or overshoot.

Unity-gain followers, A_2 and A_3, convert the current and voltage signals to the low impedance needed to drive the 4455 multiplier. The impedance transformation also allows easy monitoring of the respective signals by a voltmeter or a multiplexing data-acquisition system. Switchable meter M_1 provides a "ballpark" indication of the voltage or current at the load. A_1 and A_2 feed the multiplier, which provides the feedback signal for the power mode of operation. Regulation-mode switch S_2 selects which feedback signal (E, W or I) is sent to servo amplifier A_1, thereby determining the regulation mode of the instrument. R_2, a 22 MΩ resistor, prevents the servo loop from running wild during the transient condition that exists when the mode switch is operated.

As might be suspected, the servo loop is very prone to oscillation. C_3 and C_4 were included to insure loop stability, but slow it down as well. Loop response is about 75 msec (no load to full load), so transient response clearly is not this circuit's forte.

Pre-chopper keeps a constant drop

The pre-chopper is essentially a servo that keeps the drop across pass transistor Q_7 at a constant, low voltage, regardless of inverter demand conditions. This lowers dissipation and insures reliability. A_4 looks differentially across the Q_7 pass element. A_4's negative input is biased through the 10V zener, D_5, and its output voltage is compared to a 120-Hz line-synchronized ramp by amplifier, A_5. This op amp functions as a pulse-width modulator, and drives the Q_3, Q_4 combination that delivers phase-controlled power to C_2 and the collector of Q_7. Diode D_4 insures that Q_4 will not be reverse biased when

the 120-Hz signal is below the dc across the capacitor.

Since A_4's negative input is routed through the 10V zener, Q_7's emitter will always be 10V below the collector, despite the required inverter input power. This value, 10V, is low enough to keep dissipation down, yet high enough to insure good regulation characteristics.

Loop inside a loop

The battle-scarred veterans among those reading this article will realize the unpleasant surprises that can be encountered by running a servo loop within a servo loop. Here, these embarassments have been avoided by giving the pre-chopper slower response time than the main servo loop. C_1, the 2.2-μF capacitor across A_4, satisfies this condition.

The 120-Hz reference ramp arrives at A_5 via the 2N2646 unijunction transistor Q_2. Q_2, in turn, is driven by Q_1, the 2N2907 current source. SCR_1, D_1 and R_1—which is connected to −15V—assure a true zero-volt reset for the ramp. D_2 and D_3 provide the synchronizing signal, which cannot be taken from the bridge rectifier because the bridge output waveform is heavily influenced by the phase angle at which Q_8 and Q_9 fire.

Carry a crowbar for protection

A 1339 amplifier (A_6) helps protect the supply from excessive output current. The amplifier looks at the current-feedback signal and will swing its output to positive saturation if that signal exceeds 10V. In turn, SCR_2 is triggered and grounds the inverter drive signal, resulting in a supply shut-down. The "overload indicate" light (I_1) will come on to alert the operator to the situation. To reset, the "overload reset" button is pressed, commutating the SCR and enabling the inverter to again receive bias. D_6, a 1N914 in the base line of Q_6, assures a clean turn-off when the SCR comes on.

Overvoltage protection is provided by D_{10}, D_9 and D_8, the 10V zener diode and the 1N914's, which are connected between the "voltage" output signal and SCR_2. This arrangement prevents the supply from running away in the event of a load dropout when in the "current" or "power" regulation modes.

Preventing catastrophes

Physical layout of the supply is not critical except for the point grounding considerations common to any precision circuit. The inverter ground return (from Q_8 and Q_9 collectors) contains fast, high-current spikes and should be returned directly to supply common. Returns from the reference diode, its potentiometer and the amplifiers are also critical. They also should be connected directly to the supply ground.

Particularly insidious failures can result from a malfunction in the pre-chopper circuitry. As an example, assume an emitter-to-collector short in Q_4. All of the 120-Hz waveform will then be supplied to the 3500-μF integrating capacitor, and the dc potential at Q_7's collector will rise to maximum voltage. The power supply will, however, continue to function in an apparently normal fashion—that is, until Q_7 achieves its molten state. This most unwelcome state of affairs is prevented by the 175°F thermal switch (S_5) mounted next to Q_7. Closing of the switch will blow the fuse at the transformer primary. □

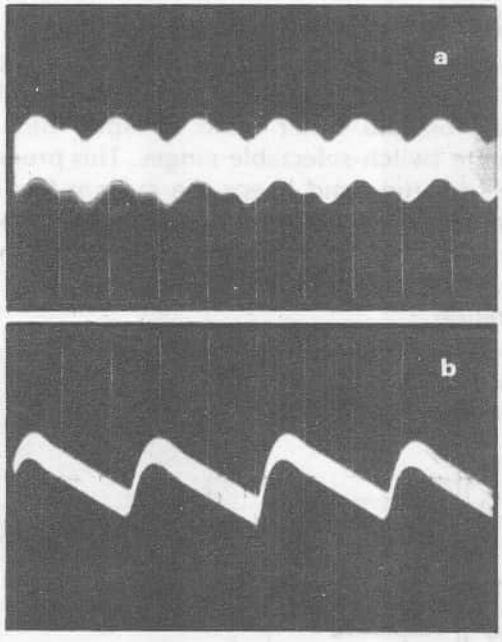

Fig. 5—Power-supply output noise is shown (at TP_7) when the supply was delivering 750V into a 15 kΩ resistive load. In (**a**) the scope was calibrated to show the low-frequency residual pre-chopper noise (0.5V and 10 msec/div.), while in (**b**) the sweep speed was changed to 20 μsec/div. to clearly show the high-frequency noise (inverter frequency related).

Author's biography

Jim Williams is a member of the technical staff at Teledyne Philbrick, as well as a senior engineer in MIT's Dept. of Nutrition and Food Science. He studied psychology at Wayne State Univ. and holds two patents (two more are pending). When not busy in electronics, Jim keeps himself occupied with travel, motorcycles, photography and sculpture.

High-powered booster circuits enhance op-amp output

Although modern IC op amps simplify linear-circuit design, their output power is limited. Well-designed booster stages can solve this problem without sacrificing amplifier performance.

Jim Williams, National Semiconductor Corp

You can use the circuits presented here to substantially increase an IC amplifier's voltage and/or current output drive. Although the circuits were developed to solve specific problems, they are general enough to satisfy a variety of applications.

A booster is a gain stage with its own inherent ac characteristics. Therefore, in applying these circuits, you can't ignore such parameters as phase shift, oscillation and frequency response if you want the booster and amplifier to work well together. Designing booster stages that maintain good dynamic performance is a difficult challenge, especially because the booster circuitry changes with the application.

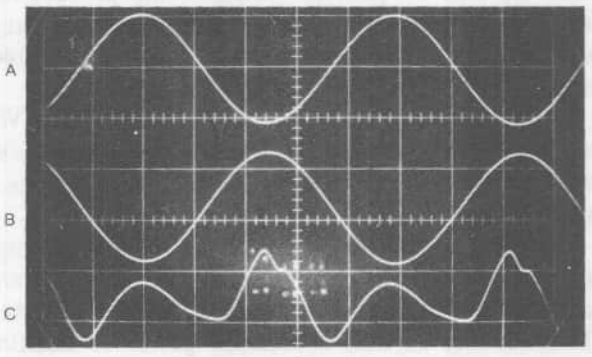

TRACE	VERTICAL
A	10V/DIV
B	10V/DIV

(b)

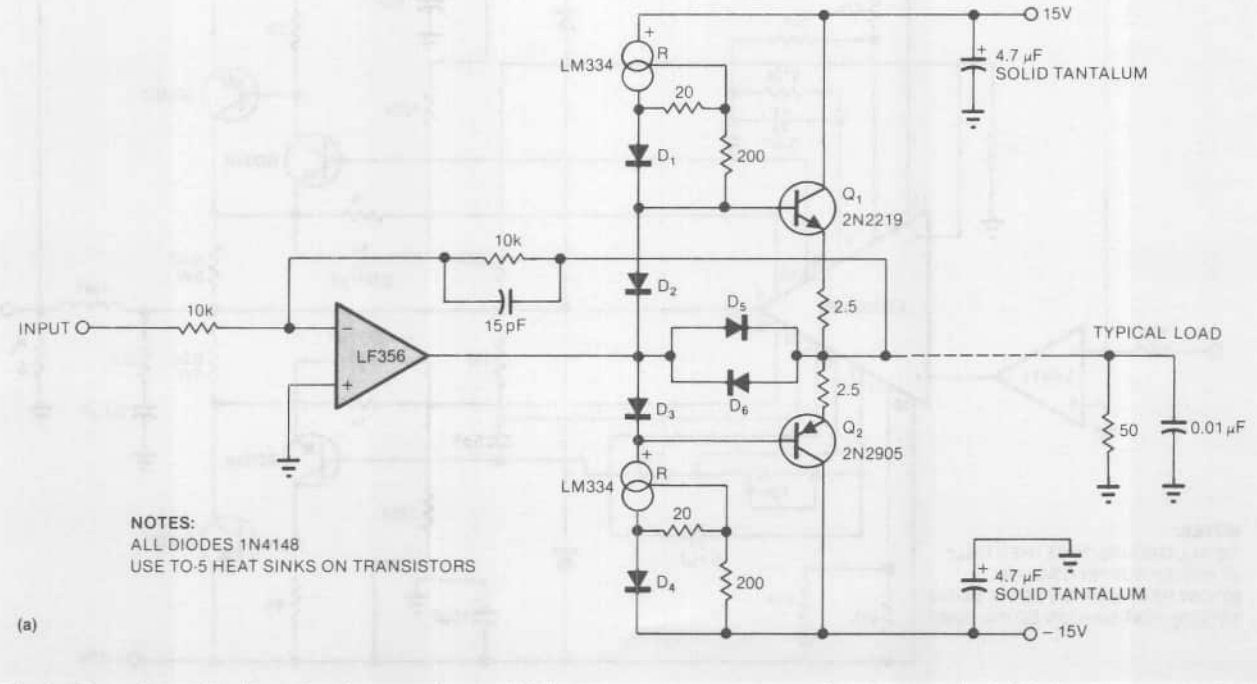

(a)

Fig 1—Complete with short-circuit protection *and fully temperature compensated, a booster circuit* ***(a)*** *develops a ±200-mA output current. Even with a heavy load (50Ω in parallel with 10,000 pF), response is quick and clean* ***(b)****; overall circuit distortion measures less than 0.05% (trace C).*

Feedforward design technique increases current-booster speed

Start with some current-gain stages

The circuit shown in **Fig 1a** boosts the output-current level of an LF356 (a unity-gain inverting amplifier) to ±200 mA while maintaining a full ±12V output swing. In it, LM334 current sources, set for a 3.5-mA output by the 20Ω resistors, bias the complementary emitter followers, which provide drive and sink functions for the LF356 output. The RC feedback network creates a gain roll-off above 2 MHz.

The circuit's diodes satisfy several needs. D_1 and D_4, along with their associated 200Ω resistors, temperature-compensate the current sources. D_2 and D_3 eliminate crossover distortion in the output stage, while D_5 and D_6 provide short-circuit protection by shunting the drive to Q_1 and Q_2 when the output current exceeds 275 mA. For best results, thermally couple D_2 and D_3 to the transistors' heat sinks.

Circuit response (**Fig 1b**) is quick and clean. When you drive a 20V p-p sine wave into a heavy load (50Ω in parallel with 0.01 μF), output distortion measures less than 0.05%.

The circuit depicted in **Fig 2** accommodates higher current applications; it drives 3A (±25V pk) into an 8Ω load. As in **Fig 1a**'s design, the booster network—LM391-80 driver and associated power transistors—lies within the op amp's feedback loop. Booster-network bandwidth, set by the 5-pF capacitor at pin 3 of the LM391-80, is greater than 250 kHz.

Feedback resistors set the loop gain at 10, with the 100-pF capacitor introducing a roll-off at 100 kHz to ensure stability for the amplifier/booster combination. The output RC network, along with the 4-μH inductor, prevents circuit oscillations. You set the output-stage quiescent current at 25 mA by monitoring the voltage drop across the 0.22Ω resistors while adjusting the 10-kΩ pot at pins 6 and 7 of the 391.

How to increase speed

These first two circuit designs stress stability at the expense of speed. For example, **Fig 1a**'s booster network has a much wider bandwidth than the LF356 op amp. Unfortunately, the network's presence within the amplifier's feedback loop means that the LF356 dictates overall circuit response time.

However, there are ways to accentuate speed. In **Fig 3a**, for example, a feedforward network lets ac signals bypass the LM308 op amp and directly drive a very-high-bandwidth 200-mA current-boost stage. And because the LM308 provides the signal path for dc and low frequencies, the circuit achieves fast response with no sacrifice in overall dc stability.

Current sources Q_1 and Q_2 bias the complementary emitter followers (Q_3/Q_6 and Q_4/Q_7). Because this output stage introduces signal inversion, circuit output feeds back to the LM308's noninverting input. The 10-kΩ/15-

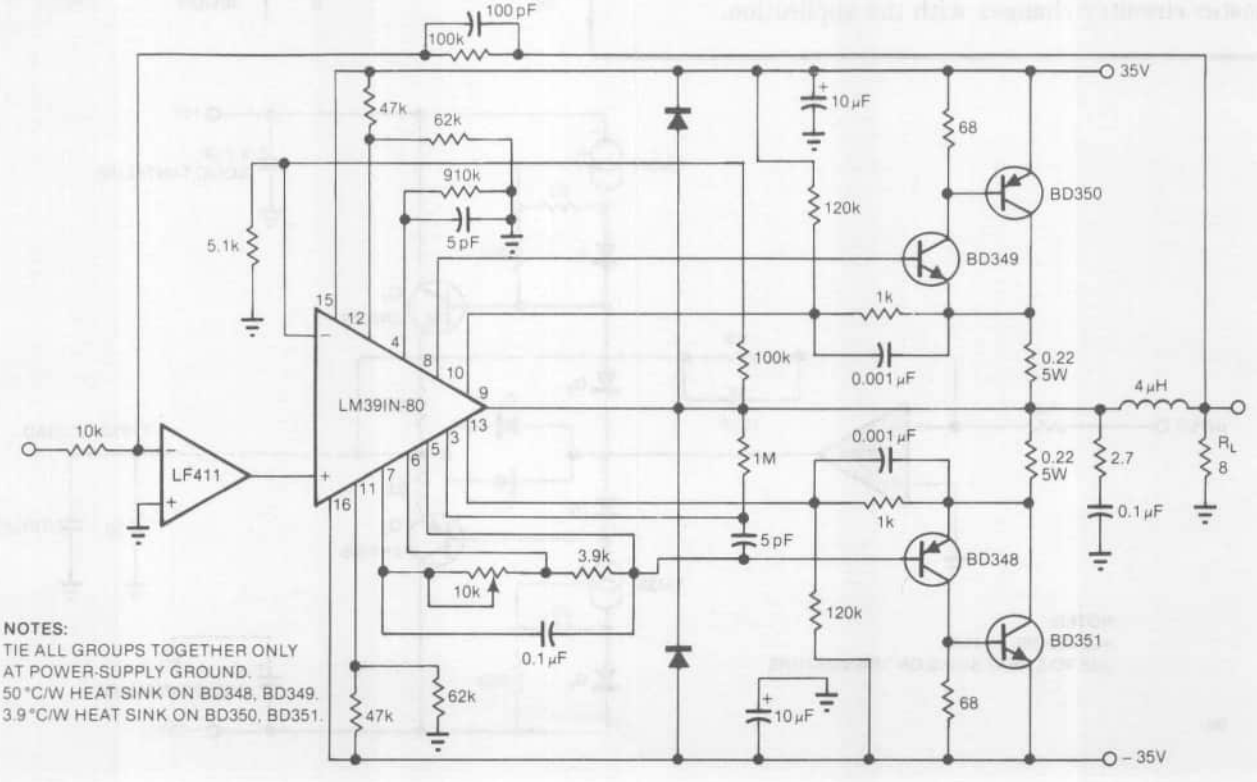

Fig 2—Designed to satisfy high-current needs, *this booster network drives 3A into an 8Ω load. The output RCL network prevents circuit oscillations, and the 10-kΩ pot sets output-stage quiescent current.*

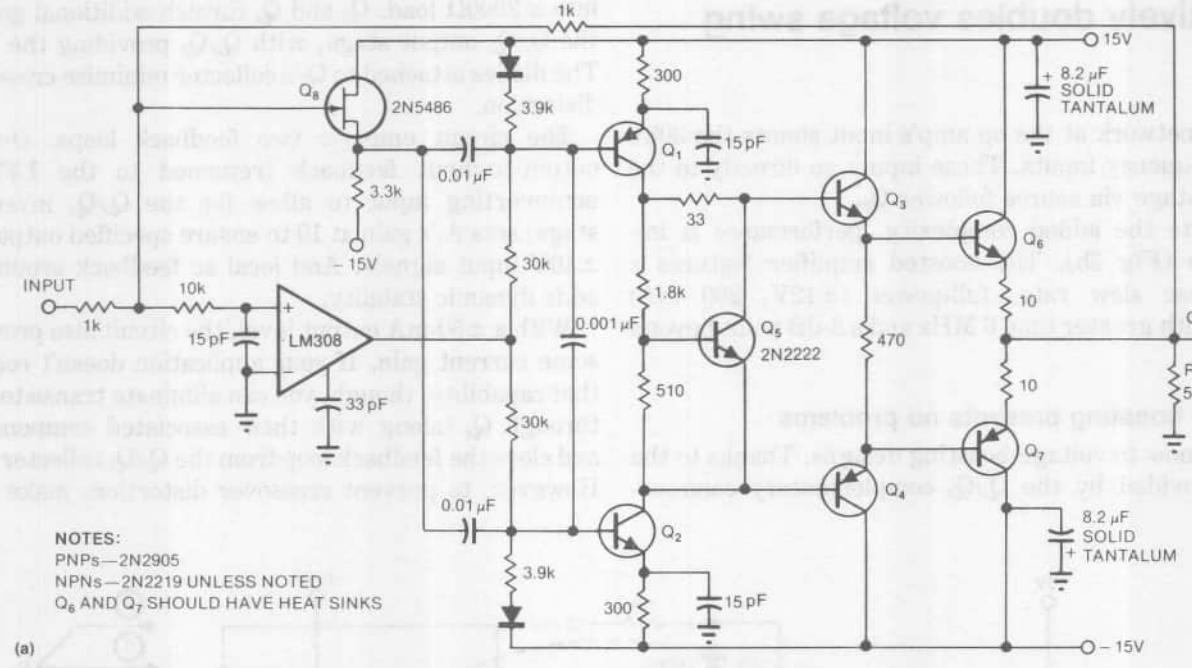

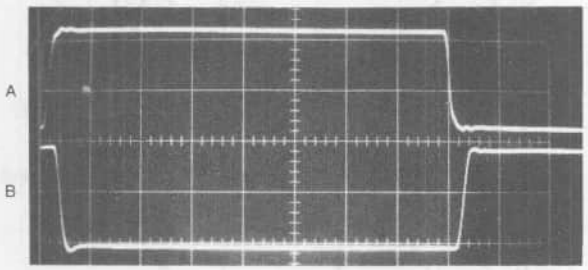

TRACE	VERTICAL	HORIZONTAL
A	5V/DIV	100 nSEC/DIV
B	5V/DIV	100 nSEC/DIV

(b)

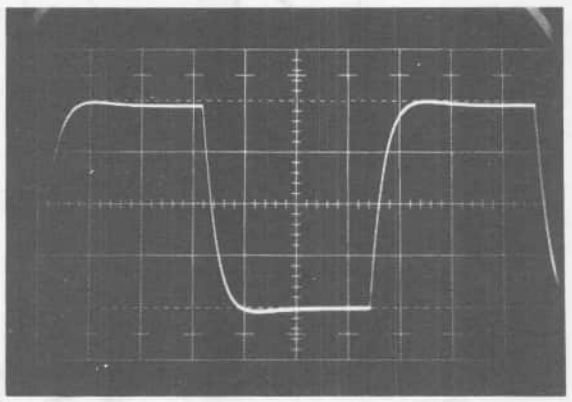

VERTICAL HORIZONTAL
50V/DIV 5 μSEC/DIV

(b)

Fig 3—To increase speed, *a booster circuit* ***(a)*** *employs a feedforward network that allows ac signals to bypass the op amp and directly drive the high-bandwidth current-boost stage. Driving a 10V pulse into 50Ω, the booster evidences clean settling characteristics* ***(b);*** *rise and fall times measure less than 15 nsec.*

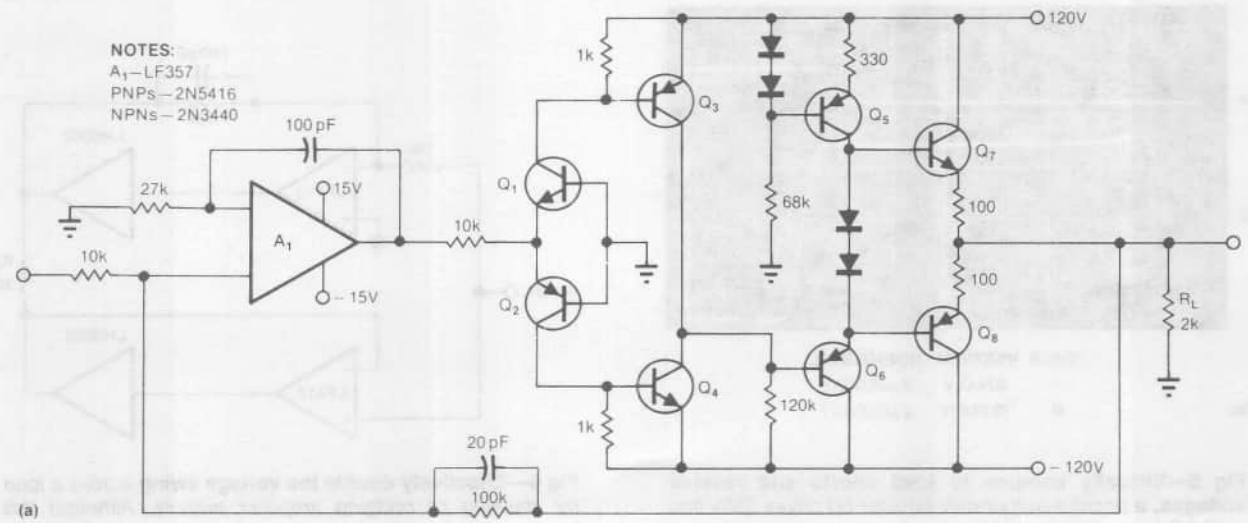

Fig 4—If you need extra voltage, *a booster design* ***(a)*** *develops ±100V across a 2-kΩ load. And it readily accommodates 30-kHz signals* ***(b).***

Stacking amplifier outputs effectively doubles voltage swing

pF RC network at the op amp's input shunts the 308's high-frequency inputs. These inputs go directly to the output stage via source follower Q_8.

Despite the added complexity, performance is impressive (**Fig 3b**). The boosted amplifier features a 750V/μsec slew rate, full-power (±12V, 200 mA) bandwidth greater than 6 MHz and a 3-dB point beyond 11 MHz.

Voltage boosting presents no problems

Turn now to voltage-boosting designs. Thanks to the gain provided by the Q_1/Q_2 complementary common-base stage, the circuit shown in **Fig 4a** drives ±100V into a 2000Ω load. Q_3 and Q_4 furnish additional gain to the Q_7/Q_8 output stage, with Q_5/Q_6 providing the bias. The diodes attached to Q_5's collector minimize crossover distortion.

The circuit employs two feedback loops. Overall output-to-input feedback (returned to the LF357's noninverting input to allow for the Q_3/Q_4 inverting stage) sets A_1's gain at 10 to ensure specified output for ±10V input signals. And local ac feedback around A_1 adds dynamic stability.

With a ±50-mA output level, the circuit also provides some current gain. If your application doesn't require that capability, though, you can eliminate transistors Q_5 through Q_8 (along with their associated components) and close the feedback loop from the Q_3/Q_4 collector line. However, to prevent crossover distortion, make sure

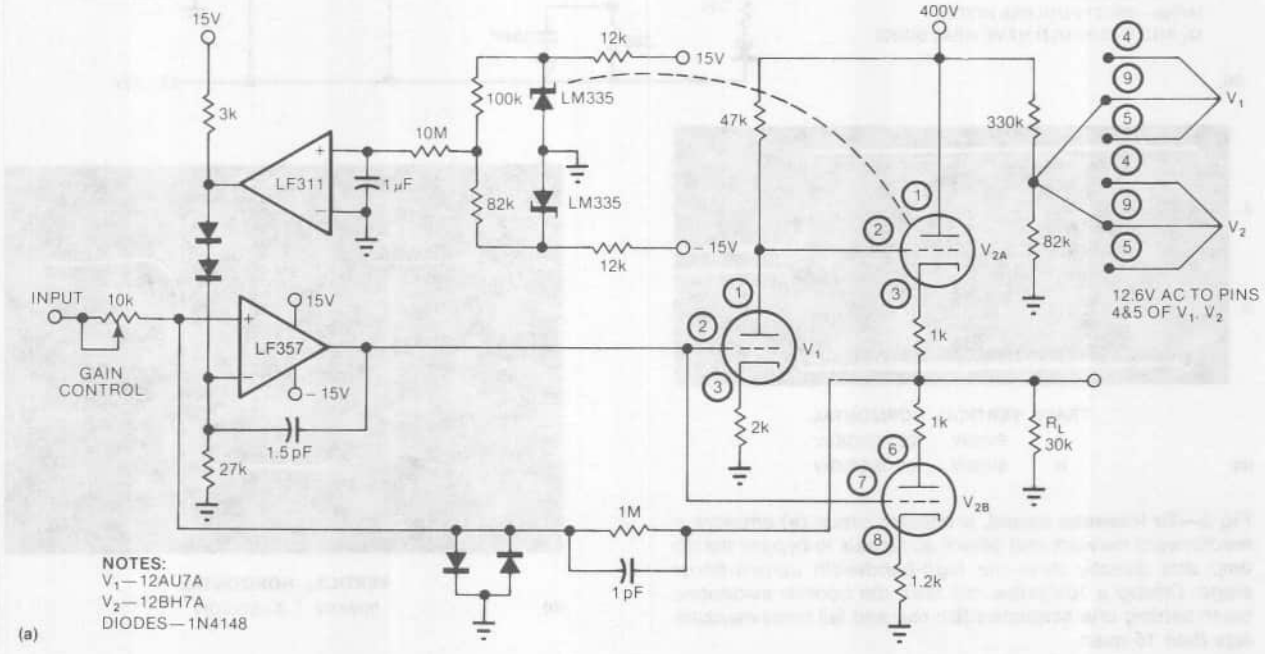

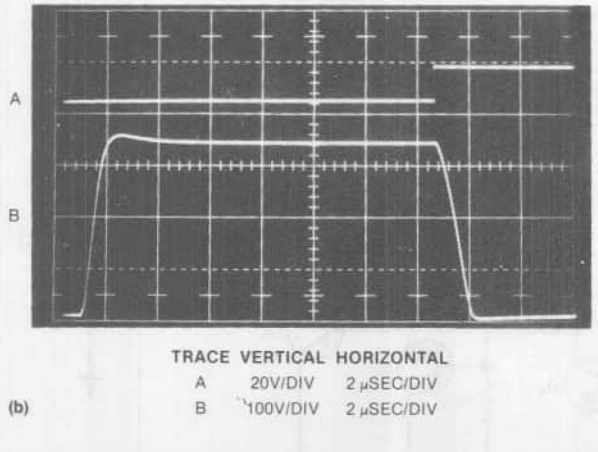

Fig 5—Virtually immune to load shorts and reverse voltages, *a positive-output-only booster* ***(a)*** *drives 350V into a 30-kΩ load. With a 15V input pulse, the output rises in 1 μsec and settles in less than 5 μsec* ***(b).*** *The falling edge slews just as rapidly and settles within 4 μsec.*

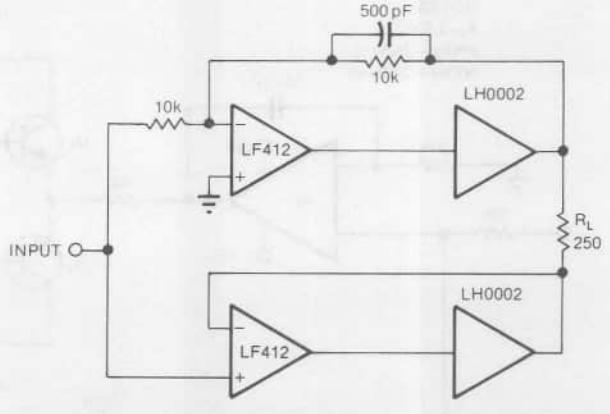

Fig 6—Effectively double the voltage swing *across a load by stacking or bridging amplifier outputs. Although this booster-circuit design is simple and requires no high-voltage supplies, you do have to float the load with respect to ground.*

that resistive output loading doesn't exceed 1 MΩ.

Fig 4b shows the boosted amplifier driving a ±100V square wave into a 200Ω load at 30 kHz. A second high-voltage booster circuit **(Fig 5a)** drives 350V into a 30-kΩ load and is virtually immune to load shorts and reverse voltages. And although the circuit has a 350V limit, tubes with higher plate-voltage ratings can extend the output capacity to several kilovolts.

In **Fig 5a,** the tubes are arranged in a common-cathode (V_{2B}), loaded-cathode-follower (V_{2A}) output configuration driven from a common-cathode (V_1) gain stage. Booster output feeds back to the LF357's noninverting input, with the 1-pF capacitor rolling off loop gain at 1 MHz. Local feedback stabilizes the LF357. The diodes at the summing junction protect the amplifier against high voltages during circuit start-up and slew-rate limiting. **Fig 5b** shows the booster's response at a gain of approximately 25.

In general, tubes are much more tolerant of load shorts and reverse voltages than transistors and are much easier to protect. In this circuit, one of the two LM335 temperature sensors is in contact with V_2, and its output gets compared with that of the second LM335, which monitors ambient temperature.

Under normal operating conditions, V_2 runs about 45°C above ambient temperature, generating a −100-mV signal at the LF311's noninverting input and forcing its output low. When a load fault occurs, V_2's plate dissipation increases causing its associated sensor's output to rise. This action in turn forces the LF311 output high, drives the LF357 output low and shuts down the output stage. V_2's thermal time constant, along with the 10-MΩ/1-μF delay network in the LF311's input line, provides adequate hysteresis.

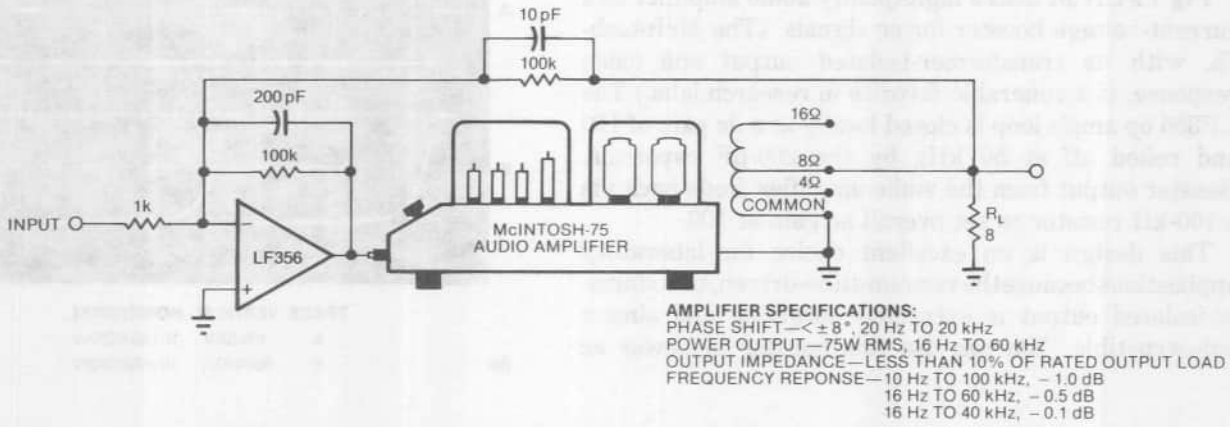

Fig 7—Voltage and current boosting are a snap *when you use a high-quality audio amplifier. For loads in the 4 to 16Ω range, this circuit produces 75W.*

BOOSTER-CIRCUIT PERFORMANCE

FIGURE	VOLTAGE GAIN	CURRENT GAIN	BANDWIDTH	COMMENTS
1	NO	YES (200-mA OUTPUT)	DEPENDS ON OP AMP: 1 MHz TYP.	FULL ± OUTPUT SWING. STABLE INTO 50Ω/10,000-pF LOAD. INVERTING AND NONINVERTING OPERATION. SIMPLE.
2	YES (± 30V OUTPUT)	YES (3A OUTPUT)	50 kHz	FULL ± OUTPUT SWING. ALLOWS INVERTING OR NONINVERTING OPERATION.
3	NO	YES (200-mA OUTPUT)	FULL OUTPUT TO 6 MHz, − 3-dB POINT AT 11 MHz.	ULTRAFAST, 750V/μSEC. FULL BIPOLAR OUTPUT. INVERTING OPERATION ONLY.
4	YES (100V OUTPUT)	YES (50-mA OUTPUT)	50 kHz	FULL ± OUTPUT SWING. ALLOWS INVERTING OR NONINVERTING OPERATION. CAN BE SIMPLIFIED TO DRIVE CRT DEFLECTION PLATE.
5	YES (350V OUTPUT)	NO	500 kHz	OUTPUT VERY RUGGED. GOOD SPEED. POSITIVE OUTPUTS ONLY.
6	YES (24V OUTPUT)	NO	DEPENDS ON OP AMP	REQUIRES THAT THE LOAD FLOAT ABOVE GROUND.
7	YES (70V OUTPUT)	YES (3A OUTPUT)	100 kHz	OUTPUT EXTREMELY RUGGED. WELL SUITED FOR DRIVING DIFFICULT LOADS IN LAB SETUPS. FULL BIPOLAR OUTPUT. AC ONLY.
8	YES (1000V OUTPUT)	YES (300-mA OUTPUT)	50 Hz	HIGH VOLTAGE AT HIGH CURRENT. SWITCHED-MODE OPERATION ALLOWS USE OF ± 15V SUPPLIES. GOOD EFFICIENCY. LIMITED BANDWIDTH WITH ASYMETRICAL SLEWING. POSITIVE OUTPUTS ONLY.

Designs boost current and voltage simultaneously

Multifunction boosting's also possible

Three additional circuit designs all provide combined current- and voltage-output boosting. **Fig 6,** for example, depicts a simple way to effectively double the voltage swing across a load by stacking or bridging amplifier outputs. Each LF412 output feeds an LH0002 amplifier to provide current-drive capability. Because only one of the LF412s inverts, though, the combination produces 24V across the 250Ω load (±12V swings from each leg).

The circuit is simple and requires no high-voltage supplies. However, you must float the load with respect to ground.

Fig 7's circuit uses a high-quality audio amplifier as a current-voltage booster for ac signals. (The McIntosh-75, with its transformer-isolated output and clean response, is a venerable favorite in research labs.) The LF356 op amp's loop is closed locally at a dc gain of 100 and rolled off at 50 kHz by the 200-pF capacitor. Booster output from the audio amplifier feeds back via a 100-kΩ resistor to set overall ac gain at 100.

This design is an excellent choice for laboratory applications because the vacuum-tube-driven, transformer-isolated output is extremely forgiving and almost indestructible. You can use this booster to power ac variable-frequency supplies and shaker-table, motor and gyro drives, as well as other difficult-to-handle inductive and active loads. Power output into 4 to 16Ω loads equals 75W; you can drive 1Ω loads at reduced power output levels.

In **Fig 8a,** the LF411 op amp controls as much as 300W for positive outputs ranging to 1000V. The booster achieves this performance without sacrificing efficiency because it operates in switching mode. Additionally, it requires only ±15V supplies to develop its high-potential outputs.

An integral dc/dc converter directly generates the required high output voltage. The LM3524 regulator chip pulse-width-modulates transistors Q_1 through Q_4 to provide switched 20-kHz drive to the stepup transform-

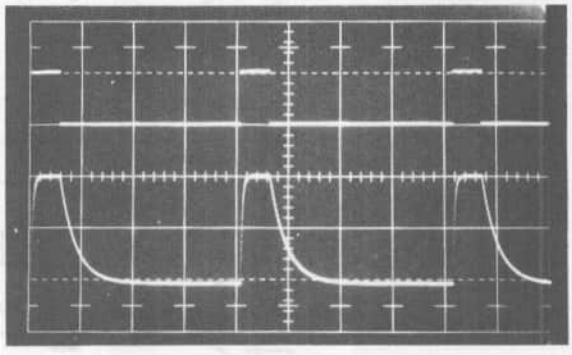

(b)

TRACE	VERTICAL	HORIZONTAL
A	10V/DIV	10 mSEC/DIV
B	500V/DIV	10 mSEC/DIV

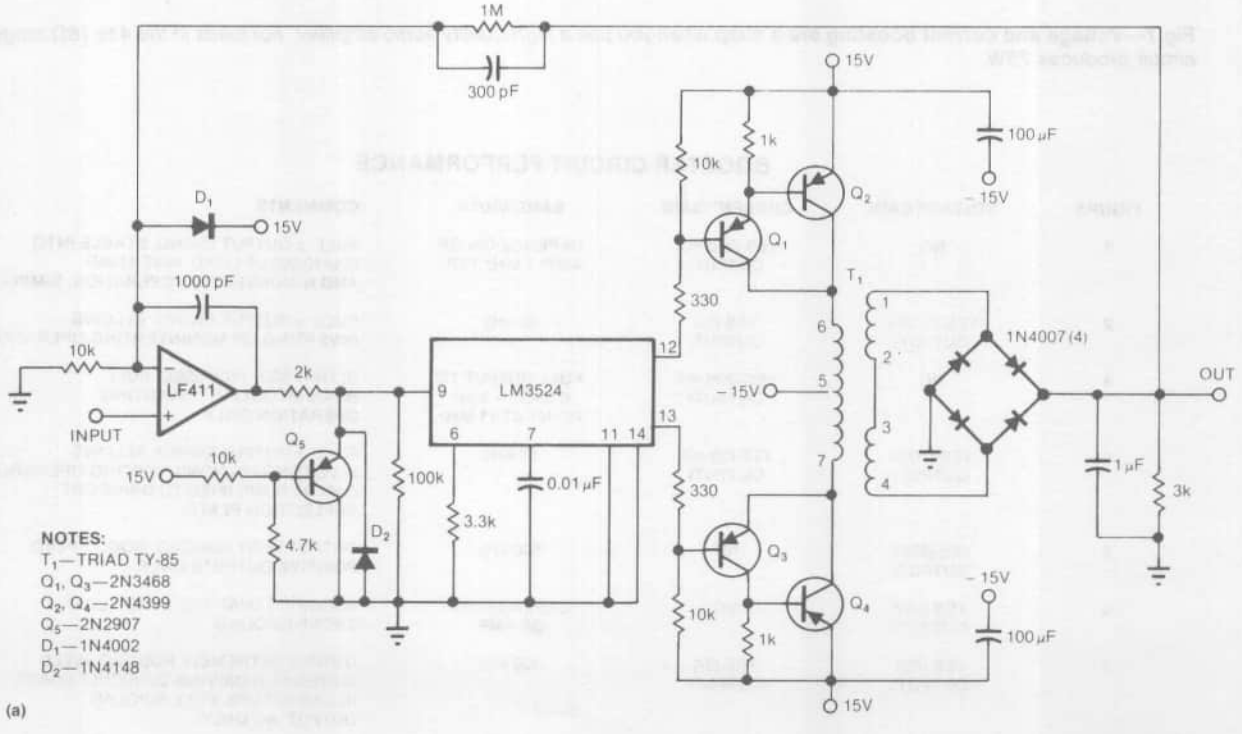

(a)

Fig 8—Operating in switching mode, *a high-power booster design* ***(a)*** *features 300W (1000V/300 mA) output capability. Performance is impressive* ***(b):*** *Output rise time equals 1 msec, while fall time measures about 10 msec (due to capacitor discharge time). Slew-rate limiting comes into play during output-pulse rise time—toroid switching action is barely visible on the output pulse's leading edge.* ***(Caution: Output levels are lethal!)***

Watch out for lethal voltage levels

er. The transformer output, rectified and filtered, feeds back to the LF411, which controls the LM3524 input. Therefore, op-amp feedback action has the same stabilizing effect found in the previous circuit designs.

Two protection networks are provided. The Q_5/diode combination clamps the LF411 output to prevent LM3524 damage during circuit start-up. And the diode at the LF411's summing junction prevents high-voltage transients coupling through the feedback capacitor from destroying the amplifier.

For the component values shown, the circuit exhibits a full-power sine-wave output frequency of 55 Hz. Resistor feedback sets amplifier gain at 100, so a 10V input produces a 1000V output. Although the 20-kHz switching rate sets the upper limit on loop information-transmission speed, the 1-μF capacitor at the output restricts circuit bandwidth. **Fig 8b** shows the LF411's boosted response with a 10V pulse applied to the circuit input.

A word of caution: Approach the construction, testing and applicaton of this circuit *with extreme care*. The output potentials developed are far above lethal levels.

As a design aid, the **table** summarizes pertinent points discussed in this article. Using it can greatly simplify the task of matching a booster circuit to your application. EDN

References

1. Gussow, S, "Vacuum-tube amplifiers," Massachusetts Institute of Technology, private communication.
2. Dobkin, R C, "Feedforward amplifiers," National Semiconductor Corp, private communication.

Author's biography

Jim Williams, manager of National Semiconductor Corp's Linear Applications Group (Santa Clara, CA), has made a specialty of analog-circuit design and instrumentation development. Before joining National, he was a consultant with Arthur D Little Inc in analog systems and circuits. From 1968 to 1977, Jim directed the Instrumentation Development Lab at the Massachusetts Institute of Technology, where in addition to designing experimental biomedical instruments, he was active in course development and teaching. A former student of psychology at Wayne State University, he lists tennis, art and collecting antique scientific instruments as his leisure interests.

Low-cost, linear A/D conversion uses single-slope techniques

Improvements in components and circuit design have brought back the single-slope converter as a viable performer. Here's how it's done.

Jim Williams, Arthur D Little Inc

The increasing popularity of voltage-to-frequency (V/F) converters and digital voltmeters using single-slope A/D conversion highlights the return of this low-cost technique to the circuit board. Some early DVM's and data converters used single-slope conversion, but the advent of the dual-slope integrator, with its inherent error-cancellation characteristics, relegated single-slope techniques to a minor role.

Now, however, the single-slope converter is back. Its weaknesses remain the same, but improvements in components and circuit design have achieved significant performance benefits at low cost.

Basic design uses V/F technique

All single-slope converters are basically voltage- or current-to-time converters. A voltage-to-frequency scheme, shown in **Fig 1**, furnishes a model.

Amplifier A_1 integrates the input voltage until its output has the same absolute value as the reference voltage. At this point, A_2, acting as a comparator, trips and causes the one-shot to close the switch across the integrating capacitor. The length of time required to trip the comparator is directly proportional to the input voltage.

Fig 2 shows a more practical incarnation of the same concepts. Here, the comparator and one-shot have been replaced by a unijunction transistor, whose intrinsic standoff ratio and the 1N821 form a reference that determines the reset point of the 301A integrator. That device's output ramps negative until the UJT switches, producing a large imbalance at the integrator's inputs and thus driving the output positive at a high slew rate. Because of the UJT's negative resistance characteristic, the amplifier moves its output all the way to zero before the UJT reverts to its high-resistance state. The positive edge of the 301A output is differentiated by the 2.2k/500 pF network and then level-shifted by the transistor to provide a logic-compatible pulse.

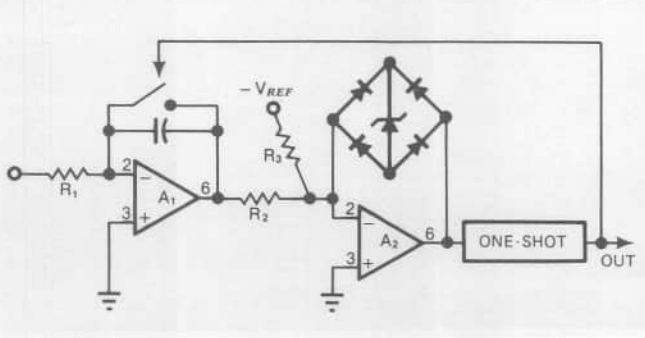

Fig 1—Simple voltage-to-frequency converter *demonstrates the basic single-slope conversion technique.*

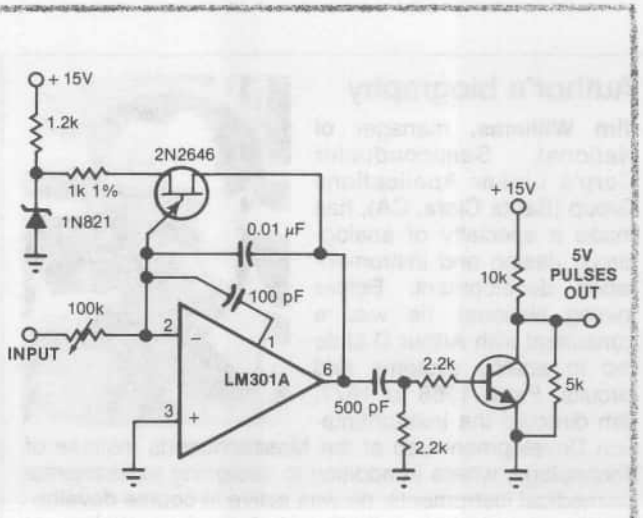

Fig 2—Single-slope conversion *can suffer from nonlinearity arising from the capacitor's reset time.*

Nonlinearity errors can be overcome, but at the cost of circuit simplicity

Nonlinearity comes from several sources

A 100 pF feed-forward capacitor between the inverting input (pin 2) and the balance/compensation input (pin 1) increases the slew rate of the 301A; however, capacitor reset requires 900 nsec. At 1 kHz, this figure represents about 0.1% dead time and produces a nonlinearity error. At 10 kHz FS, the nonlinearity arising from this effect would reach 10 Hz.

There are some other architectural weaknesses in this particular circuit, including the gain error that arises from any change in the integrating capacitor's value. Drifts in the UJT can also introduce errors. You can overcome any and all of these problems by trading off circuit simplicity.

Another way to do it

Charge dispensing, the method used in most industrial V/F converters, was first applied by R A Pease. **Fig 3** gives an example.

The output state of the amplifier switches C_1 between a reference voltage provided by the diode bridge and its inverting input. R_1 limits the current through the zener to its specified zero-TC value. Output pulse width is unimportant so long as it permits complete discharge and charge of the capacitor. The network formed by R_2 and C_2 reinforces the direction of the output's movement. Any negative-going output is followed by a positive edge after a time governed by the R_2C_2 time constant.

The actual integration capacitor in the circuit, C_3, never charges beyond 10 to 15 mV because it is constantly being reset by charge dispensed from switching C_1. Whenever the amplifier's output goes negative, C_1 dumps a quantity of charge into C_3, forcing it to a lower potential. A negative-going output causes the transfer of a short pulse through C_3 to the noninverting input. When this negative pulse decays out and the noninverting input is at a higher potential than the inverting input, C_1 can receive a charge and the cycle repeats. The diodes in C_1's path compensate for the diodes in the bridge.

Preventing lock-up

The circuit must deal with several lock-up conditions; any condition that allows C_3 to charge beyond 10 to 20 mV causes the amplifier to go to the negative rail and stay there. The 2N2907A transistor prevents such an occurrence by pulling the inverting input toward −15V. The RC network in the base circuit (33k and 10 μF) then determines at what point the transistor will come ON. When the circuit is running normally, the transistor is biased OFF and effectively remains out of the circuit. The 50k potentiometer trims

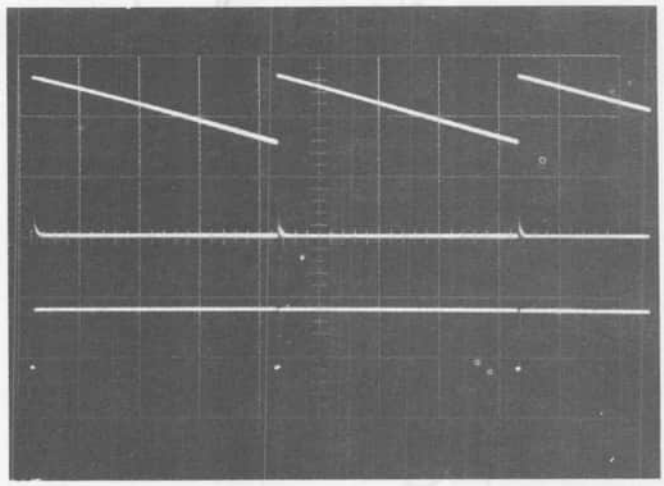

The V/F converter scheme *illustrated in* ***Fig 2*** *produces these waveforms. The top trace is the integrator's output, the middle one the diffentiated output and the bottom one the output pulse.*

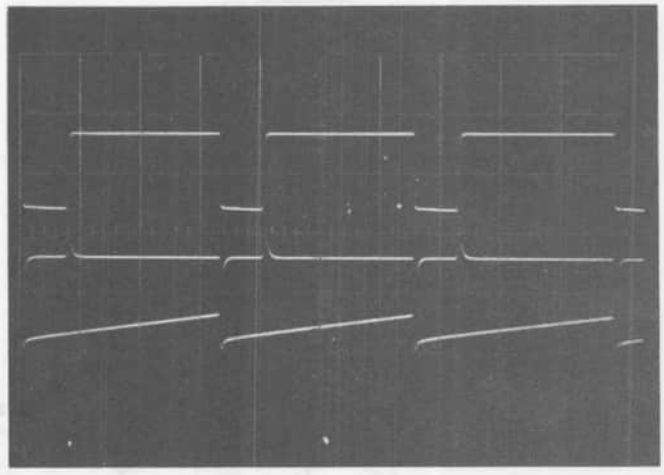

Improved linearity *results with the use of charge-dispensing techniques. The top trace shows the amplifier output for* ***Fig 3,*** *while the middle and bottom traces represent the noninverting and inverting inputs, respectively.*

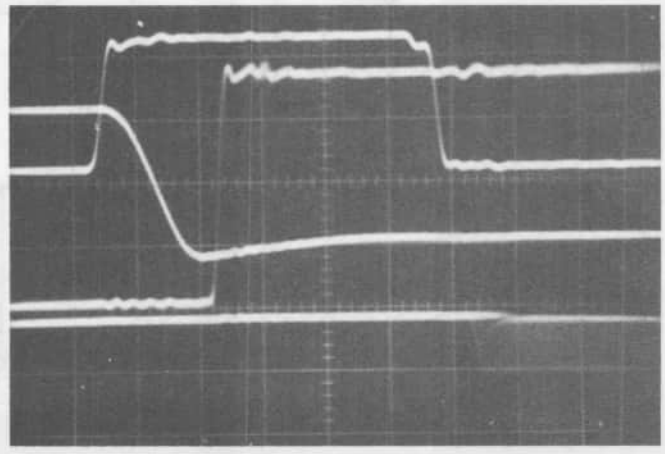

Blazing speed *is the strong point of the ultra-high-speed A/D converter shown in* ***Fig 4.*** *Horizontal scale here equals 30 nsec/div. The top trace shows the ramp resetting, the second trace is the convert command, the third is the comparator output and the bottom is data out.*

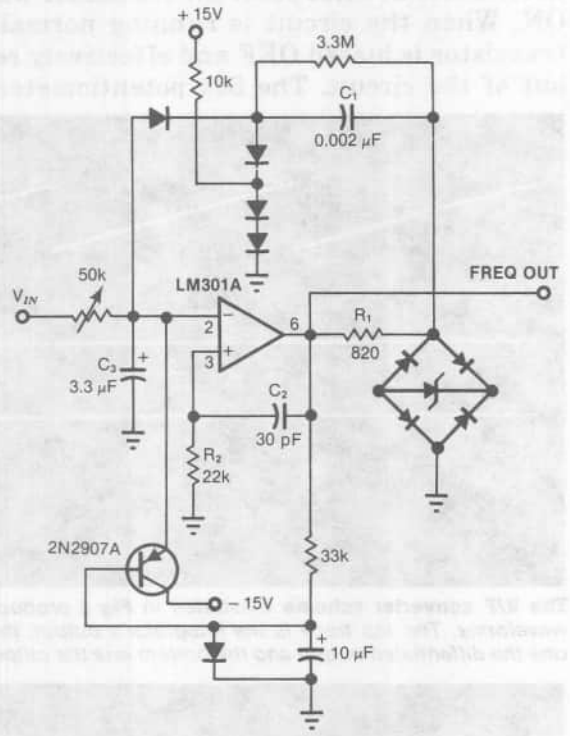

Fig 3—Charge-dispensing techniques *provide better linearity but require slightly more complex circuitry.*

the full-scale output, while the amplifier's offset limits zero frequency. This offset can be trimmed at the amplifier trim terminals or by summing a current of the appropriate polarity to the inverting input.

With proper selection of C_1, this circuit can deliver 0 to 10 kHz output with 0.01% linearity for a 0 to 10V input. Slight nonlinearity does still exist and manifests itself as a bow in the response over the total dynamic range. Normally this factor would limit linearity to about 0.05%, but the 3.3M resistor across the 0.002 μF capacitor corrects for the effect by altering the capacitor's charge characteristic. The slew rate and bandwidth limitations in the amplifier, and the difficulty of resetting the integrator, are the stumbling blocks for high-speed operation with single-slope converters. The solution is achievable, however, and in an economical (about $20 worth of parts) fashion.

Picking the players for performance

A low cost, high speed, single-slope 10-bit A/D converter appears in Fig 4. The discrete-component current source is the secret here. A 1N827 temperature-compensated zener diode, dual transistor and two film resistors constitute the reference-current source. One-half of the transistor provides temperature compensation

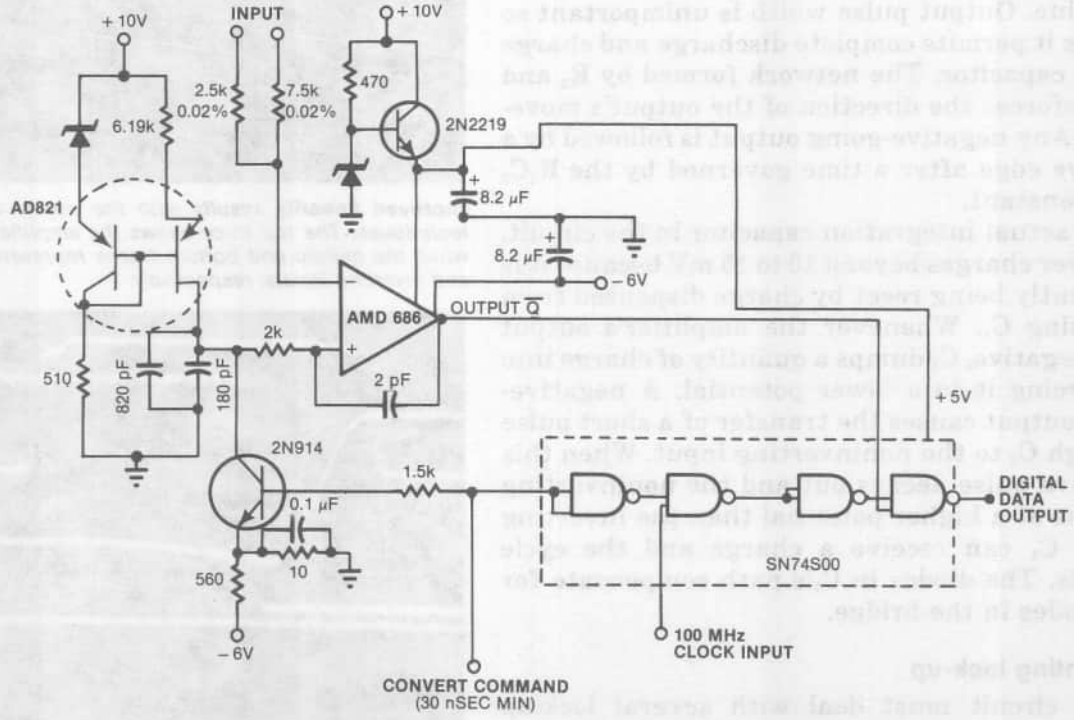

Fig 4—A discrete-component current source *allows high-speed operation with full 10-bit accuracy.*

Slew-rate and bandwidth limitations are the bars to high-speed operation

for the current-pump half, and the 510Ω film resistor ensures that the zener receives its zero-TC current—7.5 mA. The 6.19k resistor determines the magnitude of the current delivered by the current pump. Although the transistor halves run at different current densities (7.5 and 1 mA), the circuit achieves adequate temperature compensation.

The 1000 pF capacitor comprises polystyrene and silver-mica units in a ratio that cancels the temperature drifts of the individual units. In addition, the dielectrics selected have excellent aging characteristics and very low soakage (dielectric absorption). This parallel-capacitor approach has been used successfully by manufacturers, and the resulting temperature and time drifts are well documented. At least one manufacturer provides a dual-electric capacitor.

The current source provides a ground-referenced output that allows easy reset of the capacitor. Operational-amplifier-based current sources do not allow the fast integration (10-μsec) and reset (30-nsec) times without extravagant compensation techniques. Finally, note that the current source runs at all times—even when the capacitor is being reset to zero, thus eliminating errors caused by switching the current on and off.

Each time a pulse is applied to the convert-command input, the 2N914 resets the 1000 pF capacitor to 0V. This resetting action takes 30 nsec—the minimum acceptable convert-command pulse width. On the falling edge of the convert-command pulse, the capacitor begins to charge linearly; in precisely 10 μsec, it charges to 2.5V. Normally, the 2N914 would not be able to reset the capacitor to 0V because of its V_{CE} saturation voltage, but returning the 2N914 emitter to −0.1V compensates for this effect. The 560Ω resistor is selected from standard 1/4W values to give the right voltage at the 2N914's emitter to enable a reset within 1 mV (much less than 1 LSB) of ground.

The 10-μsec ramp is applied to the AMD 686 "+" input and compared with the unknown at its "−" input. For a 0 to 2.5V range, the input is applied to the 2.5k resistor. For a 0 to 10V input range, the 2.5k resistor is grounded and the input applied to the 7.5k resistor. Under both conditions, source impedance is the same. The 2.0k resistor at the "+" input provides balanced source impedance, and the 2N2219 emitter follower drops the +10V supply to +5V to run the comparator. The 686 outputs a pulse whose width is directly dependent on the value of the input; this pulse width is then used to gate a 100 MHz clock. The 74S00 gate achieves this function and also gates out the portion of the 686 output caused by the convert-command pulse. Thus, the 100 MHz clock-pulse bursts that appear at the output are proportional to the input. For a 0 to 10V input, 1024 pulses appear at full scale, 512 at 5V, etc. **EDN**

References

1. Pease, R A, "A New Ultra-Linear Voltage-to-Frequency Converter," 1973 NEREM Record, Vol 1, pg 167.
2. Pease, R A, US Patent 3,746,968, "Amplitude-to-Frequency Converter."
3. Williams, James, "Comparator IC Forms 10-Bit A/D Converter," *Electronics*, April 17, 1975, pg 146.
4. Component Research Corporation—Catalog JB.
5. Eckhardt, R A, "An Analysis of Errors in Single-Slope Integrators," SB Thesis, MIT, 1974.
6. "The Secret Life of Capacitors," ECD Corp, Cambridge, MA.
7. Williams, James, "An Experimental Microprocessor-Controlled 18-Bit Single-Slope A/D Converter with 1-ppm Linearity," MIT Department of Nutrition and Food Science, Cambridge, MA, 1975.
8. Williams, James, "Characterization, Measurement, and Compensation of Errors in Capacitors...a Compendium of Study, Hacks, Some Good Stuff and a Few Pearls," MIT Department of Nutrition and Food Science, Cambridge, MA, 1975.

Author's biography

Jim Williams is a consultant at Arthur D Little Inc, Cambridge, MA. Previously he was a senior engineer at MIT's Dept of Nutrition and Food Science, where he designed experimental biomedical instrumentation. Jim enjoys a variety of outside activities, including sculpture, travel, art, skiing, tennis, and collecting antique scientific instruments.

A few proven techniques ease sine-wave-generator design

Perhaps the most fundamental of all signals, sine waves present generating-circuit design tasks that are anything but fundamental. Next time you design such a circuit—whether it's for 1 Hz or 1 MHz—try one of the techniques described here.

Jim Williams, National Semiconductor Corp

Because sine-wave oscillators come in as many forms as the units that use them, choosing the best circuit type and implementation for an application can prove difficult. This article, however, helps simplify those choices and furnishes guidelines for controlling critical design specs such as frequency, amplitude and distortion.

You can apply many analog and digital techniques to achieve your sine-wave-generator design goals; each realization offers unique strengths and weaknesses. You'll probably find that one of those listed in the **table** will meet your requirements. The specific circuit

SINE-WAVE-GENERATION TECHNIQUES

TYPE	TYPICAL FREQUENCY RANGE	TYPICAL DISTORTION (%)	TYPICAL AMPLITUDE STABILITY (%)	COMMENTS
PHASE SHIFT	10 Hz-1 MHz	1-3	3 (TIGHTER WITH SERVO CONTROL)	SIMPLE, INEXPENSIVE TECHNIQUE. EASILY AMPLITUDE SERVO CONTROLLED. RESISTIVELY TUNABLE OVER 2:1 RANGE WITH LITTLE TROUBLE. GOOD CHOICE FOR COST-SENSITIVE, MODERATE-PERFORMANCE APPLICATIONS. QUICK STARTING AND SETTLING.
WEIN BRIDGE	1 Hz-1 MHz	0.01	1	EXTREMELY LOW DISTRORTION. EXCELLENT FOR HIGH-GRADE INSTRUMENTATION AND AUDIO APPLICATIONS. RELATIVELY DIFFICULT TO TUNE—REQUIRES DUAL VARIABLE RESISTOR WITH GOOD TRACKING. TAKES CONSIDERABLE TIME TO SETTLE AFTER A STEP CHANGE IN FREQUENCY OR AMPLITUDE.
LC NEGATIVE RESISTANCE	1 kHz-10 MHz	1-3	3	DIFFICULT TO TUNE OVER WIDE RANGES. HIGHER Q THAN RC TYPES. QUICK STARTING AND EASY TO OPERATE IN HIGH FREQUENCY RANGES.
TUNING FORK	60 Hz-3 kHz	0.25	0.1	FREQUENCY-STABLE OVER WIDE RANGES OF TEMPERATURE AND SUPPLY VOLTAGE. RELATIVELY UNAFFECTED BY SEVERE SHOCK OR VIBRATION. BASICALLY UNTUNABLE.
CRYSTAL	30 kHz-200 MHz	0.1	1	HIGHEST FREQUENCY STABILITY. ONLY SLIGHT (PPM) TUNING POSSIBLE. FRAGILE
TRIANGLE-DRIVEN BREAK-POINT SHAPER	<1 Hz-500 kHz	1-2	1	WIDE TUNING RANGE POSSIBLE WITH QUICK SETTLING TO NEW FREQUENCY OR AMPLITUDE.
TRIANGLE-DRIVEN LOGARITHMIC SHAPER	<1 Hz-500 kHz	0.3	0.25	WIDE TUNING RANGE WITH QUICK SETTLING TO NEW FREQUENCY OR AMPLITUDE. TRIANGLE AND SQUARE WAVE ALSO AVAILABLE. EXCELLENT CHOICE FOR GENERAL-PURPOSE REQUIREMENTS NEEDING FREQUENCY-SWEEP CAPABILITY WITH LOW-DISTORTION OUTPUT.
DAC-DRIVEN LOGARITHMIC SHAPER	<1 Hz-500 kHz	0.3	0.25	SIMILAR TO ABOVE BUT DAC-GENERATED TRIANGLE WAVE GENERALLY EASIER TO AMPLITUDE-STABILIZE OR VARY. ALSO, DAC CAN BE ADDRESSED BY COUNTERS SYNCHRONIZED TO A MASTER SYSTEM CLOCK.
ROM-DRIVEN DAC	1 Hz-20 MHz	0.1	0.01	POWERFUL DIGITAL TECHNIQUE THAT YIELDS FAST AMPLITUDE AND FREQUENCY SLEWING WITH LITTLE DYNAMIC ERROR CHIEF DETRIMENTS ARE REQUIREMENT FOR HIGH-SPEED CLOCK (EG, 8-BIT DAC REQUIRES A CLOCK THAT IS 256 × OUTPUT SINE-WAVE FREQUENCY) AND DAC GLITCHING & SETTLING, WHICH WILL INTRODUCE SIGNIFICANT DISTORTION AS OUTPUT FREQUENCY INCREASES.

1-IC Wein-bridge oscillators provide low-distortion signals

examples presented in this article, implementing the design techniques summarized in the **table,** demonstrate how easy it is to design a sine-wave source and achieve the kind of performance you need.

Phase-shift oscillators operate simply

Fig 1 depicts a 1-IC, 1-supply, amplitude-stabilized, phase-shift sine-wave oscillator. The LM389 audio-power-amplifier package contains the three discrete npn transistors shown (Q_1 through Q_3) in addition to the amplifier. Q_2 and the RC network constitute a phase-shift configuration that oscillates at about 12 kHz. The remaining circuitry provides amplitude stability.

The high-impedance output at Q_2's collector drives the LM389 amplifier's input via the 10-μF, 1-MΩ series network; the 1-MΩ resistor, in combination with the LM389 amplifier's internal 50-kΩ resistance, divides Q_2's output by 20—necessary because the amplifier has a fixed gain of 20. In this manner, the amplifier functions as a unity-gain current buffer capable of driving an 8Ω load.

The amplifier's positive output peaks are rectified and stored in the 5-μF capacitor, and the resulting potential then feeds to Q_3's base. As a result, Q_3's collector current varies with the difference between its base and emitter voltages. Because the LM313 1.2V reference fixes the emitter voltage, Q_3 performs a comparison function and utilizes its collector current to modulate Q_1's base voltage. Q_1 (an emitter follower) provides servo-controlled drive to the Q_2 oscillator.

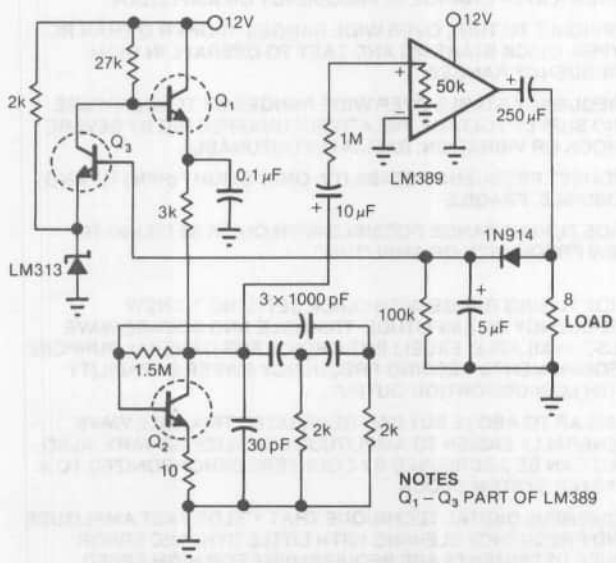

Fig 1—Phase-shift sine-wave oscillators *combine simplicity with versatility. This 12-kHz design can deliver 5V p-p to the 8Ω load with about 2% distortion.*

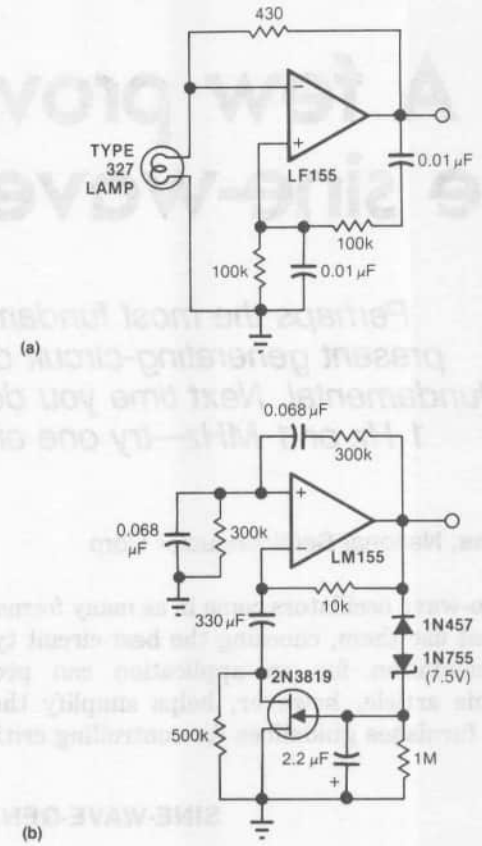

Fig 2—A basic Wein-bridge design (a) *employs a lamp's positive temperature coefficient to achieve amplitude stability. A more complex version* **(b)** *provides the same feature with the additional advantage of loop time-constant control.*

Note that you can realize an amplitude-control function with this circuit if you open Q_3's emitter and drive it with an external voltage. The LM389 output can deliver 5V p-p (1.75V rms) into an 8Ω load with about 2% distortion. A ±3V power-supply variation causes less than ±0.1-dB amplitude shift at the output.

A Wein bridge yields low distortion

In many applications, a phase-shift oscillator's distortion levels become unacceptable. A Wein bridge, however, can provide very low distortion levels. With this configuration, stable oscillation can occur only if loop gain remains at unity at the oscillation frequency. The circuit depicted in **Fig 2a** achieves this control by using a small lamp's positive temperature coefficient to regulate gain as the oscillator output attempts to vary—a classic technique for achieving low distortion that's been used by numerous circuit designers (including William Hewlett and David Packard, who built a few of this type of circuit in a Palo Alto garage about 40 yrs ago). The smooth limiting action of the bulb, in combination with the Wein network's near-ideal characteristics, yields very high performance.

The circuit shown in **Fig 2b** indicates how an electronic equivalent of a light bulb can also control loop gain. The zener diode determines output amplitude,

and the 1-MΩ/2.2-μF combination sets the loop time constant. The 2N3819 FET, biased by the voltage across the 2.2-μF capacitor, controls ac loop gain by shunting the oscillator's feedback path. This circuit is more complex than the one diagrammed in **Fig 2a,** but it offers a way to control the loop time constant while maintaining almost the same distortion performance.

Fig 3 shows the performance of the **Fig 2a** circuit. The upper trace is the oscillator's output, and the middle trace shows that waveform's downward slope, greatly expanded. The slight aberration in the latter results from crossover distortion in the FET-input LF155, distortion almost totally responsible for the design's measured 0.01% distortion level. A distortion analyzer's output appears in the bottom trace.

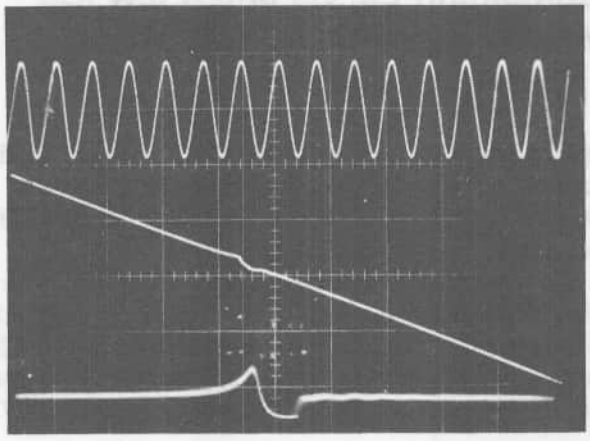

TRACE	VERTICAL	HORIZONTAL
TOP	10V/DIV	10 mSEC/DIV
MIDDLE	1V/DIV	500 NSEC/DIV
BOTTOM	0.5V/DIV	500 NSEC/DIV

Fig 3—Low-distortion output (top trace) *is a Wein-bridge-oscillator feature. The very low crossover-distortion level (middle) results from the LF155's output stage. A distortion analyzer's output signal (bottom) indicates this design's 0.01% distortion level.*

You can achieve high voltages, too

Another dimension in sine-wave-oscillator design is stable amplitude control. In **Fig 4**'s oscillator version, not only does servo control stabilize the amplitude, but the servo loop includes voltage gain.

The circuit's ability to produce a 100V rms output stabilized to 0.025% demonstrates the technique's value. Although complex in appearance, the circuit requires only three IC packages. An LS-52 audio transformer provides voltage gain within a tightly controlled servo loop, and the LM3900 Norton amplifiers constitute a 1-kHz amplitude-controllable oscillator. The LH0002 buffer furnishes low-impedance drive to the transformer. By driving the transformer's secondary and taking the ouput from the primary, the circuit achieves a voltage gain of 100.

A current-sensitive negative-absolute-value amplifier—composed of two amplifiers in an LF347 quad—generates a negative, rectified feedback signal. The third LF347 amplifier (A_7) compares this signal with the LM329 dc reference and amplifies the

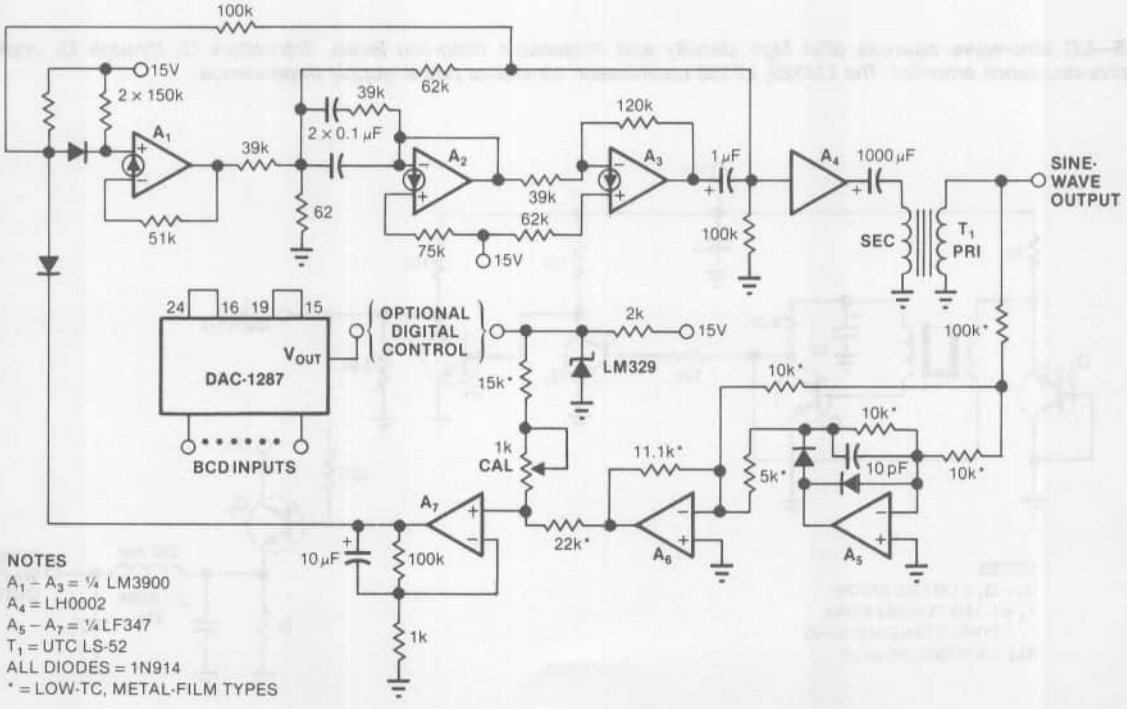

Fig 4—Generate high-voltage sine waves *using IC-based circuits by driving a transformer in a step-up mode. You can realize digital amplitude control by replacing the LM329 voltage reference with the DAC1287.*

Combining Ls, Cs and a few ICs yields high-stability sine waves

difference at a gain of 100. The 10-μF feedback capacitor sets the loop's frequency response. This stage's output controls the amplitude of the LM3900 oscillator, thereby closing the loop.

As shown, the circuit oscillates at 1 kHz with less than 0.1% distortion for a 100V rms (285V p-p) output. If you replace the summing resistors from the LM329 with a potentiometer, you can adjust the loop to remain stable for output settings ranging from 3 to 190V rms (542V p-p) with no frequency change. And if a DAC1287 D/A converter replaces the LM329 reference, a digital input code can control the ac output voltage with 3-digit calibrated accuracy.

Combine L, C and negative R for stability

All of the circuits presented so far rely on RC time constants to achieve resonance. But LC combinations can also serve and offer good frequency stability, high Q and fast starting.

A negative-resistance LC sine-wave oscillator appears in **Fig 5**, for example. The Q_1, Q_2 pair provides a 15-μA current source; Q_2's collector current in turn sets Q_3's peak collector current. The 300Ω pot and the Q_4, Q_5

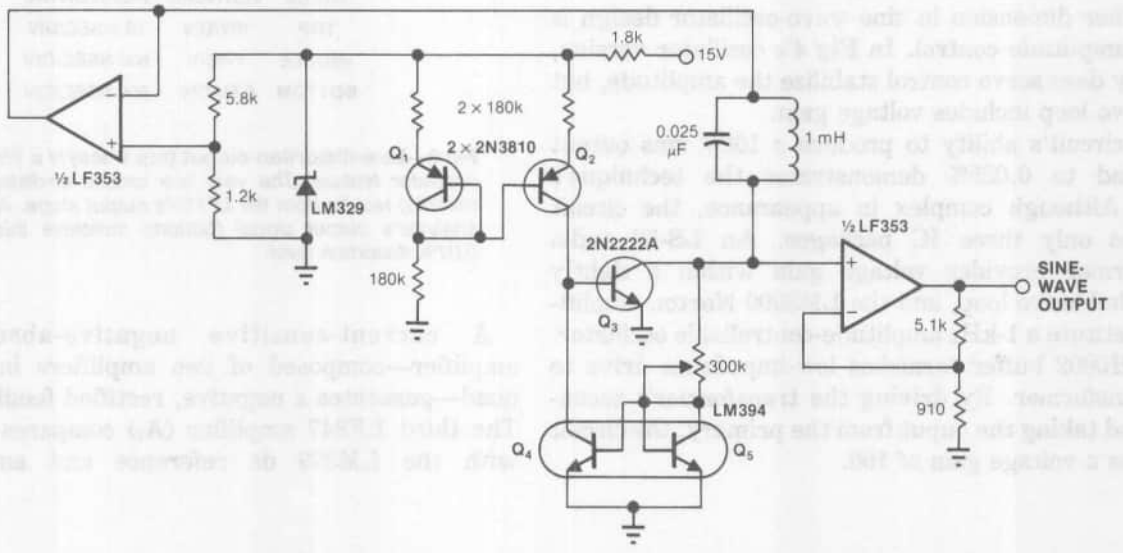

Fig 5—LC sine-wave sources *offer high stability and reasonable distortion levels. Transistors Q_1 through Q_5 implement a negative-resistance amplifier. The LM329, LF353 combination eliminates power-supply dependence.*

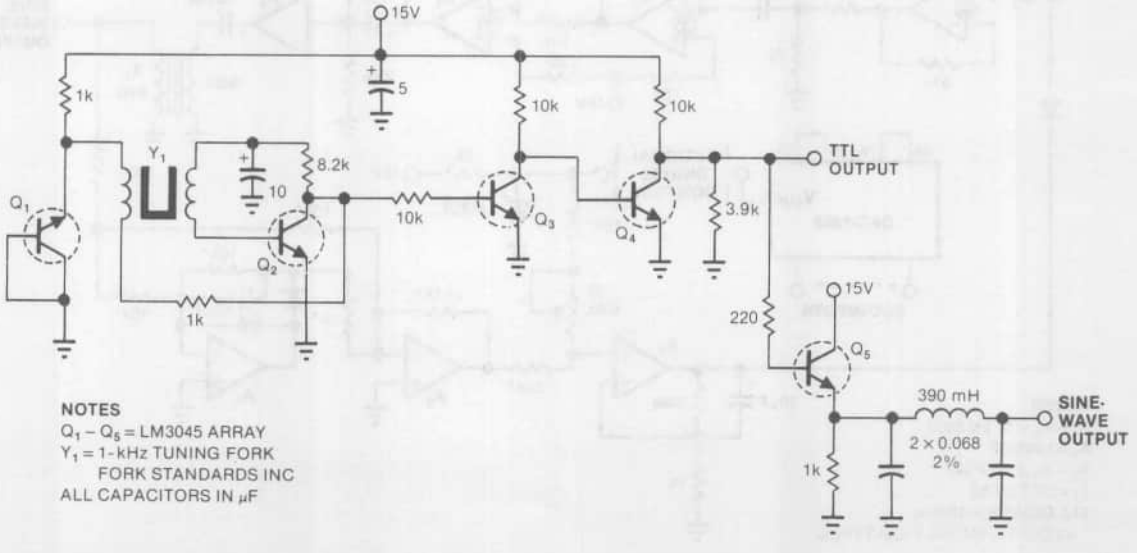

Fig 6—Tuning-fork-based oscillators *don't inherently produce sinusoidal outputs. But when you do use them for this purpose, you achieve maximum stability when the oscillator stage (Q_1, Q_2) limits. Q_3 and Q_4 provide a TTL-compatible signal, which Q_5 then converts to a sine wave.*

LM394 matched pair accomplish a voltage-to-current conversion that decreases Q_3's base current when this transistor's collector voltage rises—a process that furnishes the negative-resistance characteristic that permits oscillation.

The LC circuit in the Q_3, Q_5 collector line determines the oscillator circuit's operating frequency, and the LF353 FET amplifier provides gain and buffering. An LM329 zener diode and LF353 unity-gain follower eliminate power-supply dependence. This circuit starts quickly, and distortion remains within 1.5%.

Tuning forks offer another approach

Although oscillators for many applications can rely on combinations of passive components—whether RC or LC—to achieve resonance at the oscillation frequency, some circuits must utilize inherently resonant elements to achieve very high frequency stability. Such oscillators can generate stable low-frequency outputs under high-mechanical-shock conditions that would fracture quartz crystals.

In **Fig 6**'s circuit, for instance, a tuning fork works in a feedback loop with one of the transistors (Q_2) in an LM3045 array to achieve a stable 1-kHz output. Zener-connected Q_1 performs a combined reference and signal-limiting function. And because the oscillator is allowed to limit—a conventional technique in fork designs—it doesn't require amplitude stabilization. Q_3 and Q_4 speed up the oscillator's signal edges and furnish a TTL-compatible output level. Emitter follower Q_5 then drives an LC filter to produce a sine-wave output.

Fig 7 shows the circuit's TTL and sine-wave outputs. The 0.7% sine-wave distortion displayed in the bottom trace is a distortion analyzer's output signal.

Quartz crystals furnish high-frequency stability

If an application demands high-frequency stability—higher than a tuning-fork circuit can deliver—in the face of changing power-supply and temperature parameters, try a quartz-crystal oscillator. **Fig 8a** shows a simple example of a 100-kHz crystal oscillator—a Colpitts-class circuit that improves stability by using a JFET for low crystal loading. Voltage regulation eliminates the small effects (less than 5 ppm for a 20% shift) introduced by supply variations. And shunting the crystal with small-value capacitors allows very fine frequency trimming.

Crystals typically drift less than 1 ppm/°C, and temperature-controlled ovens can eliminate even this variation (**Fig 8b**). The RC feedback values depend upon the thermal time constants of the oven used; the values shown are typical. Set oven temperature to coincide with the crystal's zero temperature coefficient or "turning-point" temperature, which the manufacturer specifies.

An alternative to temperature control (**Fig 8c**) places a varactor diode across the crystal. The varactor receives its bias via a temperature-dependent voltage from a circuit similar to the one shown in **Fig 8b** but without the output transistor. As ambient temperature

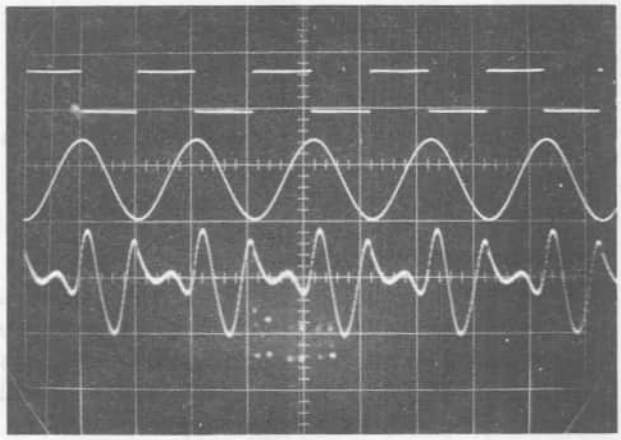

TRACE	VERTICAL	HORIZONTAL
TOP	5V/DIV	
MIDDLE	50V/DIV	500 μSEC/DIV
BOTTOM	0.2V/DIV	

Fig 7—Various output levels *are provided by the tuning-fork oscillator shown in* **Fig 6.** *This design easily produces a TTL-compatible signal (top trace) because the oscillator is allowed to limit. Low-pass filtering this square wave generates a sine wave (middle). The oscillator's 0.7% distortion level is indicated (bottom) by an analyzer's output.*

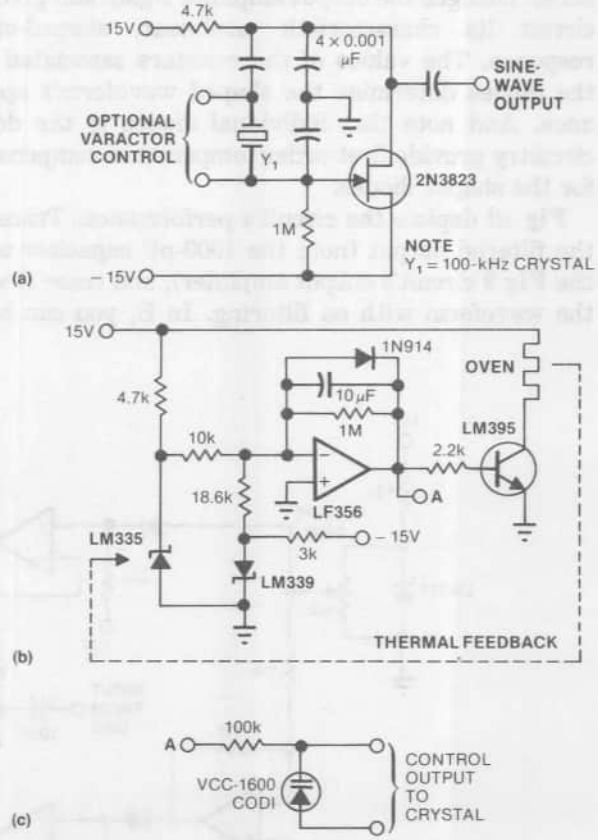

Fig 8—Stable quartz-crystal oscillators *can operate with a single active device* **(a).** *You can achieve maximum frequency stability by mounting the oscillator in an oven and using a temperature-controlling circuit* **(b).** *A varactor network* **(c)** *can also accomplish crystal fine tuning. Here, the varactor replaces the oven and retunes the crystal by changing its load capacitances.*

Quartz-crystal-based oscillators permit fine frequency trimming

varies, the circuit changes the voltage across the varactor, which in turn changes its capacitance. This capacitance shift trims the oscillator frequency.

Approximate sine waves

With the exception of the tuning-fork design, all of the preceding circuits operate as *inherent* sine-wave generators: Their normal operating mode supports and maintains a sinusoidal characteristic. Another oscillator class consists of circuits that *approximate* the sine function using a variety of techniques—usually a more complex approach but one that offers increased versatility in controlling amplitude and oscillation frequency. The adaptability of digital controls to these circuit types has markedly increased their popularity.

As an example, **Fig 9** diagrams a circuit that shapes a 20V p-p triangle-wave input into a sine-wave output. The two amplifiers in the center of the circuit establish stable bias potentials for the diode shaping network, which operates by turning individual diodes on or off depending upon the input triangle's amplitude. This action changes the output amplifier's gain and gives the circuit its characteristic nonlinear, shaped-output response. The values of the resistors associated with the diodes determine the shaped waveform's appearance. And note that individual diodes in the dc-bias circuitry provide first-order temperature compensation for the shaper diodes.

Fig 10 depicts the circuit's performance. Trace A is the filtered output (note the 1000-pF capacitor across the **Fig 9** circuit's output amplifier), and trace B shows the waveform with no filtering. In B, you can barely detect a breakpoint at the top and bottom of the waveform, but all the breakpoints become clearly identifiable in the distortion-analyzer output (trace C). Note that in **Fig 9**'s circuit, if the amplitude or symmetry of the input triangle wave shifts, the output waveform degrades badly. Typically, you can employ a D/A converter to provide input drive. Distortion in this circuit specs below 1.5% when filtered and about 2.7% without filtering.

Log shaping yields 10,000:1 frequency range

Applications that call for a wide frequency range can make good use of the shaper circuit shown in **Fig 11**, a complete sine-wave generator that you can tune from 1 Hz to 10 kHz using one variable resistor. Amplitude stability remains within 0.02%/°C, and distortion measures 0.35%. In addition, desired frequency shifts occur instantaneously because no control-loop time constants apply.

The circuit works by placing an integrator inside a comparator's positive feedback loop to produce triangle waves for shaping into sine waves. The LM311 drives a symmetrical temperature-compensated clamp arrangement, which then biases the LF356 integrator. The LF356 integrates this current into a linear ramp. At the 311's input, this ramp is summed with the clamp's output until the ramp voltage nulls out the bound voltage. At this time, the comparator changes state and the integrator output reverses.

The resultant repetitive triangle waveform then feeds to a sine-shaper section that utilizes the nonlinear, logarithmic relationship between V_{BE} and the collector current in the transistors to smooth the triangle wave. The LM394 dual transistor handles the actual shaping, while the 2N3810 provides current drive. The LF351 allows adjustable, low-impedance output-amplitude control.

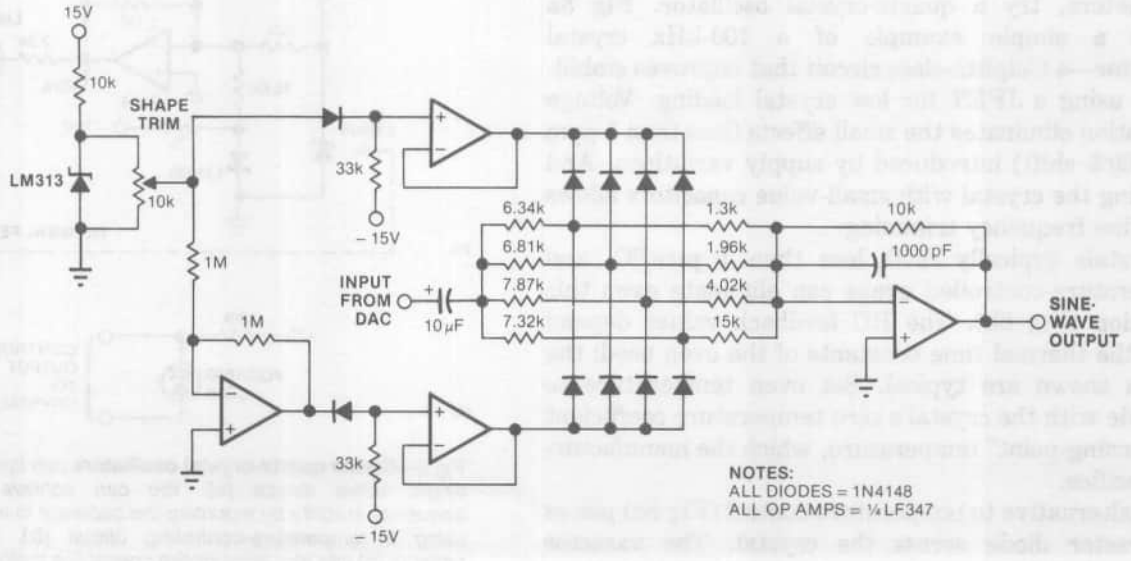

Fig 9—Breakpoint-shaping networks *employ diodes that conduct in direct proportion to an input triangle wave's amplitude. This action changes the output amplifier's gain to produce the sine function.*

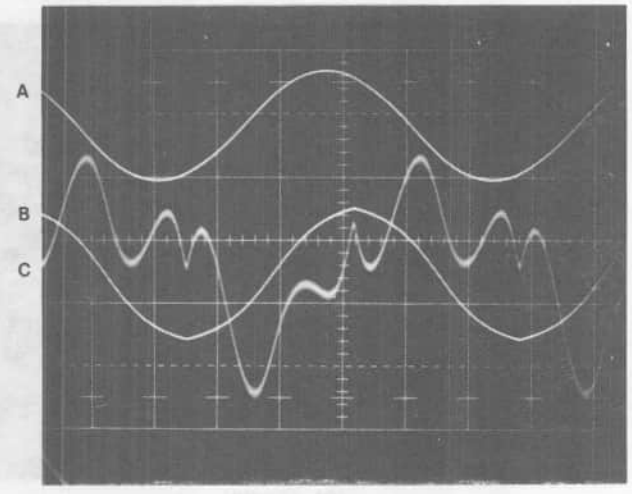

TRACE	VERTICAL	HORIZONTAL
A	5V/DIV	
B	5V/DIV	20 μSEC/DIV
C	0.5V/DIV	

Fig 10—A clean sine wave results (trace A) *when* ***Fig 9****'s circuit's output includes a 1000-pF capacitor. When the capacitor isn't used, the diode network's breakpoint action becomes apparent (trace B). The distortion analyzer's output (trace C) clearly shows all the breakpoints.*

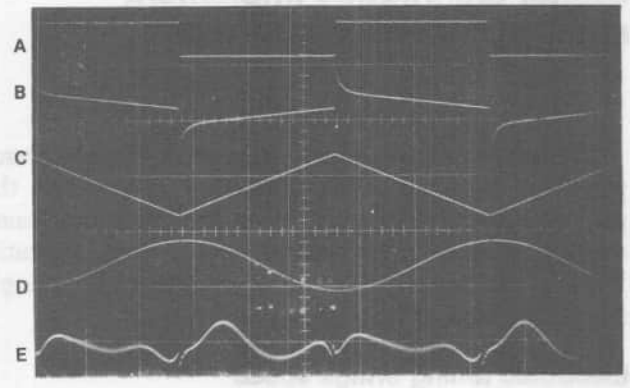

TRACE	VERTICAL	HORIZONTAL
A	20V/DIV	
B	20V/DIV	20 μSEC/DIV
C	10V/DIV	
D	10V/DIV	
E	0.5V/DIV	

Fig 12—Logarithmic shapers *can utilize a variety of circuit waveforms. The input to the LF356 integrator* ***(Fig 11)*** *appears here as trace A. The LM311's input (trace B) is the summed result of the integrator's triangle output (C) and the LM329's clamped waveform. After passing through the 2N3810/LM394 shaper stage, the resulting sine wave is amplified by the LF351 (D). A distortion analyzer's output (E) represents a 0.35% total harmonic distortion.*

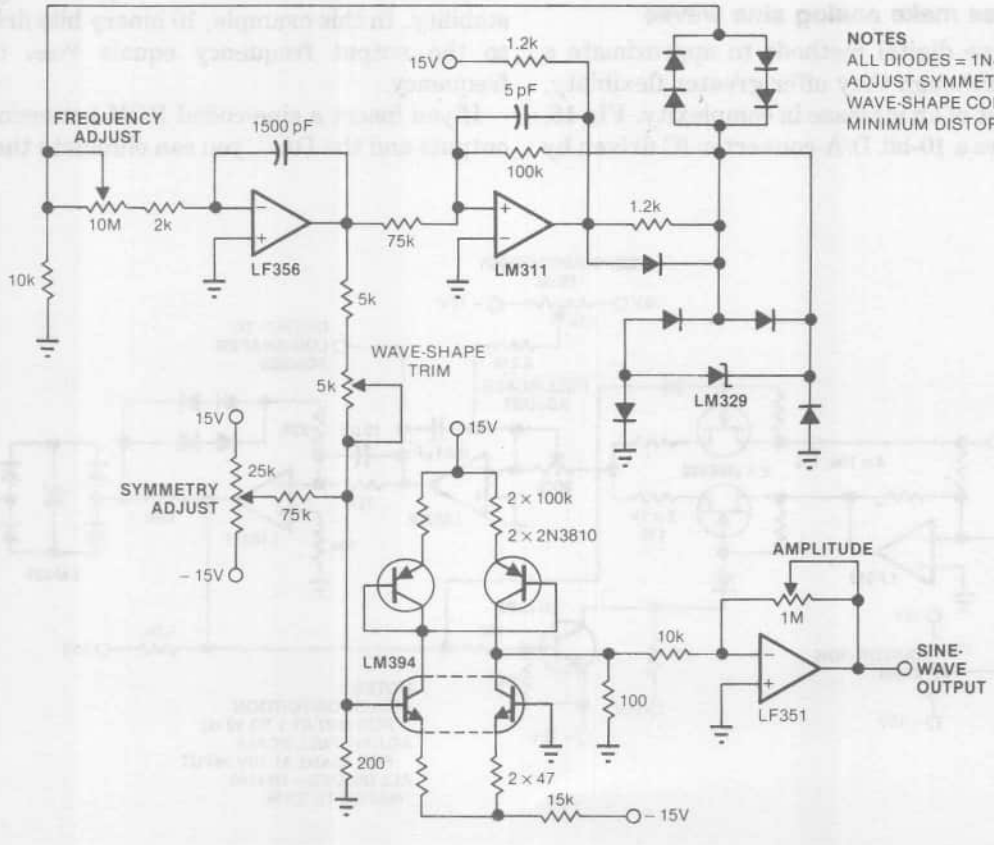

Fig 11—Logarithmic shaping schemes *produce a sine-wave oscillator that you can tune from 1 Hz to 10 kHz with a single control. Additionally, you can shift frequencies rapidly because the circuit contains no control-loop time constants.*

Digital techniques implement analog sine-wave sources

Typical circuit waveforms appear in **Fig 12.** Should you need an even wider frequency range than that provided by this circuit, bear in mind that more sophisticated versions (**references**) achieve operation from 1 Hz to 1 MHz while retaining the single-frequency-control feature.

Electronic tuning brings speed

A very-high-performance version of **Fig 11**'s log shaper design appears in **Fig 13.** Here, the LF356 integrator's input voltage is an externally supplied control voltage, rather than the zener-bridge output previously used. Inverted by the LF351, the control voltage is gated by the 2N4392 FET switches, which are in turn controlled by the LM311's output. Thus, oscillator frequency varies directly with the input control voltage. And because limiting rather than a servo-loop process determines the circuit's amplitude, an almost instantaneous frequency change occurs as the result of a step input.

A 10V input sweeps the oscillator from 1 Hz to 30 kHz with less than 0.4% distortion (**Fig 14**). Additionally, control-voltage input vs frequency-output linearity lies within 0.25%.

Digital techniques make analog sine waves

You can also use digital methods to approximate a sine wave. But, although they offer greater flexibility, it's only at the cost of an increase in complexity. **Fig 15,** for instance, shows a 10-bit D/A-converter IC driven by

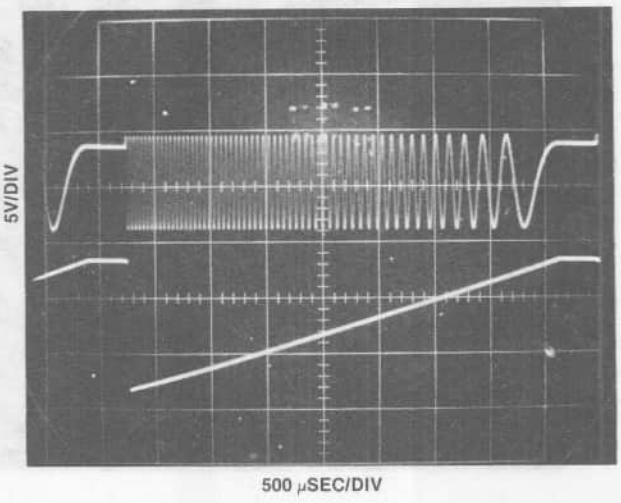

Fig 14—Rapid frequency sweeping *is an inherent feature of* ***Fig 13****'s voltage-controlled sine-wave oscillator. You can sweep this VCO from 1 Hz to 30 kHz with a 10V input signal; the output settles quickly.*

up/down counters to deliver an amplitude-stable triangle current into the LF357 FET amplifier. The LF357 then drives a shaper circuit of the type shown in **Fig 9.** The sine wave's amplitude remains stable, and its frequency depends solely on the clock speed used to drive the counters. If the clock is crystal controlled, the output sine wave reflects the crystal's high frequency stability. In this example, 10 binary bits drive the DAC, so the output frequency equals $1/1024$ of the clock frequency.

If you insert a sine-coded ROM between the counter outputs and the DAC, you can eliminate the sine shaper

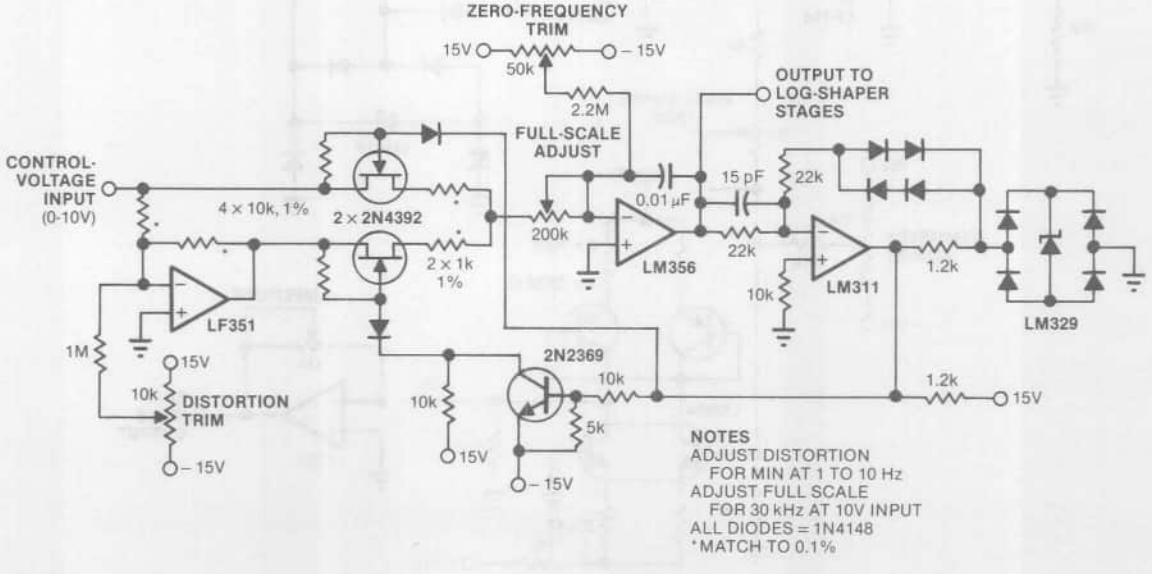

Fig 13—A voltage-tunable oscillator *results when* ***Fig 11****'s design is modified to include signal-level-controlled feedback. Here, FETs switch the integrator's input so that the resulting summing-junction current is a function of the input control voltage. This scheme realizes a frequency range of 1 Hz to 30 kHz for a 0 to 10V input.*

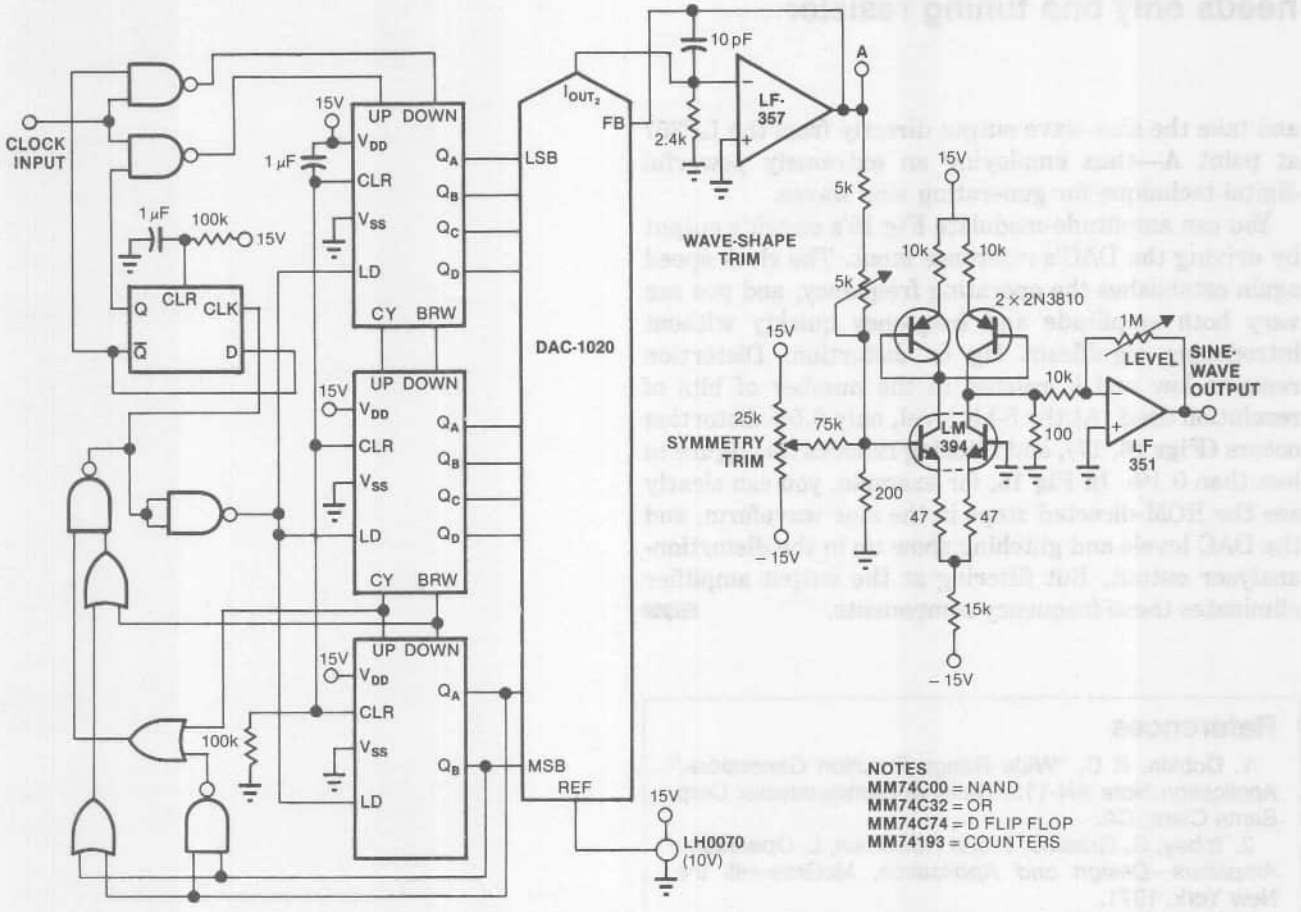

Fig 15—Digital techniques *produce triangular waveforms that methods employed in* **Fig 11** *can then easily convert to sine waves. This digital approach divides the input clock frequency by 1024 and uses the resultant 10 bits to drive a DAC. The DAC's triangular output—amplified by the LF357—drives the log shaper stage. You could also eliminate the log shaper and place a sine-coded ROM between the counters' outputs and the DAC, then recover the sine wave at point A.*

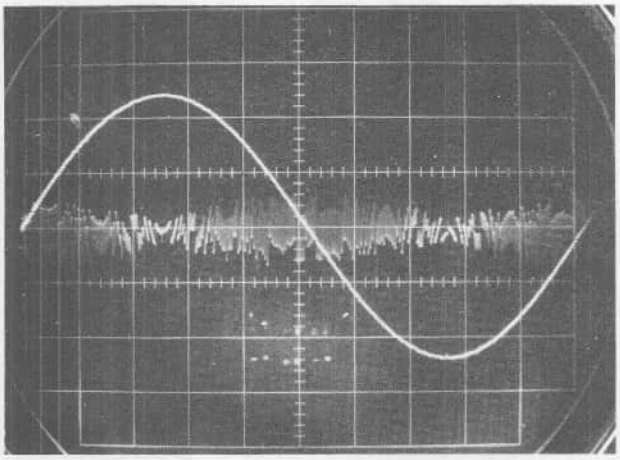

TRACE	VERTICAL	HORIZONTAL
SINE WAVE	1V/DIV	200 μSEC/DIV
ANALYZER	0.2V/DIV	

Fig 16—An 8-bit sine-coded-ROM version of Fig 15's circuit *produces a distortion level less than 0.5%. Filtering the sine output—shown here with a distortion analyzer's trace—can reduce the distortion to below 0.1%.*

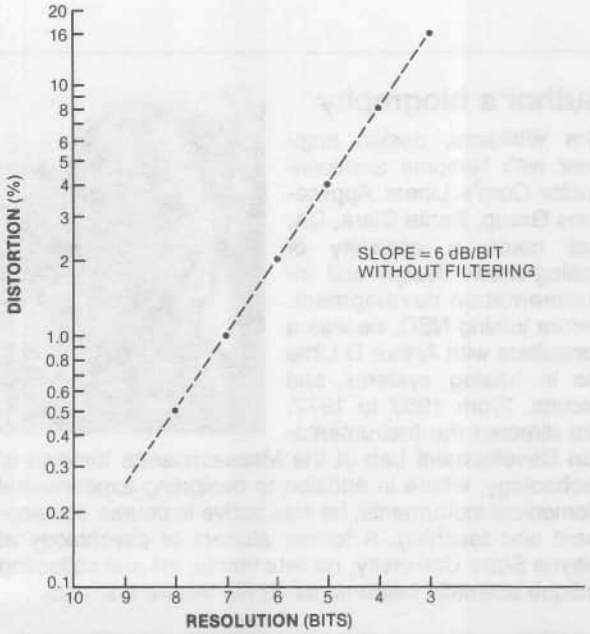

Fig 17—Distortion levels decrease *with increasing digital-word length. Although additional filtering can considerably improve the distortion levels (to 0.1% from 0.5% for the 8-bit case), you're better off using a long digital word.*

and take the sine-wave output directly from the LF357 at point A—thus employing an extremely powerful digital technique for generating sine waves.

You can amplitude-modulate **Fig 15**'s circuit's output by driving the DAC's reference input. The clock speed again establishes the operating frequency, and you can vary both amplitude and frequency quickly without introducing significant lag or distortion. Distortion remains low and is related to the number of bits of resolution used. At the 8-bit level, only 0.5% distortion occurs (**Figs 16, 17**), and filtering reduces this figure to less than 0.1%. In **Fig 16,** for example, you can clearly see the ROM-directed steps in the sine waveform, and the DAC levels and glitching show up in the distortion-analyzer output. But filtering at the output amplifier eliminates these frequency components. **EDN**

References

1. Dobkin, R C, "Wide Range Function Generators," Application Note AN-115, National Semiconductor Corp, Santa Clara, CA.

2. Tobey, G; Graeme, J; and Huelsman, L, *Operational Amplifiers—Design and Application,* McGraw-Hill Inc, New York, 1971.

3. Williams, J, "A 0.1-Hz Sine Wave Oscillator Using Thermal Feedback," Massachusetts Institute of Technology, Cambridge, MA.

4. *Application Manual for Operational Amplifiers,* Teledyne Philbrick, Dedham, MA, 1969.

Author's biography

Jim Williams, design engineer with National Semiconductor Corp's Linear Applications Group, Santa Clara, CA, has made a specialty of analog-circuit design and instrumentation development. Before joining NSC, he was a consultant with Arthur D Little Inc in analog systems and circuits. From 1968 to 1977, Jim directed the Instrumentation Development Lab at the Massachusetts Institute of Technology, where in addition to designing experimental biomedical instruments, he was active in course development and teaching. A former student of psychology at Wayne State University, he lists tennis, art and collecting antique scientific instruments as his leisure interests.

Low-cost dual, quad FET op amps implement complex functions

Multiple general-purpose FET op amps in one package offer more than basic gain and control capabilities. By fully exploiting their high-performance potential, you can derive a variety of low-cost special-purpose circuits.

Jim Williams, National Semiconductor Corp

FET op amps in dual and quad packages furnish the same performance as their single-op-amp relatives, but they cost less per amplifier, occupy less board area and require fewer bypass capacitors and power-supply buses. To show you how to implement these advantages effectively, this article examines temperature-control, sine-wave-oscillator and A/D-converter circuit designs that each utilize one dual or quad FET op-amp package.

Controller maintains stable temperature

Fig 1, for example, shows a complete high-efficiency pulse-width-modulating oven-temperature controller. A single LF347 package contains the four op amps shown (A_1 through A_4).

A_1 functions as an oscillator whose output (**Fig 2,** trace A) periodically resets integrator A_2's output

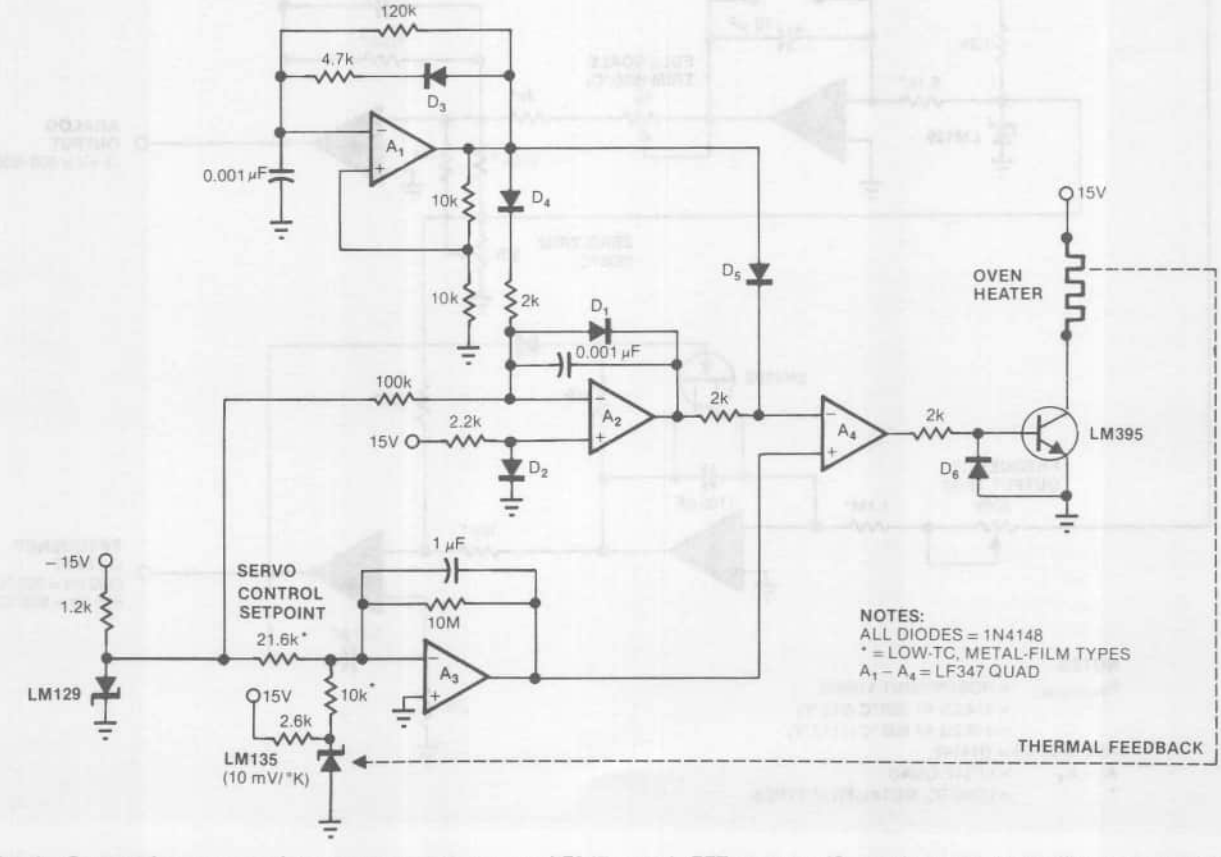

Fig 1—Connecting appropriate components *to an LF347 quad FET-op-amp IC produces a high-efficiency precision oven-temperature controller. This design can hold a temperature within 0.05°C despite wide ambient-temperature fluctuations.*

FET op amps serve efficiently in temperature-measurement circuits

(trace B) to 0V. Each time A_1's output goes high, a large positive current flows into A_2's summing junction. This current overcomes the negative current flowing through the 100-kΩ resistor into the LM329 reference. As a result, A_2's output heads negative, ultimately limited by D_1's feedback bound.

Diode D_2 provides bias at A_2's positive input to compensate for D_1. Accordingly, A_2's output settles close to 0V. When A_1's positive output pulse ends, the positive current into A_2's summing junction ceases. Then A_2's output ramps linearly until the next reset pulse.

A_3 operates as a current-summing servo amplifier that compares the currents derived from the LM135 temperature sensor and the LM329 reference. In this configuration, A_3 achieves a gain of 1000, and the 1-μF feedback capacitor permits a 0.1-Hz servo response. A_3's output represents the amplified difference between the LM135's temperature and the desired control setpoint. You can vary the setpoint by changing the

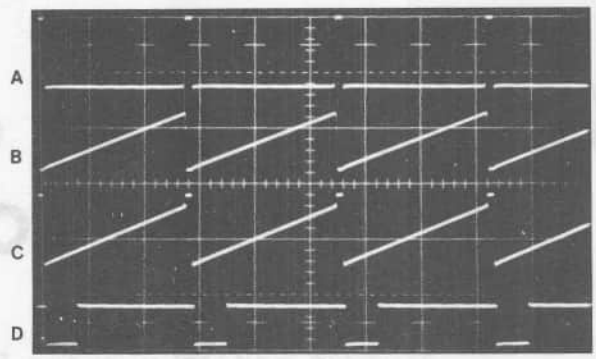

TRACE	VERTICAL	HORIZONTAL
A	20V/DIV	
B	10V/DIV	50 μSEC/DIV
C	10V/DIV	
D	20V/DIV	

Fig 2—Oven-controller waveforms *from* ***Fig 1****'s circuit show A_1's oscillator output (trace A) and A_2's integrator output (B) as the latter resets periodically to 0V. Trace C displays A_4's ramp output, and D indicates the LM395's power input to the oven heater.*

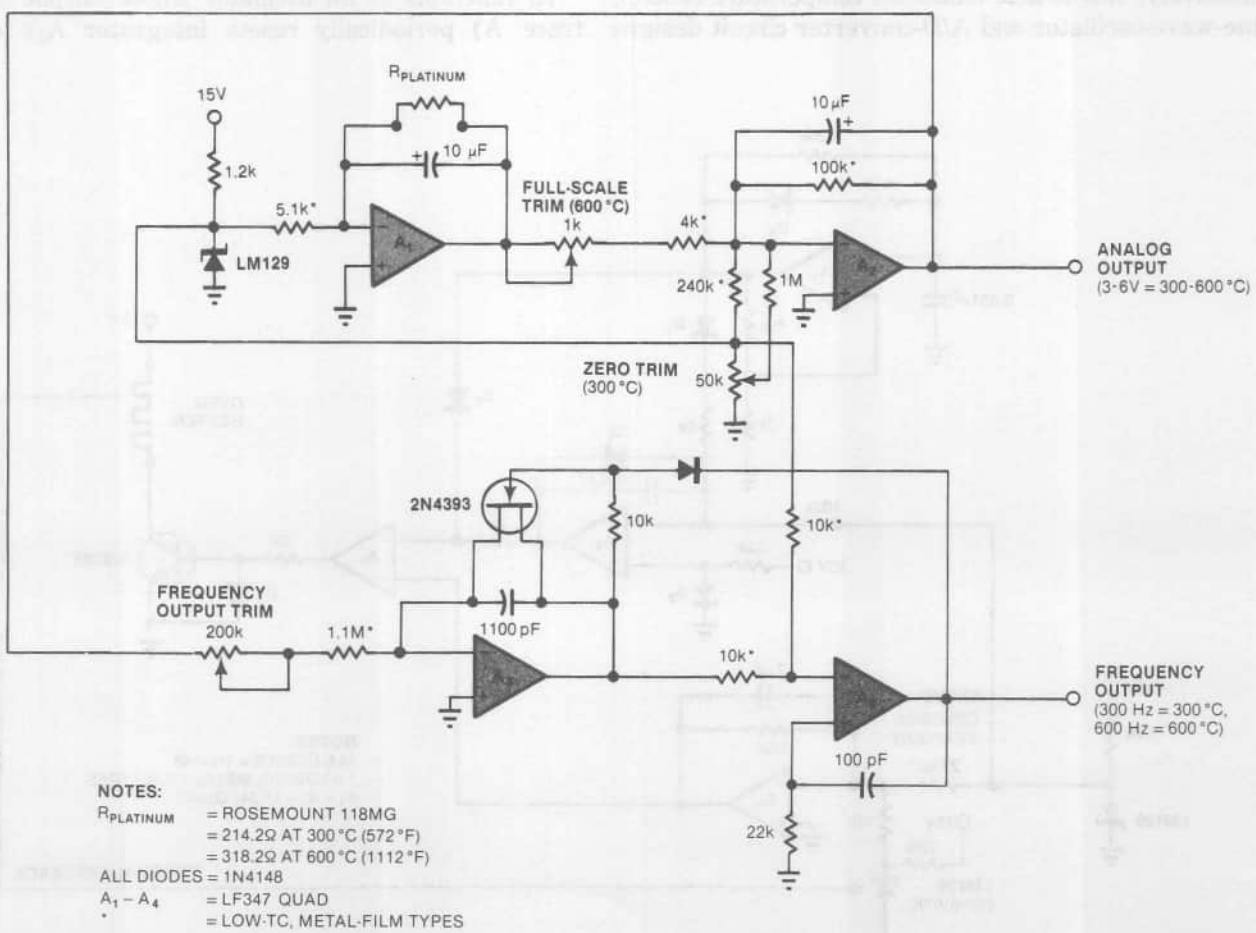

Fig 3—Generate simultaneous analog-level and frequency outputs *using one LF347 package by signal-conditioning a platinum RTD sensor. You can calibrate this high-temperature (300 to 600°C) measuring circuit to ±1°C by using three trimming pots.*

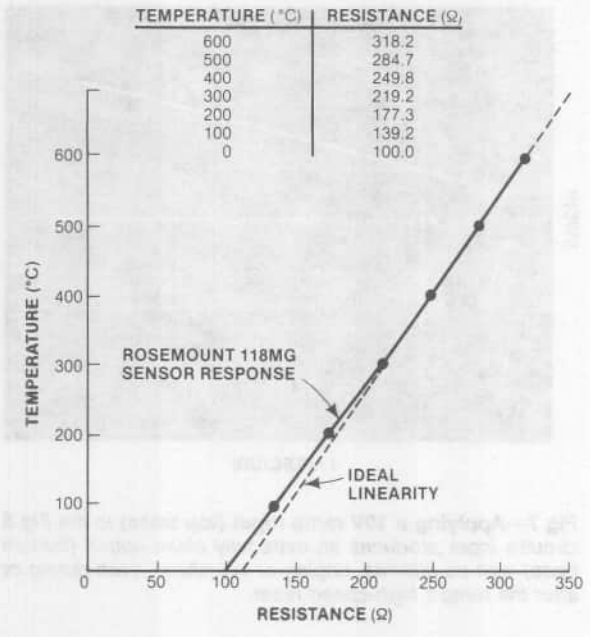

Fig 4—A platinum RTD sensor's resistance *decreases linearly from 600 to 300°C. Then, from 300 to 0°C, the sensor's resistance deviates from a straight-line slope and degrades the* ***Fig 3*** *circuit's accuracy beyond ±1°C.*

21.6-kΩ resistor's value. In **Fig 1**'s version, the 21.6-kΩ resistor provides a setpoint of 49°C (322°K).

Configured as a comparator, A_4 measures A_3's output against A_2's ramp output. Specifically, A_4's output is high only when A_3's output exceeds the ramp voltage. The ramp-reset pulse from A_1 is diode summed with the ramp output (trace C) at A_4 to prevent A_4's output from going high during the reset-pulse period.

Additionally, A_4's output biases the LM395 power transistor, which switches power (trace D) to the heater. If you tightly couple the LM135 sensor to the heater and adequately insulate the oven, this controller circuit can easily hold a setpoint within 0.05°C over wide ambient-temperature excursions.

Sensor circuit generates dual outputs

Another temperature-related circuit employing one LF347 package appears in **Fig 3.** In this design, the LF347 op amps signal-condition a platinum RTD sensor and provide simultaneous analog-level and frequency outputs. These outputs stay accurate to ±1°C over 300 to 600°C (572 to 1112°F). Although the conditioning circuit can maintain linearity over an even wider range, the sensor's nonlinear response from 0 to 300°C limits overall accuracy (**Fig 4**).

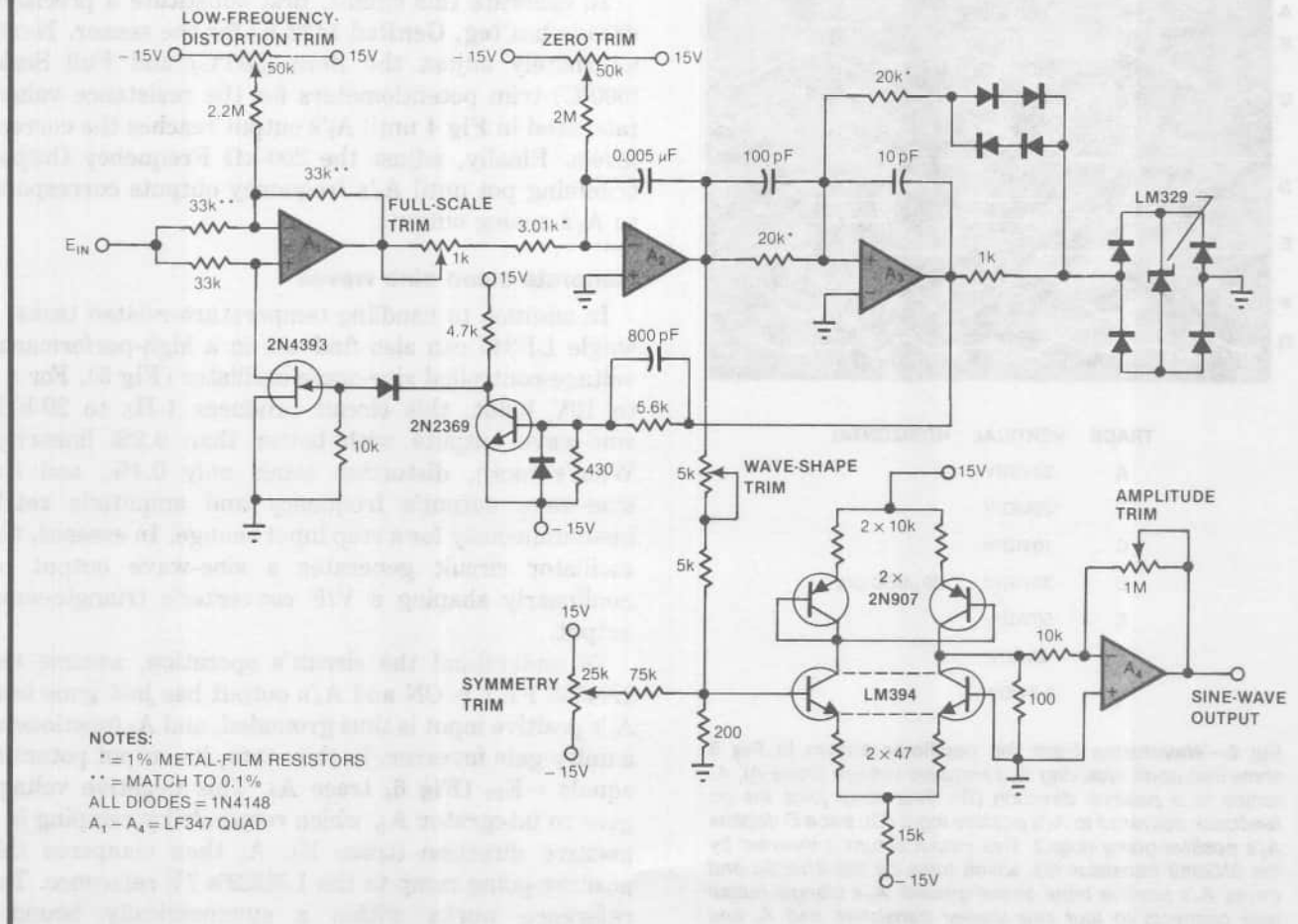

Fig 5—An LF347-based voltage-controlled sine-wave oscillator *combines high performance with versatility. For 0 to 10V inputs, this circuit generates 1-Hz to 20-kHz outputs with better than 0.2% linearity and only 0.4% distortion.*

Low-distortion oscillator generates clean sine waves

A_1 functions as a negative-gain inverter and drives a constant current through the platinum sensor. Both the LM329 and the 5.1-kΩ resistor supply the current reference. Because A_1 provides negative gain, the sensor's developed voltage remains extremely low and eliminates self-heating-induced errors.

A_1's output potential—which varies with the sensor's temperature—goes to A_2. In turn, A_2 furnishes scaled gain and offsetting to produce an analog output that ranges from 3 to 6V for a corresponding 300 to 600°C temperature swing at the sensor.

Performing as a voltage-to-frequency (V/F) converter, A_3 and A_4 generate a 300- to 600-Hz output from A_2's 3 to 6V analog output. A_3 integrates in a negative-going direction with a linear slope that depends on A_2's output voltage. Then A_4 compares A_3's negative ramp with the LM329's positive reference voltage by current-summing in the 10-kΩ resistors. When the ramp's negative potential barely exceeds the LM329's reference voltage, A_4's output goes positive. This action turns on the 2N4393 FET and resets A_3's integration process. At A_4, ac feedback causes "hang-up" in the positive state long enough to completely discharge A_3's integrator capacitor.

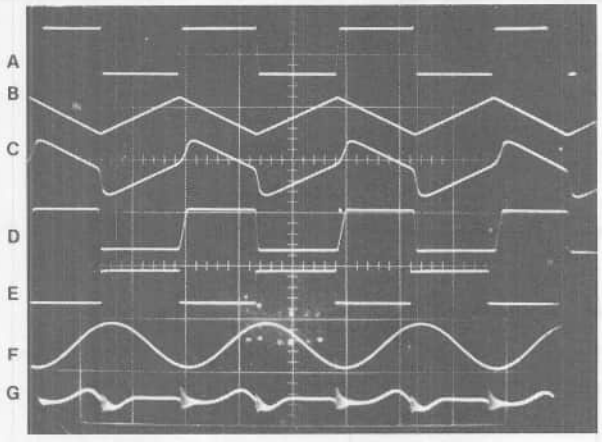

TRACE	VERTICAL	HORIZONTAL
A	20V/DIV	
B	20V/DIV	
C	10V/DIV	
D	20V/DIV	20 μSEC/DIV
E	50V/DIV	
F	2V/DIV	
G	0.2V/DIV	

Fig 6—Waveforms from the oscillator shown in Fig 5 *show that upon receiving A_1's negative voltage (trace A), A_2 ramps in a positive direction (B). This ramp joins the ac feedback delivered to A_3's positive input (C); trace D depicts A_3's positive-going output. This output in turn is inverted by the 2N2369 transistor (E), which turns off the 2N4393 and drives A_1's positive input above ground. A_2's triangle output also connects to four sine-shaper transistors and A_4 and finally emerges as the circuit's sine-wave output (F). A distortion analyzer's output (G) shows the circuit's minimum distortion products after trimming.*

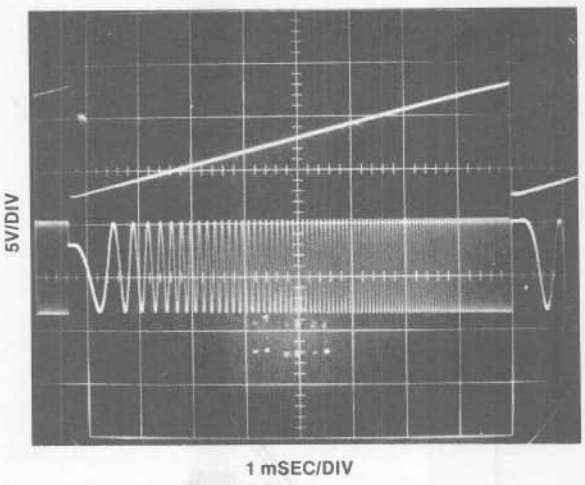

Fig 7—Applying a 10V ramp input (top trace) *to the **Fig 5** circuit's input produces an extremely clean output (bottom trace) with no glitches, ringing or overshoot, even during or after the ramp's high-speed reset.*

To calibrate this circuit, first substitute a precision decade box (eg, GenRad 1432-K) for the sensor. Next, alternately adjust the Zero (300°C) and Full Scale (600°C) trim potentiometers for the resistance values tabulated in **Fig 4** until A_2's output reaches the correct levels. Finally, adjust the 200-kΩ Frequency Output trimming pot until A_4's frequency outputs correspond to A_2's analog outputs.

Generate clean sine waves

In addition to handling temperature-related tasks, a single LF347 can also find use in a high-performance voltage-controlled sine-wave oscillator **(Fig 5).** For a 0 to 10V input, this circuit produces 1-Hz to 20-kHz sine-wave outputs with better than 0.2% linearity. What's more, distortion totals only 0.4%, and the sine-wave output's frequency and amplitude settle instantaneously for a step input change. In essence, the oscillator circuit generates a sine-wave output by nonlinearly shaping a V/F converter's triangle-wave output.

To understand the circuit's operation, assume the 2N4393 FET is ON and A_1's output has just gone low. A_1's positive input is thus grounded, and A_1 functions as a unity-gain inverter. In this state, its output potential equals $-E_{IN}$ **(Fig 6,** trace A). This negative voltage goes to integrator A_2, which responds by ramping in a positive direction (trace B). A_3 then compares this positive-going ramp to the LM329's 7V reference. The reference works within a symmetrically bounded positive feedback loop, within which the parallel diodes compensate the bridge diodes.

When the positive-going ramp voltage barely nulls

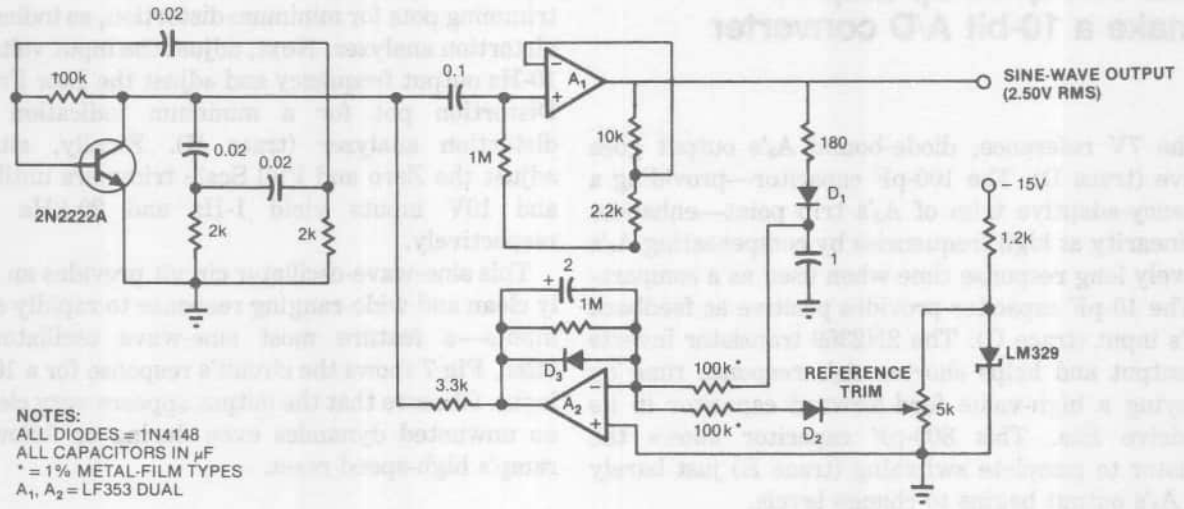

Fig 8—Reduce parts count and save money *by basing this precision sine-wave voltage reference on an LF353 dual FET-op-amp IC. This circuit generates a 1-kHz sine wave at 2.50V rms. The 2N2222A transistor functions as a phase-shift oscillator. The A_1, A_2 combination amplifies and amplitude-stabilizes the circuit's sine-wave output.*

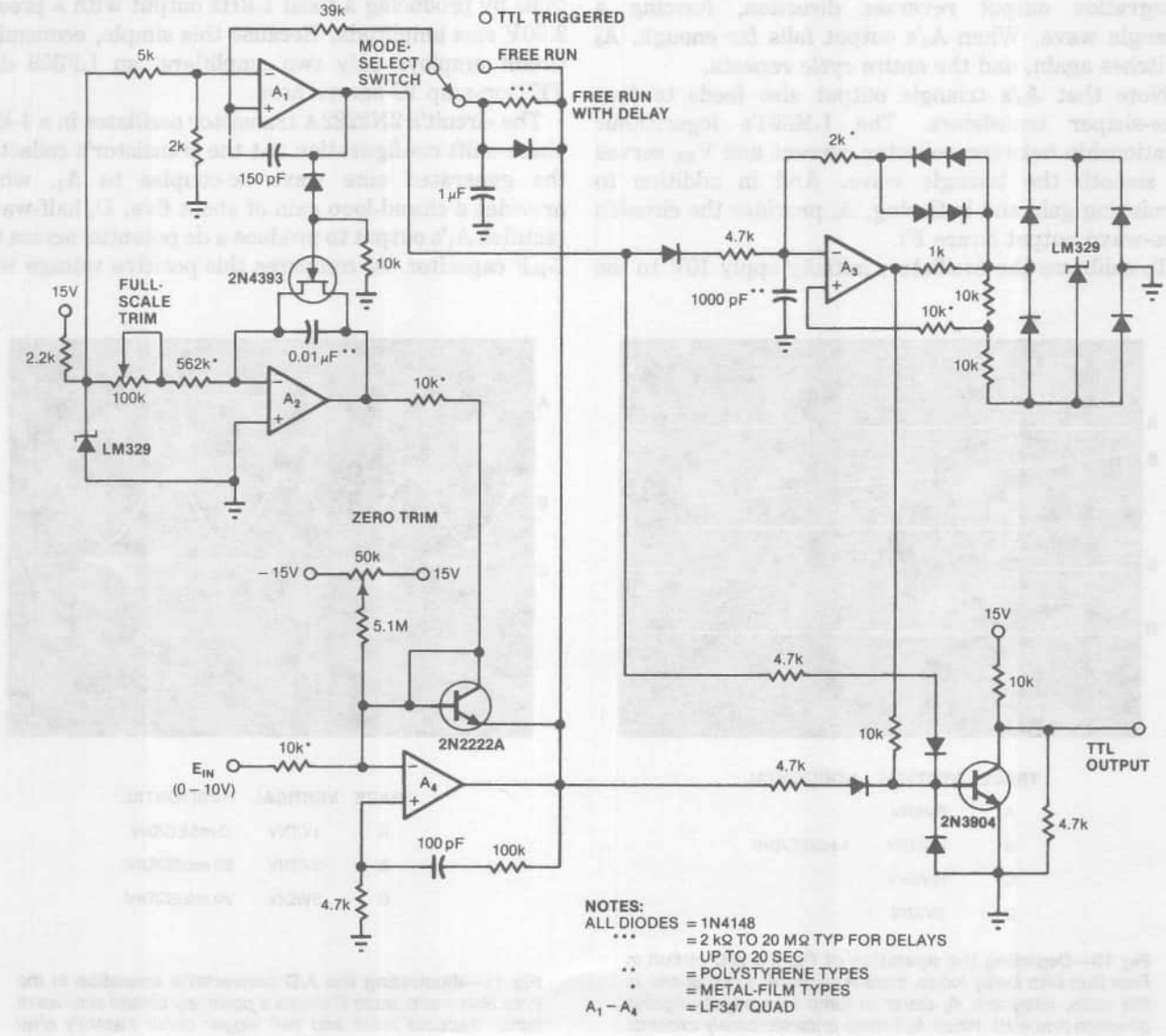

Fig 9—Three Mode Select switch positions *offer a choice of internal or external trigger conditions for this integrating A/D converter. Over 15 to 35°C, this trimmable converter provides a 10-bit serial output, converts in 10 msec and accepts 0 to 10V inputs.*

Utilize one quad op-amp IC to make a 10-bit A/D converter

out the 7V reference, diode-bound A_3's output goes positive (trace D). The 100-pF capacitor—providing a frequency-adaptive trim of A_3's trip point—enhances V/F linearity at high frequencies by compensating A_3's relatively long response time when used as a comparator. The 10-pF capacitor provides positive ac feedback to A_3's input (trace C). The 2N2369 transistor inverts A_3's output and helps shorten A_3's response time by employing a high-value feed-forward capacitor in its base-drive line. This 800-pF capacitor allows the transistor to complete switching (trace E) just barely after A_3's output begins to change levels.

The 2N2369's negative output turns off the 2N4393. As a result, A_1's positive input rises above ground and causes A_1 to act as a unity-gain follower. A_1's output then slews immediately to the value of E_{IN}, and A_2's integration output reverses direction, forming a triangle wave. When A_2's output falls far enough, A_3 switches again, and the entire cycle repeats.

Note that A_2's triangle output also feeds to four sine-shaper transistors. The LM394's logarithmic relationship between collector current and V_{BE} serves to smooth the triangle wave. And in addition to furnishing gain and buffering, A_4 provides the circuit's sine-wave output (trace F).

To calibrate the oscillator, initially apply 10V to the input and adjust the Wave Shape and Symmetry trimming pots for minimum distortion, as indicated on a distortion analyzer. Next, adjust the input voltage for a 10-Hz output frequency and adjust the Low Frequency Distortion pot for a minimum indication on the distortion analyzer (trace G). Finally, alternately adjust the Zero and Full Scale trimmers until 500-μV and 10V inputs yield 1-Hz and 20-kHz outputs, respectively.

This sine-wave-oscillator circuit provides an unusually clean and wide-ranging response to rapidly changing inputs—a feature most sine-wave oscillators don't offer. **Fig 7** shows the circuit's response for a 10V-ramp input. Observe that the output appears very clean, with no unwanted dynamics even during or following the ramp's high-speed reset.

Set up a sine-wave voltage reference

Common applications for sine-wave outputs include use as ac-calibration or amplitude-stabilized sources. Another sine-wave circuit (**Fig 8**) suits these applications by producing a fixed 1-kHz output with a precise 2.50V rms amplitude. Because this simple, economical circuit employs only two amplifiers, an LF353 dual FET-op-amp IC serves here.

The circuit's 2N2222A transistor oscillates in a 1-kHz phase-shift configuration. At the transistor's collector, the generated sine wave ac-couples to A_1, which provides a closed-loop gain of about five. D_1 half-wave-rectifies A_1's output to produce a dc potential across the 1-μF capacitor. A_2 compares this positive voltage with

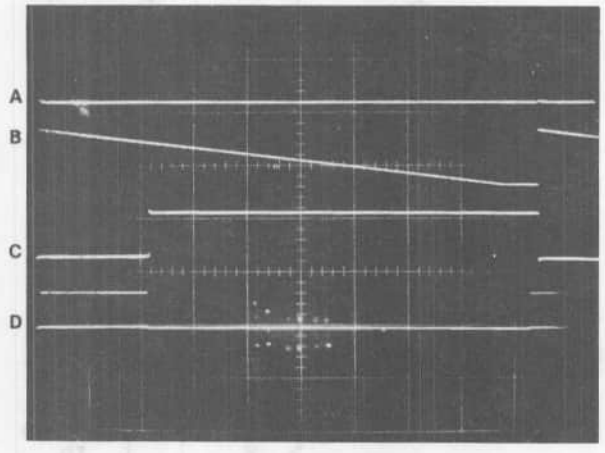

TRACE	VERTICAL	HORIZONTAL
A	5V/DIV	
B	10V/DIV	1 mSEC/DIV
C	10V/DIV	
D	5V/DIV	

Fig 10—Depicting the operation of Fig 9's A/D circuit *in Free Run With Delay mode, trace A shows A_1's output low. In this state, integrator A_2 starts to ramp in a negative-going direction (trace B). When A_2's ramp potential barely exceeds the input voltage's negative value, A_4's output goes high (C). This transition turns on the 2N3904 transistor, which shuts off the TTL output pulse train (D).*

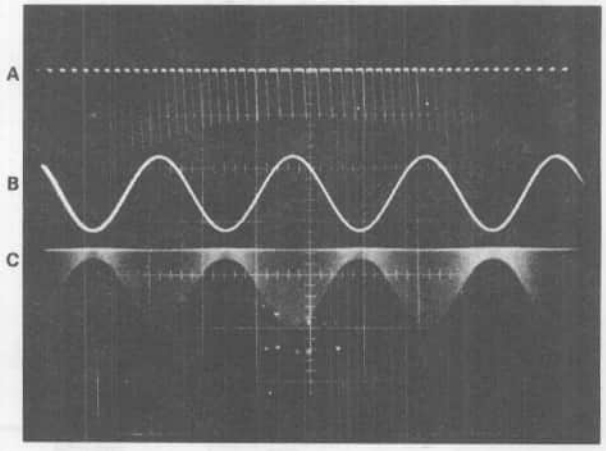

TRACE	VERTICAL	HORIZONTAL
A	1V/DIV	2 mSEC/DIV
B	5V/DIV	20 mSEC/DIV
C	5V/DIV	20 mSEC/DIV

Fig 11—Illustrating the A/D converter's operation *in the Free Run mode, trace B shows a positively biased sine-wave input. Because reset and self trigger occur instantly after conversion, A_2's output produces a ramp-constructed envelope of the input (trace C). Trace A shows a time-expanded form of the envelope waveform.*

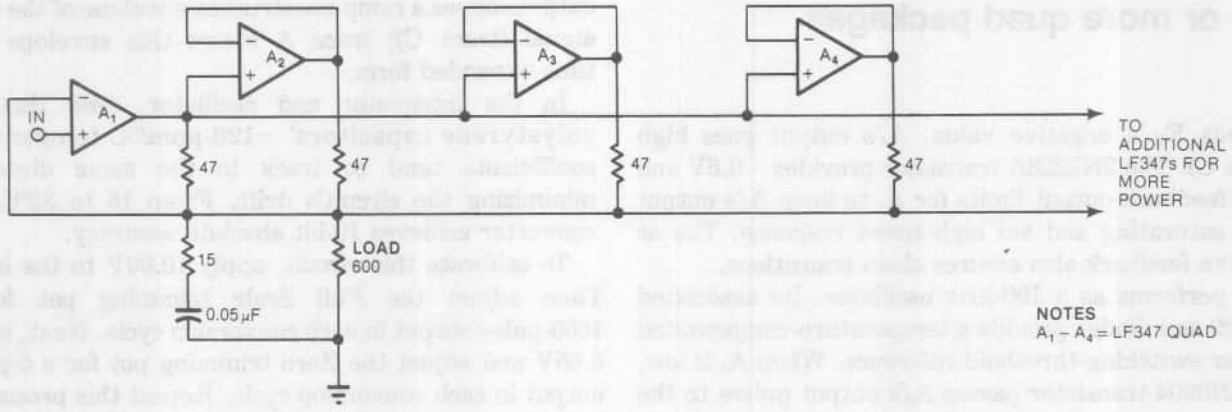

Fig 12—Utilizing current-amplifying capabilities, *one LF347 can drive a 600Ω load to ±11V. For additional power, two LF347s can supply an output current of ±40 mA.*

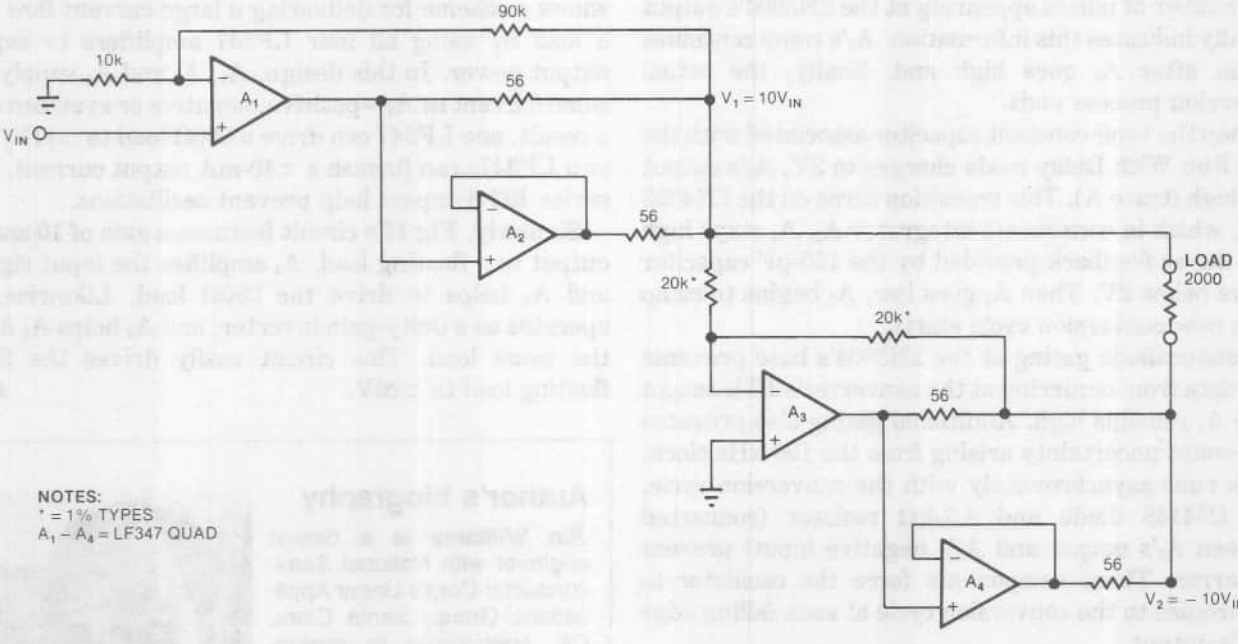

Fig 13—Configured as a high-output-current amplifier *with a gain of 10, this LF347 circuit can drive a 2000 Ω floating load to ±20V.*

a voltage derived from the LM329 reference. Diode D_2, located in the Reference pot's wiper arm, compensates for D_1. In A_2's feedback loop, D_3 prevents negative voltages from conducting to the transistor and the electrolytic 2-µF feedback capacitor upon start-up.

At a gain of 10, A_2 amplifies the difference between the reference and output signals. Additionally, A_2's output provides collector bias for the 2N2222A, completing an amplitude-stabilizing feedback loop around the oscillator. The electrolytic capacitor furnishes stable loop compensation.

To set the circuit's output amplitude, adjust the 5-kΩ pot until a precision voltmeter reads 2.50V rms at the sine-wave output terminal. For a ±5V variation in either power supply, the sine-wave output shifts less than 1 mV. Other key specs include 250-µV/°C typ drift and less than 1% distortion.

Versatile A/D converter employs quad op-amp IC

In addition to temperature- and oscillator-type circuits, the LF347 quad IC further demonstrates its versatility by implementing an integrating A/D converter (**Fig 9**). Either internally or externally triggered, this circuit delivers a 10-bit serial output word in 10 msec (full-scale conversion time).

To understand this circuit's operation, assume that the Mode Select switch is set to the Free Run With Delay position and the 2N4393 FET has just turned off. The A_2 integrator—biased from the LM329 reference—then begins to ramp in a negative-going direction (**Fig 10**, trace B). A_4 compares this ramp with the positive E_{IN} input voltage. When A_2's ramp potential barely

Obtain high output current using one or more quad packages

exceeds E_{IN}'s negative value, A_4's output goes high (trace C). The 2N2222A transistor provides −0.6V and +7V feedback-output limits for A_4 to keep A_4's output from saturating and aid high-speed response. The ac positive feedback also assures clean transitions.

A_3 performs as a 100-kHz oscillator. Its associated LM329 and diodes provide a temperature-compensated bipolar switching-threshold reference. When A_4 is low, the 2N3904 transistor passes A_3's output pulses to the TTL output terminal. When A_4 goes high, the 2N3904 is biased ON, and the transistor shuts off the output pulses (trace D).

Because A_2 generates a linear output ramp, the time A_4 spends low is directly proportional to E_{IN}'s value. The number of pulses appearing at the 2N3904's output digitally indicates this information. A_2's ramp continues to run after A_4 goes high and, finally, the actual conversion process ends.

When the time-constant capacitor associated with the Free Run With Delay mode charges to 2V, A_1's output goes high (trace A). This transition turns on the 2N4393 FET, which in turn resets integrator A_2. A_1 stays high until the ac feedback provided by the 150-pF capacitor decays below 2V. Then A_1 goes low, A_2 begins to ramp and a new conversion cycle starts.

Resistor/diode gating at the 2N3904's base prevents false data from occurring at the converter's TTL output while A_1 remains high. Additional gating also prevents a ±1-count uncertainty arising from the 100-kHz clock, which runs asynchronously with the conversion cycle. The 1N4148 diode and 4.7-kΩ resistor (connected between A_1's output and A_3's negative input) prevent this error. These components force the oscillator to synchronize to the conversion cycle at each falling edge of A_1's output.

You can adjust the time between conversions in Free Run With Delay mode by changing the RC components connected to this selection-switch position. Moreover, you can trigger the converter externally using a 2V source.

In Free Run mode, the converter self-triggers immediately after A_4 goes high. The conversion time thus varies with the input voltage. Here, a positively biased sine wave (**Fig 11**, trace B) feeds to the converter's input. Because the converter resets and self triggers immediately after converting, A_2's ramp output shapes a ramp-constructed envelope of the input signal (trace C); trace A shows this envelope in a time-expanded form.

In the integrator and oscillator, note that the polystyrene capacitors' −120-ppm/°C temperature coefficients tend to track in the same direction, minimizing the circuit's drift. From 15 to 35°C, the converter achieves 10-bit absolute accuracy.

To calibrate this circuit, apply 10.00V to the input. Then adjust the Full Scale trimming pot for a 1000-pulse output in each conversion cycle. Next, apply 0.05V and adjust the Zero trimming pot for a 5-pulse output in each conversion cycle. Repeat this procedure until the adjustments converge.

Amplifiers supply high output current

Yet another role the LF347 quad can play is as an element in high-output-current amplifiers. **Fig 12** shows a scheme for delivering a large current flow into a load by using all four LF347 amplifiers to supply output power. In this design, A_2, A_3 and A_4 supply the same current as A_1—positive, negative or even zero. As a result, one LF347 can drive a 600Ω load to ±11V, and two LF347s can furnish a ±40-mA output current. The series RC dampers help prevent oscillations.

Similarly, **Fig 13**'s circuit features a gain of 10 and an output to a floating load. A_1 amplifies the input signal, and A_2 helps to drive the 200Ω load. Likewise, A_3 operates as a unity-gain inverter, and A_4 helps A_3 drive the same load. This circuit easily drives the 200Ω floating load to ±20V. **EDN**

Author's biography

Jim Williams is a design engineer with National Semiconductor Corp's Linear Applications Group, Santa Clara, CA, specializing in analog-circuit and instrumentation development. Previously, he worked as an analog systems and circuit consultant at Arthur D Little Inc and directed the Instrumentation Development Lab at the Massachusetts Institute of Technology. Jim studied psychology at Wayne State University. In his spare time, he enjoys tennis, skiing, art and collecting antique scientific instruments.

An elegant 6-IC circuit gauges relative humidity

"It's not the heat, it's the humidity"—traditionally an easy claim to make and a difficult one to prove. But now a few low-cost devices and some novel circuit tricks simplify humidity measurements.

Jim Williams, National Semiconductor Corp

For use in critical applications such as food processing, paper and lumber production, pollution monitoring and comfort control, the humidity-meter design presented here requires only about $30 worth of parts—in contrast to other configurations, which are far more expensive and often don't perform any better. This design also overcomes the calibration and signal-conditioning difficulties that complicate traditional approaches.

Consider some relatively simple concepts

The key to the relative-humidity (RH) meter lies in the signal conditioning it applies to the output of a humidity sensor. **Fig 1** depicts such a transducer's sensing characteristic—an approximately exponential resistance change spanning nearly four decades. You can linearize this response by taking the logarithm of the sensor's resistance and utilizing a breakpoint-approximation technique to minimize residual nonlinearities.

Consider further that no significant dc current component should be allowed to pass through the sensor; the device must be excited by an unbiased ac waveform to preclude detrimental electrochemical migration. Exhibiting a 0.36 RH-unit/°C positive temperature coefficient, the sensor consists of a chemically treated styrene copolymer, and because its humidity-sensitive portion resides at its surface, it responds fairly rapidly (on the order of seconds) to humidity changes.

Fig 2 illustrates the technique chosen to instrument the sensor. An amplitude-stabilized square wave (symmetrical about 0V) provides a precision alternating current through the sensor, satisfying the requirement for a zero-dc-component drive. To obtain a linear signal, the sensor's output feeds a current-sensitive logarithmic amplifier, whose input is at virtual ground. The circuit then scales, rectifies and filters this amplifier's output to provide a dc level proportional to relative humidity. In this final stage, breakpoint techniques compensate for residual nonlinearity arising from the sensor's nonlogarithmic response below 40% RH.

The hardware realization of these functions appears in **Fig 3.** Operating as a positive-feedback oscillator, A_{1A} outputs a symmetrical square wave (**Fig 4**) whose amplitude is stabilized by an LM334 current-source/diode-bridge combination. Biased by a 15Ω resistor, the 334 current-limits at about 5 mA, forcing

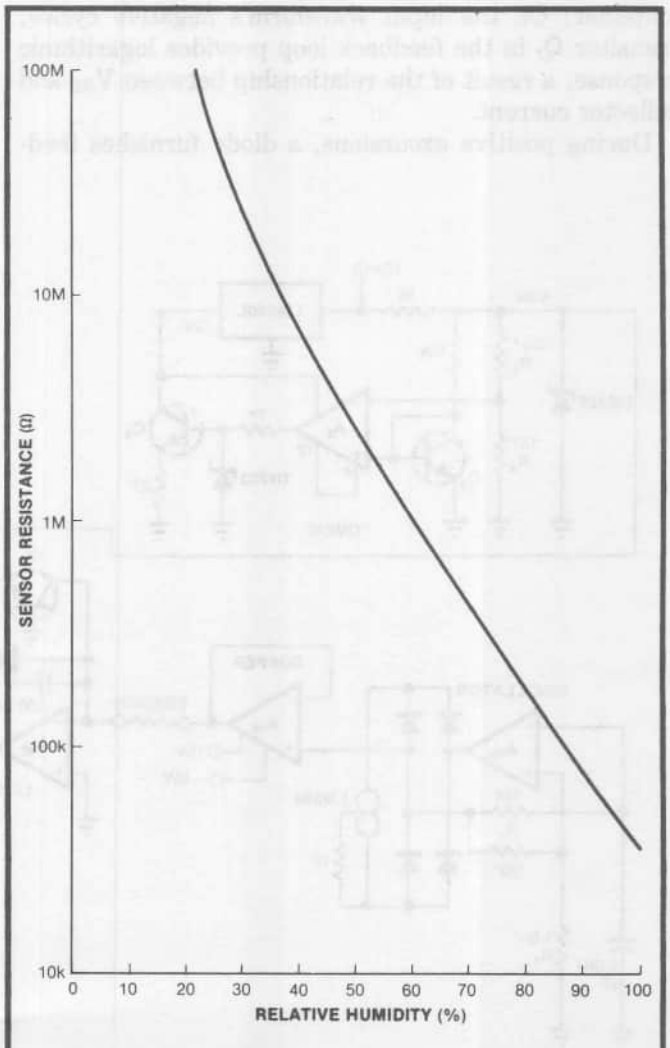

Fig 1—Resistance variation *with humidity follows a nearly log/lin relationship in a PCRC-11 sensor. Breakpoint circuit techniques can compensate for the slope change below 40% relative humidity.*

Accurate humidity measurement requires temperature stability

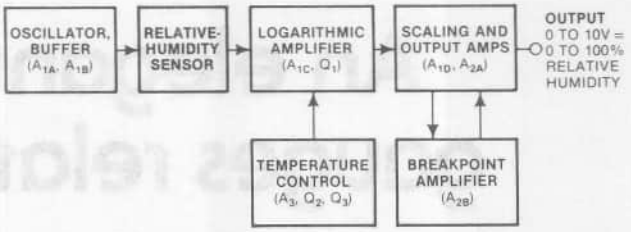

Fig 2—A humidity meter *employs a sensor to convert a temperature-compensated square-wave voltage generator into a humidity-controlled current source. Logarithmic-to-linear signal conversion is followed by a scaling amplifier and a gain-corrected output stage. (Device designations in parentheses refer to* ***Fig 3.****)*

the voltage across a divider (R_1, R_2) to stabilize at about ±8V. The waveform's amplitude stability depends upon the 334's 0.33%/°C temperature coefficient. (This TC was designed into the device to allow use in temperature-sensing and -compensation applications.)

The LM334's TC reduces the humidity sensor's −0.36%/°C temperature dependence by more than an order of magnitude, causing the sensor's thermally induced inaccuracy to drop out as an error term. (In practice, mount the LM334 near the humidity sensor.) The residual −0.03%/°C temperature coefficient is negligibly small compared with the sensor's ±1% accuracy specification and the circuit's overall 2% accuracy.

A transistor provides logarithmic response

Functioning as a buffer, A_{1B} drives a current through the sensor and into the summing junction of A_{1C}, the log amplifier. On the input waveform's negative cycles, transitor Q_1 in the feedback loop provides logarithmic response, a result of the relationship between V_{BE} and collector current.

During positive excursions, a diode furnishes feedback to the amplifier's summing junction. Thus, the summing junction always remains at virtual ground, while a negative-going square wave expresses the input current in logarithmic form at the transistor's emitter. Because the summing junction always remains at ground potential, the sensor sees the required symmetrical drive (**Fig 5**).

The log amplifier's output feeds to A_{1D}, an amplifier used to sum a 40%-RH trim with the main signal and provide adjustable gain to set a 100%-RH trim. A_{1D}'s output is filtered to dc and routed to A_{2A}, which unloads the filter and provides additional gain.

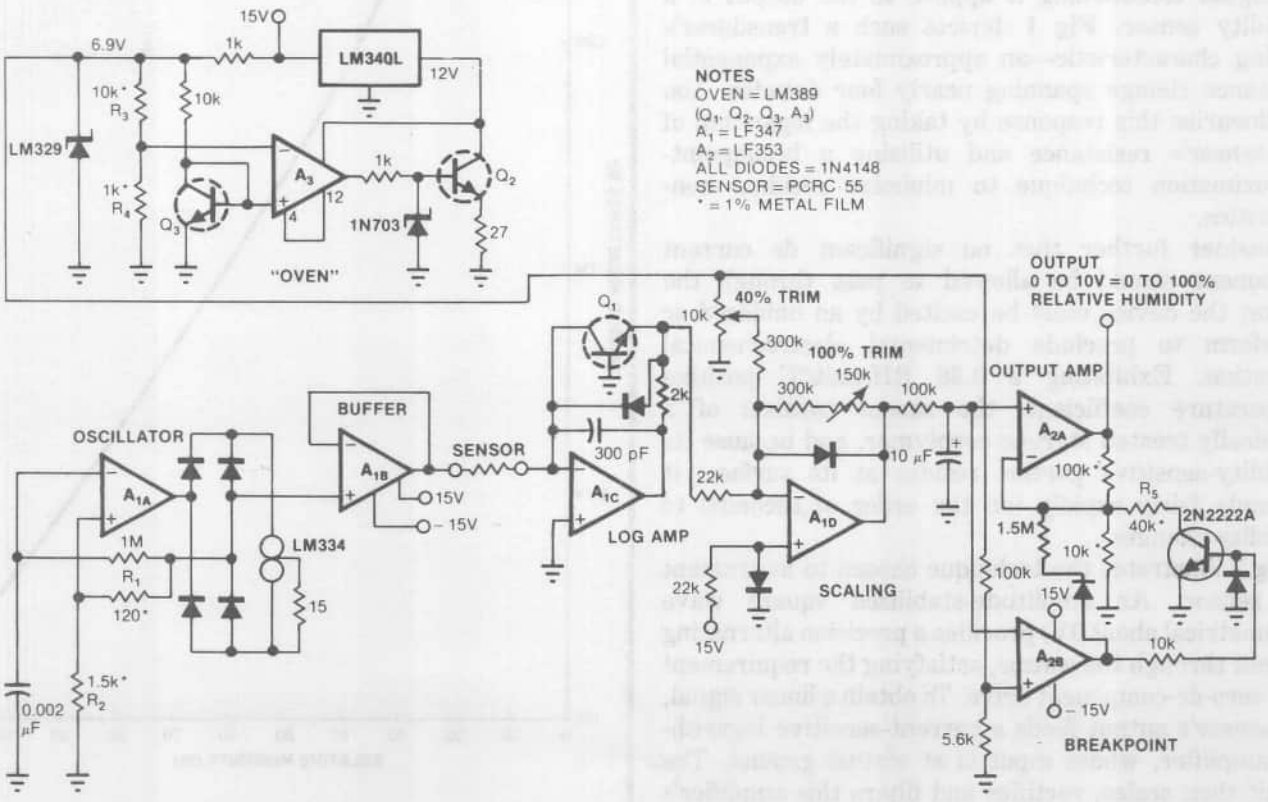

Fig 3—Novel circuit concepts *and a few ICs make low-cost humidity measurement a reality. Controlling the A_{1A} oscillator's amplitude compensates for the sensor's negative temperature coefficient. An oven-like environment (within the LM389, which senses and regulates its own temperature) stabilizes the operation of logging transistor Q_1.*

Breakpoint amplifier A_{2B} compensates for the sensor's departure from logarithmic conformity below 40% RH by changing A_{2A}'s gain for RH readings below that level. It performs this function by sensing the input to A_{2A} and swinging positive when this input goes below RH=40 (about 0.36V at A_{2A}'s positive terminal). This swing turns a 2N2222A on, causing the required gain change at the output amplifier. For RH values above 40%, the transistor is OFF, and the log amplifier alone determines the circuit's linearizing function.

An IC becomes an oven

In a logarithmic configuration such as this circuit, Q_1's dc operating point (and thus logging accuracy) varies wildly with temperature. This factor would normally mandate careful and extensive temperature compensation, which in turn would result in the expense normally associated with log amplifiers. But here, an LM389 (an audio-amplifier IC that also contains three discrete transistors) accomplishes the required temperature stabilization in a rather unorthodox—and inexpensive—manner.

LM389 transistor Q_3 functions as a chip-temperature sensor, while Q_2, another of the device's transistors, serves as a heater. The 389's amplifier, A_3, senses Q_3's temperature-dependent V_{BE} and drives Q_2, servoing the chip temperature to the setpoint established by a voltage divider (R_3, R_4). Q_1, the logging transistor, also resides in the 389 and thus operates in a tightly controlled thermal environment (typically at 50°C), immune to ambient-temperature shifts. (An LM329 voltage reference ensures power-supply independence for the temperature setpoint, and an LM340L 12V regulator provides safe operation from the 15V supply for the 12V temperature controller.)

How does the oven work? When the circuit first turns on, the voltage at Q_2's emitter is about 3.3V, resulting in a current flow of 120 mA. This current forces Q_2 to dissipate about 1.5W, which raises the chip to operating temperature very rapidly. At this point, the thermal servo takes control and reduces the power.

The LM340 regulator has only 3V across it, so its dissipation never exceeds about 0.3W. A zener at the base of Q_2 prevents servo lockup during circuit initialization. Because the LM389's chip is small, it warms quickly and consumes little power.

Fig 6 shows the thermal servo's performance for a step function of 7 °C change in setpoint. Note how the output responds almost instantaneously, and how complete settling to the new setpoint occurs within 100 msec.

Simple adjustments calibrate the circuit

To adjust this circuit, ground Q_2's base, apply circuit power and measure Q_3's collector potential at a known room temperature. Next, calculate Q_3's collector potential at 50°C, allowing −2.2 mV/°C. Select R_4's value (≈ 1 kΩ) to yield a voltage at A_3's negative input close to the calculated 50°C potential. (This adjustment can be a fairly loose trim, because the exact chip

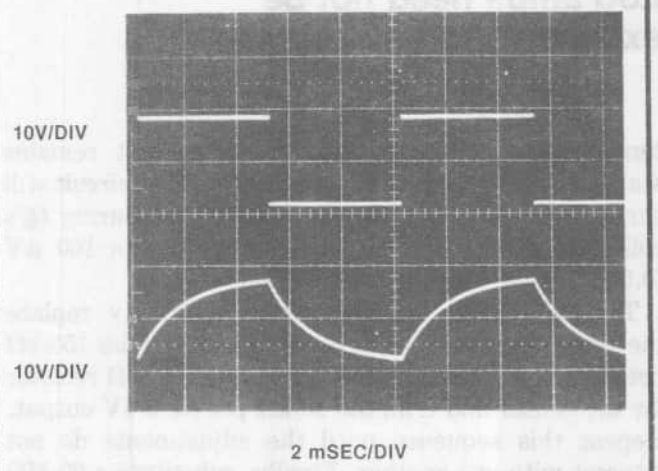

Fig 4—An amplitude-stabilized square wave *(upper trace) drives the humidity sensor. Operating as a positive-feedback oscillator, A_{1A} in* **Fig 3** *switches when its negative input port reaches threshold level (lower trace).*

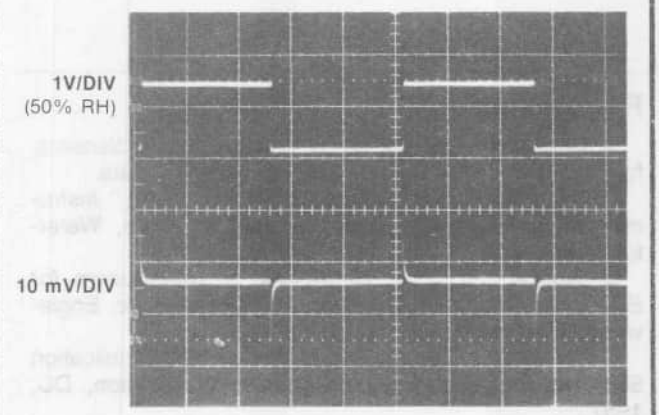

Fig 5—Sensor linearization *is accomplished by the Q_1/A_{1C} stage in* **Fig 3.** *A signal at Q_1's emitter (upper trace) is logarithmically converted and fed back to the op amp's summing junction (lower trace). The residual peaks cancel, leaving a true dc level proportional to measured humidity.*

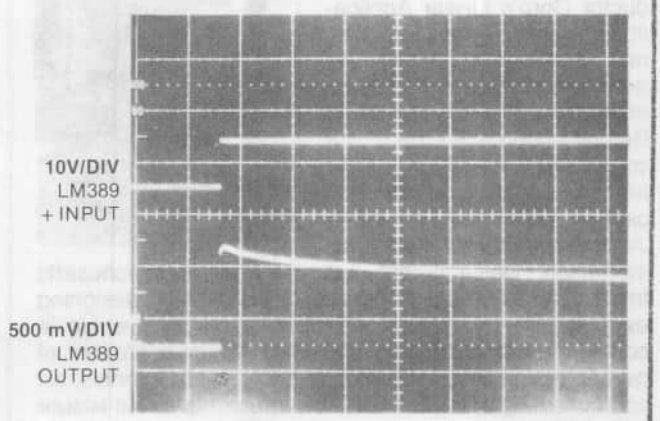

Fig 6—Rapid thermal regulation *results with the LM389 "oven." The circuit completely stabilizes an equivalent 7°C change in setpoint temperature (upper trace) within 100 msec (lower trace).*

Log amps need not be expensive to be accurate

temperature is unimportant so long as it remains stable.) Finally, unground Q_2's base, and the circuit will servo. You can check this function by measuring Q_3's collector voltage and noting stability within 100 μV (0.05°C) while blowing on the LM389.

To calibrate the circuit for relative humidity, replace the sensor with a 35-kΩ resistor and trim the 150-kΩ pot for a 10V output. Next, substitute a 5-MΩ resistor for the sensor and trim the 10-kΩ pot for a 4V output. Repeat this sequence until the adjustments do not interact with one another. Finally, substitute a 60-MΩ resistor for the sensor and select an R_5 value (nominally 40 kΩ) for a reading of RH=24% (2.4V). The circuit is now calibrated and will read ambient relative humidity when the PCRC-55 sensor is connected. **EDN**

References

1. Phys-Chemical Research Corp, *Humidity Sensors,* for Models PCRC-11 and PCRC-55 technical data.
2. Widerhold, P R, "Humidity Measurement," *Instrumentation Technology,* General Eastern Corp, Watertown, MA.
3. Norton, Harry N, *Handbook of Transducers for Electronic Measuring Systems,* Prentice-Hall Inc, Englewood Cliffs, NJ, 1969.
4. Wexler, A, *Electric Hygrometers,* NBS Publication 586, National Bureau of Standards, Washington, DC, 1957.

Author's biography

Jim Williams, design engineer with National Semiconductor Corp's Linear Applications Group, Santa Clara, CA, has made a speciality of analog circuit design and instrumentation development. Before joining NSC, he was a consultant with Arthur D Little Inc in analog systems and circuits. From 1968 to 1977, Jim was director of the Instrumentation Development Lab at the Massachusetts Institute of Technology, where in addition to designing experimental biomedical instruments, he was active in course development and teaching. A former student of psychology at Wayne State University, he lists tennis, art and collecting antique scientific instruments as his leisure interests.

Designer's Guide to: Temperature measurement

Having selected the optimum sensor for your application, you now must convert its output into a useable signal.

Jim Williams, Dept. of Nutrition and Food Science, Massachusetts Institute of Technology

Part 1 of this tutorial reviewed the characteristics of the various transducers that can sense levels of heat. But whatever device you choose for your temperature-measurement application, you will also need signal-conditioning circuitry—the subject of this article.

Signal-conditioning circuitry must accurately convert the sensor's output into information meaningful to the user. Requirements for such circuitry vary considerably. In some applications, the electronics exists in a low-noise laboratory environment but must perform ultra-precise measurements. In others, it's located thousands of feet from the sensor and in a high-noise environment, but the accuracy requirements are relaxed. Whatever the case, you should recognize that sensor characteristics, signal conditioning and qualitative results are interrelated, inseparable issues.

For straightforward problems—simple solutions

Designers can take simple and reliable "GO/NO-GO"-type temperature measurements with thermoswitches and electrical-output mercury thermometers. A single thermoswitch can determine if an object or process has reached a predetermined temperature, or it can also perform dual limit functions. **Fig. 1a** shows how a mercury thermometer with two switch contacts can be used on an assembly line to inexpensively check the temperature of an instrument's component ovens. The technician inserts the thermometer bulb into a well in the oven, then the bulb will light only if the temperature lies within preset limits.

Fig. 1b shows a similar arrangement. Here, two thermoswitches monitor the wall temperature of a chemical vat that must remain between 45 and 60°C while being filled. If the wall temperature is within these limits, the relay is energized and issues a command to fill the vat. At lower or higher temperatures, the relay deenergizes, stopping the filling process.

Analog readouts are easily obtained with a thermistor or other resistive sensor in a simple, uncalibrated deviation bridge **(Fig. 2).** Here the meter reads zero when $R_1 = R_2$ and indicates deviations from this point. This type of readout serves "ballpark" checks of equipment. Despite the fact that both the sensor and bridge responses are nonlinear, the meter reading will be approximately linear for small deviations and/or can be calibrated for large spans.

An unreferenced thermocouple can also read deviations from a reference temperature. In **Fig. 3,** a thermocouple monitors temperatures inside a furnace. Of course, the exact temperature proves difficult to determine because the thermocouple is unreferenced. But since the meter is only calibrated in terms of "hot" and "cold," the measurement scheme sufficies. The op amp

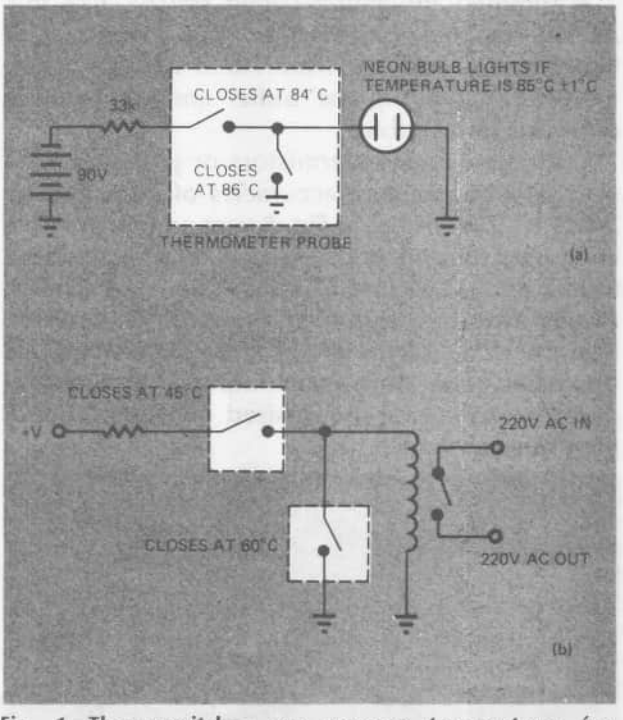

Fig. 1—Thermoswitches can measure temperatures for GO/NO-GO situations. In **a,** a mercury thermometer with two switched contacts provides a ±1° check on crystal ovens during assembly. In **b,** an arrangement of snap-action devices determines the temperature in a vat and issues switching commands to a fill control relay.

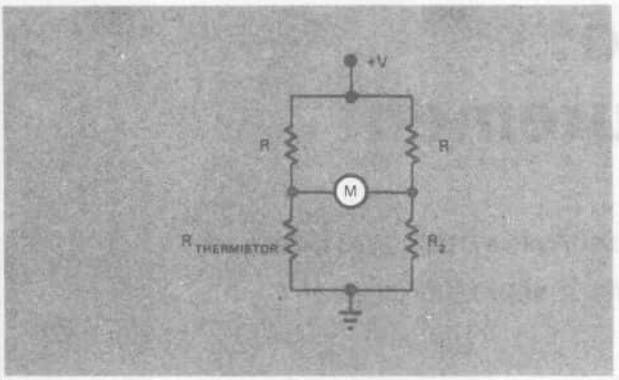

Fig. 2—As the thermistor's value approaches that of R_2, the meter reading approaches zero. Despite nonlinearities in the bridge and sensor response, a linearly calibrated meter proves quite accurate for small temperature ranges.

provides the gain needed to drive the meter.

When greater accuracies are needed....

Calibrated systems require more sophistication. In **Fig. 4,** a low-cost sensor (1N914 diode) provides ±1° accuracy over 0 to +100°C. Calibration is simple: Put the diode in a 0°C environment and adjust the zero potentiometer for 0V output, then place the diode in a 100°C environment and adjust the F.S. potentiometer for a 10V output. (This procedure should be repeated until interaction between the adjustments ceases.) Although this circuit is inexpensive, its calibration is time consuming.

A trimmed integrated-circuit sensor, like the AD590, requires no calibration at all. The circuit of **Fig. 5** reads within ±1° from 148 to 473°K (−125 to +200°C). Offsetting the buffer amplifier makes other scales possible.

Calibrated linear thermistors or platinum sensors provide absolute accuracies of from 0.15 to >0.01°C. The circuit of **Fig. 6** uses an inexpensive linearized thermistor composite to achieve absolute accuracy of 0.15°C over 0 to +100°C. The AD580 band-gap reference drives the 741J, which has the YSI 44018 temperature sensor in its feedback loop. The voltage output of A_1 feeds A_2, and the latter sets the desired output gain and provides zeroing.

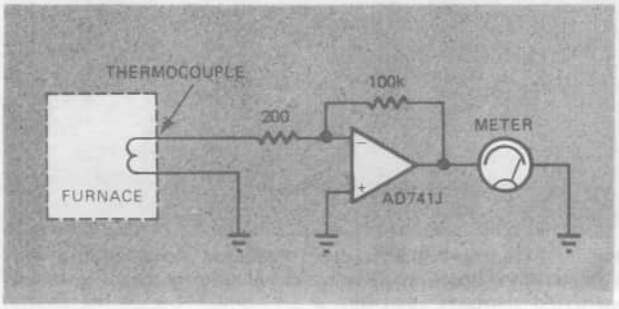

Fig. 3—To get a "hot" or "cold" indication of the heat in a furnace, an unreferenced thermocouple driving a simple amplifier suffices.

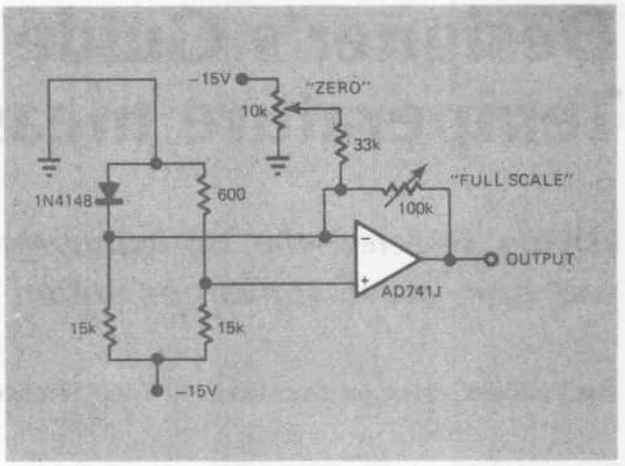

Fig. 4—After a 2-point calibration, this circuit provides ±1° accuracy over 0 to +100°C.

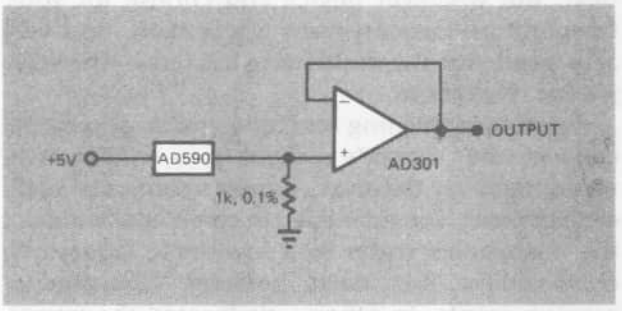

Fig. 5—Factory trimming of the AD590 IC temperature sensor permits this circuit to measure temperatures from −125 to +200°C with 1° accuracy.

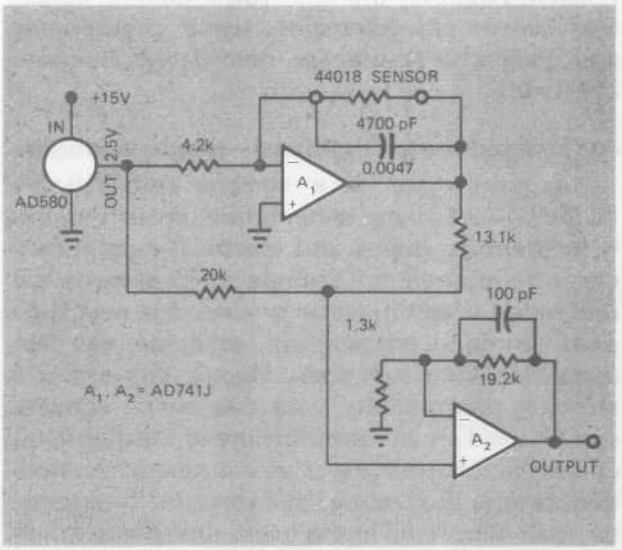

Fig. 6—An inexpensive, linearized thermistor generates the temperature-dependent signal, then A_2 provides needed gain and offset. Circuit achieves 0.15°C absolute accuracy over 0 to +100°C.

A high-resolution differential thermometer

Fig. 7 diagrams a high-performance, extremely versatile temperature-measuring instrument that can handle applications ranging from determining heat-sink temperature rise to performing microcalorimetry. It reads a thermistor sensor

from any of eight switch-selected inputs to 100 μ° resolution over a 0 to +100°C range with 0.15°C absolute accuracy. Additionally, this device measures the temperature difference between two sensors to 100 μ° sensitivity.

The circuit is basically the thermometric equivalent of a differential voltmeter. Temperature is directly dialed out on the 5-decade Kelvin-Varley voltage divider. Differences between this temperature and that of the sensor are observed on the meter. Full-scale sensitivity of the meter varies from 50 to 0.001°C and is controlled by the gain of the chopper-stabilized null detector. Fully floated from instrument ground, the null detector provides high sensitivity and low noise and drives both the meter and a 275J isolation amplifier. The latter supplies a ground-referenced strip chart recorder output.

In the "Read Absolute" mode, the null detector compares the voltage from the sensor network to that at the Kelvin-Varley divider output. Since both the sensor network and K-V divider are driven from the same potential, the measurement is ratiometric and a stable reference is not

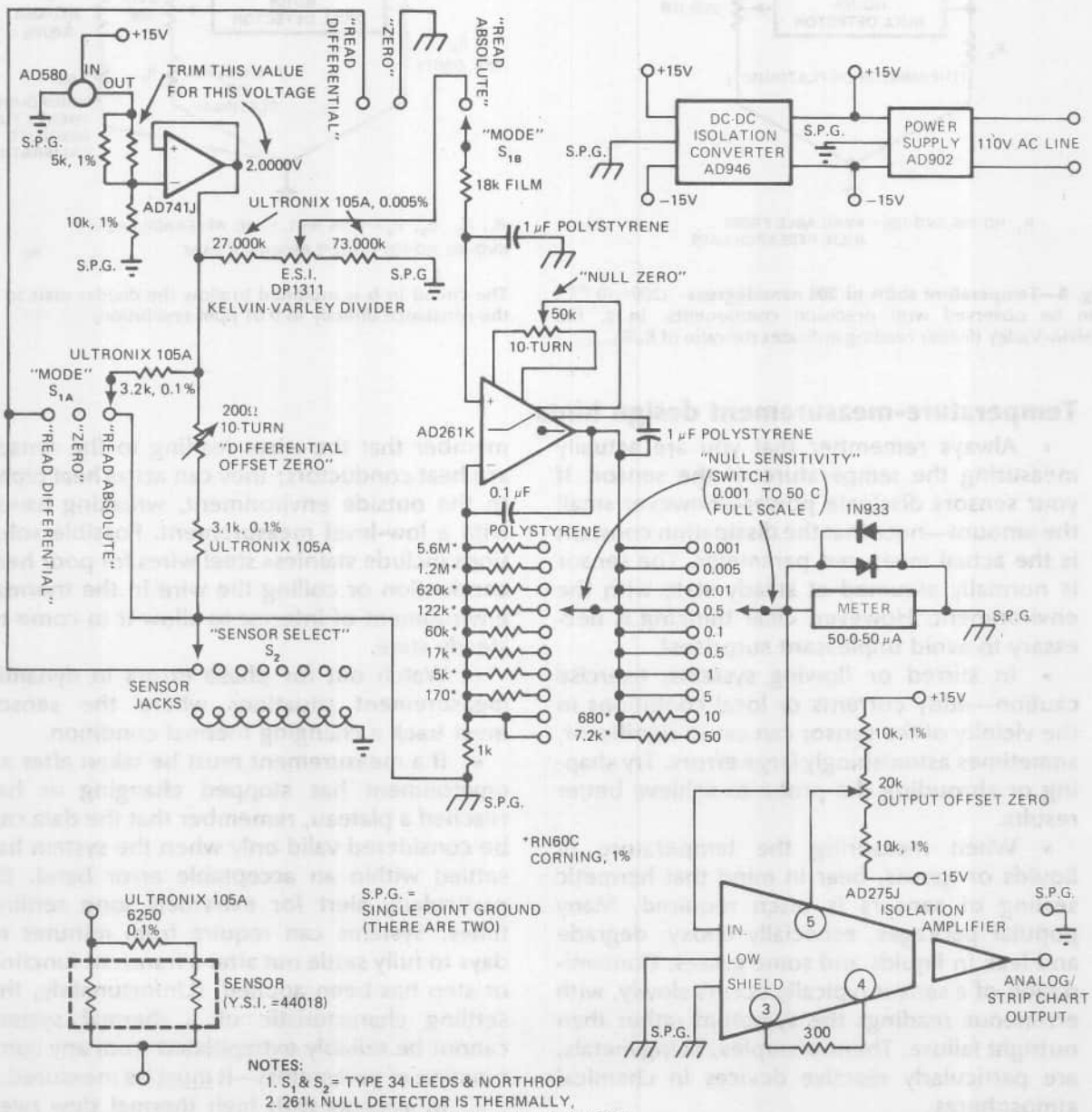

Fig. 7—Kelvin-Varley voltage divider setting reads temperature directly in this differential thermometer. Gain of the null detector varies the F.S. sensitivity from 0.001 to 50°C. Unit can indicate 100 μ° shifts in sensitivity.

required. In this mode, the temperature of an environment or surface can be determined to 0.15°C absolute accuracy. Moreover, shifts in stability of 100 μ° are directly readable.

In the "zero" mode, the null detector offset can be trimmed out with the "zero" control.

In the "Read Differential" mode, sensor number 1 reads differentially against any of the other seven switch-selected sensors. This mode can be used for microcalorimetry, where both sensors are in close physical proximity in a controlled thermal environment. Typically, one sensor is

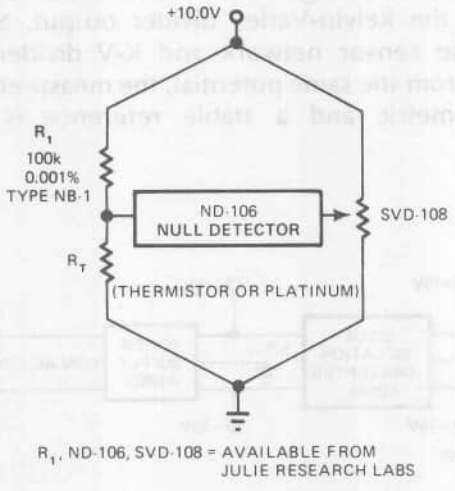

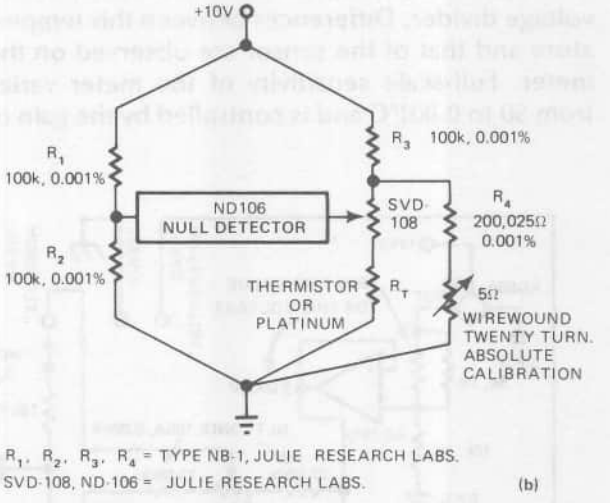

Fig. 8—Temperature shifts of 200 nanodegrees (200×10^{-7}°C) can be observed with precision components. In **a,** the Kelvin-Varley divider reading indicates the ratio of $R_1/R_{thermistor}$. The circuit in **b** is modified to allow the divider dials to read the resistance directly to 0.01 ppm resolution.

Temperature-measurement design hints

- Always remember that you are actually measuring the temperature of the sensor. If your sensors dissipate power—however small the amount—note that the dissipation constant is the actual measured parameter. The sensor is normally assumed at steady state with the environment. However, clear thinking is necessary to avoid unpleasant surprises!
- In stirred or flowing systems, exercise caution—eddy currents or local conditions in the vicinity of the sensor can cause significant, sometimes astonishingly large errors. Try shaping or shrouding the probe to achieve better results.
- When measuring the temperature of liquids or gasses, bear in mind that hermetic sealing of sensors is often required. Many popular packages, especially epoxy, degrade and leak in liquids and some gasses. Contamination of a sensor typically occurs slowly, with erroneous readings the symptom rather than outright failure. Thermocouples, being metals, are particularly reactive devices in chemical atmospheres.
- In precision measurements, keep the dissipation in the sensor down when looking for high absolute accuracy or when attempting to detect small changes in temperature. Remember that the wires leading to the sensor are heat conductors; they can act as heat pipes to the outside environment, wreaking havoc with a low-level measurement. Possible solutions include stainless steel wires for poor heat conduction or coiling the wire in the thermal environment of interest to allow it to come to steady state.
- Watch out for phase errors in dynamic measurement situations where the sensor must track a changing thermal condition.
- If a measurement must be taken after an environment has stopped changing or has reached a plateau, remember that the data can be considered valid only when the system has settled within an acceptable error band. Be particularly alert for extremely long settling times. Systems can require from minutes to days to fully settle out after a transient function or step has been applied. (Unfortunately, the settling characteristic of a thermal system cannot be reliably extrapolated from any combination of parameters—it must be measured.)
- In systems with high thermal slew rates over wide temperature ranges, monitor sensor performance very carefully. All sensors show some calibration shift after repeated exposure to thermal shock.

coated with reactive biochemicals, while its uncoated twin serves as a reference. When additional biochemical agents are introduced, the coated sensor becomes 100 to 300 μ° warmer than the reference (due to heat of reaction), and the instrument reads this difference. The "Read Differential" mode can also serve such common applications as determining the gradient between a power transistor and various points on its heat sink.

Taking good ideas one step further

Really precise measurements of absolute temperature and temperature deviations call for state-of-the-art components. **Fig. 8** shows an arrangement for reading a thermistor or platinum sensor to better than 0.01 ppm resolution. The 8-decade resolution Kelvin-Varley divider allows tracking of 0.001Ω shifts in a 100 kΩ thermistor. This arrangement provides the electronic capability to detect 200 nanodegree (200×10^{-9}°C!) temperature shifts and has been used to perform 500 pW microcalorimetry. (A single human cell operates at about the nanowatt level.)

The K-V divider readout gives the ratio of the sensor to R_{std}, from which the absolute value of the sensor can be calculated. If you alter the bridge structure **(Fig. 8b),** the divider dials can indicate the absolute value of the sensor directly in ohms.

Note that the concepts employed in these ultra-precision circuits are merely extensions of the simple circuits presented in the beginning of this article—the major differences being the greater difficulty of manufacture and the substantial increase in cost.

This T-to-F converter uses a diode sensor

Many measurement situations call for digital output of temperature information. **Fig. 9a** depicts a direct temperature-to-frequency converter that can be built for a parts cost of less than $5. The circuit uses a diode sensor for economy and responds with a 0 to 1 kHz output for 0 to +100.0°F. Accuracy is ±0.3°F.

Operation is basically that of an operational-amplifier controlled relaxation oscillator, where the −2.2 mV/°C temperature shift of the diode determines the charging rate of the 4300 pF capacitor. The 100 pF capacitor provides feed-forward compensation for the 301 amplifier, decreasing the oscillator's reset time to ensure linearity. A 1N821 compensated zener stabilizes the circuit against supply-voltage changes. At the output, the 680 pF/2.2 kΩ network differentiates the 400 nsec reset edge of the op amp's negative-going output ramp and drives the single transistor inverter.

Note that a current source does not drive the sensor diode as you might expect. Instead, the loading error that the "−" input resistor imposes on the 1k potentiometer's output has been calculated to offset the slightly nonlinear response of the voltage-driven 1N4148.

Variations of T-to-F's abound. **Fig. 9b** shows a circuit that uses the current-source output of a current-ratioed, differential pair IC temperature transducer for low parts count. This scheme provides 125 to 470 Hz for 125 to 470°K. But if even greater simplicity is desired, **Fig. 9c** shows how the on-chip temperature sensor in an AD537 IC voltage-to-frequency converter can perform direct T-to-F conversion using only four external parts.

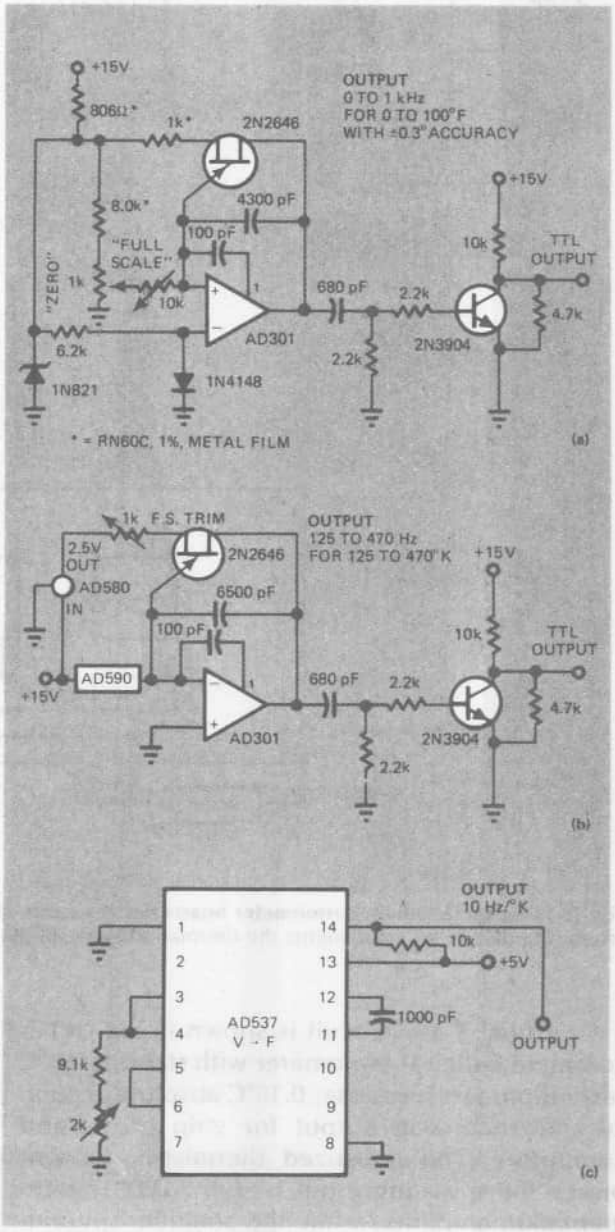

Fig. 9—Variations on a theme: Each of these circuits produces an output pulse train whose frequency is proportional to temperature.

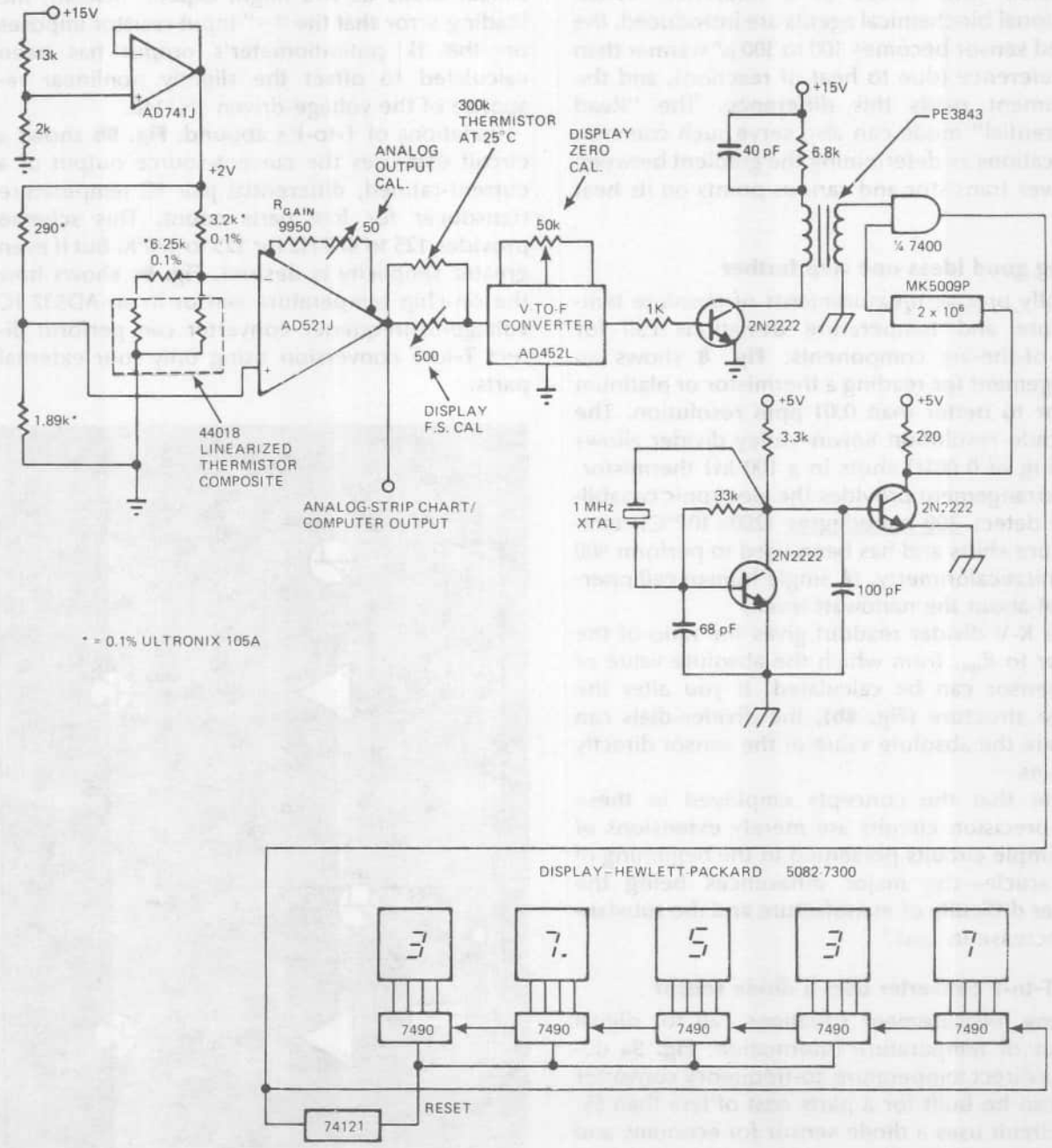

Fig. 10—Complete 5-digit thermometer boasts fast response, stable 0.001°C resolution and 0.15°C absolute accuracy. The 2-sec readout update rate complements the thermal response of the thermistor network.

One final T-to-F circuit is shown in **Fig. 10**—a complete 5-digit thermometer with stable 0.001°C resolution, fast response, 0.15°C absolute accuracy and an analog output for strip charts and computers. The linearized thermistor network biases the inverting input of the AD521 instrumentation amplifier, while the amplifier's noninverting input is driven from the same reference that drives the sensor. Output of the AD521—a precise 0 to 10V for 0 to +100°C—feeds the voltage-to-frequency converter that digitizes the analog signal.

The circuit's 2-sec update rate complements the sensor's thermal response. Further, the thermistor across the V-to-F's gain setting resistor provides sufficient temperature compensation to achieve stable 0.001°C resolution over a 20 to 30°C instrument ambient.

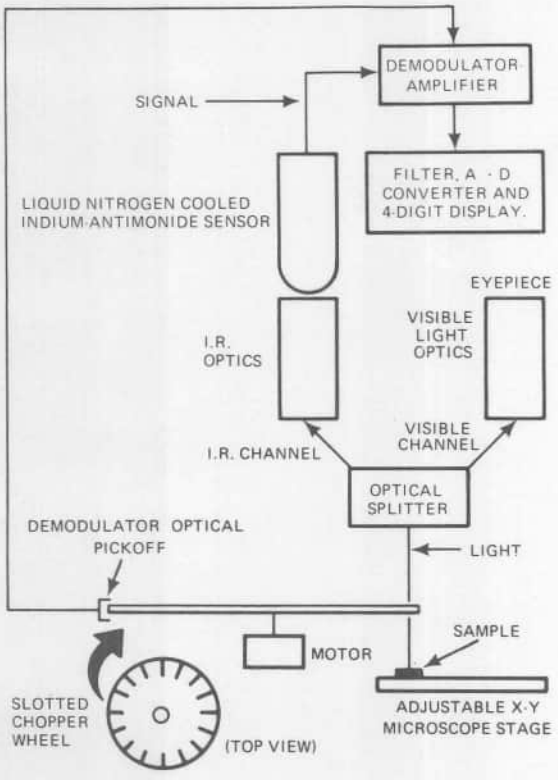

Fig. 11—Noncontact temperature measurements to 0.01°C resolution can be achieved by this IR thermal microscope.

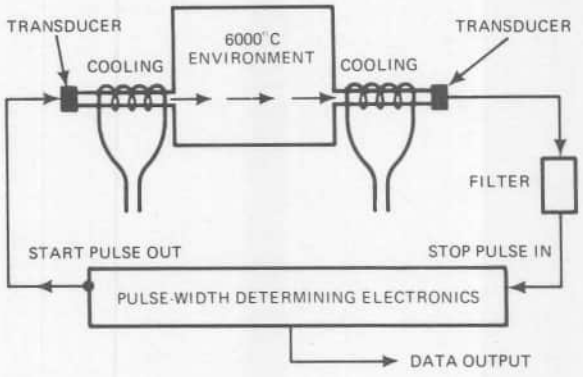

Fig. 12—For measurements at temperature extremes, an acoustic thermometer fills the bill. The medium through which the pulse must travel must be known, however.

Look, but don't touch...

Part 1, the May 5th article, described applications that require noncontact temperature measurements, detailed the infrared (IR) sensors that can be used in such cases and briefly mentioned an IR thermal microscope being developed at M.I.T.'s Nutrition and Food Science Instrumentation Laboratory. **Fig. 11** block diagrams that unit. Its 0.01°C resolution and digital display will permit researchers to monitor the progress of cancerous cells across a piece of tissue. The unit can also be used in IC design to determine the exact temperature difference between the input transistors of a low-drift op amp. From this data the optimum thermal layout can be determined.

In operation, a slotted wheel optically chops the light from the sample. The chopped light is then split into infrared and visible channels, the latter being used in the normal fashion. The IR channel, however, is sensed by a high-performance detector which is cooled by liquid nitrogen to keep noise as low as possible. The detector's output feeds an amplifier that is switched at the chopping frequency. The resultant synchronously demodulated output is filtered, converted to digital and displayed on a 4-digit readout.

Acoustic thermometers can also take accurate noncontact measurements at temperature extremes if the medium through which the sonic pulse must travel is known. **Fig. 12** shows an acoustic thermometer being used to determine the temperature of a 6000°C environment. The sonic transducers are maintained at relatively low temperatures outside the super-hot area. Of course, the pathlengths of the extension tubes must be thermally and sonically defined, because they must be subtracted out as an offset by the circuitry that determines the temperature-related pulse width.

Control comes next....

In our June 20, 1977 issue, Part 3 will conclude this series with an in-depth treatment of thermal control systems. We will emphasize practice rather than theory: Nine different actual working circuits will be presented, including one that can hold the temperature in an oven to within 3.3 μ° over a 3-hr period. A potpourri of general design hints will provide a reference overview and series wrap-up. □

Bibliography

1. Julie, L., Laboratory Manual for DC Measurement, Julie Research Labs., New York, NY.
2. Koch, C., "Diode or Transistor Makes Fully Linear Thermometer," Electronics, May 13, 1976.
3. Williams, J., "T - F Direct Reading Converter Yields Temperature," Electronics, April 3, 1975.
4. Williams, J., "Temperature Control to Microdegrees," M.I.T. Dept. of Nutrition and Food Science, Cambridge, MA.
5. Williams, J., "Prevent Low Level Amplifier Problems," Electronic Design, Feb. 15, 1975.

Low-cost instrument measures 4-decade power

Using standard parts, a watt/watt-hour meter calculates power consumption for line-powered devices over an extremely wide measurement range—2W to 2 kW FS. And its multiple analog and digital outputs allow both direct and time-related power readings.

Jim Williams, National Semiconductor Corp

If you must monitor the usage of costly electricity in commercial, industrial or consumer equipment designs, build the inexpensive but versatile watt/watt-hour meter described in this article. It resolves power measurements to as low as 0.1W, achieving 2% accuracy over 25±5°C. And it can determine the power consumption of any 115V ac unit, from large factory machines to small hand-held tools. The instrument requires only about $175 worth of off-the-shelf parts, whereas many conventional power meters cost much more and provide lower performance.

To handle a wide variety of power measurements, mostly in cases where energy conservation has high priority, the instrument provides three analog and two digital power-related outputs. One analog output—serving a 200-μA FS meter—displays power values in watts. Another furnishes 0 to 5V for driving strip-chart recorders, while the third supplies instantaneous-power-output levels for use in external-tracking applications. One of the digital outputs—a readout—indicates time-based or watt-hour readings; the second supplies watt-hour data for use by external equipment.

A look at the overall approach

The watt/watt-hour meter's design is straightforward (**Fig 1**). The device under measurement plugs into a standard 115V ac outlet mounted on the instrument's front panel. With line power applied, the ac voltage across the monitored load passes through a resistor divider and feeds (via an op amp) to an analog

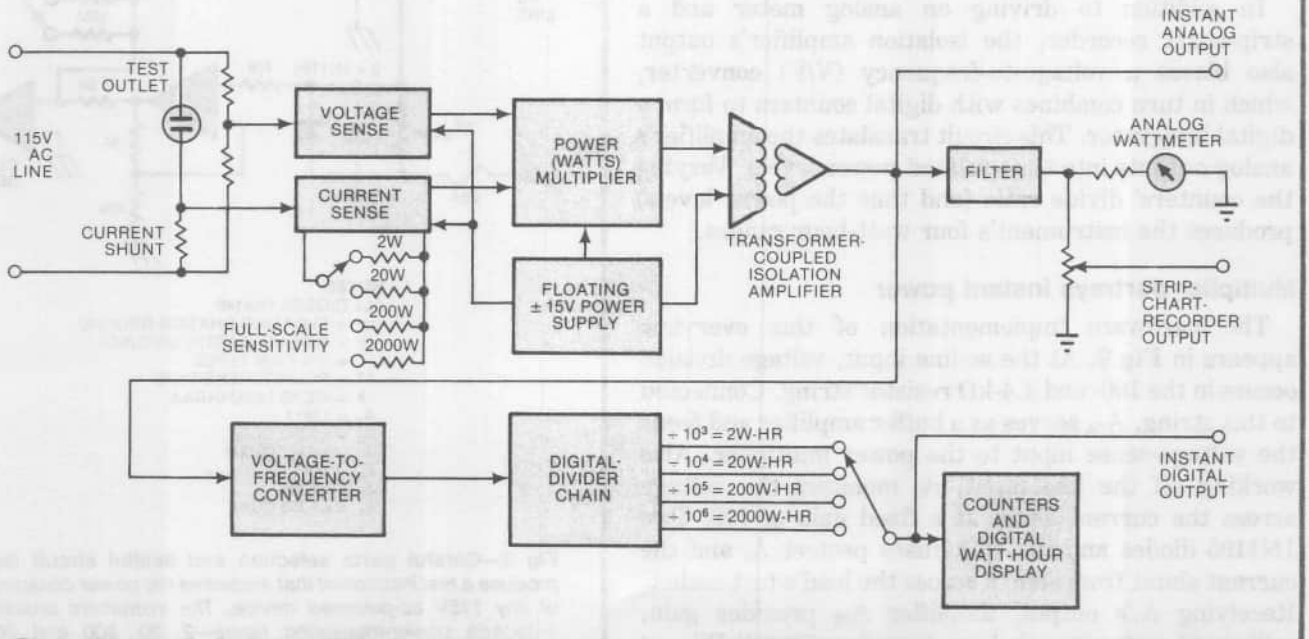

Fig 1—An inexpensive watt/watt-hour meter *incorporates (in series) a current shunt, voltage- and current-sense amplifiers, a power multiplier and a transformer-coupled isolation amplifier. These circuits generate amplitude-modulated pulses that represent the monitored device's instantaneous power consumption, measured in watts. Voltage-to-frequency conversion precedes a counter and a digital display of power levels in watt-hours.*

Single low-resistance shunt handles all four power ranges

power multiplier.

The voltage across a low-resistance shunt represents the current through the load. Even when measuring a 20A max flow, this shunt needs only 133 mV—a feature that eliminates high-resistance-current-shunt inaccuracies. Additionally, by accommodating all four power ranges—2, 20, 200 and 2000W FS—the single shunt eliminates the need to switch-in high-impedance shunts for high-sensitivity scales.

The instrument's measurement technique utilizes the low input error in a current-sense amplifier, whose output also goes to a power multiplier. Switchable gain within the amplifier makes possible the 4-decade sensitivity setting. A 4-quadrant configuration, the power multiplier produces an output representing the test load's true instantaneous-power product (E×I), regardless of the load's relative voltage and current phases.

Because the multiplier and its associated voltage- and current-sense amplifiers connect directly to the ac line, though, they require a floating ±15V power supply. Consequently, you can't safely monitor their outputs with grounded test equipment, such as strip-chart recorders. To deal with this problem, the multiplier's output drives an isolation amplifier that operates at unity gain but has no galvanic connection between its input and output terminals. The amplifier employs pulse-amplitude-modulation techniques in conjunction with a small transformer. By grounding its output, you can safely connect test equipment to all circuits following the transformer.

In addition to driving an analog meter and a strip-chart recorder, the isolation amplifier's output also biases a voltage-to-frequency (V/F) converter, which in turn combines with digital counters to form a digital integrator. This circuit translates the amplifier's analog outputs into time-related power levels. Varying the counters' divide ratio (and thus the power levels) produces the instrument's four watt-hour ranges.

Multiplier portrays instant power

The hardware implementation of this overview appears in **Fig 2.** At the ac-line input, voltage division occurs in the 100- and 4.4-kΩ resistor string. Connected to this string, A_{2A} serves as a buffer amplifier and feeds the voltage-sense input to the power multiplier. Also working off the line input, A_1 monitors the voltage across the current shunt at a fixed gain of 100. Two 1N1195 diodes and two 20A fuses protect A_1 and the current shunt from shorts across the load's test socket. Receiving A_1's output, amplifier A_{2B} provides gain, calibrated wattage switching from 2 to 2000W FS and the power multiplier's current-sense input.

Composed of amplifiers A_{3C} and A_{3D} and an LM394 IC's dual transistors, the multiplier—a variable transconductance type—uses its current-sense input to vary a 2N2222 transistor amplifier's gain. This amplifier receives A_{2A}'s voltage-sense output as its input.

At the multiplier's output, A_{3C} produces an output representing the load's instantaneous power consumption (**Fig 3,** trace A). This output in turn biases a pulse-amplitude-modulating isolation amplifier (A_{3A} and A_{3B}) and three transistors (Q_1 to Q_3).

Generating an oscillator output (trace B), A_{3A} biases the Q_1/Q_2 switch connected across the transformer's primary. Meanwhile, A_{3B}'s negative input measures the pulses' amplitude at the transformer's primary. A_{3B} then servo-controls the pulses to the same amplitude as those received at its positive input (biased by the multiplier's output). Transistor Q_3 provides current-drive capability and completes A_{3B}'s feedback path.

Trace C in **Fig 3** illustrates how Q_3's emitter voltage changes to meet the servo-loop requirements. Trace D shows the pulses applied to the transformer. Note that these pulses' amplitudes form an envelope whose amplitude equals the multiplier's output.

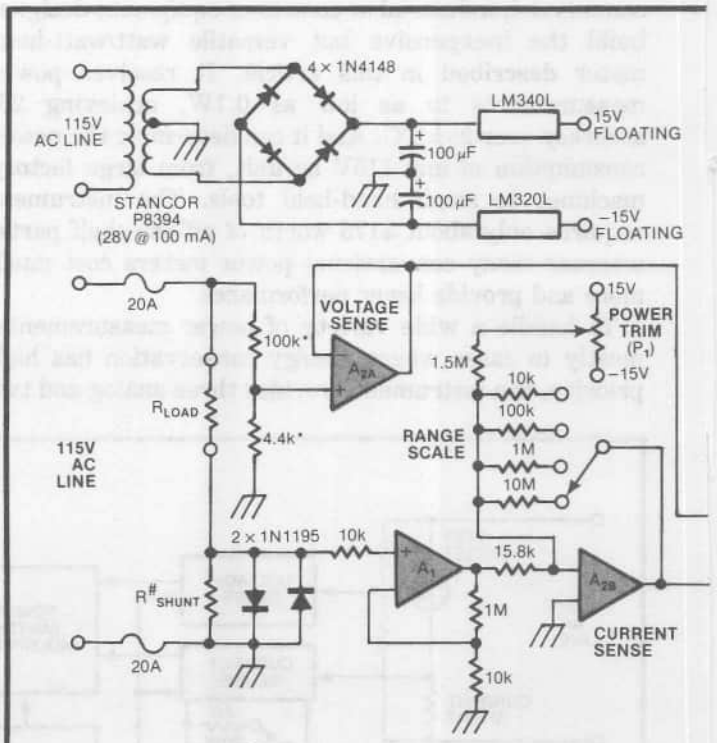

Fig 2—Careful parts selection and skillful circuit design *produce a test instrument that measures the power consumption of any 115V ac-powered device. The instrument provides a 4-decade power-measuring range—2, 20, 200 and 2000W FS—at 2% accuracy and over 25±5°C. Three analog and two digital outputs accommodate a wide variety of internal and external power-measurement applications.*

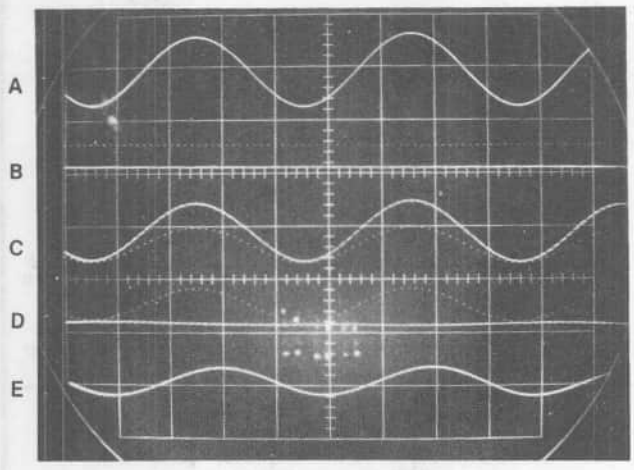

TRACE	VERTICAL	HORIZONTAL
A	5V/DIV	
B	50V/DIV	
C	5V/DIV	2 mSEC/DIV
D	10V/DIV	
E	10V/DIV	

Fig 3—During instrument operation, the power multiplier's output *(trace A) represents the monitored device's instantaneous power consumption. Biased by this output, A_{3A}'s oscillator output (refer to* **Fig 2***) biases the Q_1/Q_2 switch (trace B). Completing the feedback path to A_{3B}, Q_3 changes its emitter voltage to maintain servo-loop needs. Via Q_1, Q_2, Q_3, A_{3A} and A_{3B}, amplitude-modulated pulses arrive at the isolation transformer's primary (trace D). Connected to this transformer's secondary, A_5's output represents a sampled version of the monitored device's power consumption (E).*

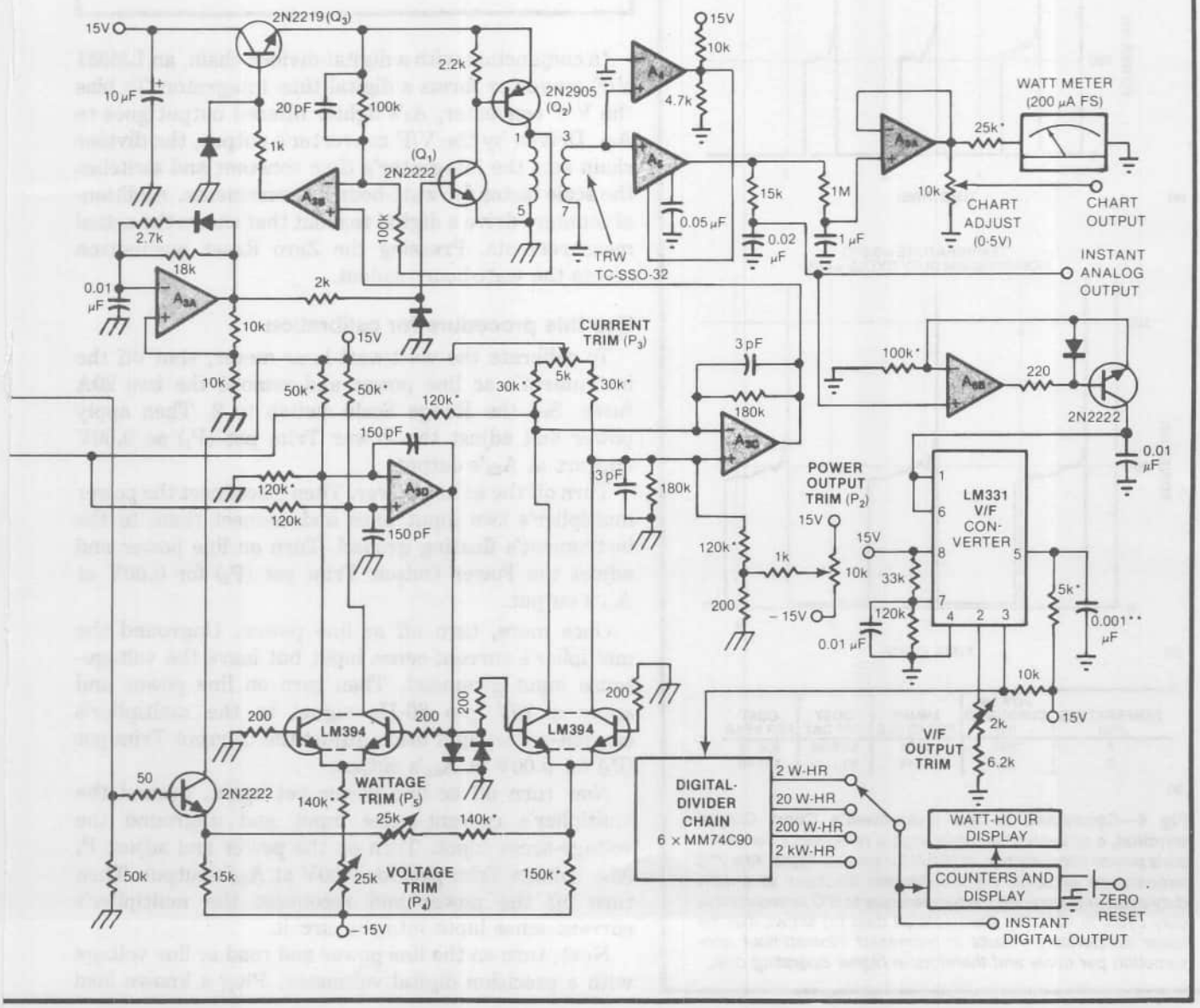

Pulse sampling and filtering smooth out power-signal levels

The amplitude-modulated pulses appear at the transformer's secondary, which is referenced to the instrument's earth ground. Each pulse's amplitude gets measured by a sample/hold amplifier (A_5) whenever A_4 generates a Sample command. Lightly filtered by the 15-kΩ, 0.02-μF network, A_5's output provides a sampled version of the load's instantaneous power consumption (trace E). Heavy filtering by the 1-MΩ, 1-μF network's time constant produces a smoother version of the sampled power signal. This signal drives the watts analog-meter and strip-chart-recorder outputs via the A_{6A} buffer.

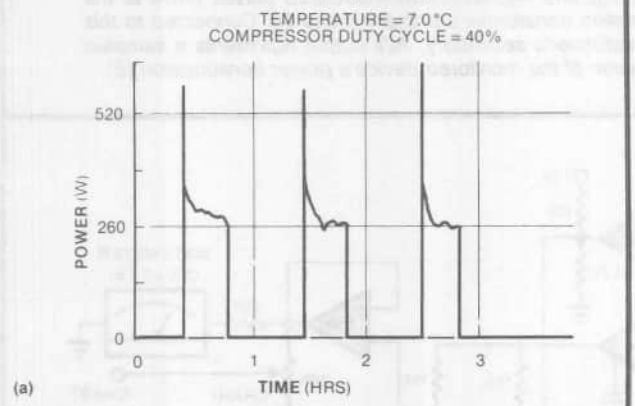

(a)

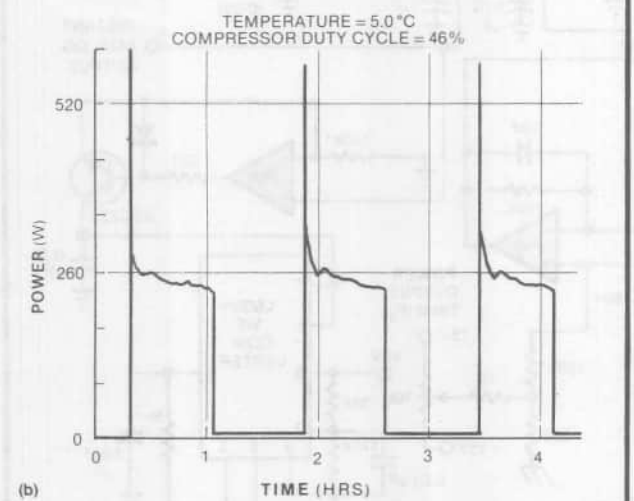

(b)

TEMPERATURE (°C)	POWER CONSUMED (W)	kW-HR PER CYCLE	COST PER DAY	COST PER YEAR
7	260	0.104	$0.0998	$36.44
5	260	0.119	$0.1147	$41.89

(c)

Fig 4—Connected to the instrument's Chart Output terminal, *a strip-chart recorder logs a refrigerator compressor's power consumption at 260W for several hours. At a 7°C temperature setpoint, the compressor functions at a 40% duty cycle* ***(a)****; lowering the temperature to 5°C increases this duty cycle to 46%* ***(b)****. Extrapolated data* ***(c)*** *shows that the lower temperature results in increased kilowatt-hour consumption per cycle and therefore in higher operating cost.*

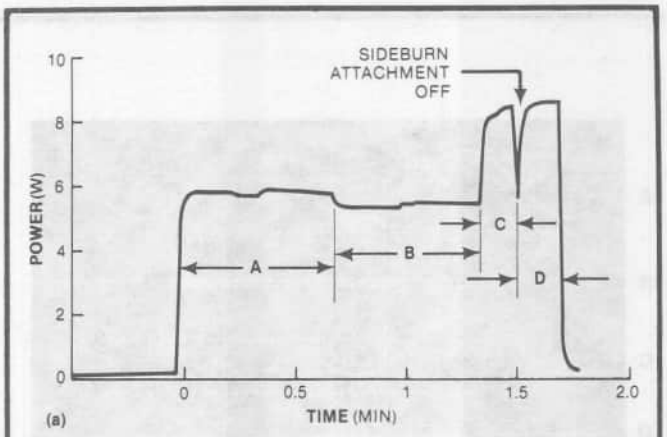

(a)

FACIAL AREA	POWER CONSUMED (W)	WATT-HOURS	COST PER SHAVE* (CENTS)
CHEEKS (A)	5.8	0.173	0.00692
UPPER & LOWER LIPS (B)	5.4	0.123	0.00492
RIGHT SIDEBURN (C)	8.4	0.063	0.00252
LEFT SIDEBURN (D)	8.4	0.061	0.00244

*BASED ON $0.04 PER kW-HR

(b)

Fig 5—Monitoring the power consumption *of a small electric razor via a strip-chart recorder, the watt/watt-hour meter generates instantaneous readings over short intervals* ***(a)****. With this accumulated data, you can make detailed power-cost calculations* ***(b)****.*

In conjunction with a digital-divider chain, an LM331 V/F converter forms a digital time integrator. To bias the V/F converter, A_5's lightly filtered output goes to A_{6B}. Driven by the V/F converter's output, the divider chain sets the integrator's time constant and switches the scale factor for watt-hour measurements. Additional counters drive a digital readout that shows the actual measurements. Pressing the Zero Reset pushbutton resets the watt-hour readout.

Use this procedure for calibration

To calibrate the watt/watt-hour meter, shut off the instrument's ac line power and remove the two 20A fuses. Set the Range Scale switch to 2. Then apply power and adjust the Power Trim pot (P_1) so 0.00V appears at A_{2B}'s output.

Turn off the ac line power. Then disconnect the power multiplier's two input lines and connect them to the instrument's floating ground. Turn on line power and adjust the Power Output Trim pot (P_2) for 0.00V at A_{6A}'s output.

Once more, turn off ac line power. Unground the multiplier's current-sense input but leave the voltage-sense input grounded. Then turn on line power and apply a 10V p-p 60-Hz signal to the multiplier's current-sense input lead. Adjust the Current Trim pot (P_3) for 0.00V at A_{6A}'s output.

Now turn off ac line power yet again, ground the multiplier's current-sense input and unground the voltage-sense input. Turn on the power and adjust P_4 (the Voltage Trim pot) for 0.00V at A_{6A}'s output. Then turn off the power and reconnect the multiplier's current-sense input into the circuit.

Next, turn on the line power and read ac line voltage with a precision digital voltmeter. Plug a known load

(eg, a 1% power resistor) into the instrument's test outlet. Adjust the Wattage Trim pot (P_5) until the analog meter reads the correct wattage (watts equals line voltage times load resistance).

Finally, turn off line power and disconnect A_{6B}'s positive input line. Then turn on the power and apply 5.00V to A_{6B}'s positive line. Adjust the V/F Output Trim pot (P_6) until the LM331's output at pin 3 runs at 27.77 kHz. Then turn off line power and reconnect A_{6B}'s positive input line.

A watt/watt-hour meter calibrated in this manner can accurately measure the power consumption of any 115V ac-powered device, large or small. Connecting the instrument to a home refrigerator demonstrates its prowess with large equipment: In one test, the refrigerator operated for 3½ hrs at a temperature setpoint of 7°C (**Fig 4**), and each time its compressor turned on, it consumed approximately 260W. As the compressor warmed up, power consumption actually decreased slightly. Changing the refrigerator's temperature control to 5°C increased the compressor's duty cycle by 15%. This power change reflects directly in the unit's per-cycle kilowatt-hour consumption.

Connecting the watt/watt-hour meter to an electric razor demonstrates its ability to monitor small equipment. In this setup, the meter recorded the electric razor's power consumption during a face-shaving exercise (**Fig 5**). Note that various facial areas cost more to shave than others.

Time-related power computations revealed that a complete daily shave costs about $0.09 per year. If this is excessive, a user could economize by growing a beard. **EDN**

Author's biography

Jim Williams is a design engineer with National Semiconductor Corp's Linear Applications Group, Santa Clara, CA, specializing in analog-circuit and instrumentation development. Previously, he worked as an analog-systems and -circuit consultant at Arthur D Little Inc and directed the Instrumentation Development Lab at the Massachusetts Institute of Technology. Jim studied psychology at Wayne State University and in his spare time enjoys skiing, art and collecting antique scientific instruments.

EDN

A Cahners Publication / 275 Washington St., Newton, MA 021581 (617) 964-3030

Cahners Publishing ☐ Publishers of 33 specialized business magazines in Building & Construction ☐ Electronics & Computers ☐ Foodservice ☐ Manufacturing ☐ Health Care ☐